

CHARACTERIZATION OF THE RESPONSE REGULATOR  
OMPR FROM *ESCHERICHIA COLI*

by

Kirsten Anne Mattison

A DISSERTATION

Presented to the Department of Molecular Microbiology and Immunology  
and the Oregon Health and Science University

School of Medicine

in partial fulfillment of

the requirements for the degree of

Doctor of Philosophy

June 2003


School of Medicine  
Oregon Health and Science University


---

CERTIFICATE OF APPROVAL


---


This is to certify that the Ph.D. thesis of  
Kirsten Anne Mattison  
has been approved

  
Dr. Linda J. Kenney

  
Dr. Scott Landfear

  
Dr. Richard G. Brennan

  
Dr. David Farrens

  
Dr. Hans Peter Bächinger

## TABLE OF CONTENTS

Table of Contents	i
List of Figures	x
List of Tables	xiv
List of Abbreviations	xv
Acknowledgements	xxi
Abstract	xxii
Preface	xxiv
Chapter 1: Introduction	1
1.0 Introduction	2
1.1 The osmoregulatory response in <i>Escherichia coli</i>	3
1.2 The OmpF and OmpC porins	6
1.3 Two component signal transduction	9
1.4 EnvZ and OmpR regulate porin gene expression	10
1.4.1 The EnvZ sensor kinase	11
1.4.1.1 EnvZ senses changes in osmolarity	12
1.4.1.2 EnvZ is autophosphorylated	15
1.4.1.3 EnvZ-P phosphorylates OmpR	16
1.4.1.4 EnvZ dephosphorylates OmpR-P	17

1.4.2 The OmpR response regulator	18
1.4.2.1 The OmpR phosphorylation domain	19
1.4.2.2 The OmpR DNA binding domain	20
1.4.2.3 Communication between the phosphorylation and DNA binding domains of OmpR	22
1.5 The porin gene promoters	24
1.6 The affinity model of porin gene regulation	28
1.7 Summary of the work presented in this thesis	29
Chapter 2: A Phosphorylation Site Mutant of OmpR Reveals Different Binding Conformations at <i>ompF</i> and <i>ompC</i>	43
2.0 Preface	43
2.1 Abstract	44
2.2 Introduction	45
2.3 Results	49
2.3.1 T83I cannot activate transcription <i>in vivo</i>	49
2.3.2 T83I is not phosphorylated by acetyl phosphate or by phosphoramidate	49
2.3.3 T83I is phosphorylated by the kinase EnvZ	51
2.3.4 T83I is phosphorylated slowly compared to wild-type OmpR	52
2.3.5 T83I binds EnvZ as well as wild-type OmpR	53
2.3.6 T83I binds to the high affinity sites F1 and C1	54

2.3.7 T83I does not saturably bind the composite site C1-C2-C3	55
2.3.8 T83I and wild-type OmpR protect the same regions of the <i>ompF</i> promoter	56
2.3.9 The pattern of protection by T83I is different from wild-type OmpR at the <i>ompC</i> promoter	57
2.3.10 The OmpF <sup>-</sup> OmpC <sup>-</sup> phenotype of T83I is co-dominant	57
2.3.11 T83I fails to activate <i>ompF</i> transcription	58
2.4 Discussion	60
2.4.1 The T83I mutant phenotype is OmpF <sup>-</sup> OmpC <sup>-</sup>	60
2.4.2 Phosphorylation properties are altered in T83I	62
2.4.3 The T83I substitution in the amino terminus alters the DNA binding properties of the carboxyl terminus	64
2.4.4 Differential activation of <i>ompF</i> and <i>ompC</i> transcription	66
2.4.5 Conclusion	68
2.5 Materials and Methods	68
2.5.1 Construction of mutants by PCR	68
2.5.2 Purification of T83I and T83I/D55A protein	69
2.5.3 $\beta$ -galactosidase assay	69
2.5.4 Phosphorylation of T83I by acetyl phosphate	70

2.5.5 Phosphoramidate synthesis and phosphorylation	71
2.5.6 EnvZ115 purification and phosphorylation	71
2.5.7 Measurement of ATPase activity	72
2.5.8 EnvZ binding	72
2.5.9 DNA binding	73
2.6 Acknowledgements	75
Chapter 3: The Linker Region Plays an Important Role in the Inter-domain Communication of the Response Regulator OmpR	102
3.0 Preface	102
3.1 Abstract	103
3.2 Introduction	104
3.3 Results	107
3.3.1 Changes in the sequence of the linker region of <i>ompR</i> result in altered porin expression	107
3.3.2 Longer and shorter linker sequences abrogate <i>ompR</i> function	108
3.3.3 Sequence changes in the linker affect OmpR phosphorylation and dephosphorylation by the kinase EnvZ	109
3.3.4 Changes in the linker alter DNA binding at <i>ompC</i>	113
3.4 Discussion	114

3.4.1 Changing the length of the OmpR linker inhibits transcriptional activation	114
3.4.2 Substitutions in the OmpR linker reveal new classes of OmpR mutants	116
3.4.3 Mutations that confer an OmpF <sup>+</sup> OmpC <sup>-</sup> phenotype do so by different mechanisms	118
3.5 Materials and Methods	119
3.5.1 Construction of mutants	119
3.5.2 Protein purification	120
3.5.3 $\beta$ -galactosidase assays	120
3.5.4 Phosphorylation assays and measurement of ATPase activity	121
3.5.5 DNase I footprinting	121
3.6 Acknowledgements	121
Chapter 4: A new model for OmpR dimerization	139
4.0 Preface	139
4.1 Abstract	140
4.2 Introduction	141
4.3 Results	146
4.3.1 DNA binding stimulates OmpR dimerization	146
4.3.2 Cysteine mutants of OmpR form homodimers, not heterodimers	148
4.3.3 OmpR cysteine substitutions S163C and V225C	

are impaired in porin gene expression	150
4.3.4 The carboxyl terminal $\beta$ sheet of OmpR	151
4.3.5 The $\beta$ sheet substitutions defective in porin gene expression are dominant to wild-type <i>ompR</i>	153
4.3.6 DNA binding stimulates phosphorylation of the cysteine mutants	153
4.3.7 Cysteine substitutions in the carboxyl terminal $\beta$ sheet of OmpR cross-link as homodimers	154
4.3.8 The cross-linked proteins are phosphorylated by the kinase EnvZ	157
4.3.9 The cross-linked proteins bind to DNA	157
4.3.10 The cross-linked proteins bind only to the high affinity site C1	160
4.4 Discussion	161
4.4.1 Oligomerization occurs after DNA binding	161
4.4.2 F140C is OmpC <sup>-</sup> and dominant to wild-type	162
4.4.3 An asymmetric tandem model for OmpR dimer formation	163
4.5 Materials and Methods	167
4.5.1 Construction of mutants by PCR	167
4.5.2 Protein purification	167
4.5.3 $\beta$ -galactosidase assays	167



4.5.4 Phosphorylation of mutant proteins	168
4.5.5 Cross-linking of mutant proteins	169
4.5.6 Electrophoretic mobility shift assays	170
4.5.7 DNase I footprinting	171
4.6 Acknowledgements	171
Chapter 5: Phosphorylation Alters the Interaction of the Response	
Regulator OmpR with its Sensor Kinase EnvZ	208
5.0 Preface	208
5.1 Abstract	209
5.2 Introduction	210
5.3 Results	213
5.3.1 Phosphorylation decreases the affinity of OmpR for EnvZ	213
5.3.2 The role of DNA in phosphorylation	215
5.3.3 The effect of DNA on GGK phosphorylation by EnvZ	216
5.3.4 The GGK mutant displays increased turnover in the presence of EnvZ and DNA	217
5.4 Discussion	218
5.4.1 <i>In vivo</i> relevance	222
5.5 Materials and Methods	224
5.5.1 Protein purification	224
5.5.2 Fluorescence anisotropy	225

5.5.3 Phosphorylation by acetyl phosphate	226
5.5.4 Phosphorylation by EnvZ115	226
5.5.5 ATPase assays	226
5.6 Acknowledgements	226
Chapter 6: A phosphatase mutant of EnvZ demonstrates altered binding to the response regulator OmpR	240
6.0 Preface	240
6.1 Abstract	241
6.2 Introduction	242
6.3 Results	244
6.3.1 EnvZ T247R is phosphorylated slightly faster than EnvZ	245
6.3.2 OmpR-P produced by EnvZ T247R or by low amounts of EnvZ is relatively stable	246
6.3.3 EnvZ T247R binds OmpR and OmpR-P with higher affinity than EnvZ	250
6.4 Discussion	254
6.5 Materials and Methods	258
6.5.1 Protein purification	258
6.5.2 ATPase assays	259
6.5.3 Phosphorylation reactions	259
6.5.4 Fluorescence anisotropy	261
6.5.5 Isothermal titration calorimetry	261

6.6 Acknowledgements	261
Chapter 7: Discussion	281
7.0 Preface	281
7.1 A new model for porin gene osmoregulation	282
7.2 Some OmpR mutants bind at C1 but not C2 or C3	284
7.3 A new model for OmpR dimerization	287
7.4 The role of the EnvZ phosphatase in osmoregulation	288
7.5 Conclusion	290
References	291

## LIST OF FIGURES

1.1	The EnvZ sensor kinase	36
1.2	The OmpR response regulator	38
1.3	The <i>ompF</i> and <i>ompC</i> promoter regions	40
2.1	Ribbon diagram of the active site of response regulator phosphorylation	77
2.2	The effect of <i>ompR</i> and mutant <i>ompRT83I</i> on transcription of <i>ompF-lacZ</i> and <i>ompC-lacZ</i> fusions <i>in vivo</i>	79
2.3	Phosphorylation of OmpR and T83I by small molecule phosphate donors	81
2.4	Phosphorylation of OmpR and T83I by EnvZ115	83
2.5	OmpR-stimulation of EnvZ115 ATPase activity	85
2.6	OmpR and T83I binding to EnvZc	87
2.7	DNA binding of OmpR and T83I to the high affinity F1 and C1 binding sites	89
2.8	DNase I footprinting analysis of OmpR and T83I binding at the <i>ompF</i> and <i>ompC</i> promoters	91
2.9	The effect of <i>ompRT83I</i> and <i>ompRT83I/D55A</i> on transcription of <i>ompF-lacZ</i> and <i>ompC-lacZ</i> fusions in the presence of <i>ompR</i>	93
2.10	The effect of <i>ompR</i> and <i>ompRT83I</i> on transcription from an <i>ompF-lacZ</i> promoter lacking the F4 binding site	95

2.11	Schematic depiction of DNase I footprinting result	97
2.12	Model for the differential regulation of transcription from the <i>ompF</i> and <i>ompC</i> promoters	99
3.1	Transcriptional activation by OmpR with random linker sequences	124
3.2	Transcriptional activation by OmpR with various linker lengths	126
3.3	Phosphorylation of linker mutants by EnvZ115	128
3.4	ATPase assay with the linker mutants	130
3.5	DNase I footprinting analysis of OmpR-P, G129D-P, P131S-P, and GGK-P binding at the <i>ompC</i> promoter	132
3.6	Model for the different conformational states of OmpR	134
3.7	Western blot analysis of linker mutant expression	136
4.1	OmpR cross-linking with BS <sup>3</sup>	173
4.2	The amino and carboxyl terminal domains of OmpR	175
4.3	Cross-linking of four cysteine substitutions with BMH	177
4.4	Cross-linking of combinations of cysteine substitutions with BMH	179
4.5	<i>In vivo</i> phenotype of the cysteine substitutions S163C and V225C	181
4.6	Cross-linking with BMH	183
4.7	Summary of cross-linking results with maleimide cross-linkers	185

4.8	Example of phosphorylation of cross-linked cysteine mutants	187
4.9	DNA binding by cross-linked cysteine mutants	189
4.10	Example of cross-linking by diluted proteins	191
4.11	DNA binding by diluted protein	193
4.12	DNase I footprinting analysis of uncross-linked and cross-linked G148C binding at the <i>ompC</i> promoter	195
4.13	Model of OmpR dimerization	197
5.1	Model for OmpR phosphorylation and DNA binding	229
5.2	EnvZc binding to OmpR by fluorescence anisotropy	231
5.3	Phosphorylation of OmpR and GGK by acetyl phosphate	233
5.4	EnvZ115 phosphorylation of OmpR and GGK	235
5.5	ATPase assay with OmpR and GGK	237
5.6	Phosphorylation of fluorescein labeled OmpR	239
6.1	Autophosphorylation of EnvZ and EnvZ T247R	264
6.2	Phosphorylation of OmpR by EnvZ and EnvZ T247R	266
6.3	ATPase assays with EnvZ and EnvZ T247R	268
6.4	Dephosphorylation of OmpR-P by EnvZ and EnvZ T247R	270
6.5	Isothermal titration calorimetry of OmpR with EnvZ	272
6.6	Fluorescence anisotropy of OmpR with EnvZ and EnvZ T247R	274
6.7	OmpR-P is maintained in the presence of EnvZ and phosphoramidate	276



## LIST OF TABLES

1.1	Phases of the response to osmotic shock in <i>Escherichia coli</i>	42
2.1	DNA binding by T83I	101
3.1	Oligonucleotides used in mutant construction	138
4.1	Sequence of oligonucleotides used for site-directed mutagenesis	199
4.2	Phenotypes of cysteine mutants in the $\beta$ sheet	201
4.3	Dominance of the cysteine mutants in the $\beta$ sheet to wild-type OmpR	203
4.4	Phosphorylation of the cysteine mutants with acetyl phosphate	205
4.5	Cross-linking of the cysteine mutants with maleimide based cross-linkers	207
6.1	Isothermal titration calorimetry data	280



## LIST OF ABBREVIATIONS

A (protein context)	alanine
A (DNA context)	deoxyadenosine
A <sub>x</sub>	absorbance at x nm
α	alpha
α-CTD	alpha-carboxyl terminal domain
AcPi	acetyl phosphate
Ala	alanine
AMP-PNP	β, γ-imidoadenosine-5'-triphosphate
Arg	arginine
Asn	asparagine
Asp	aspartic acid
ATP	adenosine triphosphate
ATPase	adenosine triphosphatase
β	beta
β-ME	beta-mercaptoethanol
bp	base pairs
BSA	bovine serum albumin
C (protein context)	cysteine
C (DNA context)	deoxycytosine
C-	carboxyl-
C4	four carbon

°C	degrees Celsius
Cl	chloride
CO <sub>2</sub>	carbon dioxide
CO <sub>3</sub>	carbonate
Cys	cysteine
D	aspartic acid
d(I-C)	deoxy(inosine-cytosine)
DNA	deoxyribonucleic acid
DNase	deoxyribonuclease
DTT	dithiothreitol
E	glutamic acid
EDTA	ethylenediaminetetraacetate
EnvZ*	EnvZ lacking TM1
EnvZ115	EnvZ lacking part of TM1
EnvZc	EnvZ cytoplasmic domain
EnvZ-P	phosphorylated EnvZ
EtOH	ethanol
F	phenylalanine
FA	fluorescence anisotropy
G (protein context)	glycine
G (DNA context)	deoxyguanosine
γ	gamma
Gln	glutamine

Glu	glutamic acid
Gly	glycine
H (protein context)	histidine
H (chemical compounds)	hydrogen
h	hour
H <sub>2</sub> O <sub>2</sub>	hydrogen peroxide
His	histidine
HPLC	high pressure liquid chromatography
I	isoleucine
Ile	isoleucine
IM	inner membrane
IPTG	isopropyl- $\beta$ -D-thiogalactoside
ITC	isothermal titration calorimetry
K (protein context)	lysine
K (chemical compounds)	potassium
K <sub>d</sub>	equilibrium dissociation constant
kb	kilobase pairs
kDa	kiloDalton
k <sub>phos</sub>	rate of phosphorylation
L	leucine
LB	Luria broth
Leu	leucine

LPS	lipopolysaccharide
Lys	lysine
M	methionine
Met	methionine
Mg	magnesium
mRNA	messenger RNA
μCi	microCurie
μg	microgram
μl	microlitre
μM	micromolar
ml	millilitre
mM	millimolar
min	minute
M	molar
N	asparagine
N-	amino-
Ni	nickel
ng	nanogram
nm	nanometer
nmol	nanomole
nM	nanomolar
NMR	nuclear magnetic resonance
OmpR1	OmpF <sup>-</sup> OmpC <sup>-</sup> OmpR mutant

OmpR <sub>2</sub>	OmpF <sup>+</sup> OmpC <sup>-</sup> OmpR mutant
OmpR <sub>3</sub>	OmpF <sup>-</sup> OmpC <sup>+</sup> OmpR mutant
OmpR <sub>c</sub>	carboxyl terminal domain of OmpR
OmpR <sub>N</sub>	amino terminal domain of OmpR
OmpR-P	phosphorylated OmpR
ONPG	o-nitrophenyl-β-D-galactoside
P	proline
PA	phosphoramidate
PAGE	polyacrylamide gel electrophoresis
PCR	polymerase chain reaction
%	percent
Phe	phenylalanine
P <sub>i</sub>	inorganic phosphate
PO <sub>4</sub>	phosphate
PP	periplasm
Pro	proline
Q	glutamine
R	arginine
RNA	ribonucleic acid
S	serine
SDS	sodium dodecyl sulfate
sec	seconds
Ser	serine

SO <sub>4</sub>	sulfate
t	time
T (protein context)	threonine
T (DNA context)	deoxythymidine
Thr	threonine
TM1	first transmembrane region of EnvZ
TM2	second transmembrane region of EnvZ
Trp	tryptophan
Tyr	tyrosine
V	valine
v/v	volume per volume
Val	valine
W	tryptophan
w/v	weight per volume
Y	tyrosine

## **Acknowledgements**

This thesis could not have been accomplished without the guidance and support of many people. I would like to thank all the members of the Kenney laboratory with whom I have worked for innumerable discussions, advice and encouragement. I owe particular thanks to Ricardo Oropeza for also being a dear friend. The members of my thesis committee, Hans Peter Bächinger, Richard Brennan, David Farrens and Scott Landfear have my gratitude for all of their support, in both helping me to work out ideas and providing aid with specific experiments.

I would also like to express my indebtedness to a group of people who have made my stay in Portland enjoyable: Aaron Farnsworth, Ben Brooks, Colin Crump, Paul Crump, Manuela DiLorenzo, Ryan Estep, Kirsten Gaarder, Kim Goldsmith, Shawn Lee, Diane LoPiccolo, Ryan Melnychuk, Shane McAllister, Michael Munks, Maho Nagasawa, Kristine Rose, Patrick Rose, Ken Ryan, Martha Sommer, Michiel Stork, Ronald Ullers and Joel Walker. My family has always been very supportive, and I would not be here without their lifelong love and encouragement.

## Abstract

The response to osmotic shock in *Escherichia coli* culminates in the regulation of expression of the porin genes *ompF* and *ompC* such that OmpF predominates in the outer membrane at low osmolarity and OmpC is present at high osmolarity. This transcriptional regulation is achieved by a two component system that consists of the sensor kinase EnvZ and the response regulator OmpR.

OmpR-P binds at the *ompF* and *ompC* promoter regions in order to activate transcription of *ompF* at low osmolarity and activate transcription of *ompC* while repressing *ompF* at high osmolarity. Previous studies in our laboratory concluded that the affinity model for the alternate regulation of porin gene expression by OmpR-P was not supported by biochemical analysis. Using OmpR mutants, I advance new models for the osmoregulation of *ompF* and *ompC* by OmpR-P. In addition, I find that the current model for OmpR dimer formation is unsubstantiated by cross-linking studies and present a new model that implicates a  $\beta$ -sheet of previously unknown function in forming the OmpR dimer interface.

I present an analysis of the interaction between the EnvZ kinase and the OmpR response regulator, which suggests that dephosphorylation of OmpR-P by EnvZ is unlikely to occur at *in vivo* concentrations. I confirm predictions made by these studies, that the EnvZ phosphatase is inactive at low EnvZ concentrations, and propose



an alternative explanation for the *in vivo* phenotype of an EnvZ phosphatase mutant.

## Preface

The work presented in this dissertation was performed by the author under the supervision of Dr. Linda J. Kenney in the program of Molecular Microbiology and Immunology at Oregon Health and Science University. The data in this thesis are presented in five chapters, three of which have been published in peer reviewed journals. Chapter 2 ("A phosphorylation site mutant of OmpR reveals different binding conformations at *ompF* and *ompC*") was published in the Journal of Molecular Biology (315: 497-511, 2002). This paper describes the biochemical characterization of an OmpR mutant and advances a new model for the regulation of porin gene expression by OmpR. Chapter 3 ("The linker region plays an important role in the inter-domain communication of the response regulator OmpR") was published in the Journal of Biological Chemistry (277: 32714-32721, 2002) and describes the characterization of a number of mutants in the linker region of OmpR. A refinement of the previous model for the regulation of porin gene expression is presented. In Chapter 4 ("A new model for OmpR dimerization"), a new model for the DNA-bound OmpR dimer is presented based on cross-linking studies. Chapter 5 ("Phosphorylation alters the interaction of the response regulator OmpR with its sensor kinase EnvZ") was published in the Journal of Biological Chemistry (277: 11143-11148). This publication describes the difference between the OmpR/EnvZ interaction and the OmpR-P/EnvZ interaction and

concludes that the EnvZ phosphatase activity is unlikely to control OmpR-P levels *in vivo*. Chapter 6 ("A phosphatase mutant of EnvZ demonstrates altered binding to the response regulator OmpR") confirms the prediction of the previous chapter that EnvZ does not dephosphorylate OmpR when present at low levels, and shows that a phosphatase mutant of EnvZ has altered interactions with OmpR which may explain its phenotype without invoking a role for the phosphatase *in vivo*. Chapter 2 is preceded by an Introduction which puts the work in the context of current knowledge in the field, and Chapter 6 is followed by a Discussion which attempts to address issues raised by my research.

# **Chapter 1**

## **Introduction**

## 1.0 Introduction

In response to changing environmental osmolarity, *Escherichia coli* undergo a variety of adaptive responses, one of which is to change the porin expression profile (Csonka, L. N., 1989). OmpF, with a larger pore and a faster flow rate, is expressed at low osmolarity and OmpC is expressed at high osmolarity (Nikaido, H. and E. Y. Rosenberg, 1983; van Alphen, W. and B. Lugtenberg, 1977). The regulation of porin gene expression is accomplished by the two component signaling system consisting of the EnvZ sensor kinase and the OmpR response regulator (Hall, M. N. and T. J. Silhavy, 1981c).

EnvZ mediates its own phosphorylation by intracellular ATP and transfers the phosphoryl group to OmpR (Igo, M. M. *et al.*, 1989b; Igo, M. M. and T. J. Silhavy, 1988). OmpR-P interacts with the promoter regions of *ompF* and *ompC*, resulting in the activation of *ompF* transcription at low osmolarity and the concomitant repression of *ompF* and activation of *ompC* at high osmolarity (Aiba, H. and T. Mizuno, 1990; Huang, K. J. *et al.*, 1997; Igo, M. M. *et al.*, 1989a). The affinity model of porin gene expression does not account for the observed pattern of osmoregulation (Head, C. G. *et al.*, 1998). In this thesis I present analyses of OmpR mutants, which led to the proposal of new models for the regulation of porin gene expression (Chapters 2 and 3) (Mattison, K. *et al.*, 2002a; Mattison, K. *et al.*, 2002b). Further characterization of OmpR is also

presented which refines the current model of OmpR dimer formation (Chapter 4).

EnvZ also dephosphorylates OmpR-P *in vitro* (Igo, M. M. *et al.*, 1989b). This phosphatase activity has been proposed to modulate the level of OmpR-P *in vivo* (Jin, T. and M. Inouye, 1993; Yang, Y. and M. Inouye, 1993). I present data in this thesis which indicates that OmpR-P and EnvZ do not interact at physiological concentrations, and as such the phosphatase activity is unlikely to be relevant to *in vivo* osmoregulatory responses (Chapters 5 and 6) (Mattison, K. and L. J. Kenney, 2002). Biochemical characterization of an EnvZ mutant is also presented which suggests that the presence of  $Mg^{2+}$  in the active site of OmpR-P may be important for appropriate osmoregulation of the porin genes (Chapter 6).

### **1.1 The osmoregulatory response in *Escherichia coli***

*Escherichia coli* are frequently exposed to dramatic changes in environmental osmolarity (Csonka, L. N., 1989). These cells, enclosed in semi-permeable membranes, are readily affected by the change in osmolarity as they transition from the external environment to the mammalian intestinal tract and vice versa (Nikaido, H. and M. Vaara, 1985; Wood, J., 1999). Osmotic shock induces an initial rapid efflux or influx of water, after which the bacteria initiate a set of responses that allow adaptation to growth in the new environment (Wood, J., 1999).

The best-characterized response is to osmotic upshift, transition from low to high osmolarity (Csonka, L. N., 1989; Wood, J., 1999). After this transition, the bacterial cell has lost water and most cellular metabolic processes have ceased (Wood, J., 1999). The response increases the internal concentration of specific solutes such that the bacteria return to a state in which the cytoplasm has a slightly higher solute concentration than the external medium (Csonka, L. N., 1989; Wood, J., 1999).

Potassium enters *Escherichia coli* cells through a constitutively expressed transporter almost immediately following osmotic upshift (Meury, J. *et al.*, 1985). The result is that intracellular  $K^+$  concentration varies directly with the osmolarity of the growth medium (Epstein, W. and S. G. Schultz, 1965). This has led some groups to propose that  $K^+$  may act as a secondary messenger of osmotic upshift (see 1.4.1.1) (Jung, K. *et al.*, 2001). Concomitant with  $K^+$  uptake, putrescine is extruded, in order to maintain the electroneutrality of the cytosol (Munro, G. F. *et al.*, 1972). Glutamate concentration also increases in the cell, balancing the positive charge of  $K^+$  (Richey, B. *et al.*, 1987; Tempest, D. W. *et al.*, 1970).

Potassium glutamate accumulation is insufficient as an osmoprotective response since many cellular enzymes are inhibited by high concentrations of these ions (Cayley, S. *et al.*, 1992). Further adaptation to growth after osmotic upshift is characterized by the accumulation of compatible solutes, so named because they may be

accumulated to high levels without interfering with cellular processes (Arakawa, T. and S. N. Timasheff, 1985; Cayley, S. *et al.*, 1992). Proline is immediately taken up, if available, by the constitutively expressed ProP transporter (Kaback, H. R. and T. F. Deuel, 1969; Milner, J. L. *et al.*, 1988). Transcriptional responses begin to be apparent after K<sup>+</sup> glutamate and proline accumulate to levels sufficient for cytosol rehydration (Csonka, L. N., 1989; Meury, J., 1994). A higher affinity K<sup>+</sup> transporter is transcribed, as is the ProU transporter with a high affinity for glycine betaine, this last is the favored compatible solute taken up by *E. coli* (Cairney, J. *et al.*, 1985; Gowrishankar, J., 1986; Laimins, L. A. *et al.*, 1981; Perroud, B. and D. LeRudulier, 1985). In the absence of exogenous proline and glycine betaine, some strains of *E. coli* synthesize glycine betaine by oxidation of choline (Andersen, P. A. *et al.*, 1988; Landfald, B. and A. R. Strom, 1986). The operon involved in choline transport and oxidation is located close to *lac* on the *E. coli* chromosome and has been deleted from our wild-type MC4100 strain (Andersen, P. A. *et al.*, 1988; Casadaban, M. J., 1976). In the absence of these preferred compounds, *E. coli* synthesize trehalose as an osmoprotective compatible solute (Giaever, H. M. *et al.*, 1988).

It is at this stage of transcriptional activation that the regulation of the porin genes is achieved (Wood, J., 1999). The timing of the transcriptional response is highly dependent on growth conditions (Wood, J., 1999). When osmotic upshift is induced by the addition of



0.3M NaCl to *E.coli* growing exponentially in rich laboratory medium, transcription from *ompF* is repressed within 2.5 minutes, and transcription of *ompC* is activated 10 minutes after the osmotic shock (Jovanovich, S. B. *et al.*, 1988).

The response to osmotic downshift essentially proceeds in reverse, and the response is completed more rapidly (Wood, J., 1999). After an initial influx of water, stretch-activated (or mechanosensitive) channels open to let small molecules exit (Cui, C. *et al.*, 1995; Schleyer, M. *et al.*, 1993; Stock, J. B. *et al.*, 1977). More specific solute influx and efflux systems are then used to restore the starting balance between internal and external solute concentrations (Wood, J., 1999). Transcription from the *ompF* promoter is activated under these conditions and transcription of *ompC* decreases (Hall, M. N. and T. J. Silhavy, 1981a; van Alphen, W. and B. Lugtenberg, 1977).

See Table 1.1 for a summary of the responses to osmotic shock in *Escherichia coli*.

## **1.2 The OmpF and OmpC porins**

The outer membrane of *Escherichia coli* provides a strong permeability barrier that protects the cell from harmful agents, such as digestive enzymes and bile salts (Nikaido, H. and T. Nakae, 1979). This protection derives mostly from the presence of lipopolysaccharide (LPS) in the outer leaflet of the outer membrane (Nikaido, H. and M. Vaara, 1985). LPS is made up of lipid A and the polysaccharide chains anchored

to it, which extend from the surface and carry many negative charges (Luderitz, O. *et al.*, 1982). These charged groups bind divalent cations that stabilize the outer membrane structure (Galanos, C. and O. Luderitz, 1975; Schindler, M. and M. J. Osborn, 1979). This hydrophilic surface protects the cell from harm, but also limits free diffusion of nutrients into the periplasm (Decad, G. M. and H. Nikaido, 1976; Nakae, T. and H. Nikaido, 1973, 1975). Small molecules must therefore access the bacterial periplasm through protein channels known as porins (Nakae, T., 1976). OmpF and OmpC are the two major outer membrane porins found in *Escherichia coli* (Argast, M. and W. Boos, 1980; Tommassen, J. and B. Lugtenberg, 1980). They form non-specific diffusion channels through which nutrients enter and waste products exit the cell (Nikaido, H. and E. Y. Rosenberg, 1983; Nikaido, H. and M. Vaara, 1985). The *ompF* gene is located at 21 minutes on the *E. coli* chromosome, while *ompC* is at 47 minutes (Hall, M. N. and T. J. Silhavy, 1981a).

OmpF and OmpC have a high degree of homology, and many functional chimeric porins have been formed that contain some OmpF and some OmpC sequences (Mizuno, T. *et al.*, 1987; Nogami, T. *et al.*, 1985). However, OmpF and OmpC are notably different in that diffusion rates through OmpF are much faster than through OmpC. This is a result of the larger diameter of the OmpF pore (1.16 nm) compared to that of OmpC (1.08 nm) (Nikaido, H. and E. Y. Rosenberg, 1983). OmpF

and OmpC are reciprocally regulated such that the total amount of porin is constant, while OmpF is preferentially expressed at low osmolarity and OmpC is preferentially expressed at high osmolarity (Hall, M. N. and T. J. Silhavy, 1981a).

It has been suggested that the osmoregulation of porin gene expression may not have physiological relevance for *E. coli* nutrient uptake. These conclusions are based on studies that generated porin-deficient mutants or exchanged the promoters for *ompF* and *ompC*, resulting in a strain that expressed *ompC* at low osmolarity and *ompF* at high osmolarity (Matsuyama, S. *et al.*, 1984; Nikaido, H. and M. Vaara, 1985). In both cases, wild-type generation times were observed in laboratory media. However, carbon sources are provided at millimolar concentrations in such media, while the half-maximal rate of glucose diffusion under wild-type conditions has been calculated to occur at an external concentration of only 7  $\mu$ M (Nikaido, H. and M. Vaara, 1985). In this diffusion process, the rate is directly proportional to both the concentration gradient and the permeability coefficient of the membrane. As such, near maximal rates of nutrient uptake and subsequent growth could occur in media containing 2 mM glucose as long as the permeability coefficient was not decreased by more than 300-fold. An even larger decrease in membrane permeability would be tolerated in rich media. By contrast, carbon sources in an aquatic environment are expected to be in the micromolar range and alteration of the porin profile

is expected to have grave consequences under these real environmental conditions (Koch, A. L., 1971; Nikaido, H. and M. Vaara, 1985). In addition, the OmpC porin is predicted to have protective effects in the mammalian intestinal tract, as the penetration rates of large, hydrophobic or multiply negatively charged compounds are selectively decreased upon expression of this porin (Nikaido, H. and E. Y. Rosenberg, 1983).

### **1.3 Two component signal transduction**

Two component signaling systems are characterized by an alternating arrangement of two protein domains, a histidine kinase domain and a response regulator domain. These serve to transfer a phosphoryl group from the environmental sensor to the effector domain. In a paradigm phosphotransfer system, two components are involved. The first component is the sensor kinase, an integral membrane protein that senses environmental conditions and autophosphorylates at a histidine residue. The second is the response regulator, which is phosphorylated at an aspartic acid residue by the histidine kinase. This phosphorylation event often regulates the DNA binding affinity of the response regulator, but may also alter its protein-protein interactions or enzymatic activity. (Foussard, M. *et al.*, 2001; Hackenbeck, R. and J. B. Stock, 1996; Stock, A. M. *et al.*, 2000)

Two component signaling systems are the predominant signal transduction pathways of prokaryotes and as such control innumerable

cellular processes (for reviews see (Hoch, J. A. and T. J. Silhavy, 1995)). In addition, these systems control diverse responses in eukaryotic organisms such as *Saccharomyces cerevisiae*, *Candida albicans*, *Dictyostelium*, *Arabidopsis thaliana*, and *Aspergillus nidulans* (Appleyard, M. V. C. L. *et al.*, 2000; Aubry, L. and R. Firtel, 1999; Calera, J. A. and R. A. Calderone, 1999; D'Agostino, I. B. and J. J. Kieber, 1999; Janiak-Spens, F. *et al.*, 1999). Thus, mechanisms of activation and signal transduction that are elucidated for one system have the potential to give insight into the mode of action of many regulatory processes.

#### **1.4 EnvZ and OmpR regulate porin gene expression**

EnvZ and OmpR comprise the two component signaling system that controls porin gene expression in *E. coli*. They are encoded in the *ompB* operon, located at 74 minutes on the chromosome (Hall, M. N. and T. J. Silhavy, 1981b, 1981c; Wurtzel, E. T. *et al.*, 1981). Within *ompB*, the gene order is *ompR-envZ* (Wurtzel, E. T. *et al.*, 1982). The *ompR* gene is translated efficiently from *ompB* mRNA, but *envZ* is translated at a much lower frequency. This is due to an overlap between the stop codon for *ompR* and the start codon for *envZ* at an ATGA sequence (Comeau, D. E. *et al.*, 1985; Liljestrom, P. *et al.*, 1988). The *envZ* gene lacks a Shine-Dalgarno ribosome binding site, and so its translation is thought to initiate when the ribosome re-initiates at the overlapping region (Comeau, D. E. *et al.*, 1985; Liljestrom, P. *et al.*, 1988; Shine, J. and L. Dalgarno, 1975). Quantitative Western blotting has estimated that

during exponential growth there are approximately 3500 molecules of OmpR and 100 molecules of EnvZ present per cell (Cai, S. J. and M. Inouye, 2002).

The EnvZ/OmpR system is required for expression of both OmpF and OmpC, thus when *ompB* is deleted, no porin gene expression is detected (Mizuno, T. and S. Mizushima, 1987). The sensor kinase, EnvZ, acts through the response regulator, OmpR, which directly regulates the transcriptional activity of the *ompF* and *ompC* promoters (Slauch, J. M. *et al.*, 1988).

In the absence of the EnvZ kinase, OmpR-P is formed and mediates some gene expression *in vivo* (Forst, S. *et al.*, 1988; Garrett, S. *et al.*, 1983; Garrett, S. *et al.*, 1985; Kanamaru, K. and T. Mizuno, 1992; Mizuno, T. and S. Mizushima, 1987; Villarejo, M. and C. C. Case, 1984). This is thought to occur largely due to phosphorylation of OmpR by intracellular acetyl phosphate (Matsubara, M. and T. Mizuno, 1999; McCleary, W. R. and J. B. Stock, 1994; McCleary, W. R. *et al.*, 1993; Pruss, B. M., 1998). It is also possible that phosphorylation of OmpR occurs through other sensor kinases; such cross-talk is possible *in vitro*, and may occur *in vivo* in the absence of EnvZ (Igo, M. M. *et al.*, 1989b; Ishige, K. *et al.*, 1994; Matsubara, M. *et al.*, 2000).

#### **1.4.1 The EnvZ sensor kinase**

EnvZ is a 450 amino acid protein found as a dimer at the inner membrane of *E. coli* (Comeau, D. E. *et al.*, 1985; Forst, S. *et al.*, 1987;

Mizuno, T. *et al.*, 1982; Tokishita, S. and T. Mizuno, 1994; Yang, Y. and M. Inouye, 1991). It consists of a short (15 amino acid) amino terminal cytoplasmic domain, two transmembrane regions separated by periplasmic domain, and a large carboxyl-terminal cytoplasmic domain (hereafter referred to as the cytoplasmic domain) (Forst, S. *et al.*, 1987). Figure 1.1 shows the structure of the EnvZ kinase. EnvZ senses changes in environmental osmolarity, autophosphorylates on a histidine residue, transfers the phosphoryl group to an aspartic acid residue of OmpR, and can dephosphorylate OmpR-P (Forst, S. *et al.*, 1989b; Hall, M. N. and T. J. Silhavy, 1981b; Igo, M. M. *et al.*, 1989b).

#### **1.4.1.1 EnvZ senses changes in osmolarity**

The amino terminus of EnvZ is responsible for sensing changes in environmental osmolarity and transmitting this information to OmpR. This region includes both transmembrane regions as well as the periplasmic domain that separates them. A truncated form of EnvZ that lacks only part of the first transmembrane domain is unable to direct osmoregulation of the porin genes (Igo, M. M. and T. J. Silhavy, 1988). This is likely to be due to the mis-localization of the truncated protein to inclusion bodies instead of to the cell surface (Igo, M. M. and T. J. Silhavy, 1988). A chimeric protein consisting of the amino terminal half of the Tar chemoreceptor to the cytoplasmic domain of EnvZ does not respond to changes in osmolarity (Utsumi, R. *et al.*, 1989).

The periplasmic domain is a clear candidate for the EnvZ sensor. Deletions in the periplasmic domain that did not affect protein localization were shown to confer aberrant osmoregulatory phenotypes (Tokishita, S. *et al.*, 1991). Further work showed that a 12 amino acid sequence in the periplasmic domain is highly conserved among the EnvZ proteins from enteric bacteria and that mutations in this region alter the osmoregulation of porin genes (Waukau, J. and S. Forst, 1999). Other studies showed that a point mutation at the junction between the periplasmic domain and the second transmembrane region (TM2) also resulted in altered osmoregulation of porin gene expression and supported a role for the periplasmic domain in osmosensing (Russo, F. D. and T. J. Silhavy, 1991). One study proposed that the periplasmic domain is not involved in sensing environmental changes. These authors found that large stretches of the periplasmic domain could be deleted or replaced without compromising EnvZ function, and suggested that transmembrane regions were involved in osmosensing (Leonardo, M. R. and S. Forst, 1996). It should be noted, however, that the deletions and replacements in this study did not alter the conserved sequence identified as important for periplasmic osmosensing (Waukau, J. and S. Forst, 1999). A role for the transmembrane regions in transmitting information from the periplasm to the cytoplasmic domain was suggested by point mutations in both TM1 and TM2 that interfered with signal transduction (Hsing, W. *et al.*, 1998; Tokishita, S. *et al.*, 1992; Tokishita,



S. and T. Mizuno, 1994). Whatever the sensing role of the periplasmic domain, it is not thought to interact with a soluble factor. Over-expression of the isolated periplasmic domain fused to the maltose binding protein does not interfere with the osmoregulation of *ompF* and *ompC* (Egger, L. A. and M. Inouye, 1997). This soluble form of the periplasmic domain, which has structure by circular dichroism analysis, would titrate any soluble factor and interfere with signaling. In summary, there is a specific signal sensed by the amino terminus of EnvZ. This signal is detected by the periplasmic and/or transmembrane domains. The transmembrane regions are also associated with transmission of the signal to the cytoplasmic domain.

The nature of the signal sensed by EnvZ has proven enigmatic. Early studies focused on the ability of the local anaesthetic procaine to induce altered porin profiles (Rampersaud, A. and M. Inouye, 1991; Taylor, R. K. *et al.*, 1983). These effects are pleiotropic, however, altering the expression of many periplasmic and outer membrane proteins, and as such are unlikely to mimic the natural osmotic signal sensed by EnvZ (Taylor, R. K. *et al.*, 1983). A recent study suggested that the accumulation of  $K^+$  in the cytoplasm, which is induced upon transition to high osmolarity (see section 1.1), might regulate the enzymatic activity of EnvZ (Jung, K. *et al.*, 2001). It has long been recognized, however, that  $K^+$  is an essential cofactor for the phosphorylation of OmpR by EnvZ (Tokishita, S. *et al.*, 1990). Furthermore, maximal stimulation of EnvZ

function was observed at 100 mM KCl, while the *in vivo* K<sup>+</sup> levels have been measured at 150-500 mM in media ranging from low to high osmolarity (Jung, K. *et al.*, 2001, Epstein, W. and S. G. Schultz, 1965). It is therefore unlikely that such a simple scheme accounts for the osmoregulation of the porin genes by the EnvZ/OmpR system.

#### **1.4.1.2 EnvZ is autophosphorylated**

While the amino terminal regions of EnvZ are important for osmosensing and signal transduction across the inner membrane *in vivo*, the isolated cytoplasmic domain of the protein possesses all of the catalytic functions *in vitro* (Hidaka, Y. *et al.*, 1997). Therefore, many of the studies on the remaining activities of EnvZ have been performed using various truncated mutant proteins, including: EnvZ115, which lacks the first 38 amino acid residues of EnvZ (part of TM1); EnvZ\*, which lacks the first 80 amino acid residues of EnvZ (TM1); and EnvZc, which lacks the first 179 amino acid residues of EnvZ (TM1, periplasmic domain, and TM2) (Aiba, H. *et al.*, 1989a; Hidaka, Y. *et al.*, 1997; Igo, M. M. and T. J. Silhavy, 1988).

The cytoplasmic domain of EnvZ consists of two separate structural domains; a core domain which is connected to TM2 via a 50 amino acid linker, and the catalytic domain which is linked to the core domain by 12 unstructured amino acid residues (Figure 1.1)(Dutta, R. *et al.*, 1999; Park, H. and M. Inouye, 1997). The NMR solution structures of both the core and catalytic domains have been solved (Tanaka, T. *et al.*,

1998; Tomomori, C. *et al.*, 1999). They reveal that the core domain forms a homodimeric four helix bundle that stabilizes the full length EnvZ dimer (Tomomori, C. *et al.*, 1999)(Figure 1.1C). The catalytic domain consists of a hydrophobic core made up of a five stranded beta sheet and three alpha helices, with a large undefined loop near the nucleotide binding site (Tanaka, T. *et al.*, 1998)(Figure 1.1D).

EnvZ is phosphorylated *in vitro* upon incubation with ATP at histidine residue 243 (Igo, M. M. and T. J. Silhavy, 1988; Roberts, D. L. *et al.*, 1994). Histidine 243 is at the surface of the four helix bundle formed by the core domain (Tomomori, C. *et al.*, 1999)(Figure 1.1C). Autophosphorylation occurs when the catalytic domain of one subunit is juxtaposed to histidine 243 of the second subunit, in a trans-phosphorylation reaction (Park, H. *et al.*, 1998; Qin, L. *et al.*, 2000; Yang, Y. and M. Inouye, 1991).

#### **1.4.1.3 EnvZ-P phosphorylates OmpR**

The phosphoryl group from histidine 243 of EnvZ is transferred to aspartic acid residue 55 of OmpR in a reaction that requires only the presence of the phosphorylated core domain of EnvZ (Delgado, J. *et al.*, 1993; Igo, M. M. *et al.*, 1989a; Park, H. *et al.*, 1998). This reaction requires both  $K^+$  and  $Mg^{2+}$ , and as such can be stopped with the addition of EDTA to the sample (Kenney, L. J., 1997; Tokishita, S. *et al.*, 1990).

sensing domain from the chemoreceptor for aspartate (Tar + EnvZ = Taz) (Utsumi, R. *et al.*, 1989). This chimera does not support normal osmoregulation of porin genes, is not capable of *ompF* activation, only functions when the linker region is derived from Tar, and requires 1000-fold more aspartate than endogenous Tar to induce signaling (Biemann, H.-P. and D. E. J. Koshland, 1994; Jin, T. and M. Inouye, 1993; Utsumi, R. *et al.*, 1989). It is therefore unlikely that the results obtained with Taz are relevant to the osmoregulation of porin gene expression.

#### **1.4.2 The OmpR response regulator**

OmpR is a 239 amino acid protein that exists in soluble form in the cytoplasm of *Escherichia coli* (Liljestrom, P. *et al.*, 1982; Nara, F. *et al.*, 1986; Wurtzel, E. T. *et al.*, 1982). It consists of an amino terminal phosphorylation domain and a carboxyl terminal DNA binding domain, joined by a flexible linker (Kato, M. *et al.*, 1989; Tate, S. *et al.*, 1988). The structure of OmpR is shown in Figure 1.2. OmpR is phosphorylated on aspartate 55 by the EnvZ kinase, OmpR-P binds to the *ompF* and *ompC* promoter sequences (Aiba, H. and T. Mizuno, 1990; Huang, K. J. *et al.*, 1997). OmpR-P bound at the promoter regions interacts with the  $\alpha$ -subunit of RNA Polymerase and mediates both the activation of *ompF* at low osmolarity and the repression of *ompF* and activation of *ompC* at high osmolarity (Aiba, H. and T. Mizuno, 1990; Delgado, J. *et al.*, 1993; Igo, M. M. *et al.*, 1989a; Kato, N. *et al.*, 1996; Matsuyama, S. and S.

Mizushima, 1987; McCleary, W. R. *et al.*, 1993; Sharif, T. R. and M. M. Igo, 1993; Slauch, J. M. *et al.*, 1991).

#### **1.4.2.1 The OmpR phosphorylation domain**

The phosphorylation domains of response regulators are highly conserved (Baikalov, I. *et al.*, 1996; Birck, C. *et al.*, 1999; Lewis, R. J. *et al.*, 2000; Madhusudan *et al.*, 1996; Robinson, V. L. *et al.*, 2000; Sola, M. *et al.*, 1999; Stock, A. M. *et al.*, 1989; Volz, K. and P. Matsumura, 1991). All of the known structures consist of an  $(\alpha/\beta)_5$  topology, that is five alternating  $\alpha$ -helices and  $\beta$ -strands in the primary structure. A five-stranded  $\beta$ -sheet forms the core of the folded protein; this core is surrounded by the five  $\alpha$ -helices. Response regulators also share a group of conserved residues that form the active site and/or are important for signal propagation. The active site residues, located at the C-terminal end of the  $\beta$ -sheet, are the site of phosphorylation (D55 in OmpR), residues involved in binding metal ions (D11 and D12), and a residue that interacts with the incoming phosphate (K105) (Brissette, R. E. *et al.*, 1991a; Kanamaru, K. *et al.*, 1990; Lukat, G. S. *et al.*, 1991; Lukat, G. S. *et al.*, 1990; Robinson, V. L. *et al.*, 2000). Two adjacent residues, a hydroxylic residue (T83) and an aromatic ring (Y102) are thought to be involved in transmitting a conformational change whereby phosphorylation of OmpR leads to its activation (Brissette, R. E. *et al.*, 1991b; Ganguli, S. *et al.*, 1995; Kanamaru, K. and T. Mizuno, 1992; Zhu, X. *et al.*, 1996; Zhu, X. *et al.*, 1997a).

The X-ray crystal structures of activated phosphorylation domains allow further interpretation of the importance of the conserved residues listed above (Birck, C. *et al.*, 1999; Cho, H. S. *et al.*, 2000; Halkides, C. J. *et al.*, 2000; Lewis, R. J. *et al.*, 1999; Robinson, V. L. *et al.*, 2000). The  $Mg^{2+}$  essential for the phosphorylation reaction is coordinated to the phosphoryl group, and this interaction is stabilized by the conserved acidic residues (D11, D12) and water molecules. The side chain of the hydroxylic residue (T83) moves to form a charge-dipole interaction with the phosphoryl group, which exposes a hydrophobic pocket that allows the aromatic residue (Y102) to move from an exposed to a buried position. This "aromatic switch" has been proposed to be a conserved mechanism whereby phosphorylation of a response regulator is translated to its activation (Zhu, X. *et al.*, 1996; Zhu, X. *et al.*, 1997a).

#### **1.4.2.2 The OmpR DNA binding domain**

The carboxyl terminal DNA binding domain of OmpR (OmpRc) consists of a four-stranded  $\beta$ -sheet, an  $\alpha$ -helical domain, and a  $\beta$ -hairpin (Kondo, H. *et al.*, 1997; Martinez-Hackert, E. and A. M. Stock, 1997a). Three alpha helices form a helix-turn-helix motif and the  $\beta$ -hairpin is indicative of a winged helix-turn-helix DNA binding protein (Brennan, R. G., 1993). The  $\beta$ -sheet at the amino terminus of this domain is unique to the OmpR family of response regulators (Martinez-Hackert, E. and A. M. Stock, 1997b).

The function of the  $\beta$ -sheet that is conserved among OmpR family members is not well defined. The first strands of this sheet contribute to the hydrophobic core of the domain and may therefore be important for correct orientation of the helix-turn-helix motif (Martinez-Hackert, E. and A. M. Stock, 1997b). Mutagenesis has identified only one residue in this region, an arginine at position 150, as important for regulation of porin gene expression (Kato, M. *et al.*, 1995; Nara, F. *et al.*, 1986; Russo, F. D. *et al.*, 1993). In the OmpR family member PhoB, this region has been shown to form the interface between DNA bound dimers, if this is true for OmpR it is possible that the overall structure of the region is more crucial than any specific amino acid residue (Blanco, A. G. *et al.*, 2002).

The first  $\alpha$ -helix of OmpRc forms much of the hydrophobic core which stabilizes the entire domain (Martinez-Hackert, E. and A. M. Stock, 1997a). Mutations have been isolated in this region which alter porin gene expression and interfere with DNA binding, presumably by altering the structure of the domain (Kato, M. *et al.*, 1995; Martinez-Hackert, E. and A. M. Stock, 1997b; Russo, F. D. *et al.*, 1993). The second  $\alpha$ -helix is packed on the surface of OmpRc, and by analogy to other helix-turn-helix transcription factors is thought to direct appropriate positioning of the recognition helix. Mutations in  $\alpha 2$  have also been isolated which alter DNA binding and porin gene expression (Kato, M. *et al.*, 1995; Martinez-Hackert, E. and A. M. Stock, 1997b; Russo, F. D. *et al.*, 1993).  $\alpha 3$  of OmpRc is the recognition helix that is

thought to specifically interact with the bases in the major groove of OmpR binding sites (Huang, K. J. and M. M. Igo, 1996; Martinez-Hackert, E. and A. M. Stock, 1997a). Mutations here specifically interfere with DNA binding (Aiba, H. *et al.*, 1994; Nara, F. *et al.*, 1986; Russo, F. D. *et al.*, 1993). The  $\beta$ -hairpin that forms the wing of OmpRc has been proposed to play a role in DNA binding, although an additional role for this region in transcriptional activation is also suggested by mutagenesis studies (Kato, M. *et al.*, 1995; Tsuzuki, M. *et al.*, 1994).

The turn of the helix-turn-helix motif is unusually large in OmpRc, relative to other helix-turn-helix motifs (Blanco, A. G. *et al.*, 2002; Martinez-Hackert, E. and A. M. Stock, 1997a, 1997b). This region is referred to as the  $\alpha$ -loop since mutations have been isolated which indicate that it is involved in transcriptional activation (Pratt, L. A. and T. J. Silhavy, 1994; Russo, F. D. *et al.*, 1993). However, recent evidence from our laboratory indicates that these mutants may actually be defective in DNA binding (D. Walthers and L. J. Kenney, unpublished results). The mutations that seem to truly interfere with OmpR/RNA Polymerase interaction are located in the loop between  $\alpha 1$  and  $\alpha 2$ , and in the linker region (Aiba, H. *et al.*, 1994; Kato, M. *et al.*, 1995).

#### **1.4.2.3 Communication between the phosphorylation and DNA binding domains of OmpR**

Phosphorylation of the amino terminal domain of OmpR leads to an increase in the DNA binding affinity of the carboxyl terminal domain



(Aiba, H. *et al.*, 1989c; Huang, K. J. *et al.*, 1997). Similarly, the presence of high affinity DNA binding sites increases phosphorylation of the amino terminal domain *in vitro* (Ames, S. K. *et al.*, 1999; Qin, L. *et al.*, 2001). Interesting classes of mutations are those in the carboxyl terminal domain, which interfere with phosphorylation and those in the amino terminal domain, which interfere with DNA binding. A substitution in the recognition helix, V203M, was found to interfere with DNA binding as expected, but also to have a defect in its ability to be phosphorylated by small molecule phospho-donors such as acetyl phosphate (Tran, V. K. *et al.*, 2000). Two mutations in the amino terminus which were phosphorylated normally, G96A and R155S, have DNA binding defects which render them phenotypically OmpF<sup>-</sup> OmpC<sup>-</sup> (Nakashima, K. *et al.*, 1991b).

This interaction between the two domains is necessary for wild-type OmpR function. The isolated carboxyl terminus retains DNA binding ability, but with approximately 10-fold lower affinity than the full length protein (Kato, M. *et al.*, 1989; Tate, S. *et al.*, 1988)(Ann M. Stock, personal communication). OmpR<sub>C</sub> does not function *in vivo* either to activate transcription of porin genes or to interfere with activation by the full length protein (Nakashima, K. *et al.*, 1991a; Tsuzuki, M. *et al.*, 1994).

The conformational transitions that are involved in this inter-domain communication are poorly understood. Limited proteolysis by trypsin has shown that a conformational change occurs when OmpR is

phosphorylated that is centered on the inter-domain linker region (Kenney, L. J. *et al.*, 1995). The linker region of OmpR is also implicated in inter-domain communication by mutations in this region which result in defects in osmoregulation of the porin genes (Aiba, H. *et al.*, 1994; Russo, F. D. *et al.*, 1993). It is interesting to speculate that this region may play a role in transmitting the signal that increases the DNA binding affinity of the carboxyl terminus in response to phosphorylation of the amino terminus.

### **1.5 The porin gene promoters**

Both *ompF* and *ompC* require OmpR-P binding for their transcriptional activation (Inokuchi, K. *et al.*, 1985; Ramakrishnan, G. *et al.*, 1985; Taylor, R. K. *et al.*, 1985). The promoter regions of these genes have low homology with the consensus -10 and -35 regions (Hawley, D. K. and W. R. McClure, 1983; Inokuchi, K. *et al.*, 1984). If the promoter region of *ompF* is mutated such that the -10 is a better match to the consensus sequence, transcriptional activity of this locus is observed in the absence of OmpR (Dairi, T. *et al.*, 1985; Ozawa, Y. *et al.*, 1987).

OmpR thus activates transcription by binding upstream of the -35 site and enhancing the binding of RNA Polymerase to the promoter region (Mizuno, T. and S. Mizushima, 1986; Ostrow, K. S. *et al.*, 1986; Tsung, K. *et al.*, 1990). The OmpR binding sites in the *ompF* and *ompC* promoter regions are shown in Figure 1.3.

Three OmpR-P dimers bind to three sites at the *ompF* promoter termed F1, F2 and F3 (Harlocker, S. L. *et al.*, 1995; Maeda, S. *et al.*, 1991). F1 is the highest affinity site, and OmpR binds to this site even in the absence of phosphorylation (Huang, K. J. *et al.*, 1997; Norioka, S. *et al.*, 1986; Rampersaud, A. *et al.*, 1989; Tsung, K. *et al.*, 1989). It has been proposed that cooperative interactions between OmpR dimers lead to high affinity binding at the complete F1-F2-F3 region (Harlocker, S. L. *et al.*, 1995; Huang, K. J. *et al.*, 1997). Certainly, binding at F1 is necessary for high affinity binding at the downstream sites, but sigmoidal binding curves have never been observed for OmpR-P binding at *ompF* (Head, C. G. *et al.*, 1998; Huang, K. J. *et al.*, 1997). It is thought that the binding of OmpR-P to the low affinity F3 site at -40 is required for transcriptional activation, however the V203M mutant of OmpR does not appear to protect F3 from DNase I digestion and is capable of activation at *ompF* (Mizuno, T. *et al.*, 1988; Tsung, K. *et al.*, 1989). OmpR-P binding in this region leads to activation of transcription *in vitro*, and presumably *in vivo* (Igo, M. M. *et al.*, 1989a; Norioka, S. *et al.*, 1986).

There is a fourth OmpR binding site at *ompF*, located at -384 to -351 from the transcriptional start site and termed F4 (Huang, K. J. *et al.*, 1994). This site is required for repression of *ompF* transcription (Huang, K. J. *et al.*, 1994). Repression of *ompF* is thought to arise by formation of a repression loop in which the OmpR-P dimer bound at F4 interacts with a dimer bound at F2 or F3, sterically excluding RNA Polymerase from the

promoter region (Forst, S. *et al.*, 1995; Slauch, J. M. and T. J. Silhavy, 1991). Support for the repression loop model comes from the finding that the *ompF* promoter region has an intrinsic bend (Mizuno, T., 1987). Formation of this repression loop is thought to be facilitated by the binding of a histone-like protein, integration host factor (IHF), which has the ability to bend the DNA to which it binds (Friedman, D. I., 1988; Ramani, N. *et al.*, 1992). IHF binds to two sites centered at -180 and -60 of the *ompF* promoter, and *ompF* regulation is altered in IHF mutants (Ramani, N. *et al.*, 1992; Tsui, P. *et al.*, 1988).

The *micF* RNA may also contribute to down-regulation of OmpF. *micF* is divergently transcribed from the *ompC* promoter region. This RNA is antisense to and binds the Shine-Dalgarno and translation initiation sites of *ompF* mRNA, thus potentially decreasing its translation (Andersen, J. *et al.*, 1987). *micF* is highly expressed at high growth temperatures, and may play a role in decreasing OmpF expression under these conditions (Coyer, J. *et al.*, 1990). In addition, *micF* may play a role in fine tuning the repression of *ompF* upon transition to high osmolarity, but deletion of this gene does not significantly affect porin gene expression levels (Aiba, H. *et al.*, 1987; Matsuyama, S. and S. Mizushima, 1985; Pratt, L. A. *et al.*, 1996).

Three OmpR-P dimers also bind the *ompC* promoter region, at C1, C2 and C3 binding sites that are located as the F1-F2-F3 sites from -100 to -40 upstream of the transcriptional start site (Maeda, S. *et al.*, 1991).

Once again, the C1 site is bound with high affinity, while the C2 and C3 sites require C1 occupancy for OmpR-P binding (Maeda, S. and T. Mizuno, 1990; Norioka, S. *et al.*, 1986). The binding sites must be spaced such that they lie on one face of the promoter DNA for *ompC* activation to be achieved, but the region can be completely inverted without affecting promoter function (Maeda, S. *et al.*, 1988; Maeda, S. *et al.*, 1991). Binding at a promoter-proximal site is thought to be required for transcriptional activation, since re-location of the high affinity C1 site to the promoter-proximal position allows transcriptional activity of *ompC* in the absence of the other sites (Maeda, S. and T. Mizuno, 1990).

The OmpR binding sites are not highly conserved and have inherent asymmetry; both of these facts make it difficult to assign consensus sequences for OmpR binding (Huang, K. J. and M. M. Igo, 1996). An adenine and a cytosine are found juxtaposed at the 5' end of the high affinity half sites, these bases have been shown to be important for DNA recognition by OmpR *in vivo* (Figure 1.3)(Huang, K. J. and M. M. Igo, 1996; Pratt, L. A. and T. J. Silhavy, 1995). A central GXXXC motif is also conserved in each whole OmpR binding site, with the guanine base being the last in the 5' half site and the cytosine the second in the 3' half site (Figure 1.3). The X's in this motif are mostly A or T (Harlocker, S. L. *et al.*, 1995; Huang, K. J. and M. M. Igo, 1996).

## 1.6 The affinity model of porin gene regulation

An interesting problem in studies of osmoregulation of the porin genes is how a single species (OmpR-P) can alternately activate *ompF* at low osmolarity and activate *ompC* while repressing *ompF* at high osmolarity. It is known that OmpR-P is indeed the active form of the protein, and as such this modification is not sufficient to explain the transition from low to high osmolarity (Slauch, J. M. and T. J. Silhavy, 1989). A model was proposed to explain this switch based on the relative amounts of OmpR-P present in the cell and varying affinities of OmpR-P for the *ompF* and *ompC* promoter regions (Russo, F. D. and T. J. Silhavy, 1991). This model predicts that at low osmolarity there is a low amount of OmpR-P present. Therefore, at low osmolarity, OmpR-P only interacts with those sites to which it binds with the highest affinity. These are predicted to be the F1, F2, and F3 sites required for activation of *ompF* (Harlocker, S. L. *et al.*, 1995; Maeda, S. *et al.*, 1991). At high osmolarity, OmpR-P levels are predicted to rise in the cell, and the lower affinity sites would be filled. These are predicted to be the F4 site required for repression of *ompF* and the C1, C2, and C3 sites required for activation of *ompC* (Huang, K. J. *et al.*, 1994; Maeda, S. and T. Mizuno, 1990; Norioka, S. *et al.*, 1986).

The real assessment of the validity of the affinity model is to determine the affinity of OmpR-P binding to each of the sites from the *ompF* and *ompC* promoter regions. The mathematical model that was

used to show how changing OmpR-P concentration could result in changes in gene expression required a 20-fold difference in affinity between the high and low affinity sites to accurately portray the observed pattern of porin regulation (Russo, F. D. and T. J. Silhavy, 1991). However, DNA binding measurements showed that there is approximately a 2-fold difference between OmpR-P affinity for the F1-F2-F3 and C1-C2-C3 composite binding sites (Head, C. G. *et al.*, 1998). Furthermore, the high affinity F1 and C1 sites have virtually identical affinities for OmpR-P (Bergstrom, L. *et al.*, 1998; Head, C. G. *et al.*, 1998). Therefore, the affinity model does not accurately describe the behavior of OmpR-P at the various promoter sites, and as such, cannot account for the alternate regulation of *ompF* and *ompC* transcription by OmpR-P.

### **1.7 Summary of the work presented in this thesis**

The first part of this work (Chapters 2, 3 and 4) focuses on the interaction between the amino and carboxyl terminal domains of OmpR and uses the information gleaned to model how OmpR-P is responsible for activating *ompF* at low osmolarity while repressing *ompF* and activating *ompC* at high osmolarity.

In the second chapter, I examined a point mutant in which the threonine at position 83 was substituted with isoleucine (Mattison, K. *et al.*, 2002a). This mutant protein was found to have some phosphorylation defects, as expected for a substitution of one of the

residues conserved in the active site (Section 1.4.2.1). Interestingly, I also observed that T83I bound normally at the *ompF* promoter region, but interacted only with the highest affinity C1 site of the *ompC* promoter region, failing to bind C2 and C3. This finding supported the proposed importance of T83 in propagating conformational changes to the carboxyl terminal DNA binding domain (Ganguli, S. *et al.*, 1995; Zhu, X. *et al.*, 1997a). It also allowed us to propose an alternative to the affinity model whereby OmpR-P undergoes a conformational change at high osmolarity (blocked in T83I) which allows binding of the C2 and C3 sites and subsequent activation of *ompC*. This was the first time that a mutant of OmpR was seen to bind the high affinity C1 site, but not interact with the other sites at *ompC*. This finding demonstrated that the ability of a mutant protein to bind at C1 does not indicate that it interacts at the entire *ompC* promoter, which has important implications in the study of so-called activation mutants which are expected to be defective in interactions with RNA Polymerase (Pratt, L. A. and T. J. Silhavy, 1994).

In the third chapter, I examined OmpR proteins mutated in the linker region that joins the amino and carboxyl terminal domains (Mattison, K. *et al.*, 2002b). This study addressed the role of the linker region in the communication between the amino and carboxyl terminal domains of OmpR. Two point mutants and a number of random linker sequences were characterized. I found that none of the random linker mutants generated could mediate wild-type osmoregulation of *ompF* and



*ompC* expression. This led to the conclusion that the linker sequence plays a role in fine tuning the activation and repression of the porin genes. Only one of the random linker mutants was completely defective in activating both *ompF* and *ompC*; the hydrophobic nature of its linker led us to propose that hydrophobicity in the linker was inhibitory for OmpR function. Interestingly, we found that two of the linker substitutions mediated activation of *ompC* but could not repress *ompF* at high osmolarity. Conversely, one other mutant failed to activate *ompC* while retaining the ability to activate and repress *ompF* normally. This allowed us to refine the model proposed in the second chapter, to include a difference in the form of OmpR that represses *ompF* from the form that activates *ompC*; both of these conformations must co-exist in the cell at high osmolarity. Furthermore, we have shown that the two point mutants and one of the linker substitutions, which share an OmpF<sup>+</sup> OmpC<sup>-</sup> phenotype, have different molecular defects. This reinforces the validity of studying these mutants at a biochemical level in order to understand the various ways an OmpF<sup>+</sup> OmpC<sup>-</sup> phenotype may be achieved.

In the fourth chapter, I used cysteine substitutions and cross-linking studies to propose a model for OmpR dimerization on DNA. In this study, we found that dimerization of OmpR was dependent on DNA, and that the current model of OmpR dimerization was not supported by cross-linking experiments. We went on to define the  $\beta$ -sheet of the

carboxyl terminal domain as important in OmpR dimerization, and propose a new model for the mode of OmpR binding to DNA. As a refinement of the old model, this new model provides predictions that can be tested to further understanding of OmpR/DNA interactions.

The second part of this thesis (Chapters 5 and 6) is focused on the interaction between the EnvZ kinase and the OmpR regulator, with an emphasis on understanding the reported phosphatase activity of EnvZ and its *in vivo* relevance.

In the fifth chapter, I determined that OmpR binds EnvZ with much higher affinity than OmpR-P (Mattison, K. and L. J. Kenney, 2002). This led to the conclusion that at physiological concentrations OmpR-P and EnvZ would be unlikely to interact, limiting the possibility that EnvZ actively dephosphorylates OmpR-P *in vivo*. Furthermore, we found that OmpR/DNA interaction does not inhibit OmpR/EnvZ binding, that is, a ternary EnvZ/OmpR(-P)/DNA complex may be formed *in vitro*. This contradicted a previous model whereby specific DNA prevented the interaction between OmpR-P and EnvZ to stabilize the phospho-protein. We proposed that a conformational change in OmpR-P upon interaction with DNA was responsible for decreasing its rate of dephosphorylation. This was supported by a mutant form of OmpR which was bound to DNA with high affinity and was dephosphorylated more efficiently in the presence of DNA. This study suggested that neither the phosphatase

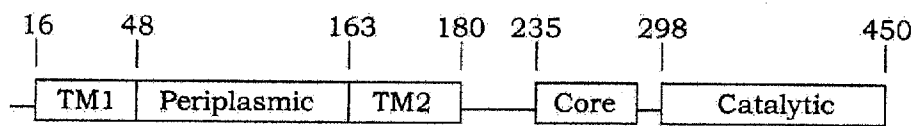
activity of EnvZ nor DNA binding by OmpR-P is likely to control intracellular OmpR-P levels.

In the sixth chapter, I tested the prediction that at low concentrations of OmpR and EnvZ the phosphatase activity of EnvZ is non-existent. I showed that as [EnvZ] is decreased relative to [OmpR] it retains the ability to phosphorylate the regulator without any detectable dephosphorylation of OmpR-P. Furthermore, I examined a mutant of EnvZ, T247R, which had been shown to be defective in its phosphatase activity. This mutant protein results in no expression of the OmpF porin and constitutive expression of the OmpC porin *in vivo*. Since we have suggested that the phosphatase activity of EnvZ is not important for porin gene regulation, the question arose, what property of T247R could account for the observed phenotype? I found that this mutant bound OmpR with much higher affinity than wild-type EnvZ in the presence of  $Mg^{2+}$ . T247R autophosphorylates in a  $Mg^{2+}$ -independent manner, and auto-dephosphorylation of response regulators depends on  $Mg^{2+}$  (Goudreau, P. N. *et al.*, 1998; Lukat, G. S. *et al.*, 1990). This led us to conclude that T247R may produce an altered form of OmpR-P which lacks  $Mg^{2+}$  in its active site and as a result dephosphorylates intrinsically more slowly. This protein would be more stable in its phosphorylated form without invoking any phosphatase activity for EnvZ, and may correspond to the high osmolarity form we predicted in our earlier models of OmpR-P function (Chapters 2 and 3).

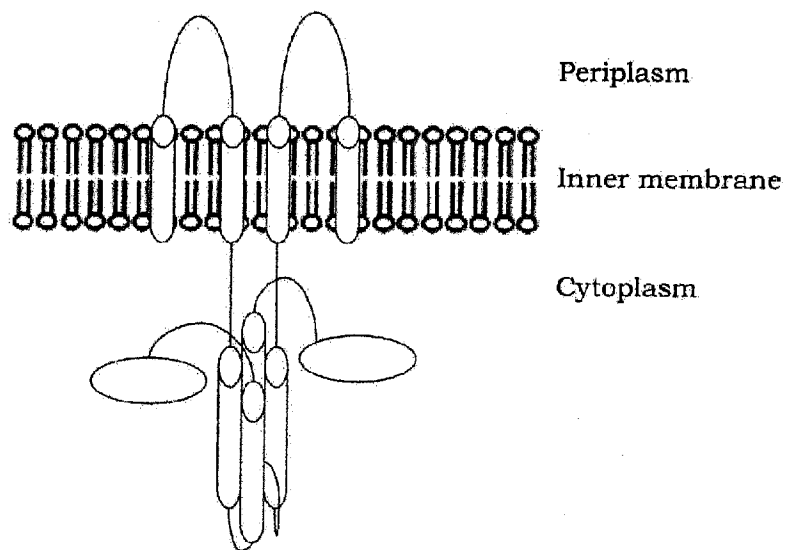
Taken together, the chapters of this thesis further our understanding of the manner in which EnvZ and OmpR interact, and of the way this interaction leads to differential activation of *ompF* and *ompC* expression in changing environmental osmolarity.

Figure 1.1. The EnvZ sensor kinase. A. The location of the domains of EnvZ in the primary amino acid sequence. Numbers indicate the amino acid residue that borders each region. B. Schematic representation of the EnvZ dimer in the inner membrane. C. The solution structure of the homodimeric core domain of EnvZ. The histidine at position 243, which is the site of phosphorylation, is shown. D. The solution structure of the catalytic domain of EnvZ. The non-hydrolysable ATP analog  $\beta$ ,  $\gamma$ -imidoadenosine-5'-triphosphate (AMP-PNP) is shown bound at the active site. Coordinates for C. and D. were from Protein Data Bank accession numbers 1JOY and 1BXD (Tanaka, T. *et al.*, 1998; Tomomori, C. *et al.*, 1999).

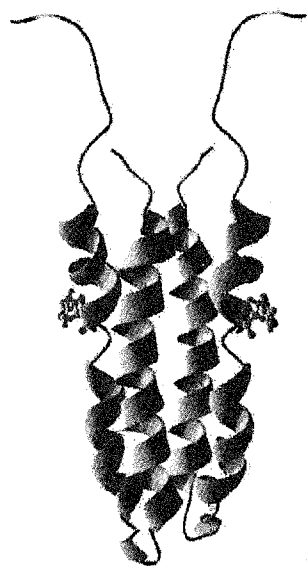
A



B



C



D

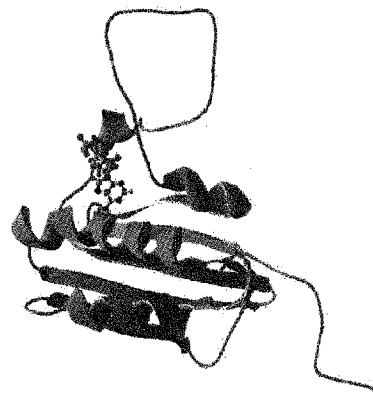
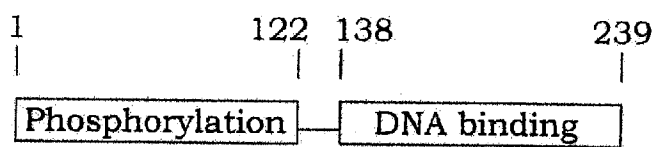
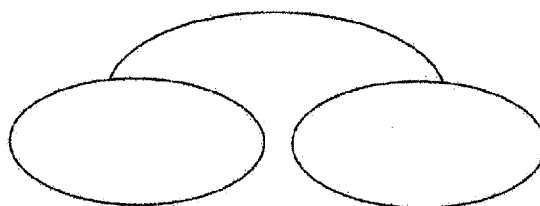


Figure 1.2. The OmpR response regulator. A. The location of the domains of OmpR in the primary amino acid sequence. Numbers indicate the amino acid residue that borders each region. B. Schematic representation of the two domains of OmpR, joined by a flexible linker region. C. The x-ray crystal structure of CheY, a response regulator homologous to the amino terminus of OmpR. The aspartate residue that is phosphorylated is indicated. D. The x-ray crystal structure of the carboxyl terminal domain of OmpR. The recognition helix is colored in red. Coordinates for C. and D. were from PDB accession numbers 1CHN and 1OPC (Martinez-Hackert, E. and A. M. Stock, 1997a; Stock, A. M. *et al.*, 1989).

A



B



C



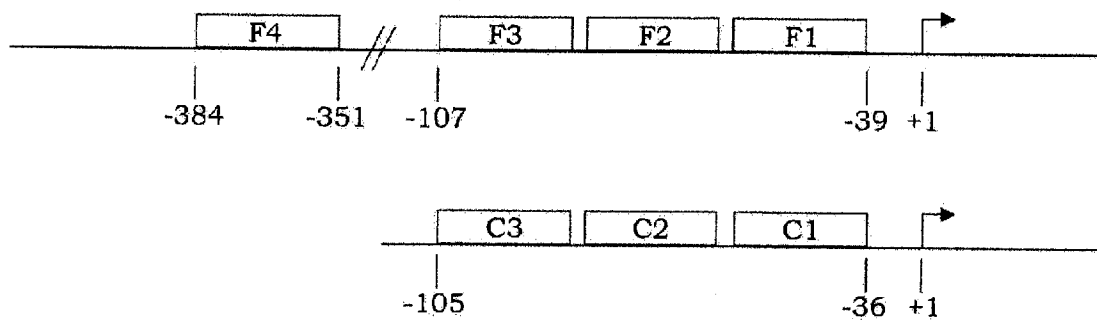
D





Figure 1.3. The *ompF* and *ompC* promoter regions. A. The OmpR binding sites in both promoter regions are diagrammed. The numbers indicate positions relative to the transcriptional start site. B. The individual OmpR binding sites are aligned to show the conserved GXXXC motif (conserved G and C residues are in bold face and underlined) and the AC bases identified as important for OmpR binding *in vivo* (arrows show the location of these sites). Data incorporated from (Harlocker, S. L. *et al.*, 1995; Huang, K. J. and M. M. Igo, 1996; Maeda, S. and T. Mizuno, 1990; Pratt, L. A. and T. J. Silhavy, 1995).

A



B

	↓ ↓	↓ ↓
F1	ACTTTTGGTTACATATTT	
F2	TCTTTTGGAAACCAAATC	
F3	TATCTTTGTAGCACTTTC	
C1	ACATTTTGGAAACATCTAT	
C2	GATAAATGAAACATCTTA	
C3	AGTTTGTAGTATCATATTC	

Table 1.1. Phases of the response to osmotic shock in *Escherichia coli*.

The responses discussed in the text to osmotic upshift and downshift are summarized. In both cases, phase I occurs immediately upon osmotic shock. During osmotic upshift, phase II may take up to 60 minutes, depending on the growth conditions, and the phase III response may not be complete until hours after the increase in osmolarity. During osmotic downshift, phase II is typically completed at times approaching the detection limit of assays used, in less than 2 minutes. Phase III of the response to a decrease in osmolarity is similarly thought to proceed more rapidly than that to osmotic upshift, but again, transcriptional responses are highly dependent on growth conditions. Adapted from (Wood, J., 1999).

Response to osmotic upshift		
Phase	Physiological change	Structural change
I	Respiration ceases Most active transport ceases K <sup>+</sup> and proline uptake begins	Cell dehydrates, shrinks Wall/membrane strain altered
II	Putrescine extruded K <sup>+</sup> glutamate accumulates Proline accumulates Respiration resumes	Rehydration begins
III	High affinity transporters expressed Glycine betaine and/or other compatible solutes accumulate Transcription of <i>ompF</i> repressed Transcription of <i>ompC</i> activated	DNA/protein synthesis resume Cell growth/division resume
Response to osmotic downshift		
Phase	Physiological change	Structural change
I	Mechanosensitive channels open	Cell hydrates, swells Wall/membrane strain altered
II	Co-solvents and water extruded	Cell shrinks
III	Mechanosensitive channels close Co-solvents re-accumulate Transcription of <i>ompF</i> activated Transcription of <i>ompC</i> decreases	DNA/protein synthesis resume Cell growth/division resume

## **Chapter 2**

### **A Phosphorylation Site Mutant of OmpR Reveals Different Binding Conformations at *ompF* and *ompC***

**(Journal of Molecular Biology 315: 497-511, 2002)**

#### **2.0 Preface**

In the following chapter, I carried out the experiments in Table 2.1, Figures 2.2, 2.3, 2.4, 2.5, 2.6, 2.7, 2.9, and 2.10, as well as the data analysis and modeling for Figures 2.11 and 2.12. Nicole Byers performed experiments contributing to the reported averages in Figures 2.2, 2.7 and Table 2.1, as well as experiments similar to those shown in Figure 2.3. Ricardo Oropeza conducted the DNase I footprinting experiments shown in Figure 2.8. The model shown in Figure 2.1 was taken from (Robinson, V. L. *et al.*, 2000).

## 2.1 Abstract

In *Escherichia coli*, the two component regulatory system that controls the expression of outer membrane porins in response to environmental osmolarity consists of the sensor kinase EnvZ and the response regulator OmpR. Phosphorylated OmpR activates expression of the OmpF porin at low osmolarity, and at high osmolarity represses *ompF* transcription and activates expression of OmpC. We have characterized a substitution in the amino-terminal phosphorylation domain of OmpR, T83I, its phenotype is OmpF<sup>-</sup> OmpC<sup>-</sup>. The mutant protein is not phosphorylated by small molecule phosphodonors such as acetyl phosphate and phosphoramidate, but it is phosphorylated by the cognate kinase EnvZ. Interestingly, the active site T83I substitution alters the DNA binding properties of the carboxyl-terminal effector domain. DNase I protection assays indicate that DNA binding by the mutant protein is similar to wild-type OmpR at the *ompF* promoter, but at *ompC*, the pattern of protection is different from OmpR. Our results indicate that all three of the OmpR binding sites at the *ompC* promoter must be filled in order to activate gene expression. Furthermore, it appears that OmpR-phosphate must adopt different conformations when bound at *ompF* and *ompC*. A model is presented to account for the reciprocal regulation of OmpF and OmpC porin expression.

## 2.2 Introduction

Homeostatic mechanisms require physiological changes at the cellular level in response to environmental conditions. Effector proteins involved in transmitting information from the environment to the cells are involved in signaling cascades and often catalyze phosphorylation and dephosphorylation reactions. In prokaryotes and lower eukaryotes, signal transduction is often accomplished via two component regulatory systems. The first component, usually a membrane protein, is a sensor kinase that responds to environmental cues and is phosphorylated by ATP on a histidine residue. The second component is a response regulator that accepts the phosphoryl group from the histidine onto an aspartic acid residue and then alters its output. The altered output may be an enhancement of DNA binding, but can also be a change in protein:protein interactions (for reviews see (Hoch, J. A. and T. J. Silhavy, 1995)).

In *Escherichia coli*, osmoregulation is mediated in part by the actions of such a two component system consisting of EnvZ and OmpR. These proteins act to control the relative levels of the outer membrane porin genes, *ompF* and *ompC*. At low osmolarity, OmpF predominates in the outer membrane, while at high osmolarity the OmpF porin is replaced by OmpC (van Alphen, W. and B. Lugtenberg, 1977). OmpF has a larger pore and a faster flow rate than OmpC (Nikaido, H. and E. Y. Rosenberg, 1983).

EnvZ is an inner membrane protein that is phosphorylated by intracellular ATP at histidine 243 in response to a signal related to the environmental osmolarity (Forst, S. *et al.*, 1987; Liljestrom, P., 1986b; Roberts, D. L. *et al.*, 1994). It transfers this phosphoryl group to aspartic acid 55 of OmpR (Delgado, J. *et al.*, 1993). It has been suggested that EnvZ also catalyzes the dephosphorylation of phospho-OmpR (OmpR-P) (Igo, M. M. *et al.*, 1989a), further controlling the cellular levels of OmpR-P. According to the affinity model of porin regulation, differential regulation of the porin genes is controlled by occupancy of OmpR-P binding sites of varying affinities (Russo, F. D. and T. J. Silhavy, 1991). However, there is only a two-fold difference in the binding affinity of OmpR-P for the *ompF* and *ompC* sites (F1-F2-F3 and C1-C2-C3), and the question of how OmpR binding site occupancy determines which porin is expressed remains (Head, C. G. *et al.*, 1998).

The response regulator OmpR (27 kDa) consists of an N-terminal phosphorylation domain and a C-terminal DNA binding domain (Kato, M. *et al.*, 1989; Tate, S. *et al.*, 1988), joined by a protease-sensitive, flexible linker of 15 amino acid residues (Kenney, L. J. *et al.*, 1995). The C-terminal domain of OmpR contains a winged helix-turn-helix DNA binding motif (Kondo, H. *et al.*, 1997; Martinez-Hackert, E. and A. M. Stock, 1997a). The phosphorylation site, aspartic acid 55, is located in the amino terminus, referred to as the receiver domain. The x-ray crystal structures of several receiver domains from homologous response



regulators have been solved, and they all reveal an  $(\alpha/\beta)_5$  topology (Baikalov, I. *et al.*, 1996; Madhusudan *et al.*, 1996; Stock, A. M. *et al.*, 1989; Volz, K. and P. Matsumura, 1991). The five parallel  $\beta$ -strands form a hydrophobic core, surrounded by two  $\alpha$  helices on one side and three on the other. The receiver domains also share a group of conserved residues at the active site that are important for phosphorylation and signal propagation. These are (see Figure 2.1): an aspartate residue that is the site of phosphorylation (D55 in OmpR), two aspartate residues that coordinate a magnesium ion (D11 and D12), a lysine residue that interacts with the phosphoryl group (K105), an aromatic residue that functions as a rotamer (Y102), and a side chain hydroxyl residue (T83) that also interacts with the phosphoryl group. Structural analysis of activated response regulators has revealed the role of these conserved residues upon activation (Birck, C. *et al.*, 1999; Cho, H. S. *et al.*, 2000; Halkides, C. J. *et al.*, 2000; Lewis, R. J. *et al.*, 1999). In the presence of the kinase or a small molecule phosphodonor such as acetyl phosphate, the acidic phosphate is coordinated to a magnesium ion in the pocket and both species are stabilized by interactions with conserved amino acid side chains and water molecules. For example, the side chain of threonine moves to form a charge-dipole interaction with the newly arrived phosphoryl moiety, a movement that is tracked by the closely packed tyrosine side chain. This “aromatic switch”, where the tyrosine moves from an exposed to a buried position, may be a general

mechanism for intramolecular signaling in the response regulator family of proteins. What remains unknown at present is how this conformational change is propagated to the C-terminal effector or DNA binding domain.

We are interested in the molecular mechanism responsible for transmission of the conformational change associated with phosphorylation of OmpR at aspartic acid 55 in the N terminus that results in enhanced affinity of the C-terminal DNA binding domain for DNA (Head, C. G. *et al.*, 1998). In the single domain chemotaxis response regulator CheY, a substitution has previously been identified that converts the conserved active site threonine at position 87 to isoleucine. The mutant is phosphorylated *in vitro*, but non-chemotactic *in vivo*, indicating a block in activation subsequent to phosphorylation (Ganguli, S. *et al.*, 1995). We made the equivalent mutation in OmpR in order to characterize its properties *in vivo* and *in vitro*. Single substitutions at this site have not been previously isolated. Our results indicate that T83I interacts differently at the *ompF* regulatory region compared to *ompC*, a result which had been suggested from our earlier studies (Tran, V. K. *et al.*, 2000). Understanding the defect of the T83I mutant in molecular terms is likely to provide a key to understanding the switch between the low osmotic form and the high osmotic form. Furthermore, our data suggest that occupancy of all three OmpR binding sites is required for *ompC* expression.

## 2.3 Results

### 2.3.1 T83I cannot activate transcription in vivo

We first determined the phenotype that resulted from the threonine to isoleucine substitution at amino acid residue 83 of OmpR. For this experiment, we expressed the T83I mutant in an *ompR101* strain that contains a small, in-frame deletion in *ompR* and either an *ompF-lacZ* or *ompC-lacZ* operon fusion (MH225.101 and MH513.101 (Hall, M. N. and T. J. Silhavy, 1981b)). The results are shown in Figure 2.2. In the absence of *ompR* (filled columns, 1 and 4),  $\beta$ -galactosidase activity is minimal in both fusion strains. When wild-type *ompR* is over-expressed in cultures grown in Luria Broth, both the *ompF-lacZ* and the *ompC-lacZ* fusions are stimulated (striped columns, 2 and 5). In the presence of *ompRT83I*,  $\beta$ -galactosidase activity is at background levels (open columns, 3 and 6). T83I also failed to activate either fusion when the strains were grown in minimal media at low and high osmolarity (data not shown). These results suggest that the T83I mutant is unable to activate transcription. Its porin phenotype is OmpF<sup>-</sup> OmpC<sup>-</sup>, regardless of the medium osmolarity.

### 2.3.2 T83I is not phosphorylated by acetyl phosphate or by phosphoramidate

We expressed and purified the mutant protein in order to examine its phosphorylation properties. Wild-type OmpR elutes as a single peak on C4 reversed phase HPLC, as shown in Figure 2.3A and E (Kenney, L.

J. *et al.*, 1995). The mutant T83I also elutes as a single peak (Figure 2.3C and G). When OmpR is incubated with acetyl phosphate, a faster peak appears, shown in Figure 2.3B, that corresponds to OmpR-P (Head, C. G. *et al.*, 1998). When the T83I mutant is incubated with acetyl phosphate and the products analyzed on C4 reversed phase HPLC, no new peak appears, and only the unphosphorylated protein peak is present (Figure 2.3D). This result suggests that T83I is not stably phosphorylated by acetyl phosphate.

Since phosphorylation by acetyl phosphate is relatively slow, we were interested in determining whether another small molecule phosphodonor, phosphoramidate, could phosphorylate T83I (Mayover, T. L. *et al.*, 1999). After a 2 hour incubation with phosphoramidate, 100% of the OmpR protein is phosphorylated (Figure 2.3F), indicating that phosphoramidate is more efficient than acetyl phosphate as a phosphodonor (compare Figures 2.3B and F). After a 2 hour incubation with phosphoramidate, T83I elutes as a single peak, at the same location as the unphosphorylated protein, indicating that the mutant protein is also not phosphorylated by this compound (compare Figure 2.3G and H). Increasing incubation times with phosphoramidate failed to produce T83I-P (data not shown).

Our laboratory has previously shown that DNA-binding stimulates the rate of OmpR phosphorylation by acetyl phosphate (Ames, S. K. *et al.*, 1999). Thus, we tested whether incubation of T83I with acetyl

phosphate and the high affinity OmpR-binding sites from the *ompF* or *ompC* promoters (F1 or C1) would stimulate phosphorylation of T83I. In the presence of DNA, we were also unable to detect a phosphorylated product (data not shown).

### **2.3.3 T83I is phosphorylated by the kinase EnvZ**

We next tested whether or not the T83I mutant was defective in phosphorylation from its cognate kinase, EnvZ. When EnvZ is incubated with [ $\gamma$ - $^{32}$ P]ATP and the product is separated by SDS-PAGE, a labeled band is visible that corresponds to EnvZ-P (Figure 2.4, lane 1). In the presence of wild-type OmpR, EnvZ-P transfers the phosphoryl group to OmpR, as evidenced by a labeled OmpR-P band (lanes 2-3). When T83I is added to the reaction in place of OmpR, it is also phosphorylated (lanes 4-5), even though it cannot be phosphorylated by small molecule phosphate donors (Figures 2.3D and 2.3H). We confirmed that T83I-P runs as a faster, resolvable peak on C4 reversed phase HPLC after incubation of T83I with EnvZ and ATP, eliminating the possibility that we could not detect phospho-protein which might have been produced by incubation with acetyl phosphate or phosphoramidate (data not shown). The level of phosphorylation of T83I is considerably lower than the level of wild-type OmpR-P (compare the lower bands in lanes 4-5 with lanes 2-3), suggesting that there is either a defect in phospho-transfer to the mutant protein or enhanced dephosphorylation of the phospho-protein T83I-P (See Discussion).

Some response regulators can be phosphorylated at non-active site residues, but these have specific structural requirements (Appleby, J. L. and R. B. Bourret, 1999; Bourret, R. B. *et al.*, 1990; Moore, J. B. *et al.*, 1993; Reyrat, J. M. *et al.*, 1994). These are: the presence of a serine residue adjacent to the phosphorylated aspartate and substitution of the phosphorylated aspartate by asparagine. This serine is not present in OmpR. In order to establish the requirement of aspartate 55 for EnvZ mediated phosphorylation of T83I, we purified the double mutant T83I/D55A and added it to the kinase reaction. Phosphorylation of T83I absolutely requires the presence of aspartate 55, as the T83I/D55A double mutant is not phosphorylated by the kinase (Figure 2.4, lanes 6-7). It is not surprising that phosphorylation does not occur with the double mutant, as there is no evidence for phosphorylation at sites other than D55 in OmpR (Tran, V. K. *et al.*, 2000).

#### **2.3.4 T83I is phosphorylated slowly compared to wild-type OmpR**

The T83I mutant exhibited lower levels of phosphorylation by EnvZ than wild-type OmpR in the kinase assay shown in Figure 2.4. This could be due to a slower rate of phosphorylation of the mutant protein or to a faster rate of dephosphorylation of the mutant phospho-protein. It was therefore of interest to compare the activity of the two proteins in an EnvZ-dependent OmpR-stimulated ATPase assay (shown in Figure 2.5). When EnvZ, ATP and OmpR are mixed together, the following reactions occur:  $\text{EnvZ} + \text{ATP} \rightarrow \text{EnvZ-P} + \text{ADP}$  (autophosphorylation);  $\text{EnvZ-P} +$

$\text{OmpR} \rightarrow \text{OmpR-P} + \text{EnvZ}$  (phosphotransfer);  $\text{EnvZ} + \text{OmpR-P} \rightarrow \text{EnvZ} + \text{OmpR} + \text{P}_i$  (phosphatase);  $\text{OmpR-P} \rightarrow \text{OmpR} + \text{P}_i$  (intrinsic dephosphorylation). The sum of these reactions is an overall ATPase activity. In the absence of OmpR, there is a low basal level of ATPase activity associated with EnvZ phosphorylation and spontaneous dephosphorylation (Kenney, L. J., 1997; Tran, V. K. *et al.*, 2000). This rate (7.1 nmol/ml/minute) was subtracted from the OmpR or T83I-stimulated rate and only the stimulated rates are shown. Upon addition of OmpR, there is a large increase in  $\text{P}_i$  production, which increases with increasing incubation time (Figure 2.5, triangles). In contrast, the ATP hydrolysis in the presence of T83I is only slightly greater than the activity associated with EnvZ alone, and  $\text{P}_i$  production remains low (Figure 2.5, circles). In the presence of T83I, the rate of  $\text{P}_i$  release is 0.5 nmol/ml/minute, compared to 4.6 nmol/ml/min for OmpR. This represents a nine-fold decrease in turnover compared to the wild-type protein. Together with the data presented in Figure 2.4, the lack of ATPase activity observed in the presence of T83I indicates that the mutant protein is phosphorylated more slowly than the wild-type.

### **2.3.5 T83I binds EnvZ as well as wild-type OmpR**

It was possible that the slow rate of phosphorylation of T83I by EnvZ was a result of the substitution disrupting the interaction between EnvZ and OmpR. In order to investigate this binding, we measured fluorescence anisotropy of an OmpR protein labeled with fluorescein at

the amino terminus. Increasing amounts of a carboxyl terminal fragment of EnvZ (EnvZc) are added, obtaining the binding curves shown in Figure 2.6. The average  $K_d$  from five similar binding curves is  $462 \pm 135$  nM. T83I also binds to EnvZ, as demonstrated by the binding curve shown in the circles in Figure 2.6. The average  $K_d$  from three such experiments is  $257 \pm 83$  nM. Thus, the mutant T83I binds to EnvZc with slightly higher affinity than wild-type OmpR, and the decrease in phosphorylation observed with T83I is not due to an inability to interact with EnvZ. The experiment shown in Figure 2.6 represents the first direct measurements of OmpR and EnvZ interaction.

### **2.3.6 T83I binds to the high affinity sites F1 and C1**

Since our previous studies have demonstrated interactions between the amino and carboxyl terminal domains of OmpR, it was of interest to determine whether the substitution that altered its phosphorylation properties would also affect its DNA binding ability (Ames, S. K. *et al.*, 1999; Tran, V. K. *et al.*, 2000). For measurements of DNA binding, we used fluorescein-labeled oligonucleotides that correspond to the high affinity sites F1 and C1 upstream from the *ompF* and *ompC* promoters, respectively (See Figure 2.11 for a diagram of the binding sites). The results are presented in Figure 2.7A and B. In Figure 2.7A, it is clear that the saturable binding curves observed upon incubation of OmpR or T83I with fluorescein-labeled F1 DNA are similar. The apparent dissociation constant ( $K_d$ ) in the experiment shown is 150



nM for wild-type OmpR (triangles) and 180 nM for T83I (circles). The average values from repeated determinations are  $194 \pm 60$  nM for OmpR and  $175 \pm 45$  nM for T83I. In other words, the binding affinities of OmpR and T83I at the F1 site are identical, within the error of the assay. In Figure 2.7B, it can be seen that when binding to C1, T83I (circles) reaches saturation at a slightly lower concentration than the wild-type protein (triangles). The apparent dissociation constants calculated for the binding curves shown in Figure 2.7B are 59 nM for OmpR and 33 nM for T83I, less than a two-fold increase in the affinity of the mutant protein. In further determinations, this nearly two-fold difference is maintained, as the average apparent  $K_d$  for OmpR at C1 is  $101 \pm 59$  nM and for T83I it is  $59 \pm 19$  nM. Thus, at the high affinity sites F1 and C1, DNA binding by the mutant T83I is similar to wild-type OmpR.

### **2.3.7 T83I does not saturably bind the composite site C123**

T83I was able to bind to the isolated high affinity sites F1 and C1 (Figure 2.7). We next measured binding of the mutant protein to a composite site containing the two lower affinity *ompF* binding sites (F2 and F3), in addition to the high affinity site, F1 (F1-F2-F3). T83I binds to the composite site (Table 2.1).

We then examined the binding of T83I to the composite *ompC* binding site, C1-C2-C3. Surprisingly, we were unable to measure saturable binding to this site. The binding curve is easily fit by linear regression, indicating that only very low affinity ( $K_d > 3 \mu\text{M}$ ) binding

occurs (Table 2.1). In our previous studies with wild-type OmpR, we observed saturable binding to any oligonucleotide that contained either the F1 or C1 sites (Head, C. G. *et al.*, 1998). Thus, the T83I mutant, containing a single amino acid substitution, behaves differently from OmpR at the *ompF* regulatory region, where it exhibits high affinity binding, compared with the *ompC* regulatory region, where it does not exhibit saturable binding.

### **2.3.8 T83I and wild-type OmpR protect the same regions of the *ompF* promoter**

Because the inability of T83I to bind at C1-C2-C3 was so unexpected, we sought an alternative approach in order to examine DNA-T83I protein interactions. For these experiments, we used a DNase I protection assay, as shown in Figure 2.8. In Figure 2.8A and B, the result from the *ompF* regulatory region is shown. Figure 2.8A indicates pattern of DNase I protection by wild-type OmpR at the *ompF* promoter. Lane 1 shows the DNase I cleavage pattern obtained in the absence of OmpR, and lanes 2-7 indicate that as previously reported, OmpR protects three regions of *ompF* from -102 to -40 upstream of the transcriptional start site (Figure 2.8A)(Huang, K. J. and M. M. Igo, 1996; Rampersaud, A. *et al.*, 1994). In Figure 2.8B, the pattern of DNase I protection in the presence of T83I is shown. Lanes 2-7 show that T83I can also bind the *ompF* promoter from -102 to -40. It can be clearly seen

that the pattern of protection with T83I is similar to that observed with wild-type OmpR (compare Figure 2.8A and B).

### **2.3.9 The pattern of protection by T83I is different from wild-type OmpR at the *ompC* promoter**

In contrast, the T83I footprint at *ompC* is different from that seen with wild-type OmpR. Figure 2.8C and D presents the footprinting results obtained at the *ompC* regulatory region. Lanes 2 through 8 of Figure 2.8C demonstrate that wild-type OmpR binds to the three previously characterized binding regions at *ompC*, from -105 to -36 upstream of the transcriptional start site.

In Figure 2.8D, it is apparent that T83I binds the *ompC* promoter differently than does wild-type OmpR. We observe protection of most of the C1 region from DNase I cleavage, from -103 to -77 (lanes 2-8). The lower affinity C2 and C3 binding sites are not bound by T83I. Twelve DNase I hypersensitive sites are unique to T83I binding at *ompC*, these occur at positions -75, -73, -62, -60, -45, -43, -42, -40, -38, -37, -36, and -33 relative to the transcriptional start site (see arrows). Thus, in contrast to OmpR, T83I is incapable of binding outside of the C1 region at the *ompC* promoter.

### **2.3.10 The OmpF<sup>-</sup> OmpC<sup>-</sup> phenotype of T83I is co-dominant**

It is unclear why T83I fails to activate transcription of *ompF*. The mutant protein can bind to the *ompF* promoter sequences (Figure 2.8), and does not repress transcription from this promoter (Figure 2.10). If

T83I can bind to *ompF* promoter sequences *in vivo*, the T83I phenotype should be dominant to wild-type OmpR. If T83I simply fails to bind DNA, the phenotype should be recessive. We expressed *ompRT83I* in the strains MH513 and MH225, which contain a wild-type copy of *ompR* and *ompF-lacZ* or *ompC-lacZ* transcriptional fusions, respectively. The  $\beta$ -galactosidase activity expressed by these two strains is shown in lanes 1 and 5 of Figure 2.9. Addition of a plasmid-borne copy of the wild-type *ompR* gene does not negatively affect production of  $\beta$ -galactosidase (Figure 2.9, lanes 2 and 6). We found that transcription of *ompF* decreases 2.5-fold in the presence of T83I (Figure 2.9 lane 3) and transcription of *ompC* decreases 3-fold ((Figure 2.9, lane 7). T83I does not need to be phosphorylated to compete with wild-type OmpR. When OmpR and T83I/D55A are co-expressed, the  $\beta$ -galactosidase activity expressed from the *ompF* and *ompC* promoters remains less than that observed in the parent strains (Figure 2.9, lanes 4 and 8). Thus even the unphosphorylated double mutant T83I/D55A decreases transcription from *ompF* and *ompC* 2.5 and 1.8-fold, respectively. We postulate that the dominance of T83I is due to its ability to bind DNA even in the absence of phosphorylation (Figures 2.7 and 2.8).

#### **2.3.11 T83I fails to activate *ompF* transcription**

Because T83I failed to induce expression of *ompF* (Figure 2.2), it was of interest to determine whether this failure was the result of repression or due to a lack of activation. The *ompF* locus contains an

additional OmpR binding site from -384 to -351 upstream of the transcriptional start site, F4. This binding site is required for OmpR-mediated repression of *ompF* (Huang, K. J. *et al.*, 1994; Ostrow, K. S. *et al.*, 1986). We wished to determine whether the OmpF<sup>-</sup> phenotype of the mutant was the result of repression of *ompF* transcription. Strains BW25891 (F4 minus) and BW25892 (F4 plus) were grown in the presence of *ompR* or *ompRT83I* under conditions of high osmolarity, i.e. conditions that normally repress *ompF*. When the strains were assayed in the absence of *ompR*, they expressed some  $\beta$ -galactosidase activity; this value was subtracted from the data shown. In the presence of *ompR*, high levels of  $\beta$ -galactosidase are expressed from the strain lacking the F4 binding site (Figure 2.10, hatched column 3). Repression of the *lacZ* fusion containing F4 is also evident under high osmolarity conditions (see the decrease in activity of hatched column 1 compared to hatched column 3). When the F4 site is absent, T83I is still unable to activate transcription from *ompF* (Figure 2.10, open column 4). As expected from the result shown in Figure 2.2, T83I failed to activate transcription above background levels from the *lacZ* fusion containing F4 (see Figure 2.10, open column 2). Thus, T83I fails to repress transcription from this promoter and the T83I mutant is OmpF<sup>-</sup> because it cannot activate transcription, not because *ompF* transcription is repressed.

## 2.4 Discussion

### 2.4.1 The T83I mutant phenotype is OmpF<sup>-</sup> OmpC<sup>-</sup>

The replacement of the conserved threonine with an isoleucine at position 83 of OmpR results in a protein that is unable to activate expression of *ompF-lacZ* or *ompC-lacZ* fusions (Figure 2.2). This finding parallels previous data obtained for the homologous response regulators CheY and FixJ. A CheY T87I mutant is non-chemotactic and exhibits only counterclockwise flagellar rotation (Appleby, J. L. and R. B. Bourret, 1998; Ganguli, S. *et al.*, 1995). The homologous FixJ T82I mutant is seriously inhibited in its ability to activate transcription of a *p-nifA-lacZ* or a *p-fixK-lacZ* fusion (Weinstein, M. *et al.*, 1992). An isoleucine substitution at this conserved position in other response regulators is thus disruptive to signaling, just as we have shown for OmpR. A T82A substitution in SpoOF essentially abrogates sporulation in *Bacillus subtilis*, indicating that for some response regulators, removal of the hydroxyl group can interfere with function (Tzeng, Y. L. and J. A. Hoch, 1997). Not all amino acid substitutions at this position result in such extreme phenotypic consequences. A T83A substitution in OmpR was isolated because of its ability to restore a wild-type phenotype in a D55Q background. Interestingly, in the wild-type background, a T83A mutation in *ompR* results in an OmpF<sup>-</sup> OmpC<sup>+</sup> phenotype (Brissette, R. E. *et al.*, 1991b). This implies that T83 is a critical residue for OmpR function, even if some substitutions are less deleterious than the

isoleucine described here. T87A and T87C substitutions in CheY retain some ability to mediate clockwise flagellar rotation, and in the presence of a D13K substitution, these two substitutions nearly restore clockwise rotation (Appleby, J. L. and R. B. Bourret, 1998).

The crystal structures of several phosphorylated response regulators have been solved, and they suggest a role for the conserved hydroxyl and aromatic residues in signal propagation (Birck, C. *et al.*, 1999; Cho, H. S. *et al.*, 2000; Halkides, C. J. *et al.*, 2000; Lewis, R. J. *et al.*, 1999), for a review see Robinson *et al.* (Robinson, V. L. *et al.*, 2000). Upon phosphorylation, the conserved threonine (T83 in OmpR) moves towards the phosphorylated aspartate (D55), allowing the tyrosine (Y102) to rotate inwards and fill the space where T83 used to reside (see Figure 2.1). The structure of the CheYT87I mutant has been determined, and reveals that the isoleucine substitution locks the tyrosine rotamer in the solvent exposed 'out' position (Ganguli, S. *et al.*, 1995). Substitutions of the conserved tyrosine of CheY result in a range of phenotypes, from hyperactive signaling to inactivity (Zhu, X. *et al.*, 1996). Mutants of Y102 in OmpR also produce aberrant phenotypes. For example, a substitution of Y102 for cysteine results in constitutive activation of OmpR (Kanamaru, K. and T. Mizuno, 1992), suggesting that restriction of the movement of the conserved tyrosine residue contributes to the mutant phenotype of both CheYT87I and OmpRT83I.

#### **2.4.2 Phosphorylation properties are altered in T83I**

In contrast to wild-type OmpR, T83I is not phosphorylated by the small phosphate donors acetyl phosphate and phosphoramidate (Figure 2.3). However, the mutant retains the ability to be phosphorylated by the cognate sensor kinase, EnvZ (Figure 2.4). Kinase mediated phosphorylation requires aspartate 55 of the active site, when D55 is mutated to alanine, no phospho-protein is detected (Figure 2.4).

The ability of mutant response regulators to discriminate between phosphodonors has previously been observed in another OmpR mutant, V203M (Tran, V. K. *et al.*, 2000). In addition, a CheY T87I mutant is not phosphorylated by acetyl phosphate (Zhu, X. *et al.*, 1997b), yet it is phosphorylated by its kinase, CheA (Ganguli, S. *et al.*, 1995). A FixJ mutant, T82I, is phosphorylated by the FixL kinase, but with much slower kinetics. Phosphorylation of T82I was evident after 80 minutes at levels equivalent to those of wild-type FixJ after five minutes (Weinstein, M. *et al.*, 1992). A T82A substitution in SpoOF interferes with phospho-transfer reactions from both KinA and SpoOB (Tzeng, Y. L. and J. A. Hoch, 1997). There are several explanations for the observed phosphorylation characteristics of T83I. The first is that small molecule phosphodonors such as acetyl phosphate act by a different mechanism than the endogenous kinase, and that the T83I (T87I in CheY) substitution has separated the two mechanisms. This was proposed by Zhu *et al.* in their studies of CheY T87I (Zhu, X. *et al.*, 1997b). The



second possibility is that the mechanism of phosphorylation is the same for both small molecule donors and the cognate kinase, but that the kinase renders the site more accessible via protein:protein interactions. Mayover *et al.* measured the kinetics of phosphorylation of CheY by both small molecule and kinase phosphate donors (Mayover, T. L. *et al.*, 1999). They found that the rate constant for phosphorylation ( $k_{\text{phos}}$ ) by the kinase CheA was 10,000-fold faster than for phosphorylation by acetyl phosphate, and 2,000-fold faster than for phosphorylation by phosphoramidate. These authors proposed that the kinase plays an active role in orienting the active site of the regulator for effective phospho-transfer. We have shown that the EnvZ kinase binds to T83I and it is therefore likely that protein-protein interactions increase the efficiency of phospho-transfer (Figure 2.6), perhaps by increasing the local concentration of phosphodonor.

Our laboratory has previously characterized the OmpR2 mutant, V203M. It has altered dephosphorylation properties, although the substitution is located in the DNA binding domain at the carboxyl-terminus (Tran, V. K. *et al.*, 2000). Clearly, substitutions that affect the phosphorylation site are not limited to the amino-terminal phosphorylation domain of OmpR. Our laboratory and others have also shown that DNA binding in the carboxyl terminus can affect both phosphorylation and dephosphorylation kinetics at the amino terminus of OmpR (Ames, S. K. *et al.*, 1999; Qin, L. *et al.*, 2001).

### **2.4.3 The T83I substitution in the amino terminus alters the DNA binding properties of the carboxyl terminus**

T83I is capable of binding to the *ompF* promoter region, although it fails to activate transcription. Since T83I binds to both F1-F2-F3 and to F4 sites (Figure 2.8 and Table 2.1), we determined whether the *OmpF*<sup>-</sup> phenotype observed was due to a lack of activation or to repression of the *ompF* locus by the mutant protein. T83I is incapable of activating transcription from promoters lacking the F4 binding site (Figure 2.10). Thus, it seems most likely that the mutant protein is unable to interact productively with RNA Polymerase in order to activate gene expression at *ompF*. This suggests that it is defective in later events leading to transcriptional activation at the *ompF* locus. This is supported by the observed dominance of the *OmpF*<sup>-</sup> *OmpC*<sup>-</sup> phenotype, which is maintained in the absence of phosphorylation.

T83I binds to the independent site C1, presumably with one dimer bound, but saturable binding is not detectable at C1-C2-C3 (Figure 2.7B and Table 2.1). Our preferred explanation for this result is that T83I binds to C1 of the composite site (as seen by protection from DNase I digestion; Figure 2.8D), but the change in molecular volume of the composite DNA when one dimer is bound is not sufficient to observe a saturable increase in anisotropy. With wild-type *OmpR*, presumably three dimers normally bind to C1-C2-C3. Using DNase I footprinting analysis, we determined that T83I protects at the high affinity C1 site,

but fails to protect the low affinity sites, C2 and C3 (Figure 2.8D). This is in contrast to the wild-type pattern of protection observed with T83I at the *ompF* binding sites (see Figures 2.7A, 2.8A and 2.11) and demonstrates that binding of OmpR at *ompF* and at *ompC* are not equivalent events.

Our combined results from fluorescence anisotropy and DNase I footprinting indicate that a substitution in the phosphorylation site of OmpR affects its DNA binding properties in the carboxyl-terminus. T83I is defective in OmpR-mediated transcriptional activation of both the *ompF* and *ompC* promoters, but behaves differently at *ompF* and *ompC*. The mutant protein can bind at the *ompF* regulatory sites but fails to activate transcription. At *ompC*, it is unable to bind the promoter-proximal sites, C2 and C3.

The DNase I footprinting studies indicate that when OmpR is bound solely at the C1 site, it is not sufficient to activate *ompC* transcription. Therefore, the low level of *ompC* expression seen at low osmolarity *in vivo* is not due to sole occupancy of the C1 site. C1 is located approximately 40 bp upstream from the -35 region of the promoter. It has been shown that moving C1 to the promoter-proximal position normally occupied by C3 allows high levels of *ompC* expression in the absence of the C2 and C3 sites (Maeda, S. and T. Mizuno, 1990). Similarly, positioning of the strong binding sites for the UhpA response regulator closer to the transcriptional start site results in constitutive

expression of *uhpT* (Chen, Q. and R. J. Kadner, 2000). Clearly, the precise location of the high affinity binding site influences porin gene expression. It is interesting to note that the high affinity OmpR binding site at the *ompC* locus of *Salmonella typhi* is located in the C2 position, i.e. closer to the -35 region. *S. typhi* expresses *ompC* irrespective of the osmolarity of the growth medium. This altered location is not sufficient, however, to confer the constitutive phenotype, since *S. typhi ompC* is osmoregulated when it is expressed in *E. coli* (Martinez-Flores, I. *et al.*, 1999).

#### **2.4.4 Differential activation of *ompF* and *ompC* transcription**

The T83I mutant provides insight into the mechanism of differential activation of *ompF* and *ompC* transcription, by demonstrating that binding to the *ompF* and *ompC* promoters probably requires a different protein conformation. As we have shown, the small difference in the DNA binding affinity of OmpR-P at the F1-F2-F3 and C1-C2-C3 sites is not sufficient to explain the lack of *ompC* expression at low osmolarity (Head, C. G. *et al.*, 1998). We propose that at low osmolarity, OmpR-P exists in a conformation that binds at the *ompF* regulatory sites, and at the high affinity C1 region of the *ompC* promoter. This is the conformation that T83I adopts. In an environment of high osmolarity, the phospho-protein undergoes a conformational change such that the low affinity sites necessary for *ompC* activation, C2 and C3, are filled. Furthermore, since T83I is capable of binding at F4, yet does not mediate

repression of *ompF* (see Table 2.1 and Figure 2.9), we postulate that the conformation necessary for binding and activation at *ompC* is also required for repression of *ompF*. The previous finding that mutants that fail to express OmpF also constitutively express OmpC and vice versa provides support for this notion (Hall, M. N. and T. J. Silhavy, 1981c). T83I is unable to undergo this conformational transition and as such can neither activate transcription of *ompC* nor repress transcription of *ompF*. When T83I binds to C1 in the inappropriate conformation, it induces large structural changes in the downstream sequences, observed in our footprints as hypersensitive sites (Figure 2.8D). Alternatively, T83I may directly contact C2 and C3, but in a manner different from C1. We cannot exclude the possibility that C2 and C3 are occupied across the entire site, but in a manner that does not result in protection against DNase I, and instead results only in hypersensitization, e.g. with T83I exclusively occupying the major groove and expanding the minor groove. This possibility seems less likely given the absence of saturable binding observed with the composite site C1-C2-C3 using fluorescence anisotropy. It is this result that leads us to propose that T83I is locked in a low osmolarity conformation (Figure 2.12). The conformational change required for the switch to an OmpF<sup>-</sup> OmpC<sup>+</sup> configuration may be transmitted by movement of the side chain of Y102.

### **2.4.5 Conclusion**

This study of a single substitution in the phosphorylation domain of OmpR has provided insight into the mechanism of transcriptional regulation of the *ompF* and *ompC* genes. We have established that a single substitution in the amino terminus (the phosphorylation domain) of OmpR can interfere with transcriptional activation at *ompF*. We have also shown that this substitution, which alters a residue in the active site, changes the DNA binding properties of T83I at the *ompC* promoter. Our data indicate that occupancy of the high affinity C1 site is not sufficient for activation of *ompC* transcription, and that substitution of T83 influences subsequent binding. We propose that binding of OmpR to the two promoter regions has different conformational requirements, and that the transition between these two conformations accounts for the reciprocal regulation of OmpF and OmpC expression. The important question that remains is how the appropriate OmpR conformation is generated in response to high osmolarity.

## **2.5 Materials and Methods**

### **2.5.1 Construction of mutants by PCR**

*ompR* was subcloned into the Bluescript KS vector using the *Hind*III and *Xba*I sites. Two complementary oligonucleotides containing the desired mutation were used for the PCR reaction. The sequence of the oligonucleotide creating the T83I mutation is (5'-3'):

CCGATCATTATGGTGATCGCGAAAGGGAAGTG. The sequence used for

the D55A mutation is (5'-3'): CCATCTTATGGTACTC-GCGTTAATGTTACCTGGTGAAGATGGC. The PCR reaction contained 10ng of double-stranded DNA template, 100ng of each primer, 2.5mM each deoxynucleoside triphosphate, and 2.5 units of native Pfu DNA Polymerase (Stratagene) in 50  $\mu$ l. The reaction was amplified by 20 cycles of 95 °C (30 seconds), 55 °C (one minute), 68 °C (eight minutes). The product was treated with *DpnI* (New England Biolabs) in order to eliminate the methylated template and transformed into *Escherichia coli* strain DH5 $\alpha$ . Plasmids were isolated from the ampicillin-resistant colonies and the entire *ompR* gene was sequenced to confirm the presence of the desired mutation and the absence of unintended mutations.

### **2.5.2 Purification of T83I and T83I/D55A protein**

Both T83I and T83I/D55A were expressed and purified as described for wild-type OmpR (Head, C. G. *et al.*, 1998).

### **2.5.3 $\beta$ -galactosidase assay**

Wild-type *ompR* and *ompRT83I* were subcloned into pFR29\*, a derivative of pFR29 (Russo, F. D. and T. J. Silhavy, 1991) from which the *envZ* gene has been excised. The plasmid was used to transform the strains MH225.101, MH513.101, BW25891 and BW25892. MH225 contains a chromosomal *ompC-lacZ* fusion and MH513 contains a chromosomal *ompF-lacZ* fusion (Hall, M. N. and T. J. Silhavy, 1981b). The .101 strains contain a small in-frame deletion in the *ompR* gene.

BW25891 contains a chromosomal copy of an *ompF-lacZ* fusion that lacks the F4 binding site in the promoter (*F4 minus-lacZ*), and BW25892 contains an *ompF-lacZ* fusion with the entire *ompF* promoter (*F4 plus-lacZ*). These two strains are also in an *ompR* minus background. An overnight culture of bacteria was diluted 1/200 and grown to mid-exponential phase. Cultures were grown in Luria Broth (LB) at 37 °C for the experiments shown in Figure 2.2. Cultures were grown in LB with 20% sucrose added for the experiments shown in Figure 2.9. In experiments not shown, minimal A salts were used at a concentration of 0.2 or 4x; glucose, casamino acids, MgCl<sub>2</sub>, and thiamine supplements were as for 1x minimal A medium. The overexpressed wild-type OmpR confers osmoresponsiveness under these high and low osmolarity conditions. 0.1 ml of cells were added to 0.9 ml of Z buffer (60 mM Na<sub>2</sub>HPO<sub>4</sub>, 40 mM NaH<sub>2</sub>PO<sub>4</sub> (pH 7.0), 10 mM KCl, 1 mM MgSO<sub>4</sub>, 2.7 µl/ml β-mercaptoethanol), disrupted by adding 0.1% SDS and chloroform, and incubated with 0.2 ml of 4 mg/ml o-nitrophenyl-β-D-galactoside (ONPG). The reaction was carried out for 15 or 30 minutes at room temperature and stopped by the addition of 1 M Na<sub>2</sub>CO<sub>3</sub>. β-galactosidase activity was expressed in Miller units and calculated using the formula  $1000 \times (A_{420} - 1.75 \times A_{550}) / \text{time (minutes)} \times \text{culture volume (ml)} \times A_{600}$ .

#### **2.5.4 Phosphorylation of T83I by acetyl phosphate**

OmpR protein was phosphorylated using acetyl phosphate (Sigma) as described (Kenney, L. J. *et al.*, 1995). For some experiments, DNA



was added in a 1:2 molar ratio of protein to DNA (Ames, S. K. *et al.*, 1999). Samples were injected onto a C4 reversed phase HPLC column and eluted as described (Tran, V. K. *et al.*, 2000). The T83I mutant elutes approximately 5 minutes later than the wild-type protein (compare Figures 2.3E and 2.3G or 2.3A and 2.3C).

#### **2.5.5 Phosphoramidate synthesis and phosphorylation**

Ammonium hydrogen phosphoramidate (PA) was synthesized according to (Sheridan, R. C. *et al.*, 1971). The resulting crystalline product was dissolved to 0.5 M in dH<sub>2</sub>O and immediately used to phosphorylate OmpR and T83I. Phosphorylation reactions were carried out in 200 µl volumes containing 50 mM Tris (pH 7.5), 50 mM KCl, 20 mM MgCl<sub>2</sub>, 25 mM PA, and 10 µM OmpR or T83I. Reactions were incubated for 2 hours at room temperature and stopped by freezing in an ethanol/CO<sub>2</sub> bath. Samples were injected onto a C4 reversed phase HPLC column and eluted as described (Tran, V. K. *et al.*, 2000).

#### **2.5.6 EnvZ115 purification and phosphorylation**

EnvZ115 was expressed and purified as described (Igo, M. M. and T. J. Silhavy, 1988). EnvZ (~100 µg) was phosphorylated in a 90 µl reaction volume containing: 50 mM Tris (pH 7.5), 50 mM KCl, 20 mM MgCl<sub>2</sub>, 0.2 mM ATP, 10 µCi [ $\gamma$ -<sup>32</sup>P]ATP. After 15 minutes at room temperature, 40 µg of OmpR was added. At the indicated times, the reaction was stopped by addition of denaturing sample buffer (124 mM Tris-HCl (pH 6.8), 20% (v/v) glycerol, 4% (w/v) SDS, 8% (v/v)  $\beta$ -

mercaptoethanol, 0.025% (w/v) bromophenol blue) and the products were separated by SDS-PAGE. The dried gel was exposed for six hours to Kodak X-Omat Blue XB-1 film in the presence of an intensifying screen.

#### **2.5.7 Measurement of ATPase activity**

The reaction was carried out in a total volume of 0.6 ml containing 125 mM NaCl, 4 mM MgCl<sub>2</sub>, 60 mM Tris-HCl (pH 7.5), 0.75 mM EDTA, 300 µg of EnvZ 115 and 24 µg of OmpR. The reaction was initiated by the addition of 4 mM ATP and conducted at 37 °C. At different times, the reaction was stopped according to (Kenney, L. J., 1997). The absorbance of the samples at 850 nm was measured in a Beckman DU-640 spectrophotometer and compared to Na<sub>2</sub>HPO<sub>4</sub> standards. The P<sub>i</sub> produced in the presence of OmpR or T83I was obtained by subtracting the P<sub>i</sub> produced in the presence of EnvZ alone from the total P<sub>i</sub> produced.

#### **2.5.8 EnvZ binding**

The construct encoding a soluble carboxyl terminal fragment of EnvZ, EnvZc, was a kind gift from Dr. Masayori Inouye, the protein was expressed and purified as described (Park, H. *et al.*, 1998). The concentration of EnvZc was determined by its absorbance at 280 nm, using a molar extinction coefficient of 25,500. This extinction coefficient was estimated from the tryptophan and tyrosine content of the protein (Mach, H. *et al.*, 1992). Fluorescence anisotropy was used to determine the equilibrium binding of EnvZc to OmpR and the mutant derivative in solution. OmpR and T83I were N-terminally labeled using an amine

fluorescein labeling kit as per manufacturer's instructions (Panvera). The labeled proteins were separated from free label using a series of three 5 mL HiTrap desalting columns (Pharmacia). The binding assays were performed at room temperature by titrating serial dilutions of EnvZc into a binding solution containing 15 mM Na<sub>2</sub>HPO<sub>4</sub>/NaH<sub>2</sub>PO<sub>4</sub> (pH 7.4), 50 mM NaCl, 5 mM MgCl<sub>2</sub>, 0.05% (v/v) Tween-20, 50 µg/ml bovine serum albumin and 20-30 nM fluorescein-labeled protein. Fluorescent protein was excited at 490 nm and emission was measured at 530 nm on a Beacon Fluorimeter (Panvera). The samples were incubated in the fluorimeter for 60 seconds and a measurement was taken after each protein addition. Binding curves were fit by non-linear least squares regression analysis (Head, C. G. *et al.*, 1998).

### **2.5.9 DNA binding**

Fluorescence anisotropy was used to measure equilibrium binding, and the experiments were performed as described (Head, C. G. *et al.*, 1998). The sequences of the oligonucleotides used were the same as in the previous study. The results from the binding curves were fit by non-linear least-squares regression as described (Head, C. G. *et al.*, 1998). The apparent dissociation constants from two individual binding curves (Figure 2.7 A and B) are reported in the text. The mean of multiple binding curves ± the standard deviations are also reported in the text. DNase I footprinting analysis was also performed to assess the DNA binding ability of OmpR and T83I. The DNA was prepared by end-

labeling the oligonucleotides (5'-3'): GCCTTTATTTGCTTTTTTATGCCAC and (5'-3'): TAAGTTCTGTCAATAAAAATTACGG with [ $\gamma$ - $^{32}$ P]ATP (3000 Ci/mmol) using T4 polynucleotide kinase. The labeled probes were then used as primers in a PCR reaction to amplify ~250 bp of the *ompC* or *ompF* promoter regions. The forward primers in the reactions were (5'-3'): CTTAAGAATAAGTTATTGATTTTAACC and (5'-3'): CAAGAGCCAGCGCCCGCTGGC. The PCR reactions contained 20 ng of double-stranded DNA template, 100 ng of each primer, 2.5 mM each deoxynucleoside triphosphate, and 1 unit of Vent Polymerase (New England Biolabs) in 50  $\mu$ l. The reactions were amplified by 30 cycles of 95 °C (30 seconds), 60 °C (30 seconds), 72 °C (one minute). The amount of radioisotope incorporated in the product was quantified by scintillation counting. Binding reactions were prepared consisting of: 300,000 cpm DNA, 4 mM Tris-HCl (pH 7.6), 1 mM EDTA (pH 8.0), 1 mM DTT, 20 mM KCl, 12 % (v/v) glycerol, 50 mg/ml poly [d(I-C)], and a range of OmpR or T83I concentrations. The DNA binding reaction was incubated at room temperature for 20 minutes before the addition of DNase I. After DNase I incubation for two minutes, the reaction was stopped and the DNA was precipitated with 85 mM EDTA (pH 8.0), 500 mM NaAc (pH 5.5), carrier DNA and isopropanol. DNA was resuspended in 7  $\mu$ l of distilled water and 4  $\mu$ l of sequencing stop solution (95 % (v/v) formamide, 20 mM EDTA, 0.05% (w/v) bromophenol blue, 0.05% (w/v) xylene cyanol), heated at 65 °C for 5 minutes and run on an 8M urea/ 6%

polyacrylamide sequencing gel. The dried gel was exposed to Kodak X-Omat Blue XB-1 film.

## **2.6 Acknowledgements**

We thank Van Tran for constructing the T83I mutant and the *ompF-lacZ* fusions used in this study. We are grateful to Barry Wanner for *ompF* fusion strains BW25891 and BW25892. Masayori Inouye kindly provided the EnvZc-his construct. The authors would like to thank the following for helpful discussions: Ann Stock, UMDNJ-Robert Wood Johnson Medical School; James Hernandez, SUNY-Buffalo; Kozo Makino, Osaka University; Aaron Farnsworth, Manuela DiLorenzo, Don Walthers, Xiuhong Feng and Judith Dietvorst from OHSU. Jack Kaplan, OHSU and Bob Bourret, University of North Carolina, provided insightful discussions as well as comments on the manuscript. NB was a participant in the science program for high school students at OHSU and is currently an undergraduate at Bowdoin College, ME. She was a recipient of a Summer Research Fellowship from the American Heart Association-Northwest Affiliate. RO was the recipient of a Conacyt Fellowship from the Mexican government and KM is a Predoctoral Fellow of the American Heart Association-Northwest Affiliate. Supported by NSF MCB-9904658 and NIH GM-58746 to LJK.

Figure 2.1. Ribbon diagram of the active site of response regulator phosphorylation. The position of three of the conserved residues of the active site are shown before (red) and after (green) phosphorylation. The phosphoryl group is in yellow. Diagram from Robinson, *et al.* (Robinson, V. L. *et al.*, 2000), used with permission.

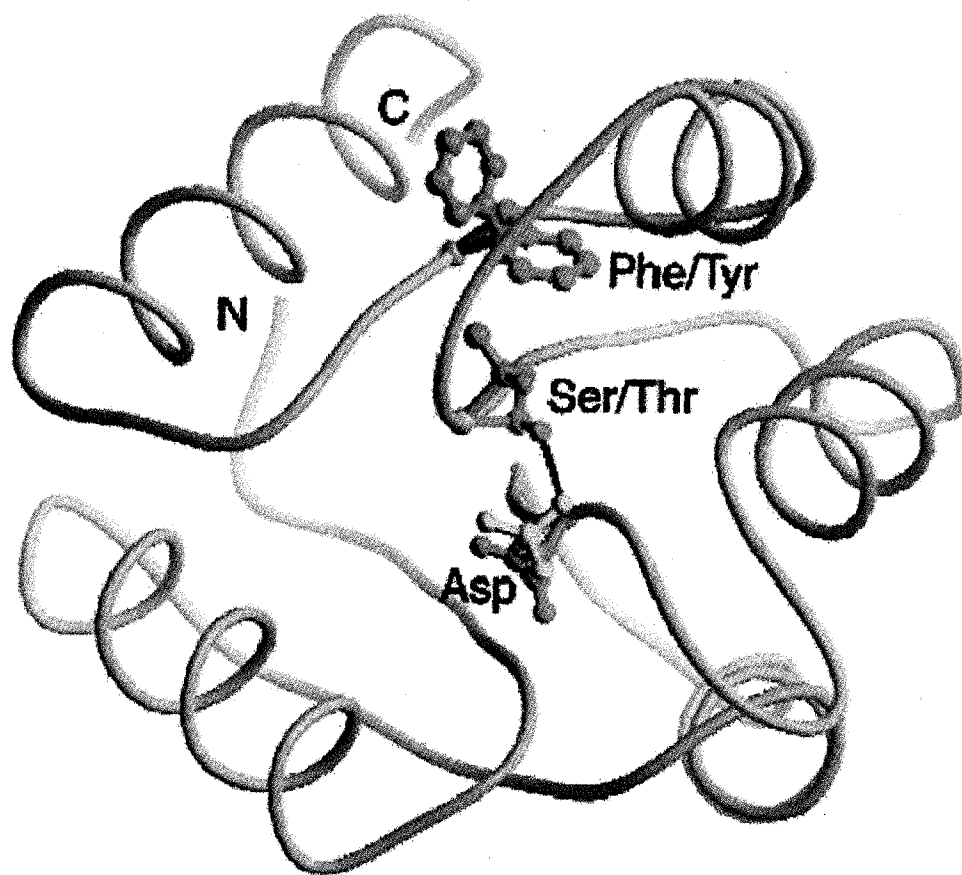


Figure 2.2. The effect of *ompR* and mutant *ompRT83I* on transcription of *ompF-lacZ* and *ompC-lacZ* fusions *in vivo*.  $\beta$ -galactosidase assays were performed as described in Materials and Methods. Activity of the *ompF-lacZ* strain MH513.101 and the *ompC-lacZ* strain MH225.101 are shown in the absence of *ompR* (solid columns), in the presence of *ompR* (striped columns), and in the presence of *ompRT83I* (open columns). At least three independent assays were performed on each strain, the standard deviation is indicated by the error bars. For columns one and three the standard deviation was negligible.



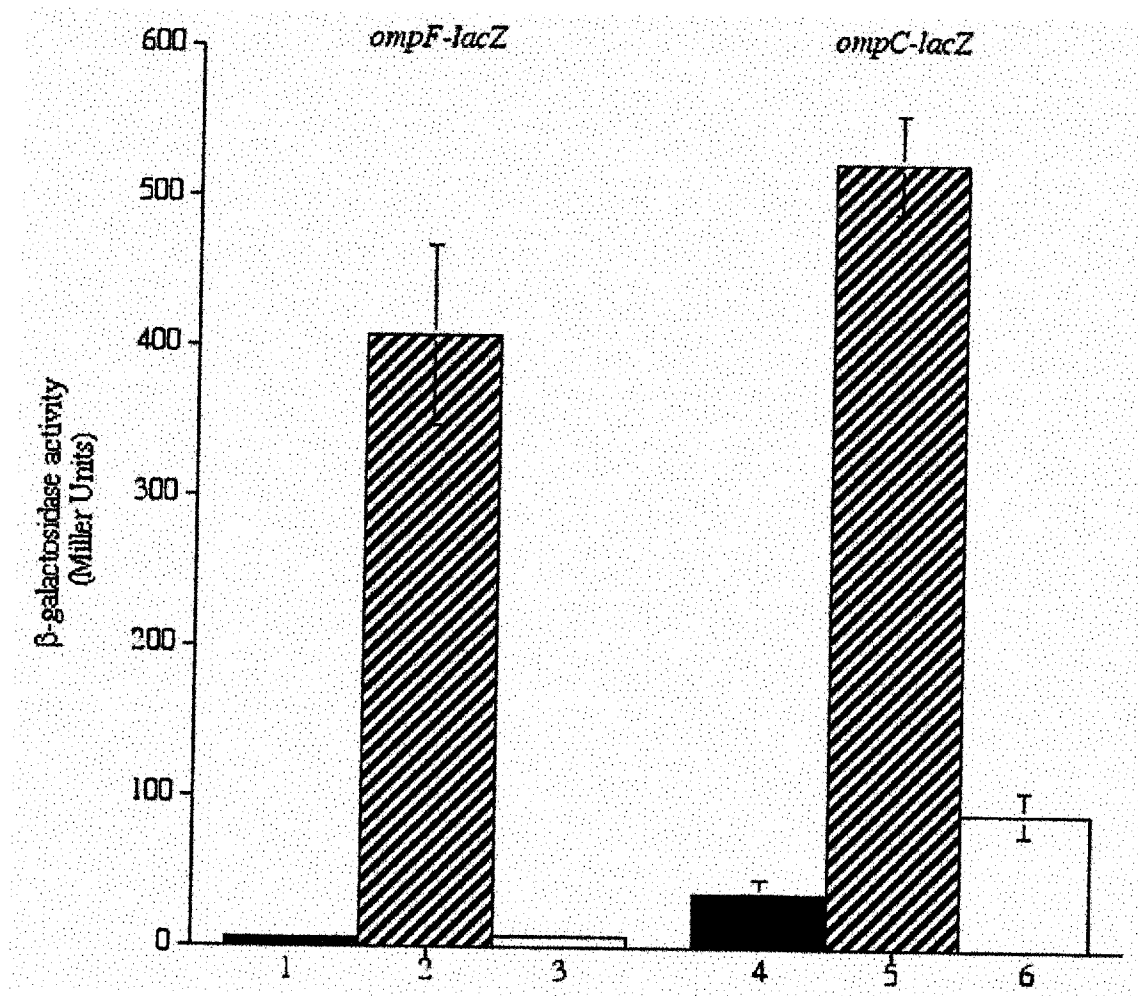


Figure 2.3. Phosphorylation of OmpR and T83I by small molecule phosphate donors. 10 $\mu$ M OmpR or T83I in a total volume of 200  $\mu$ l was injected onto a C4 reversed phase HPLC column. The sample was eluted as described (Tran, V. K. *et al.*, 2000). The profile of OmpR is shown in (A & E), and the profile of T83I is shown in (C & G). After incubation of OmpR or T83I with acetyl phosphate for three hours at room temperature, the samples were separated on C4 and two peaks corresponding to OmpR and OmpR-P are evident (B) (Head, C. G. *et al.*, 1998). In contrast, there is no additional peak in the presence of acetyl phosphate with T83I (D). After a two hour incubation with phosphoramidate, 100% OmpR-P is formed (F), and T83I remains unphosphorylated (H).

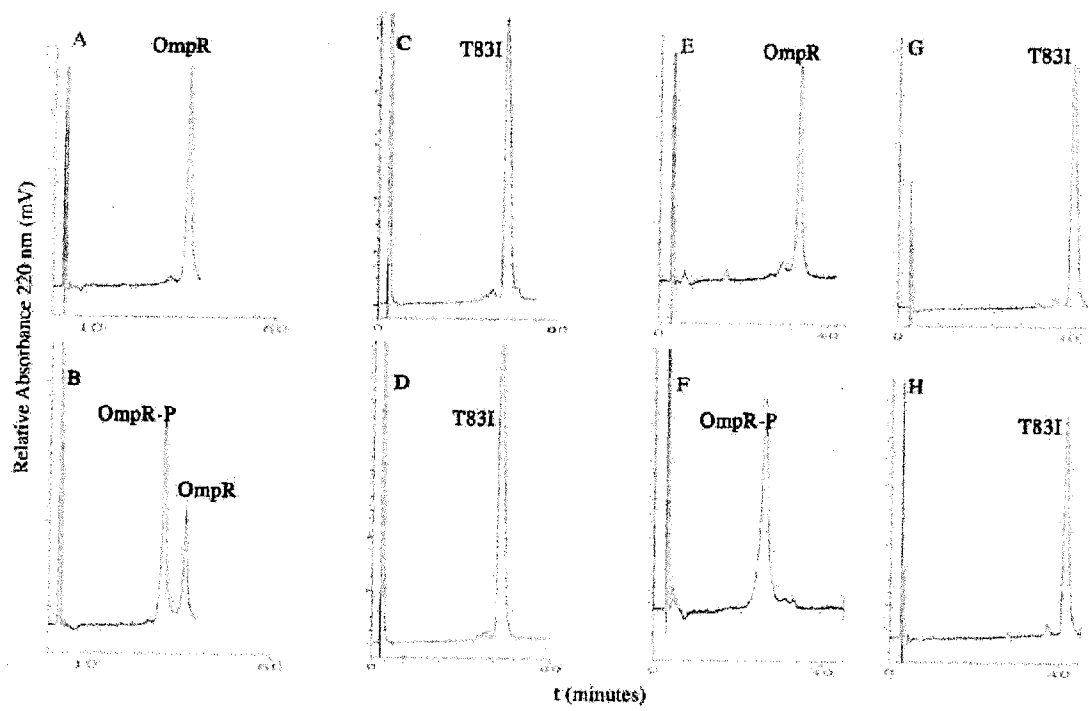


Figure 2.4. Phosphorylation of OmpR and T83I by EnvZ115.

Phosphorylation was as described in Materials and Methods. Lane 1 contains approximately 10  $\mu$ g of EnvZ115 autophosphorylated by ATP. Approximately 3 $\mu$ g of OmpR (lanes 2-3), T83I mutant (lanes 4-5), or T83I/D55A mutant (lanes 6-7) were added to phosphorylated EnvZ. The phosphotransfer reaction was stopped by the addition of denaturing sample buffer at 20 minutes (lanes 2, 4 and 6), or 60 minutes (lanes 3, 5 and 7).

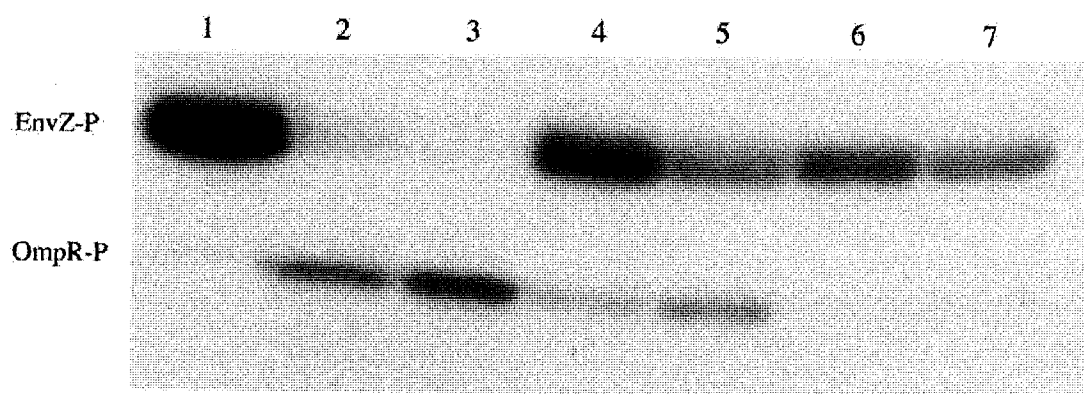


Figure 2.5. OmpR-stimulation of EnvZ115 ATPase activity. 300 $\mu$ g EnvZ115 was incubated alone, with 24 $\mu$ g OmpR or with 24 $\mu$ g T83I. The reaction was conducted at 37 °C, initiated by the addition of 4 mM ATP and stopped at the indicated times. The concentration of inorganic phosphate produced represents the OmpR-stimulated component and it was determined by subtracting the  $P_i$  produced by EnvZ alone (7.1  $\mu$ M/minute) from the total  $P_i$  produced in the presence of OmpR (triangles) or T83I (circles). At least three independent experiments were performed and the averaged values are shown. Error bars represent the standard deviation.

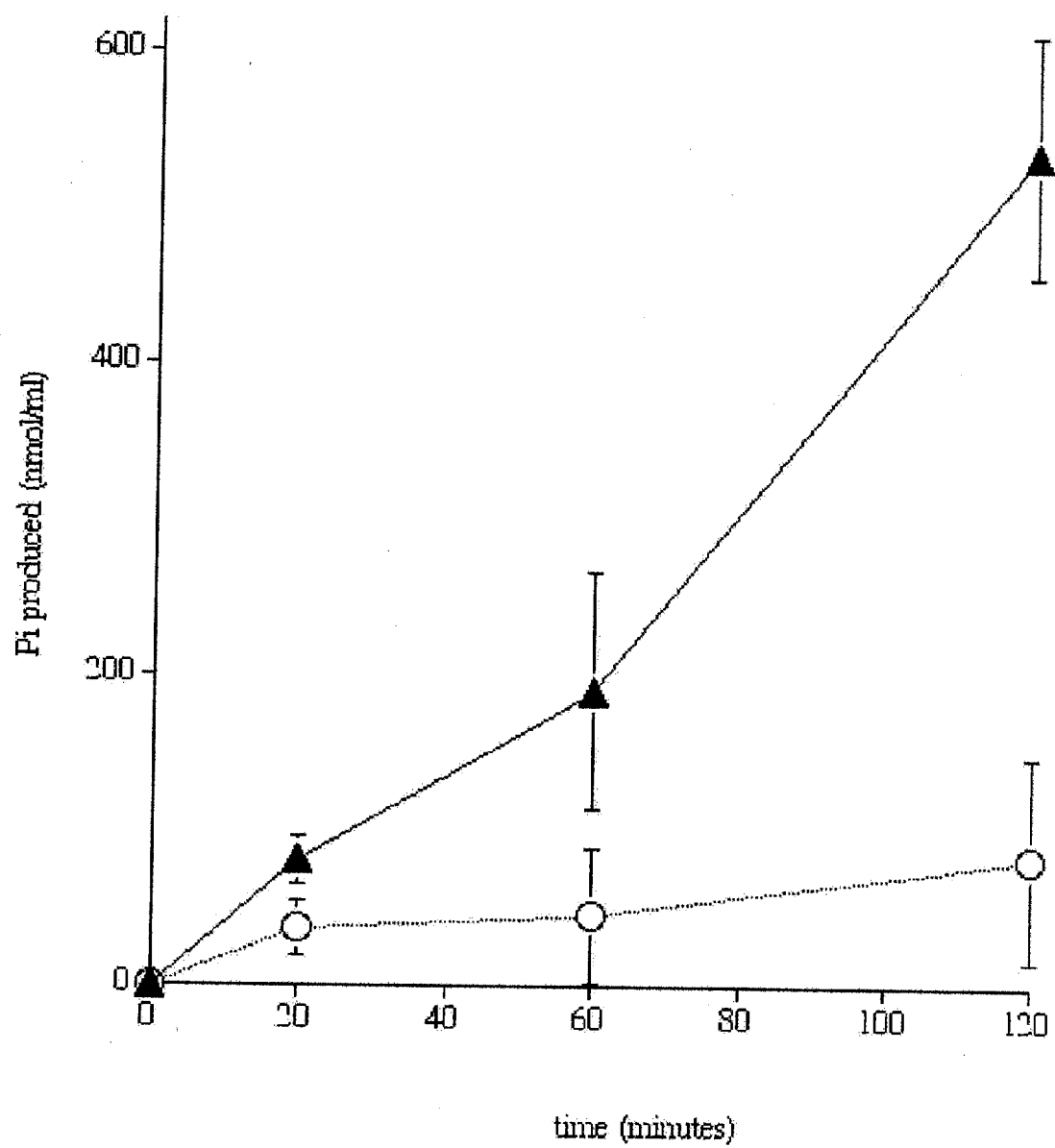


Figure 2.6. OmpR and T83I binding to EnvZc. OmpR (triangles) or T83I (circles) were labeled at the amino terminus with fluorescein succinimidyl ester and 20-30 nM protein was included in a binding reaction as described in Materials and Methods. EnvZc was titrated into this mixture and the resulting change in anisotropy is shown. All values have been normalized such that the highest value corresponds to 100%, and these values are plotted against the total EnvZc concentration. The curves are representative of multiple separate experiments, the average values for all curves are reported in the text. The apparent dissociation constant for EnvZc binding to OmpR in the curve shown is 519 nM, for T83I it is 199 nM.



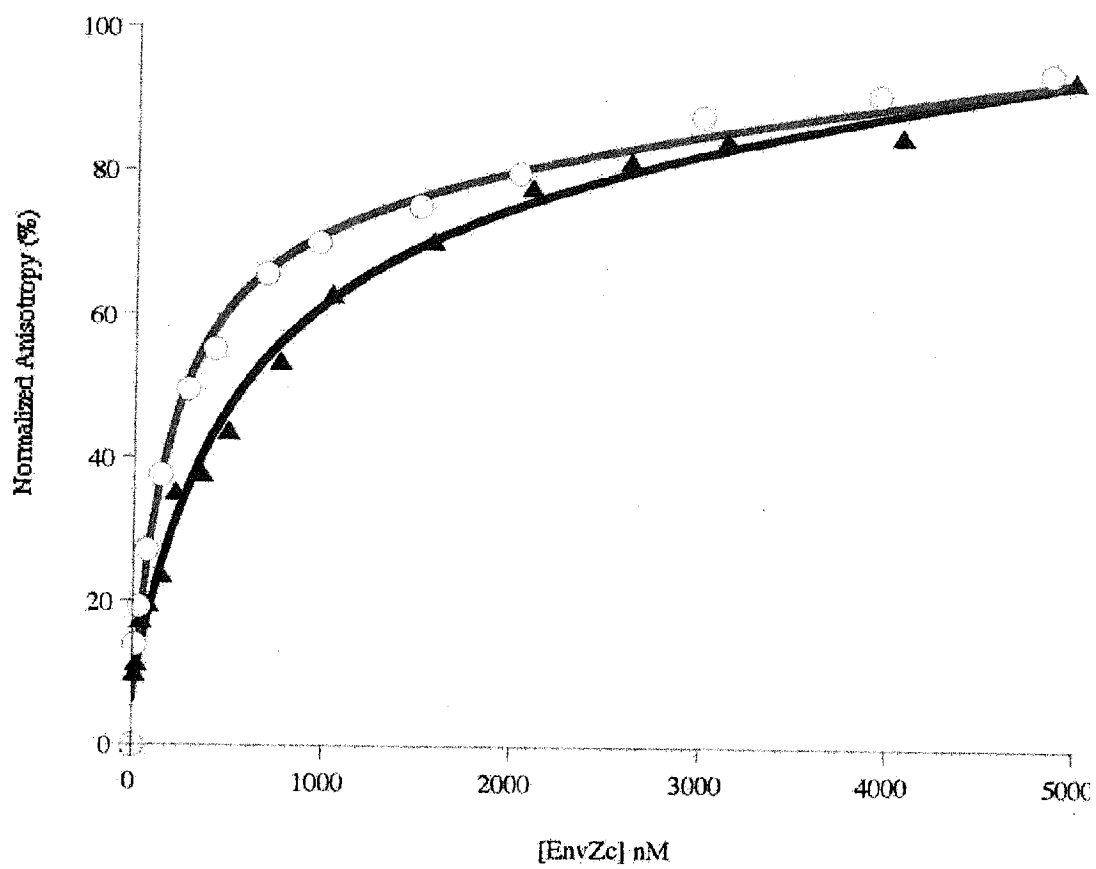


Figure 2.7. DNA binding of OmpR and T83I to the high affinity F1 and C1 binding sites. OmpR (triangles) or T83I (circles) were titrated into a binding reaction mixture with 3 nM fluorescein-labeled (A) F1 or (B) C1 oligonucleotide in a buffer containing: 15 mM  $\text{Na}_2\text{HPO}_4/\text{NaH}_2\text{PO}_4$  (pH 7.4), 50 mM NaCl, 5 mM  $\text{MgCl}_2$ , 0.05% (v/v) Tween-20, 0.1 mg/ml poly [d(I-C)], 30  $\mu\text{g}/\text{ml}$  bovine serum albumin. The curve illustrates the change in anisotropy, where the highest value has been normalized in each case to 100%, and all other values adjusted accordingly. This value is plotted as a function of the total protein concentration. The curves are representative of multiple separate experiments, the average values for all curves are reported in the text. (A) The apparent dissociation constant for OmpR binding at F1 in the curve shown is 150 nM, for T83I it is 180 nM. (B) The apparent dissociation constant for OmpR binding at C1 in this experiment is 59 nM, for T83I it is 33 nM.

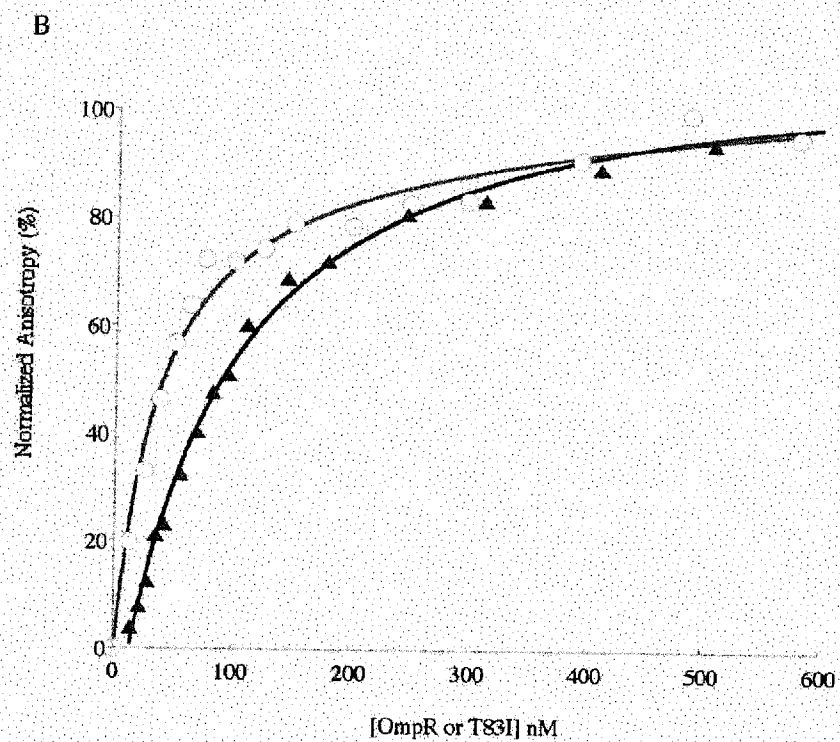
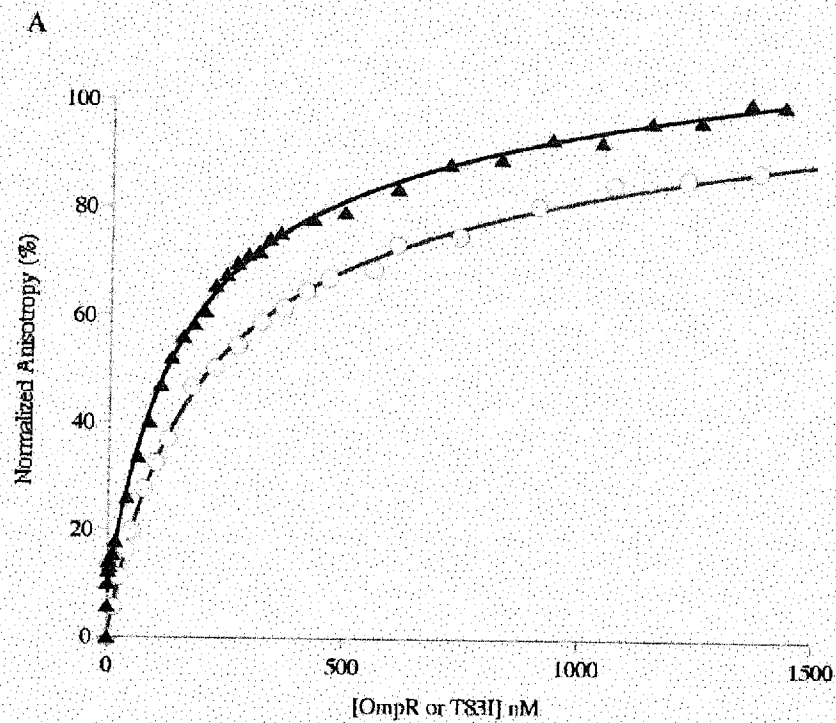


Figure 2.8. DNase I footprinting analysis of OmpR and T83I binding at the *ompF* and *ompC* promoters. Footprinting was performed as described in Materials and Methods. The previously characterized OmpR binding sites at each promoter are indicated to the right of each panel. The scale on the left of each panel refers to the position of each band in relation to the transcriptional start site for the respective promoter. Arrows indicate newly accessible DNase I cleavage sites (hypersensitive sites). (A) OmpR bound at the *ompF* promoter. Lane 1 represents DNase I cleavage in the absence of OmpR. Lanes 2-7 show the cleavage pattern obtained when 1.0, 2.0, 3.2, 4.5, 5.8, and 7.0  $\mu\text{M}$  OmpR was included in the reaction. (B) T83I bound at the *ompF* promoter. Lane 1 is DNase I cleavage in the absence of protein, lanes 2-7 show the cleavage pattern when 1.0, 2.0, 3.2, 4.5, 5.8, and 7.0  $\mu\text{M}$  T83I are bound to the DNA fragment. (C) OmpR bound at the *ompC* promoter. Lane 1 is cleavage of the unbound fragment by DNase I, lanes 2-8 show cleavage patterns with 2.9, 2.4, 2.0, 1.6, 1.2, 0.8, and 0.4  $\mu\text{M}$  total OmpR (50% of which is phosphorylated). (D) T83I bound at the *ompC* promoter. Lane 1 is DNase I cleavage in the absence of T83I, lanes 2-8 show the result obtained when 2.9, 2.4, 2.0, 1.6, 1.2, 0.8, and 0.4  $\mu\text{M}$  total T83I (26% of which is phosphorylated) is included in the reaction.

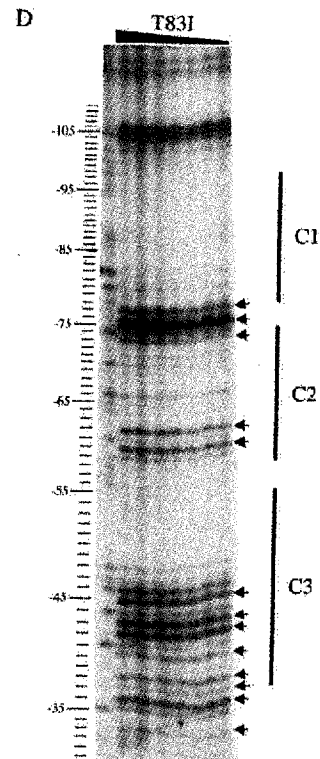
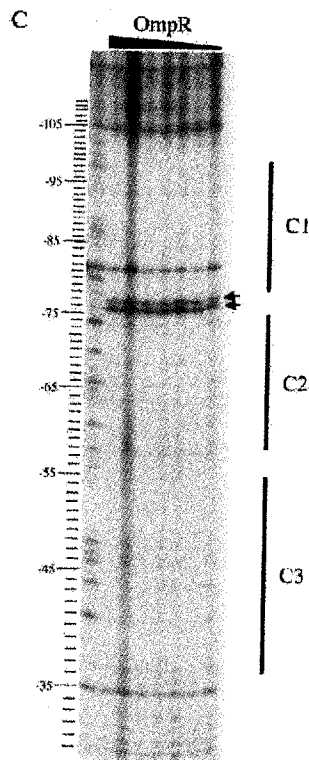
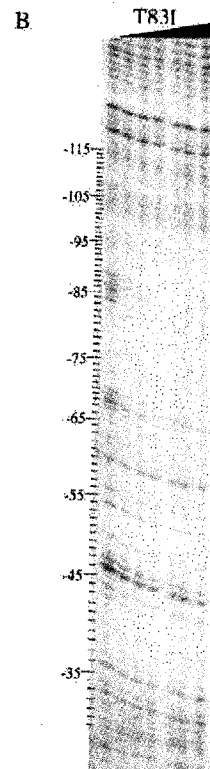
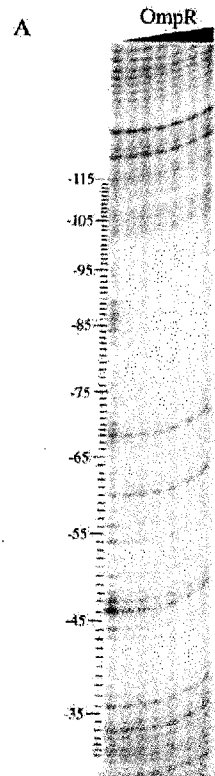


Figure 2.9. The effect of *ompRT83I* and *ompRT83I/D55A* on transcription of *ompF-lacZ* and *ompC-lacZ* fusions in the presence of *ompR*.  $\beta$ -galactosidase assays were performed as described in Materials and Methods. Activity of the *ompF-lacZ* strain MH513 and the *ompC-lacZ* fusion strain MH225 are shown in the absence of extra-chromosomal *ompR* (solid columns), in the presence of *ompR* (thick striped columns), in the presence of *ompRT83I* (open columns), and in the presence of *ompRT83I/D55A* (thin striped columns). At least three independent assays were performed on each strain, the standard deviation is indicated by the error bars.

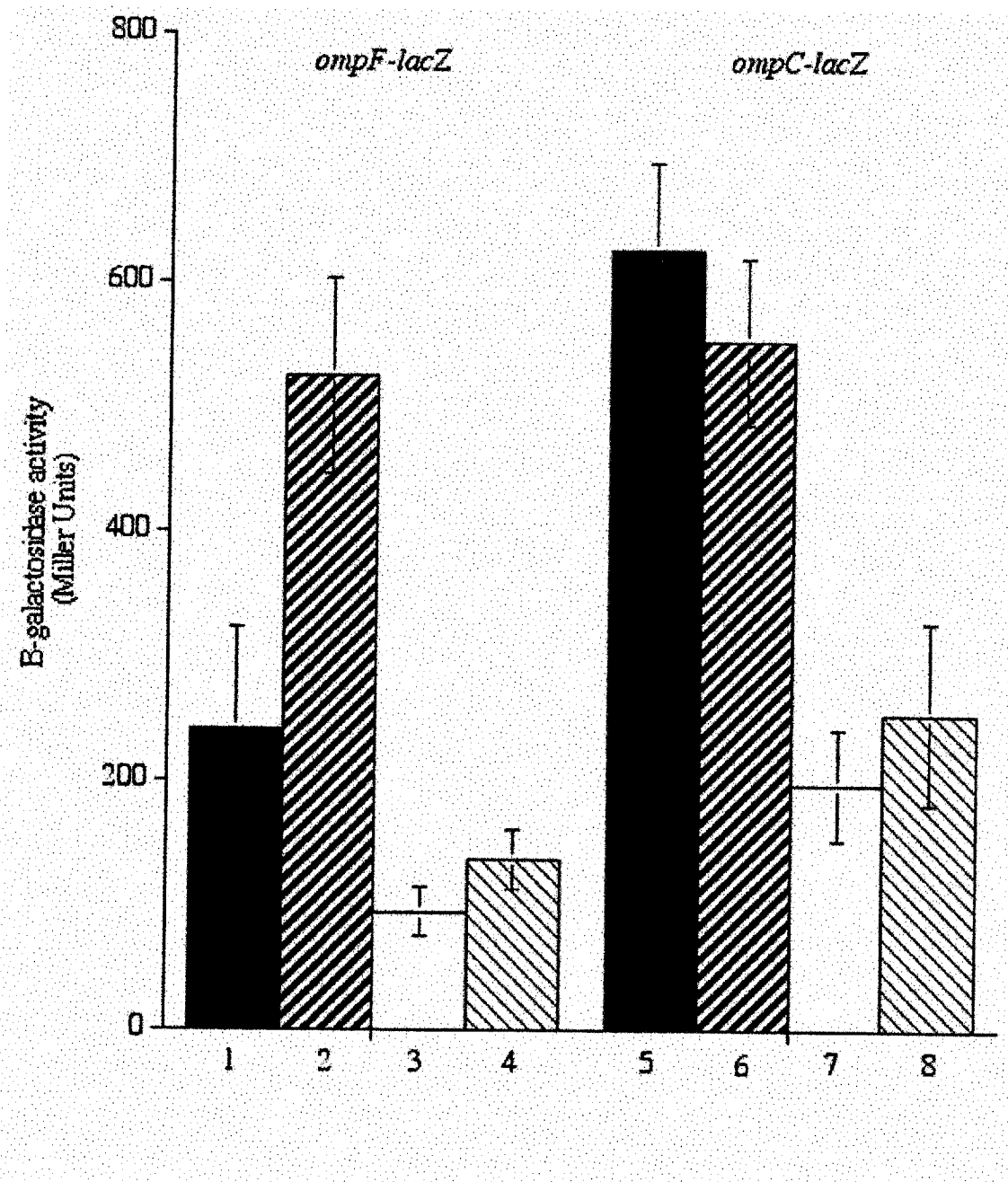


Figure 2.10. The effect of *ompR* and *ompRT83I* on transcription from an *ompF-lacZ* promoter lacking the F4 binding site.  $\beta$ -galactosidase assays were performed as described in Materials and Methods. Activity of the *F4 plus-lacZ* fusion strain BW25892 and the *F4 minus-lacZ* fusion strain BW25891 are shown in the presence of *ompR* (striped columns), and in the presence of *ompRT83I* (open columns). The activity of the strains in the absence of *ompR* has been subtracted from each column. At least three independent assays were performed on each strain, the standard deviation is indicated by the error bars. For column four, the error was negligible.



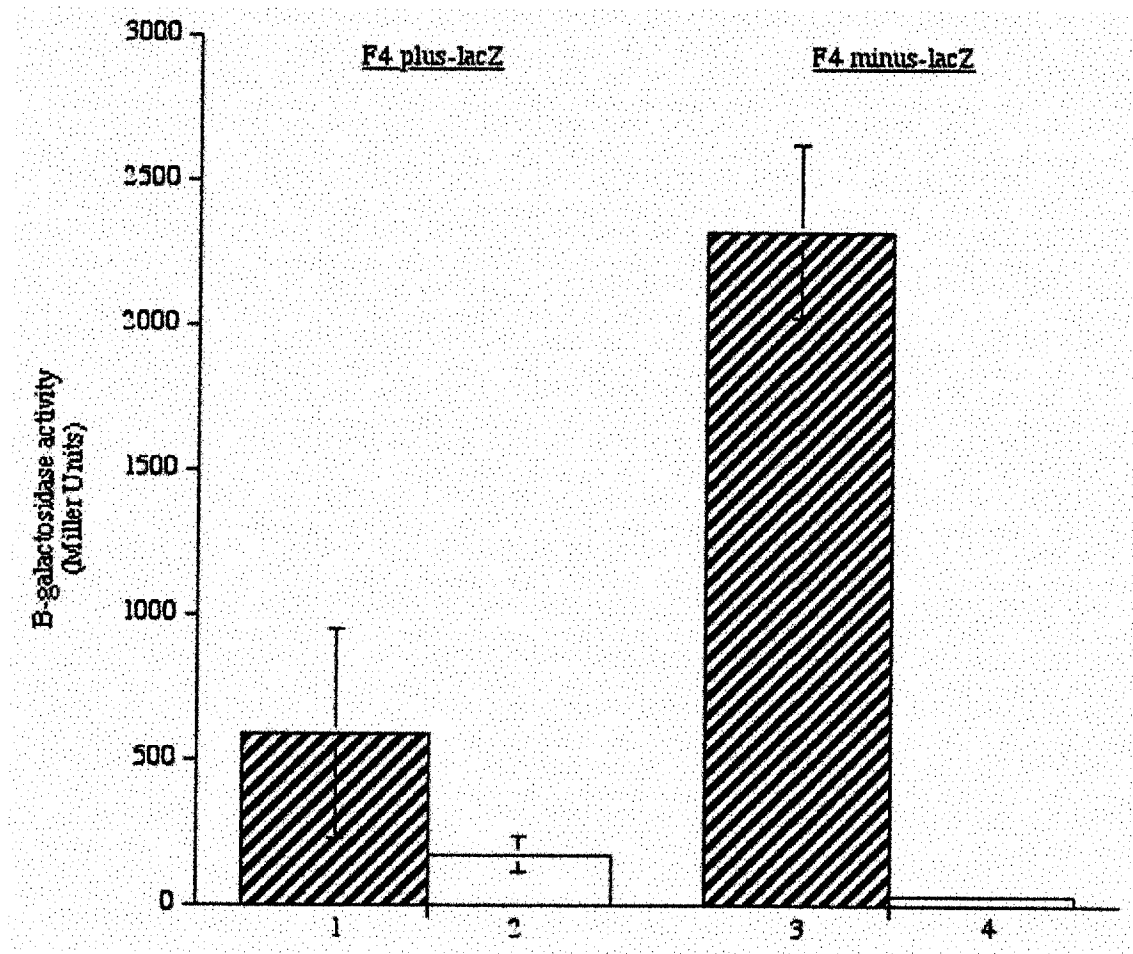


Figure 2.11. Schematic depiction of DNase I footprinting result. The sequences of the *ompF* (A and B) and *ompC* (C and D) promoter regions are shown. Boxes indicate regions of *ompF* protected by (A) wild-type OmpR or (B) T83I. Note that the protected region is the same in both cases. Boxes indicate regions of *ompC* protected by (C) wild-type OmpR and (D) T83I. Arrows indicate regions of hypersensitivity.

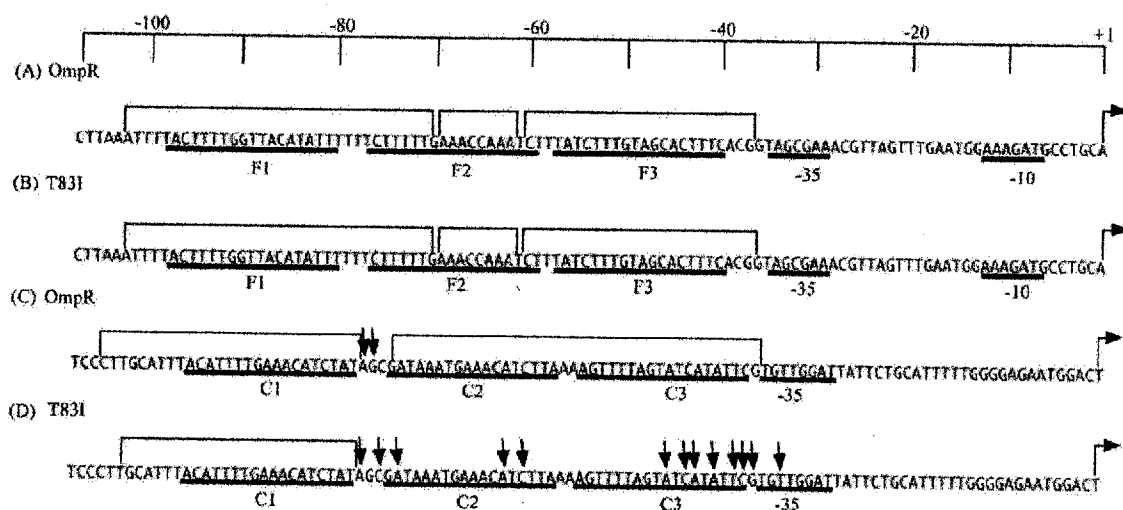
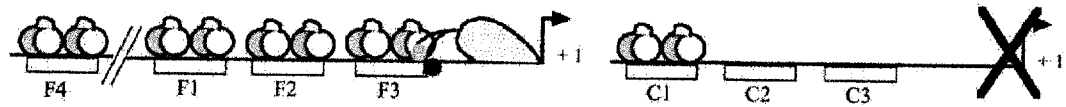


Figure 2.12. Model for the differential regulation of transcription from the *ompF* and *ompC* promoters. (A) represents the situation at low osmolarity while (B) indicates events at in high osmolarity. OmpR is represented as a two-domain molecule where striped regions denote the amino terminus and open regions indicate the carboxyl terminus, joined by a linker. Circles indicate the low osmolarity conformation that T83I is capable of assuming, and squares represent the uncharacterized conformation necessary for activation of *ompC* transcription and repression of *ompF*. The RNA Polymerase complex is included as a stippled structure, with the amino terminal domain of the  $\alpha$  subunit as a gray circle and the carboxyl terminal domain of  $\alpha$  in black. A large X indicates that transcription does not occur under conditions shown.

(A) Low osmolarity



(B) High osmolarity

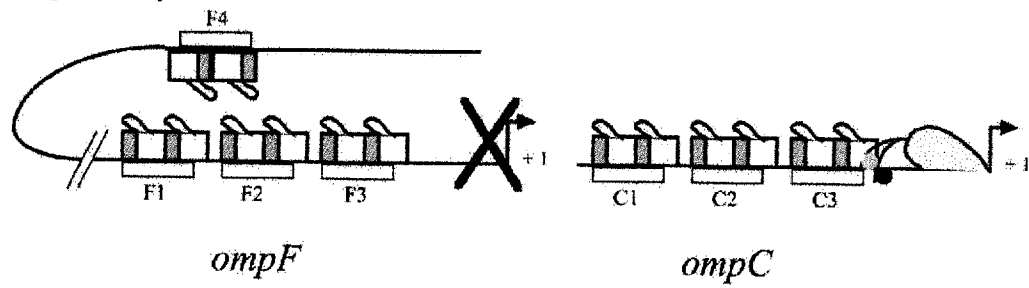


Table 2.1. DNA binding by T83I. The average values for DNA binding curves using fluorescence anisotropy. The oligonucleotide used in the binding assay is indicated in the first column. The apparent  $K_d$  calculated from the binding curves  $\pm$  the standard deviation are shown for OmpR and T83I in columns 2 and 4, respectively. The number of binding curves used in this calculation, n, is indicated in columns 3 and 5. NSB, non-saturable binding, ND, not determined. <sup>a</sup> Dissociation constants from (Head, C. G. *et al.*, 1998), <sup>b</sup> dissociation constant from (Tran, V. K. *et al.*, 2000).

Oligonucleotide	OmpR K <sub>d</sub> (nM)	<i>n</i>	T83I OmpR K <sub>d</sub> (nM)	<i>n</i>
F1	194 ± 60 <sup>a</sup>	4	175 ± 45	4
F2	NSB <sup>a</sup>	3	ND	
F3	NSB <sup>a</sup>	3	ND	
F4	355 ± 89 <sup>b</sup>	5	152 ± 36	3
F123	497 ± 61 <sup>a</sup>	4	40 ± 14	3
C1	101 ± 59 <sup>a</sup>	5	59 ± 19	5
C2	NSB <sup>a</sup>	2	ND	
C3	NSB <sup>a</sup>	2	ND	
C123	87 ± 32 <sup>a</sup>	5	NSB	3

## **Chapter 3**

### **The Linker Region Plays an Important Role in the Inter-domain Communication of the Response Regulator OmpR (Journal of Biological Chemistry 277: 32714-32721, 2002)**

#### **3.0 Preface**

In the following chapter, I carried out the experiments in Figures 3.1, 3.2, 3.3, 3.4 and 3.7, as well as the molecular biology described in Table 1 and the data analysis and modeling for Figure 3.6. Ricardo Oropeza performed the DNase I footprinting assays shown in Figures 3.5 and 3.8.



### 3.1 Abstract

OmpR is the response regulator of a two component regulatory system that controls the expression of the porin genes *ompF* and *ompC* in *Escherichia coli*. This regulator consists of two domains joined by a flexible linker region. The amino-terminal domain is phosphorylated by the sensor kinase EnvZ, and the carboxyl terminal domain binds DNA via a winged helix-turn-helix motif. *In vitro* studies have shown that amino terminal phosphorylation enhances the DNA binding affinity of OmpR and, conversely, that DNA binding by the carboxyl terminus increases OmpR phosphorylation. In the present work, we demonstrate that the linker region contributes to this communication between the two domains of OmpR. Changing the specific amino acid composition of the linker alters OmpR function, as does increasing or decreasing its length. Three linker mutants give rise to an OmpF<sup>+</sup> OmpC<sup>-</sup> phenotype, but the defects are not due to a shared molecular mechanism. Currently, functional homology between response regulators is predicted based on similarities in the amino and carboxyl-terminal domains. The results presented here indicate that linker length and composition should also be considered. Furthermore, classification of response regulators in the same subfamily does not necessarily imply that they share a common response mechanism.

### 3.2 Introduction

Two component signaling systems are the predominant signal transduction pathways in prokaryotes, and the components are highly conserved (Hoch, J. A. and T. J. Silhavy, 1995). In *Escherichia coli*, a two component system that consists of the sensor kinase EnvZ and the response regulator OmpR regulates the expression of the outer membrane porins OmpF and OmpC in response to environmental osmolarity. At low osmolarity, OmpF predominates in the outer membrane; OmpC is expressed at high osmolarity (van Alphen, W. and B. Lugtenberg, 1977). In response to an unidentified environmental signal, the EnvZ kinase autophosphorylates at histidine 243, and transfers the phosphoryl group to aspartate 55 of OmpR (Aiba, H. and T. Mizuno, 1990; Delgado, J. *et al.*, 1993; Roberts, D. L. *et al.*, 1994). At low osmolarity, OmpR-P activates transcription of *ompF*, whereas at high osmolarity OmpR-P represses *ompF* transcription and activates transcription of *ompC* (Aiba, H. and T. Mizuno, 1990; Slauch, J. M. and T. J. Silhavy, 1989).

OmpR consists of an amino terminal phosphorylation domain and a carboxyl terminal DNA binding domain, which are joined by a linker region (Kato, M. *et al.*, 1989; Tate, S. *et al.*, 1988). The two domains of OmpR influence each other. Phosphorylation of OmpR, at the amino-terminal aspartate 55, increases the DNA binding affinity of the carboxyl terminus (Aiba, H. *et al.*, 1989c; Head, C. G. *et al.*, 1998; Huang, K. J. *et*

*al.*, 1997; Rampersaud, A. *et al.*, 1994). Conversely, the presence of specific DNA binding sites increases the steady-state amount of OmpR-P formed *in vitro* (Ames, S. K. *et al.*, 1999; Qin, L. *et al.*, 2001). Our laboratory is interested in determining the mechanism responsible for this interdomain communication in OmpR.

The linker regions of response regulators are not highly homologous; however, they are relatively rich in glutamine, arginine, glutamate, serine and proline residues (Argos, P., 1990; Wootton, J. C. and M. H. Drummond, 1989). These linker regions have no predicted secondary structure. Wootton and Drummond termed these sequences Q-linkers due to the preponderance of glutamine residues (Wootton, J. C. and M. H. Drummond, 1989). These authors suggested that the Q-linkers serve the simple role of tethering the two domains to allow functional interactions to occur. However, point mutants have been isolated in the linker region of both OmpR and the homologous regulator DmsR that disrupt protein function (Aiba, H. *et al.*, 1994; Russo, F. D. *et al.*, 1993; Yamamoto, I. *et al.*, 1999). It was therefore of interest to determine whether specific amino acids were required for inter-domain communication of OmpR. In the present work, we have analyzed the effect of replacing the linker region with different amino acid sequences and found that some, but not all, linker substitutions allow OmpR-mediated transcriptional activation of the *ompF* and *ompC* genes.

OmpR orthologues are very highly conserved among enteric bacteria such as *Salmonella typhi*, *Salmonella typhimurium*, *Yersinia enterocolitica*, *Yersinia pestis*, *Enterobacter cloacae*, and *Shigella flexnerii*. As such, although the linker sequences are conserved, it is impossible to determine whether this has functional significance, as the entire protein varies by only 1-8 residues. Among more divergent species such as *Xenorhabdus nematophilus*, *Vibrio cholerae* and *Pseudomonas aeruginosa*, it appears that a central PGAP sequence (residues 128-131 in OmpR) is more highly conserved than the rest of the linker; this is where the previously isolated point mutants are located (Aiba, H. *et al.*, 1994; Russo, F. D. *et al.*, 1993; Yamamoto, I. *et al.*, 1999).

The Q-linkers of response regulators vary greatly in length as well as in sequence composition. For example, two highly homologous regulators from the same subfamily, OmpR and PhoB, have linker regions of 15 and 6 amino acid residues, respectively (Martinez-Hackert, E. and A. M. Stock, 1997a; Sola, M. *et al.*, 1999). An understanding of the molecular mechanism for transmitting information between the two domains will depend upon understanding the interface that connects them. As the putative inter-domain interface might vary with linker length, it is useful to understand the required length of the linker region for each regulator. Here we express OmpR constructs encoding linkers of various lengths and find that alterations in linker length impair OmpR function.

In our analysis of several linker mutants, it was striking that three different substitutions resulted in an OmpF<sup>+</sup> OmpC<sup>-</sup> phenotype. An examination of these OmpR mutants revealed that their porin gene expression profiles are similar, and yet they differ in their phosphorylation and DNA binding properties. Thus, there are different molecular mechanisms by which an OmpR linker mutant may present an OmpF<sup>+</sup> OmpC<sup>-</sup> phenotype *in vivo*.

### **3.3 Results**

#### **3.3.1 Changes in the sequence of the linker region of *ompR* result in altered porin expression**

Previous results indicate that the linker is important for inter-domain communication in OmpR signaling (Aiba, H. *et al.*, 1994; Kanamaru, K. and T. Mizuno, 1992; Russo, F. D. *et al.*, 1993). In order to test this hypothesis more directly, we constructed *ompR* mutants containing non-native amino acids in place of the endogenous linker sequence. These sequences replaced amino acids 123-137 of the *ompR* sequence (QANELPGAPSQEEAV) with either: QQQQQQQQQQQQQQQQ (Q15), QGSTGSSTGSTTGST (GST), GGGKGGKGGKGGKGG (GGK'), or QKINGELVISLIVES (ELVIS). The resulting constructs were expressed in the *ompF-lacZ* fusion strain MH513.101 and the *ompC-lacZ* fusion strain MH225.101 (Hall, M. N. and T. J. Silhavy, 1981b, 1981c).

We performed liquid  $\beta$ -galactosidase assays in media of low and high osmolarity to determine both the relative expression levels and the

osmoregulatory profiles of the mutants. The results are presented in Figure 3.1. Figure 3.1A shows that the *ompF-lacZ* fusion strain displays the normal osmoregulatory profile when OmpR is present, activating expression at low osmolarity, and repressing expression at high osmolarity. While both Q15 and GST activate expression of *ompF*, they fail to repress *ompF* transcription at high osmolarity. In contrast, like wild-type OmpR, GGK' is capable of both activating expression of *ompF* at low osmolarity and repressing its transcription at high osmolarity. ELVIS does not activate expression of the *ompF-lacZ* fusion.

In Figure 3.1B, results obtained in the *ompC-lacZ* fusion strain are reported. Wild-type OmpR, as well as Q15 and GST, activates expression of *ompC*. All three constructs demonstrate normal osmoregulatory profiles in the expression of this locus. Neither GGK nor ELVIS are capable of activating transcription from *ompC*.

### **3.3.2 Longer and shorter linker sequences abrogate *ompR* function**

Because *ompRQ15* expressed both *ompF* and *ompC*, it enabled us to examine the effect of changing the length of the linker sequence without concern for the specific amino acid residues deleted. We constructed Q15 variants, which added or removed amino acids from the linker region of *ompRQ15*.

The linker substitutions were examined in liquid  $\beta$ -galactosidase assays. The results are presented in Figure 3.2. When Q15 is substituted with a longer linker region of 20 amino acid residues (Q20), activation of

*ompF* is greatly diminished, although the construct still expresses *ompF* constitutively (Figure 3.2A). When OmpR contains a linker of 15 or 13 amino acids, it can activate expression of *ompF* to normal levels, but fails to mediate repression of this locus at high osmolarity. When the linker region is shortened to 11 amino acids, some loss of activation is observed, and this construct still fails to repress *ompF*. With a linker length of 10 amino acids, OmpR is barely capable of *ompF* transcriptional activation. Further reduction of linker length completely abolishes transcriptional activation.

Interestingly, the results obtained with the *ompC-lacZ* fusion clearly show that a decrease in transcriptional activation occurs with increasing and decreasing linker length (Figure 3.2B). Linkers of 20, 13 and 11 residues exhibit normal patterns of osmoregulated expression of *ompC*. However, deviation from the wild-type length of 15 decreases the level of transcription observed. When only 10 residues separate the amino and carboxyl-terminal domains of OmpR, no transcription is detected in logarithmically growing cells. Linkers of even shorter length similarly have no function. Thus, changing the length of the linker that separates the two domains of OmpR severely curtails its function *in vivo*. This finding has serious implications for function (signal output), and may limit the validity of comparisons between OmpR and closely related response regulators. For example, the recently crystallized OmpR homologue DrrD from *Thermotoga maritima* has a linker length of only 5

residues, and the limited inter-domain interface observed may not be relevant to the structure of OmpR (Bourret, R. B. *et al.*, 2002; Buckler, D. R. *et al.*, 2002; Kenney, L. J., 2002)(see Discussion).

### **3.3.3 Sequence changes in the linker affect OmpR phosphorylation and dephosphorylation by the kinase EnvZ**

Since two previously identified point mutants (G129D and P131S) of the OmpR linker region were OmpF<sup>+</sup> OmpC<sup>-</sup>, it was of interest that the GGK linker substitution also resulted in this phenotype (Aiba, H. *et al.*, 1994; Russo, F. D. *et al.*, 1993). In order to characterize the OmpF<sup>+</sup> OmpC<sup>-</sup> phenotype observed in OmpR mutants with a defective linker, we expressed and purified OmpR G129D, OmpR P131S, and OmpR GGK for *in vitro* analysis. We hypothesized that the OmpC<sup>-</sup> phenotype associated with substitutions in the linker resulted from a defect in interdomain communication, and thus it was of interest to compare the effects of DNA binding on phosphorylation and vice versa.

We performed kinase assays to determine whether phosphotransfer from the EnvZ kinase to the linker mutants was similar to wild-type OmpR. Figure 3.3 shows the results of this experiment. In Figure 3.3A, it is apparent that wild-type OmpR is phosphorylated upon incubation with  $\gamma$ -[<sup>32</sup>P]-ATP and EnvZ (lanes 1-3). The phosphorylated EnvZ is turned over as OmpR is phosphorylated and OmpR-P is dephosphorylated. Upon the addition of a two-fold molar excess of the



high affinity OmpR binding site from the *ompF* promoter (F1), slightly more OmpR-P is visible (lanes 4-6). In Figure 3.3B, P131S is phosphorylated (lanes 1-3), similar to the wild-type OmpR (Figure 3.3A). The addition of F1 DNA in this case only slightly increases the amount of P131S-P. G129D is also phosphorylated by EnvZ-P (Figure 3.3C, lanes 1-3), and in this case, the addition of DNA does not affect the phosphoprotein levels (lanes 4-6). GGK is phosphorylated by EnvZ-P (Figure 3.3D, lanes 1-3), but the addition of DNA has a remarkable effect on the level of GGK-P (lanes 4-6), as GGK-P decreases over time in the phosphorylation reaction when DNA is present. In summary, all three linker mutants are phosphorylated by EnvZ-P, but the effect of DNA on the GGK linker substitution is dramatic, causing an increase in turnover of GGK-P (Mattison, K. and L. J. Kenney, 2002).

*In vitro*, the EnvZ kinase is capable of both phosphorylating OmpR and dephosphorylating OmpR-P. When EnvZ is the phosphodonor, the observed increase in OmpR-P formation upon the addition of DNA is due to a decrease in the phosphatase activity of EnvZ (Mattison, K. and L. J. Kenney, 2002; Qin, L. *et al.*, 2001). We can quantify the effect of DNA on the phosphatase activity of EnvZ, using an assay that detects the release of  $P_i$  (Kenney, L. J., 1997). Upon incubation of OmpR, EnvZ and ATP there is a large increase in  $P_i$  production over time. The average rate of  $P_i$  release in the presence of OmpR is 7.1 nmol/ml/minute (Figure 3.4A, filled triangles). The P131S mutant possesses a net ATPase activity ( $P_i$

release) of 6.6 nmol/ml/minute, close to the level observed with wild-type OmpR (Figure 3.4A, filled circles). When G129D is incubated with EnvZ and ATP, there is a low rate of  $P_i$  production, 1.0 nmol/ml/minute (Figure 3.4A, open squares). In the presence of GGK,  $P_i$  production is barely above background (0.3 nmol/ml/minute, Figure 3.4A, open diamonds).

When specific DNA such as the region upstream of the *ompC* promoter (C1-C2-C3) is included in the ATPase reaction, the level of OmpR-stimulated ATPase activity decreases dramatically, falling to 0.3 nmol/ml/minute (Figure 3.4B, filled triangles). None of the linker mutants follow this pattern. The ATPase activity in the presence of P131S does not decrease substantially in the presence of C1-C2-C3 (4.1 nmol/ml/minute, only a 2-fold decrease) (Figure 3.4B, filled circles). The  $P_i$  release stimulated by G129D is also not affected by the presence of DNA, decreasing approximately 1.5-fold, to 0.7 nmol/ml/minute (Figure 3.4B, open squares). These differences are small when compared with the approximately 20-fold reduction in phosphate turnover seen with wild-type OmpR (Compare filled triangles in Figures 3.4A and 3.4B). Both P131S and G129D are able to bind DNA (see below), and yet DNA binding does not increase the stability of the mutant phosphoproteins as it does for wild-type OmpR-P (Compare circles or triangles in Figures 3.4A and 3.4B). When specific DNA is included in the GGK reaction, a large increase in  $P_i$  production is observed (Figure 3.4B, diamonds). This

is the opposite of the effect of DNA on wild-type OmpR. GGK also binds DNA, as shown in the footprinting assay below. The interaction of GGK with DNA decreases the stability of GGK-P, this effect is diametrically opposed to that observed for OmpR (Mattison, K. and L. J. Kenney, 2002).

#### **3.3.4 Changes in the linker alter DNA binding at *ompC***

We characterized the DNA binding ability of all three of the linker mutants using a DNase I footprinting assay. We observed that all three of the mutants were capable of protecting the *ompF* promoter to the same extent as wild-type OmpR, as expected by their OmpF<sup>+</sup> phenotypes (data not shown). The *ompC* binding data are shown in Figure 3.5.

Figure 3.5A-C reveals that the three linker mutants have different DNA binding properties at the *ompC* promoter region. Both OmpR-P and P131S-P are capable of protecting the *ompC* promoter sequences from -104 to -40, as shown in Figure 3.5A. With the G129D point mutant, a different pattern of protection is observed (Figure 3.5B). Whereas OmpR-P is capable of protecting the entire *ompC* upstream region from -104 to -40, G129D-P only binds at the high affinity C1 site, from -104 to -75. Even at protein concentrations up to 2  $\mu$ M G129D-P, no binding is evident at the C2 or C3 regions. As observed with the point mutant G129D-P, the substituted linker mutant GGK-P only binds to the high affinity C1 region (Figure 3.5C). It seems likely that the OmpC-

phenotypes of two of the linker mutants (G129D and GGK) are due to a DNA binding defect at the -35 proximal regions of the promoter (sites C2 and C3). The P131S point mutant may be incapable of interacting productively with RNA Polymerase to initiate transcription, since it can bind to the entire *ompC* promoter region but does not activate transcription from this locus. Thus, the underlying defects in G129D and GGK are distinct from that of P131S, yet they all give rise to an OmpF<sup>+</sup> OmpC<sup>-</sup> phenotype (see Discussion).

### **3.4 Discussion**

#### **3.4.1 Changing the length of the OmpR linker inhibits transcriptional activation**

We chose to use Q15 as a basis for our studies of OmpR linker length in order to eliminate concerns that specific amino acid residues were being added or deleted. We discovered that a linker of 13-15 amino acid residues is optimal for OmpR function, with shorter linkers gradually decreasing the ability of the protein to activate transcription of the porin genes (Figure 3.2). This finding has important implications for the likelihood of similarity in the activation mechanisms of closely related response regulators. One OmpR family member, PhoB, which shares a high degree of sequence homology with OmpR, has a linker of only 6 amino acid residues (Blanco, A. G. *et al.*, 2002). Chimeric protein studies with CheY/PhoB have shown that  $\alpha$ -helix 5 in the amino terminus of PhoB inhibits transcriptional activation by the carboxyl terminus;

inhibition is relieved when the amino terminus is phosphorylated (Allen, M. P. *et al.*, 2001). This is unlike the signal propagation mechanism that controls OmpR signaling. Both the amino and carboxyl termini of OmpR are necessary for its function, and neither domain is inhibitory (Tsuzuki, M. *et al.*, 1994). Similarly, although the FixJ family members UhpA and NarL share high sequence similarity, the carboxyl terminus of NarL is inhibited by its amino terminus, while that of UhpA is not (Baikalov, I. *et al.*, 1996; Webber, C. A. and R. J. Kadner, 1997). NarL has a short inter-domain linker of 6 amino acid residues, the linker of UhpA is 16 residues long (Webber, C. A. and R. J. Kadner, 1997). Thus, even within the FixJ family of response regulators, to which UhpA and NarL belong, there is a correlation between linker length and functional differences in the activation mechanism. In any attempt to predict functional homology based on sequence analysis, it may be useful to consider the length of the interdomain linker as well as the respective domain architectures.

An additional point worth noting is that longer linker sequence also reduced transcriptional activation by OmpR. Thus, a functional OmpR linker must be 13-15 amino acid residues in length. Because a linker of 20 amino acid residues should provide a similar increase in local concentration of the amino and carboxyl termini as a linker of 15 amino acid residues, it seems likely that the linker of OmpR plays some active role in directing the appropriate interaction between the two domains (Ames, S. K. *et al.*, 1999; Buckler, D. R. *et al.*, 2000; Kenney, L.

J., 2000). Evidence supporting this view comes from our studies of limited proteolysis with trypsin, which found that cleavage sites in the linker were sensitive to both phosphorylation and DNA binding in the amino and carboxyl-terminal domains, respectively (Ames, S. K. *et al.*, 1999; Kenney, L. J. *et al.*, 1995).

### **3.4.2 Substitutions in the OmpR linker reveal new classes of OmpR mutants**

Four different linker sequences were used to examine whether the sequence of the linker region was important for OmpR function. Of these, only the ELVIS linker did not activate transcription (Figure 3.1), suggesting that the linker region may require flexibility and hydrophilicity to allow appropriate interactions between the amino and carboxyl-terminal domains of OmpR. In contrast to the other substitutions, GGK' activates transcription from one locus (*ompF*<sup>+</sup>) and not the other (*ompC*<sup>-</sup>). GGK' is also the only construct that mediates repression of *ompF* expression at high osmolarity. The GGK linker is expected to be flexible, which may improve its ability to activate transcription over that of the ELVIS construct. The five positively charged residues concentrated in the linker region of GGK may allow OmpR to more readily adopt a conformation that represses *ompF* transcription at high osmolarity than one that allows expression of *ompC* (see Figure 3.6). Q15 and GST both contain hydrophilic residues and are predicted to be flexible. Thus, hydrophilicity and flexibility, as well as the length

requirement mentioned above, seem to be important for OmpR linker function.

We have shown that OmpR can retain its basic function of transcriptional activation at the *ompF* and *ompC* promoters when the endogenous amino acid sequence of the linker is altered (Figure 3.1). However, there are subtleties in porin gene regulation that are not maintained in the mutants with substituted linkers, as none of the constructs tested displayed wild-type osmoregulatory profiles (Figure 3.1A and B). With both *ompRQ15* and *ompRGST*, the ability to repress transcription of *ompF* at high osmolarity was lost (Figure 3.1A). Note that this does not result from constitutive expression of both porin genes, as osmoregulation of *ompC* is normal in these assays (Figure 3.1B).

We present a model in Figure 3.6 that incorporates these findings. We propose that unphosphorylated OmpR does not play a role in the osmoregulation of porin genes, because it interacts with the promoter regions with low affinity (Head, C. G. *et al.*, 1998). At low osmolarity, OmpR-P exists in a conformation that activates expression of *ompF* but binds only at the high affinity C1 site and as such fails to activate transcription from the *ompC* promoter (Figure 3.6A, circles). At high osmolarity, wild-type OmpR-P is capable of adopting a conformation that represses transcription of *ompF* (Figure 3.6B, squares) or one that allows binding at the downstream sites of the *ompC* promoter and activation of *ompC* expression (Figure 3.6B, triangles). The model predicts that two

different conformations of OmpR-P co-exist in the cell at high osmolarity, one of which represses *ompF* and another that activates *ompC*. The DNA binding sites at the *ompF* and *ompC* promoter regions may induce these alternate conformational changes. We can explain the phenotypes of the linker mutants using this model (Figure 3.6C). GGK-P is capable of activating and repressing *ompF* but is unable to undergo the conformational change that would allow binding at the C2 and C3 sites of the *ompC* promoter. Q15-P and GST-P are capable of activating transcription from both *ompF* and *ompC* but cannot access the conformation that would direct repression loop formation and repress transcription at *ompF*.

### **3.4.3 Mutations that confer an OmpF<sup>+</sup> OmpC<sup>-</sup> phenotype do so by different mechanisms**

The three linker mutants described in the present work share an OmpF<sup>+</sup> OmpC<sup>-</sup> porin profile but have different molecular defects. G129D and GGK fail to bind the promoter-proximal C2 and C3 sites of the *ompC* promoter region, and this explains their failure to activate transcription from *ompC* (Figure 3.5). However, a closer examination of mutant phosphorylation properties indicates that, although the mutants have similar DNA binding properties, the G129D and GGK substitutions have altered the protein in different ways. The G129D substitution appears to have only quantitatively altered the effect of DNA on the stability of the phosphoprotein (Figures 3.3 and 3.4). GGK, however, has a dramatic



phenotype (Mattison, K. and L. J. Kenney, 2002). The results obtained with GGK in assays of phospho-transfer and  $P_i$  release are diametrically opposed to those seen with wild-type OmpR.

P131S can protect the same sites at *ompC* to which OmpR binds, indicating that this residue change most likely interferes with the ability of the P131S protein to contact RNA Polymerase, as suggested by previous studies (Figures 3.4B and 3.5) (Aiba, H. *et al.*, 1994).

We have thus examined the molecular phenotypes of three OmpR linker mutants with the same porin profiles, and found that no two behave in the same way. This result, together with the possibilities for conformational changes in OmpR-P revealed by the linker substitutions and depicted schematically in Figure 3.6, underscores the sophisticated mechanism by which OmpR and EnvZ control the osmoregulation of porin gene expression.

### **3.5 Materials and Methods**

#### **3.5.1 Construction of mutants**

*ompR* was subcloned into the Bluescript KS vector using *HindIII* and *XbaI* sites. To create some of the mutations, two complementary oligonucleotides containing the desired mutation were used in a PCR reaction as described (Mattison, K. *et al.*, 2002a; Tran, V. K. *et al.*, 2000). These oligonucleotides are listed in Table 3.1 as group A. The linker is defined in this case based on structural determination by X-ray crystallography (20,21). The linker is defined by the lack of electron

density and its edges are the first residue after the  $\alpha$  5 helix in the receiver (N-terminus) domain and the last residue before the  $\beta$  strand of the C-terminal DNA binding domain. To create the linker substitutions, the endogenous *SalI* and *DraI* sites were removed from the pBluescript vector, and silent *SalI* and *DraI* sites were created in *ompR*, flanking the linker region. This mutagenesis was by the same PCR reaction (Mattison, K. *et al.*, 2002a; Tran, V. K. *et al.*, 2000). The oligonucleotides used for construction of this vector are listed as group B in Table 3.1.

Oligonucleotides corresponding to new linker sequences were then synthesized, annealed and ligated into the vector at these now unique *SalI* and *DraI* sites. The oligonucleotides used in this approach are listed as group C in Table 3.1. All of the linker mutants expressed in the strain MH225.101 except Q9 were found to be expressed in soluble form by Western Blot analysis (Figure 3.7).

### **3.5.2 Protein purification**

OmpR, G129D, P131S and GGK were expressed and purified as described (Head, C. G. *et al.*, 1998; Mattison, K. and L. J. Kenney, 2002).

### **3.5.3 $\beta$ -galactosidase assays**

All of the linker mutants were subcloned into pFR29\* using the *XbaI* and *HindIII* sites. pFR29\* is a derivative of pFR29 from which the *EnvZ* gene has been excised (Russo, F. D. and T. J. Silhavy, 1991). The plasmids were used to transform the strains MH225.101 and MH513.101. The MH225.101 genotype is  $F^- \Delta lacU169 araD139 rpsL relA$

*thiA malQ7 ompR101*  $\Phi(ompC-lacZ^+)$ 10-21 and the genotype of MH513.101 is *F<sup>-</sup>  $\Delta(lac)$  U169 rpsL relA thiA flbB ompR101  $\Phi(ompF-lacZ^+)$*  16-13 (Hall, M. N. and T. J. Silhavy, 1979, 1981c). Liquid  $\beta$ -galactosidase assays were performed exactly as described (Mattison, K. *et al.*, 2002a).

### **3.5.4 Phosphorylation assays and measurement of ATPase activity**

Phosphorylation reactions were carried out with EnvZ115 as described (Mattison, K. and L. J. Kenney, 2002). ATPase reactions were carried out as described (Mattison, K. and L. J. Kenney, 2002).

### **3.5.5 DNase I footprinting**

DNA was prepared as described (Mattison, K. *et al.*, 2002a). The proteins were phosphorylated with 25 mM acetyl phosphate (OmpR and GGK) or 25 mM phosphoramidate (OmpR, G129D and P131S) in phosphorylation buffer (50 mM Tris (pH 7.5), 50 mM KCl, 20 mM MgCl<sub>2</sub>) for three hours (acetyl phosphate) or one hour (phosphoramidate) at room temperature. The amount of OmpR-P was determined to be 74 % by C4 reversed phase HPLC analysis, and GGK-P was 58 % (Figure 3.4C). For Figures 3.4A and 3.4B, OmpR-P, G129D-P and P131S-P were 100%. Binding reactions were prepared, DNase I treated, and run on gels as described (Mattison, K. *et al.*, 2002a).

### **3.6 Acknowledgements**

The authors would like to thank the following for helpful discussions: Dr. David Farrens, Dr. Scott Landfear, Dr. Richard Brennan and Dr. Hans Peter Bächinger, OHSU; Dr. Edmundo Calva and Mario

Flores-Valdez, Universidad Nacional Autónoma de México, Cuernavaca. Jack Kaplan, OHSU, provided numerous invaluable suggestions and advice. Chantal Rison constructed the P131S mutant. We also thank the members of our laboratory, Don Walthers and Xiuhong Feng, for helpful discussions. RO was the recipient of a Conacyt Fellowship from the Mexican government and KM is a Predoctoral Fellow of the American Heart Association-Northwest Affiliate. Supported by NSF MCB-9904658 and NIH GM-58746 to LJK.

Figure 3.1. Transcriptional activation by OmpR with random linker sequences. The effect of *ompR* (WT) and the linker mutants *ompRQ15* (Q15), *ompRGST* (GST) *ompRGGK'* (GGK'), and *ompRELVIS* (ELVIS) on transcriptional activation of (A) *ompF-lacZ* and (B) *ompC-lacZ* fusions *in vivo* under conditions of low (open bars) or high (filled bars) osmolarity.  $\beta$ -galactosidase assays were performed as described (Mattison, K. *et al.*, 2002a). Four independent assays were performed on each strain, the standard deviation is indicated by the error bars.

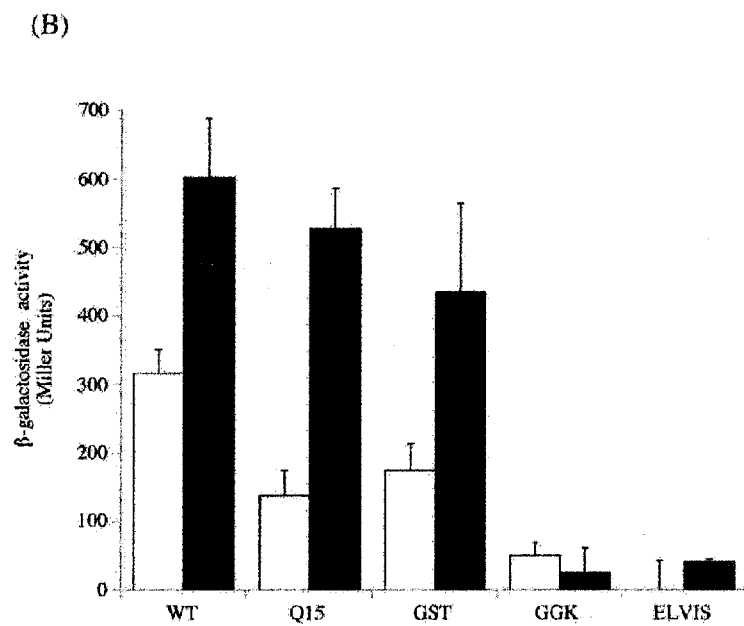
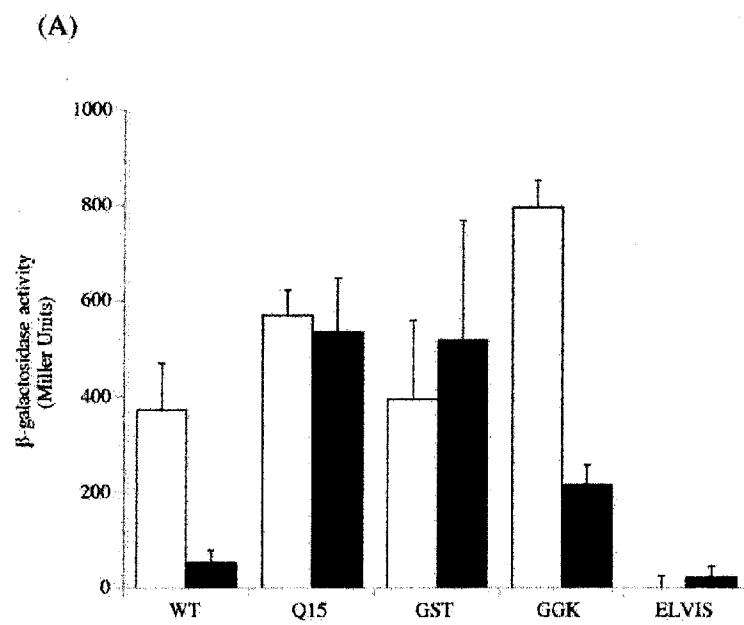
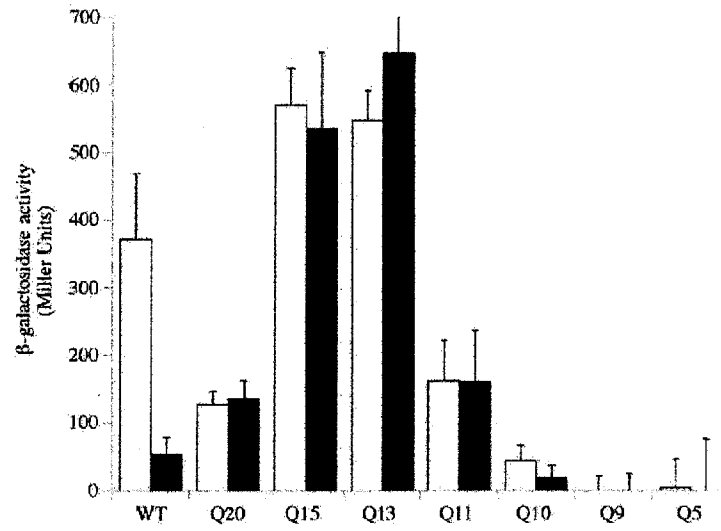


Figure 3.2. Transcriptional activation by OmpR with various linker lengths. The effect of *ompR* (WT) and the linker mutants *ompRQ20* (Q20), *ompRQ15* (Q15), *ompRQ13* (Q13), *ompRQ11* (Q11), *ompRQ10* (Q10), *ompRQ9* (Q9), and *ompRQ5* (Q5) on transcriptional activation of (A) *ompF-lacZ* and (B) *ompC-lacZ* fusions *in vivo* under conditions of low (open bars) and high (filled bars) osmolarity.  $\beta$ -galactosidase assays were performed as described (Mattison, K. *et al.*, 2002a). At least three independent assays were performed on each strain, the standard deviation is indicated by the error bars.

(A)



(B)

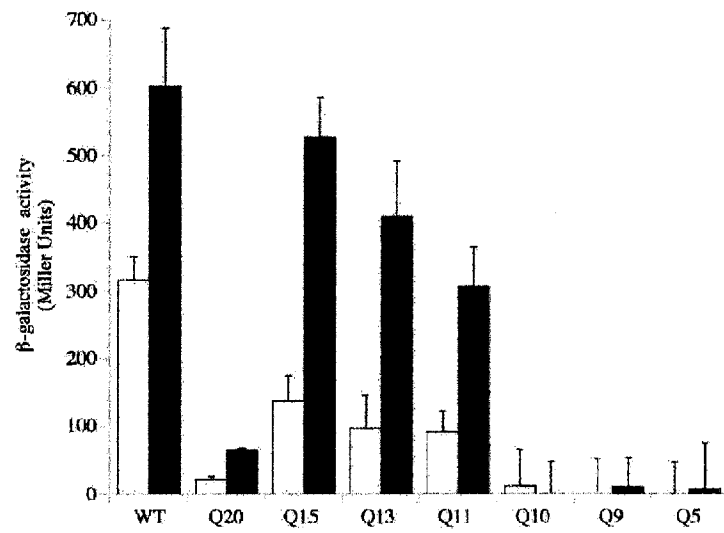




Figure 3.3. Phosphorylation of linker mutants by EnvZ 115. (A) OmpR and the linker mutants (B) P131S, (C) G129D and (D) GGK were phosphorylated as described (Mattison, K. *et al.*, 2002a). Lanes 1-3 in each panel show phosphorylation after OmpR has been incubated with [ $\gamma$ - $^{32}$ P]ATP and EnvZ 115 for 1, 2 and 3 hours. Lanes 4-6 show the same reaction performed in the presence of a 2-fold molar excess of F1 DNA (sequence as in (Head, C. G. *et al.*, 1998)).

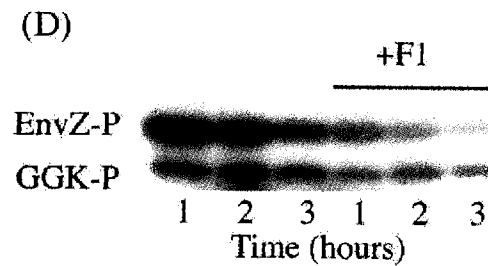
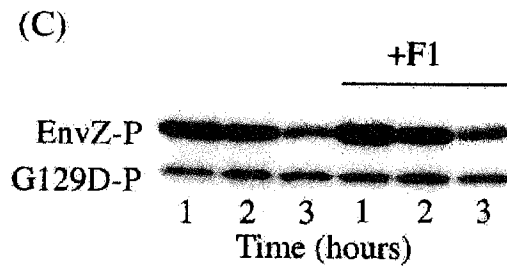
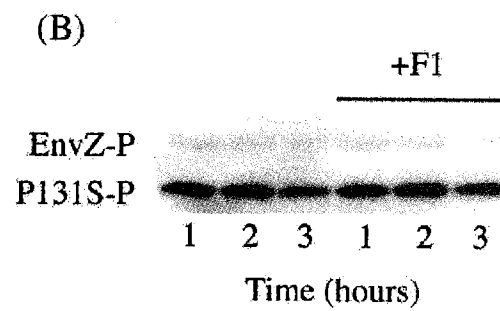
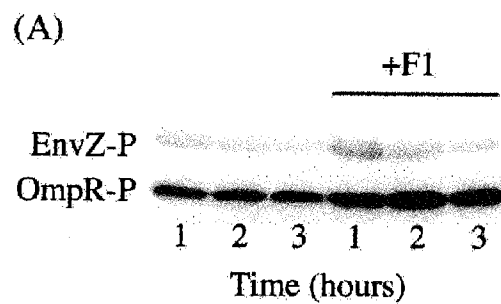
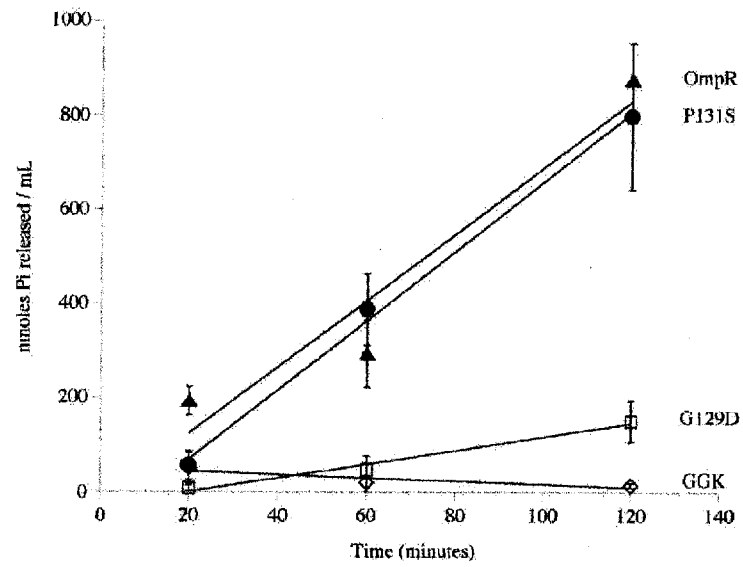


Figure 3.4. ATPase assay with the linker mutants. (A) Closed triangles show the  $P_i$  released after incubation of OmpR with EnvZ and ATP. Closed circles depict the same reaction with P131S, open squares correspond to G129D and open diamonds indicate GGK was used in the reaction. (B) The same assay was performed in the presence a 2-fold molar excess of the C1-C2-C3 oligonucleotide (sequence as in (Head, C. G. *et al.*, 1998)). The amount of inorganic phosphate produced represents the OmpR-stimulated component. At least three independent experiments were performed over 120 minutes and the values reported represent the averages from all time points taken. The error bars indicate the standard deviation.

(A) - C1-C2-C3



(B) + C1-C2-C3

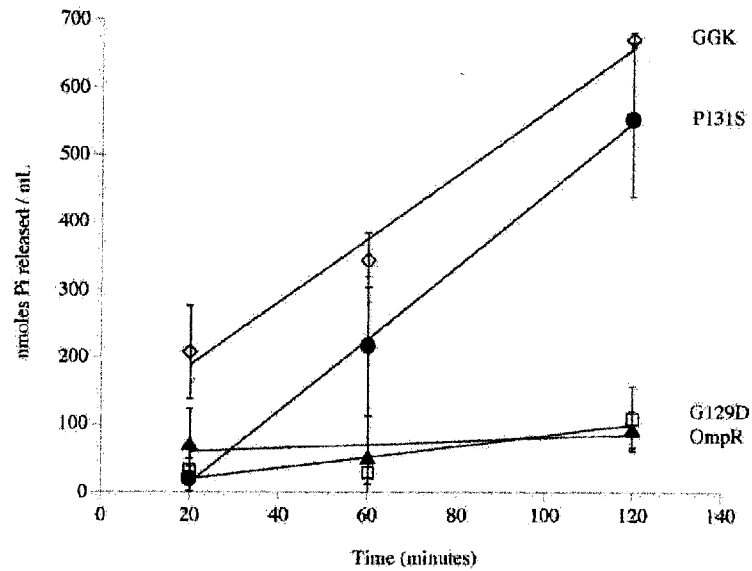


Figure 3.5. DNase I footprinting analysis of OmpR-P, G129D-P, P131S-P and GGK-P binding at the *ompC* promoter. Previously characterized OmpR binding sites are indicated to the right of each panel. The scale on the left of each panel indicates the position of each band relative to the transcriptional start site of the promoter, determined by comparison with dideoxy-termination sequencing reactions previously run in parallel with DNase I footprinting experiments. (A) OmpR-P and P131S-P binding to the *ompC* promoter. Lane 1 shows the oligonucleotide probe in the absence of protein and DNase I. Lanes 2 and 10 represent DNase I cleavage in the absence of OmpR. Lanes 3-8 and 11-16 show the cleavage pattern obtained when 0.14, 0.29, 0.73, 1.09, 1.6 and 2.1  $\mu\text{M}$  OmpR-P or P131S-P is included in the reaction. Lane 9 separates the two sections of the panel. (B) OmpR-P and G129D-P bound at *ompC*. Lanes are the same as in part A. (C) OmpR-P and GGK-P binding to the *ompC* promoter. Lanes as in part A except lanes 3-8 and 11-16 show the cleavage pattern obtained when 0.4, 0.8, 1.7, 2.5, 3.7, and 5.0  $\mu\text{M}$  GGK-P or OmpR-P is included in the reaction.

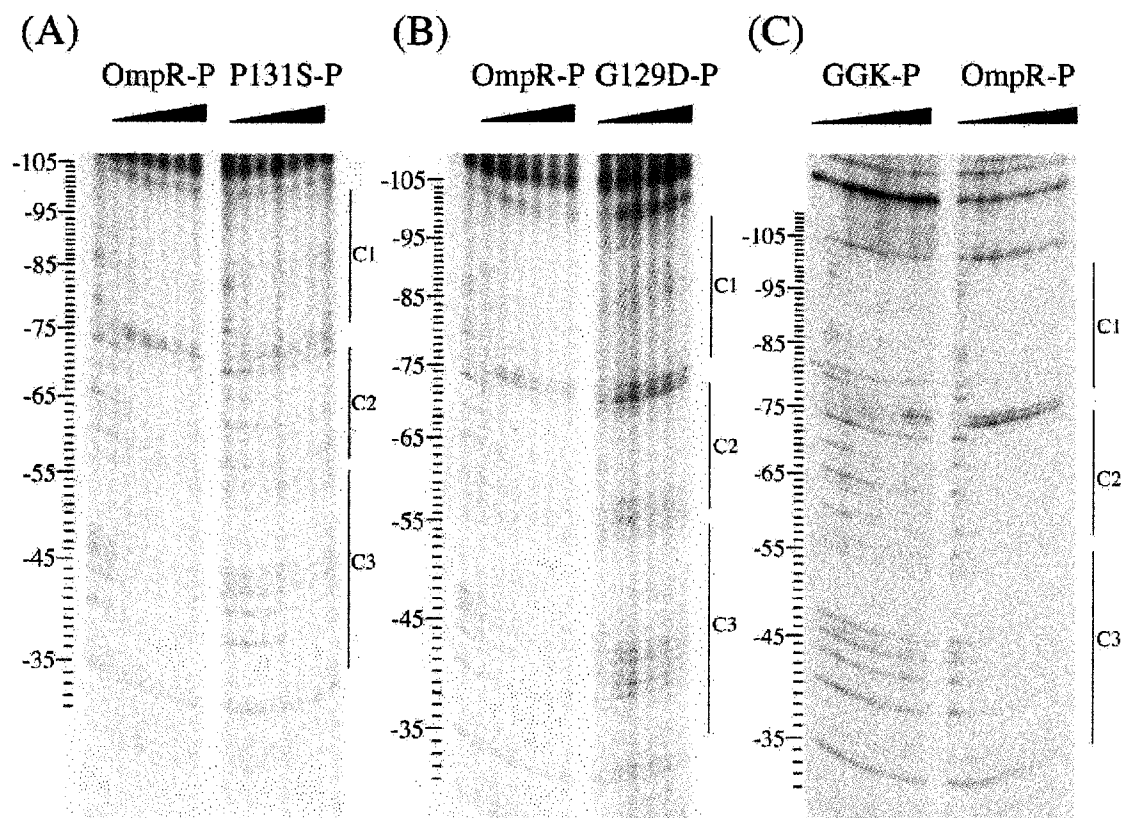
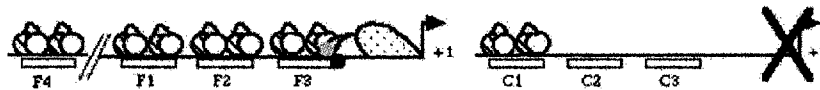
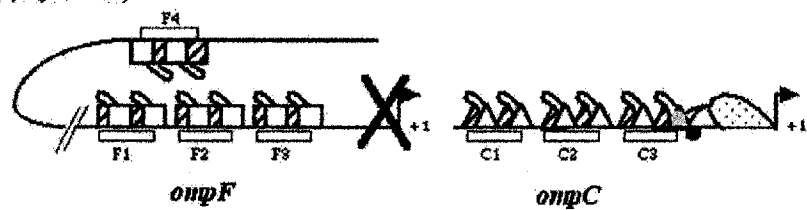


Figure 3.6. Model for the different conformational states of OmpR. (A) Is the situation at low osmolarity and (B) represents high osmolarity. OmpR is represented as a two-domain protein, with shaded regions corresponding to the amino terminus and open regions denoting the DNA-binding carboxyl-terminus. Circles indicate the low osmolarity conformation that all of the random linker mutants are capable of assuming, which leads to activation of *ompF* expression. Squares represent a conformation accessible to wild-type OmpR and GGK but not to Q15 or GST, which leads to repression loop formation and repression of *ompF* transcription. Triangles show an alternate high osmolarity conformation that is accessible to wild-type OmpR as well as to Q15 and GST (which GGK cannot adopt) and allows activation of transcription from the *ompC* locus. The RNA Polymerase complex is included as a mouse-shaped structure with the  $\alpha$ -subunit protruding as a tail-like appendage. A large X indicates that transcription does not occur under the conditions shown. (C) Shows which conformations the linker mutants are incapable of adopting.

(A) Low osmolarity



(B) High osmolarity



(C)

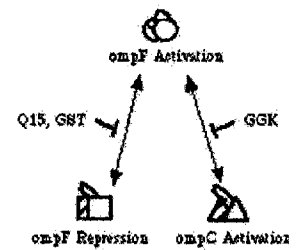




Figure 3.7. Western Blot analysis of linker mutant expression.

MH225.101 containing the various linker mutant constructs express OmpR protein in all cases but one. The linker mutant expressed is indicated at the top of each lane and the position at which an OmpR protein is expected to be found is indicated to the left of the gels.

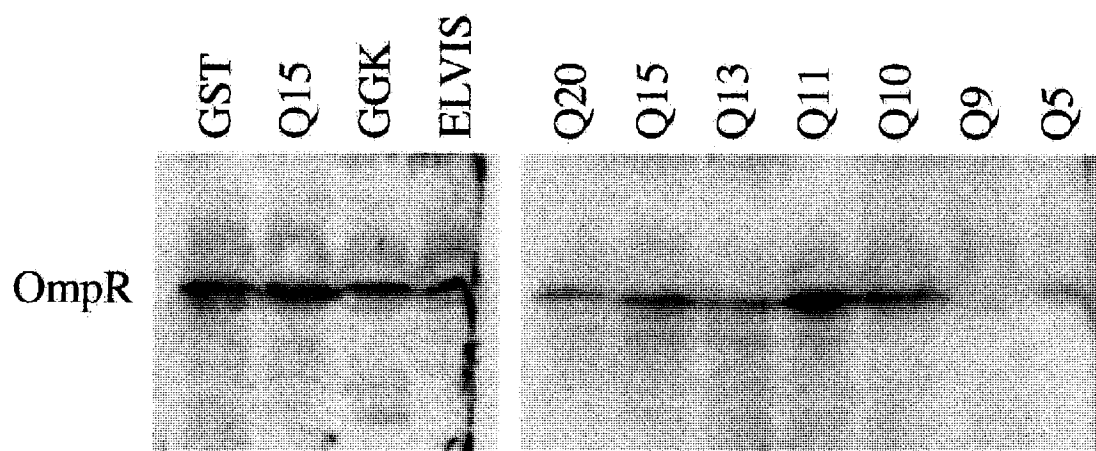


Table 3.1. Oligonucleotides used in mutant construction. As described in the Materials and Methods, the oligonucleotides in groups A and B were used with their complements in PCR reactions as described (Mattison, K. *et al.*, 2002a; Tran, V. K. *et al.*, 2000). Group C oligonucleotides were annealed to the complementary strands and ligated into the *SaII* / *DraI* cut pKAM vector.

Group	Construct Produced	Template	Oligonucleotide (5'-3')
A	<i>ompRG129D</i>	<i>ompR</i>	CAGGCGAACGAGCTCCCAGACGCACCC TCAC
	<i>ompRP131S</i>	<i>ompR</i>	ACTGCCAGGCGCATCATCACAGGAA G
	<i>ompRGGK</i>	<i>ompRGGK</i>	GCTGCGTCGAGGCGGCGGTAAAG
B	pBS-Sall	pBS	TCGATACCGTTGATCTCGAGGGGG
	pBS-Sall-DraI	pBS-Sall	CCTTTTAAGTTAAAAATGAAGTTTCAA ATCAATC
	pBS-Sall-2DraI	pBS-Sall-DraI	AGCAGAACCCTGAAAGTGCTCATC
	pBS-Sall-2DraI( <i>ompR</i> +Sall)	pBS-Sall-2DraI	GCGGTGCTGCGTCGACAGGCGAAC GA
	pKAM	pBS-Sall-2DraI( <i>ompR</i> +Sall)	TTTCGGTAAGTTTAAACTTAACCTCG
C	<i>ompRGST</i>		TCGACAGGGTTCAGGGACTGGCGGT TCCGGTACGGGCAGCGGTGGCAG ATTGCTTTCGGTAAGTTT
	<i>ompRQ15</i>		TCGACAGCAACAGCAACAGCAACAG CAACAGCAACAGCAACAGCAACAGA TTGCTTTCGGTAAGTTT
	<i>ompRQ20</i>		TCGACAGCAACAGCAACAGCAACAG CAACAGCAACAGCAACAGCAACAGC AACAGCAACAGCAAATTGCTTTCGGT AAGTTT
	<i>ompRQ13</i>		TCGACAGCAACAGCAACAGCAACAG CAACAGCAACAGCAACAGATTGCTTT CGGTAAGTTT
	<i>ompRQ11</i>		TCGACAGCAACAGCAACAGCAACAG CAACAGCAACAGATTGCTTTCGGTAA GTTT
	<i>ompRQ10</i>		TCGACAGCAACAGCAACAGCAACAG CAACAGCAAATTGCTTTCGGTAAGTT T
	<i>ompRGGK</i>		TCGACAGGGCGGTAAAGGCGGTAAA GGCGGTAAAGGCGGTAAAGGCGGT TTGCTTTCGGTAAGTTT
	<i>ompRELVIS</i>		TCGACAGAAAATTAACGGCGAACTG GTGATTAGCCTGATTGTGAAAGCAT TGCTTTCGGTAAGTTT

## **Chapter 4**

### **A new model for OmpR dimerization**

#### **4.0 Preface**

In the following chapter, I constructed all of the cysteine mutants as described in Table 4.1. I performed the cross-linking shown in Figure 4.1. Nicole Byers purified the proteins and performed the cross-linking shown in Figures 4.2, 4.3, and 4.4 under my direct supervision. Nicole and I together performed  $\beta$ -galactosidase assays, purified protein, assayed phosphorylation and performed cross-linking studies shown in Tables 4.2, 4.4, 4.5, and Figures 4.6 and 4.7. I completed the experiments shown in the rest of the Figures (4.5, 4.8, 4.9, 4.10, 4.11, and 4.12) and Table (4.3), except for the model of the OmpR dimer (Figure 4.13), which was constructed by Ann E. Maris at the University of California, Los Angeles.

## 4.1 Abstract

EnvZ and OmpR make up a two component signaling system responsible for the alternate regulation of porin gene expression in *Escherichia coli*. The OmpF porin is expressed at low osmolarity and the OmpC porin is found in the membrane at high osmolarity. The response regulator OmpR is phosphorylated by the sensor kinase EnvZ and OmpR-P controls the transcriptional activity of the promoters for *ompF* and *ompC*. Phosphorylation increases the DNA binding affinity of OmpR and OmpR is known to bind DNA as a dimer. OmpR may dimerize as a result of phosphorylation or when it binds the DNA target sites. We present evidence that the presence of specific OmpR binding sites leads to dimer formation. This indicates that the role of phosphorylation is to increase the intrinsic DNA binding affinity of each OmpR monomer, and not to promote dimer formation. Cross-linking studies do not provide support for the existing symmetric tandem model of OmpR dimer formation. We show that the  $\beta$ -sheet that begins the carboxyl terminal domain of OmpR is a key element of the OmpR dimer interface and present a new asymmetric model for OmpR dimerization.

## 4.2 Introduction

The response to environmental stimuli in prokaryotes and lower eukaryotes is often coordinated by signaling systems that utilize a histidine-aspartate phosphorelay (see (Hoch, J. A. and T. J. Silhavy, 1995) for reviews). Such systems are known as two component regulatory systems and in their basic form consist of a sensor kinase and a response regulator. The sensor kinase typically spans the inner membrane and is phosphorylated on a histidine by ATP in response to changing environmental conditions. The phosphoryl group is transferred from the phosphorylated sensor kinase onto an aspartic acid residue on the cytoplasmic response regulator. The phosphorylated response regulator controls signal output, for example, by binding to DNA and enhancing transcriptional activation of a given locus.

The two component signaling system consisting of the response regulator OmpR and the sensor kinase EnvZ plays a pivotal role in directing the expression of the porin genes *ompF* and *ompC* in response to changing environmental osmolarity (Hall, M. N. and T. J. Silhavy, 1981c; van Alphen, W. and B. Lugtenberg, 1977). The OmpF porin, with a larger pore size and concomitant faster flow rate, is expressed under conditions of low osmolarity, while OmpC is expressed at high osmolarity (Nikaido, H. and E. Y. Rosenberg, 1983).

EnvZ resides in the inner membrane and is phosphorylated at histidine 243 in response to an unidentified signal related to the

osmolarity of the growth medium (Forst, S. *et al.*, 1987; Liljestrom, P., 1986b; Roberts, D. L. *et al.*, 1994). OmpR is a cytosolic protein with two domains (Kato, M. *et al.*, 1989; Tate, S. *et al.*, 1988). The amino terminal domain contains the phosphorylation site at aspartate 55 and is highly homologous to the receiver domains of other response regulators, such as CheY and PhoB (Delgado, J. *et al.*, 1993; Sola, M. *et al.*, 1999; Stock, A. M. *et al.*, 1989; Volz, K. and P. Matsumura, 1991). The carboxyl terminal domain of OmpR (OmpRc) consists of a winged helix-turn-helix DNA binding motif (Kondo, H. *et al.*, 1997; Martinez-Hackert, E. and A. M. Stock, 1997a). There are some interesting structural similarities and differences between OmpRc and other winged helix-turn-helix proteins (Kenney, L. J., 2002). One characteristic of OmpR family members is the presence of a four-stranded  $\beta$  sheet located amino-terminally from the conserved DNA binding fold. This  $\beta$  sheet is not simply an addition to the core structure, as it packs tightly against the core and contributes several amino acid residues to the hydrophobic core of the domain (Martinez-Hackert, E. and A. M. Stock, 1997b). The function of the  $\beta$  sheet is unknown. However, in the crystal structure of PhoB (an OmpR family member) bound to DNA, it contributes residues to the dimer interface (Blanco, A. G. *et al.*, 2002). In another deviation from the usual winged helix-turn-helix motif, in the OmpRc structure, the loop between helices 2 and 3 (i.e., the turn of the helix-turn-helix motif) is unusually long (Kondo, H. *et al.*, 1997; Martinez-Hackert, E. and A. M. Stock,



1997a). This feature is not universally shared by OmpR family members. PhoB, for example, has a loop of only six residues (Blanco, A. G. *et al.*, 2002). In OmpRc, this region has been designated the  $\alpha$  loop, as it is postulated to contact the  $\alpha$  subunit of RNA Polymerase (Kondo, H. *et al.*, 1997; Martinez-Hackert, E. and A. M. Stock, 1997a; Pratt, L. A. and T. J. Silhavy, 1994; Russo, F. D. *et al.*, 1993). However, recent evidence emerging from our laboratory contradicts this view and suggests that this region is involved in DNA binding (D. Walthers and L.J. Kenney, unpublished results).

At present, there are three examples of co-crystal structures of response regulators bound to DNA: NarL, PhoB and Spo0A (Blanco, A. G. *et al.*, 2002; Maris, A. E. *et al.*, 2002; Zhao, H. *et al.*, 2002). PhoB and Spo0A are in the same subfamily as OmpR, their structures indicate a head-to-tail mode of binding (Blanco, A. G. *et al.*, 2002; Zhao, H. *et al.*, 2002). However, although OmpR and PhoB are highly homologous structurally, they are mechanistically distinct (Mattison, K. *et al.*, 2002b; Walthers, D. *et al.*, 2003). For example, the binding of DNA by the C-terminus of PhoB is prevented until the N-terminus is phosphorylated (Ellison, D. W. and W. R. McCleary, 2000). OmpR can bind DNA in the absence of phosphorylation, although it does so with lower affinity (Head, C. G. *et al.*, 1998). OmpR is a monomer in solution, PhoB is a dimer (McCleary, W. R., 1996)(K. Van Holde and L. J. Kenney, unpublished results). The isolated C-terminus of PhoB (PhoBc) can stimulate

transcription, whereas OmpRc cannot (Ellison, D. W. and W. R. McCleary, 2000; Tsuzuki, M. *et al.*, 1994). PhoB interacts with the sigma subunit of RNA Polymerase and OmpR interacts with alpha (Igarashi, K. *et al.*, 1991; Makino, K. *et al.*, 1996; Slauch, J. M. *et al.*, 1991).

The role of phosphorylation in controlling OmpR activity is not currently completely understood. Regulation of porin gene expression is mediated *via* phospho-OmpR (OmpR-P) levels and unphosphorylated OmpR does not play a role (Russo, F. D. and T. J. Silhavy, 1991; Slauch, J. M. and T. J. Silhavy, 1989). Phosphorylation of OmpR in the amino terminus increases the affinity of the carboxyl terminus for the upstream regulatory regions of both *ompF* and *ompC* (Aiba, H. *et al.*, 1989c; Harlocker, S. L. *et al.*, 1995; Head, C. G. *et al.*, 1998; Huang, K. J. and M. M. Igo, 1996). The two domains of OmpR interact as evidenced by the observation that DNA binding by the carboxyl terminus stimulates OmpR phosphorylation in the amino terminus, raising the possibility that OmpR might be activated while bound to its DNA target sites (Ames, S. K. *et al.*, 1999; Kenney, L. J., 2000). OmpR binds to each binding site within these regions as a dimer (Harlocker, S. L. *et al.*, 1995; Huang, K. J. and M. M. Igo, 1996). Phosphorylation of OmpR could stimulate dimerization, as reported for the response regulator FixJ, and Nakashima *et al.* have reported that OmpR-P cross-links more readily than does OmpR (Birck, C. *et al.*, 1999; Da Re, S. *et al.*, 1999; Nakashima, K. *et al.*, 1991b). In the present work, we demonstrate that DNA binding drives

OmpR dimer formation. The role of phosphorylation may be to increase the DNA binding affinity of each monomer.

OmpR is bound to DNA as a dimer, yet essentially nothing is known about OmpR:OmpR interactions (Harlocker, S. L. *et al.*, 1995; Huang, K. J. *et al.*, 1997). Recently, we characterized several substitutions that resulted in an unusual pattern of OmpR binding to DNA. These substitutions displayed normal footprinting behavior at *ompF*, but at *ompC*, the mutants were only capable of binding to the high affinity site C1. The substitutions were located in the phosphorylation site, in the inter-domain linker or in the turn of the helix-turn-helix motif (Mattison, K. *et al.*, 2002a; Mattison, K. *et al.*, 2002b)(D. Walthers & L.J. Kenney, unpublished results). In order to further examine OmpR protein:protein interactions, we introduced unique cysteines into the protein, followed by cross-linking using homo-bifunctional cross-linkers. Our choice of placement of the cysteine substitutions was based on a head-to-tail model for OmpR bound to DNA (Harrison-McMonagle, P. *et al.*, 1999). This model agrees well with existing data on OmpR DNA binding in that the recognition helix of each monomer contacts the major groove and adjacent monomers bind on the same face of the DNA helix. A weakness of the study lies in the fact that Cu-phenanthroline cleavage was not observed at all expected positions and some aberrant cleavage was found, resulting in the exclusion of much of the data from the eventual modeling process (Harrison-McMonagle, P. *et al.*, 1999).

Our results suggest that the previous model may not be correct. We propose a role for the  $\beta$  sheet, a unique feature of the OmpR winged HTH members, in facilitating protein:protein interactions. Thus, although response regulators such as PhoB and OmpR can share structural features such as the  $\beta$  sheet and the winged HTH motif, they are mechanistically distinct in their modes of DNA binding and transcriptional activation.

## **4.3 Results**

### **4.3.1 DNA binding stimulates OmpR dimerization**

OmpR is a monomer in solution (Harlocker, S. L. *et al.*, 1995; Jo, Y. *et al.*, 1986); K. Van Holde & L.J. Kenney, unpublished results), yet OmpR binds to DNA as a dimer. Phosphorylation of OmpR increases its affinity for the *ompF* and *ompC* promoter regions (Aiba, H. *et al.*, 1989c; Harlocker, S. L. *et al.*, 1995; Head, C. G. *et al.*, 1998; Huang, K. J. and M. M. Igo, 1996; Huang, K. J. *et al.*, 1997). Dimerization could occur as a consequence of phosphorylation, or OmpR could dimerize as it binds to DNA, as proposed for UhpA (Webber, C. A. and R. J. Kadner, 1997). In order to address this question, we used the homo-bifunctional cross-linker BS<sup>3</sup> to examine the effect of phosphorylation and DNA binding on OmpR oligomerization. A typical result is shown in Figure 4.1. In lane 1, OmpR is incubated in the presence of the cross-linking reagent BS<sup>3</sup>. The OmpR protein migrates in SDS PAGE at approximately 27 kDa, consistent with its molecular mass and no higher molecular mass

species are observed. The interaction of the cross-linker with OmpR alters its mobility on SDS PAGE, as is evident by the two bands, corresponding to modified (upper band) and unmodified (lower band) protein, respectively. Thus, as expected, OmpR exists as a monomer in solution. In the presence of the high affinity *ompF* binding site F1, a cross-linked complex is formed (lane 2). The molecular mass of the complex closely corresponds to the expected 54 kDa of an OmpR dimer. Higher order complexes of OmpR were not detected, even in the presence of composite DNA binding sites (data not shown). In lane 3, the cross-linking reaction in the presence of OmpR-P is shown. A barely detectable level of dimer is observed that is substantially less than the dimer formed in the presence of DNA (lane 2). Cross-linking in the presence of OmpR-P and F1 DNA is shown in lane 4. Again, the presence of DNA increases the level of dimer formed (compare lanes 3 and 4). Taken together, the results shown in Figure 4.1 suggest that the main consequence of phosphorylation is to promote high affinity binding to DNA and dimerization appears to be stimulated upon DNA binding. Alternatively, unphosphorylated OmpR could bind to DNA and dimerize, while phosphorylation might promote an interaction with RNA Polymerase that activates transcription. This is in contrast to other response regulators such as PhoB and FixJ, where phosphorylation stimulates dimerization in the absence of DNA (Birck, C. *et al.*, 1999; Da Re, S. *et al.*, 1999).

### 4.3.2 Cysteine mutants of OmpR form homodimers, not heterodimers

In order to identify the OmpR:OmpR dimer interface, we generated four unique cysteine substitutions at disparate positions within the OmpR protein. The locations were based on the existing model for a tandem dimer of OmpR molecules at each binding site (Harrison-McMonagle, P. *et al.*, 1999). We chose two residues each in the amino terminus and the carboxyl terminus that were predicted to be on opposite faces, based on the X-ray crystal structures of CheY and OmpRc (Martinez-Hackert, E. and A. M. Stock, 1997a; Stock, A. M. *et al.*, 1989). The positions of the cysteine substitutions are highlighted in Figure 4.2. Figure 4.2A is derived from the CheY structure (Bellsollell, L. *et al.*, 1994), the amino terminus of OmpR is predicted to fold in a similar manner. The yellow residue is alanine 103 of CheY, which corresponds to alanine 99 of OmpR. Threonine 112 of CheY is shown in red, this is the position of asparagine 108 of OmpR. The structure of the carboxyl terminal domain of OmpR is shown in Figure 4.2B. The leucine residue at position 161 is indicated in blue, the glycine at position 227 is in green. All four residues were replaced with cysteine and displayed wild-type patterns of porin gene expression, as indicated by  $\beta$ -galactosidase assays in *ompF-lacZ* and *ompC-lacZ* fusion strains (data not shown).

The four mutant proteins, each containing a unique cysteine, were used in cross-linking studies to examine OmpR:OmpR dimer formation

(shown in Figures 4.3 and 4.4). The proteins were incubated in the absence or presence of bis-maleimido-hexane (BMH), which contains two maleimides that react specifically with sulfhydryl groups separated by a six-carbon spacer arm (about 16 angstroms). In Figure 4.3A, the results of a typical cross-linking experiment with OmpR A99C are shown (represented by the yellow residue in Figure 4.2A). In lanes 1, 3 and 5, BMH is added to protein samples containing DTT and no cross-linked product is formed. In the absence of DTT and the presence of the cross-linker BMH, a low level of cross-linked product is formed that corresponds to the predicted size of an OmpR dimer (lane 2). In the presence of *ompF* or *ompC* DNA (lanes 4 and 6, respectively), there is an increase in the concentration of dimer formed. Thus, in the case of OmpR A99C, binding to DNA stimulates dimer formation. This result was surprising, since in the existing model of OmpR binding, the two cysteine residues would be too far apart to cross-link as a homodimer (Harrison-McMonagle, P. *et al.*, 1999).

Not all cysteine mutants formed homodimers, as can be seen in Figures 4.3B (N108C) and 4.3D (G227C). In either example, there is no dimer formation upon addition of the cross-linker. Thus, cysteine substitutions in the surface-exposed loop between  $\beta$  strand 5 and  $\alpha$  helix 5 in the amino terminus (N108, see Figure 4.2A), or in wing 1 (G227C, see Figure 4.2B) do not form homodimers. In the case of L161C, homodimers were formed upon addition of cross-linker (lane 2, Figure

4.3C), but the addition of DNA inhibited the dimer formation (compare lanes 4 and 6 with lane 2).

No evidence of heterodimer formation was observed when the cysteine-substituted mutants were incubated with one another (Figure 4.4). For example, when OmpR A99C was present in the reaction with N108C (Figure 4.4A), the level of cross-linked product was reduced, presumably as a consequence of decreasing the concentration of OmpR A99C (compare Figure 4.4A to Figure 4.3A). All combinations of cysteine mutants were tested, although only a subset of these are shown in Figure 4.4.

#### **4.3.3 OmpR cysteine substitutions S163C and V225C are impaired in porin gene expression**

In a previous study, results from DNA cleavage using Cu-phenanthroline conjugated to introduced cysteines in OmpR led to the proposal of a symmetric tandem orientation for OmpR binding to *ompF* (Harrison-McMonagle, P. *et al.*, 1999). The model incorporated the cleavage patterns from two OmpR mutants, S163C and V225C, yet their phenotypes were not reported. Because our cross-linking results in the present study (Figures 4.3 and 4.4) were in conflict with the proposed model, it was of interest to examine the phenotypes of the cysteine substitutions used in the previous study (shown in Figure 4.5). The cysteine substitutions were constructed by PCR and the *ompR* mutations were expressed in an *ompR* deletion strain containing either an *ompF*-



*lacZ* or *ompC-lacZ* fusion. In the absence of *ompR*, there is only a very low level of  $\beta$ -galactosidase activity (open columns). The filled columns indicate the  $\beta$ -galactosidase activity of the *ompF-lacZ* fusion (left panel) or *ompC-lacZ* fusion (right panel) in the presence of wild-type *ompR*. There is a significant stimulation in  $\beta$ -galactosidase activity of both fusions by *ompR* (dark columns). In contrast, the S163C mutant is defective in activating transcription at both *ompF* and *ompC* (light gray columns).  $\beta$ -galactosidase activity of *ompF-lacZ* is reduced to 50% of the wild-type level and at *ompC*, the defect is even more pronounced, as the activity is reduced to background levels. V225C is also defective in activating *ompC*, although it is comparable to wild-type OmpR in activating *ompF* (dark gray columns). Thus, neither mutant whose Cu-phenanthroline cleavage pattern led to the existing model of OmpR bound to DNA, mediates wild-type porin gene expression. It therefore seemed worthwhile to consider other modes of interaction of OmpR bound to DNA.

#### **4.3.4 The carboxyl terminal $\beta$ sheet of OmpR**

There are several crystal structures of the DNA binding domains of response regulators bound to DNA, including NarLc, PhoBc and Spo0Ac (Blanco, A. G. *et al.*, 2002; Maris, A. E. *et al.*, 2002; Zhao, H. *et al.*, 2002). Although OmpR is most structurally homologous to PhoB, it has many mechanistic features in common with UhpA, BvgA and NarL, members of the FixJ subfamily. These include the presence of multiple binding sites and interaction with the carboxyl-terminal domain of RpoA ( $\alpha$ -CTD), for

example. In our initial cross-linking studies, the cysteine replacement of L161 in wing 1 produced dimers in the absence of DNA. This surface of OmpRc is near the  $\beta$  sheet. Among winged HTH proteins, this structure is unique to OmpR family members and it is involved in forming the dimer interface when PhoB binds to DNA (Blanco, A. G. *et al.*, 2002; Martinez-Hackert, E. and A. M. Stock, 1997b). Within the OmpR family, the sequence of this  $\beta$  sheet is not highly conserved, suggesting that it could play a unique role (Martinez-Hackert, E. and A. M. Stock, 1997b). In order to examine the role of the  $\beta$  sheet in OmpR function, we constructed individual cysteine substitutions at each position of the 23 amino acid residues that comprise this region. The *in vivo* phenotypes of the substitutions were determined by  $\beta$ -galactosidase assays in *ompF-lacZ* or *ompC-lacZ* fusion strains in an *ompR* deletion background (Hall, M. N. and T. J. Silhavy, 1979, 1981c). The results are summarized in Table 4.2. With one exception (OmpR K142C), the cysteine mutants activated *ompF* to wild-type levels. Five of the mutants were defective in activating transcription at *ompC*: OmpR F140C, OmpR G141C, OmpR K142C, OmpR N146C and OmpR R150C (see Table 4.2). The cysteine mutants that did not exhibit wild-type expression profiles were not considered in our model of the OmpR dimer interface (see below).

#### **4.3.5 The $\beta$ sheet substitutions defective in porin gene expression are dominant to wild-type *ompR***

The five mutations in *ompR* that resulted in defective porin gene expression profiles (Table 4.2) were introduced into *ompF-lacZ* and *ompC-lacZ* fusion strains that contain a wild-type copy of the *ompR* gene (Hall, M. N. and T. J. Silhavy, 1979, 1981c). The results are shown in Table 4.3 and are expressed as a percentage of the  $\beta$ -galactosidase activity in the strain expressing wild-type *ompR*. Four of the five mutants tested were partially dominant to wild-type *ompR*; the exception was OmpR K142C. It was completely recessive to wild-type. The results from the dominance test indicate that all of the mutants (except possibly K142C) can bind to DNA and DNA binding of the mutant interferes with wild-type OmpR function.

#### **4.3.6 DNA binding stimulates phosphorylation of the cysteine mutants**

In order to determine whether the cysteine mutants could bind to DNA, we used an *in vitro* phosphorylation assay (Table 4.4). Acetyl phosphate phosphorylates OmpR slowly, but this rate is substantially increased in the presence of a two-fold molar excess of specific DNA (Ames, S. K. *et al.*, 1999). Phosphorylation by acetyl phosphate is not stimulated in the presence of non-specific DNA, or if the DNA binding sites are of low affinity (Ames, S. K. *et al.*, 1999). Thus, in order to stimulate phosphorylation, the protein has to bind to DNA with relatively

high affinity and then undergo a conformational change that alters the reactivity of the phosphorylation site. The cysteine-substituted proteins were expressed, purified and incubated with acetyl phosphate. The resulting mixture was separated by reversed phase HPLC on a C4 column and two peaks corresponding to OmpR and OmpR-P were observed. The area under the peaks was calculated and used to determine how much phospho-protein was generated (expressed as a percent of the total, see column 2, Table 4.4). A parallel reaction was also performed in the presence of the high affinity OmpR binding sites from the *ompF* (F1) or *ompC* (C1) regulatory region (columns 3 and 5, respectively) (Head, C. G. *et al.*, 1998). An increase in the level of OmpR-P in the presence of F1 or C1 DNA, compared to the level in the absence of DNA, indicates that the mutant protein is capable of high affinity binding to DNA (see fold-increase in columns 4 and 6). It is evident from Table 4.4, that the only cysteine mutant that does not bind to the C1 site with high affinity is F140C. This mutant binds to F1, the high affinity site from *ompF*, but it fails to bind to C1. This result also accounts for the OmpF<sup>+</sup> OmpC<sup>-</sup> phenotype of F140C reported in Table 4.2.

#### **4.3.7 Cysteine substitutions in the carboxyl terminal $\beta$ sheet of OmpR cross-link as homodimers**

We used the sulfhydryl-specific reagent BMH to cross-link the panel of cysteine substitutions in the carboxyl terminal  $\beta$  sheet of OmpR. The results of these experiments are summarized in Table 4.5. The

mutants fell into three classes: the first class did not form homodimers, the second class formed homodimers, but dimerization was reduced or prevented in the presence of *ompF* or *ompC* DNA. The third class exhibited an increase in the cross-linked dimer in the presence of DNA.

The first class, those that did not form homodimers, was the smallest class (Table 4.5, top panel). These residues are located in the first two strands of the  $\beta$  sheet, where it packs against helices  $\alpha 1$  and  $\alpha 3$  and contributes residues to the hydrophobic core (Martinez-Hackert, E. and A. M. Stock, 1997a). The G141C and N146C substitutions also resulted in defective porin expression profiles (Table 4.2). It appears that substitution of residues distal to the dimer interface is detrimental for expression of the *ompC* gene in particular.

More commonly, the introduced cysteine residues were cross-linked when the proteins were free in solution, but not when they were bound to DNA (Table 4.5, middle panel). M152C is an example of this class, this cross-linking experiment is shown in Figure 4.6A. M152C is cross-linked in solution (lane 2), but when bound to *ompF* DNA (lane 4) or *ompC* DNA (lane 6), cross-linking is prevented, as also observed with L161C (Figure 4.3C). Cysteines substituted at other positions that also behaved in this fashion include: F140C, F143C, T149C (i.e., homodimer formation is prevented in the presence of DNA). A related, but less severe effect was observed with many other substitutions, including: K142C,

L145C, R150C, M159C and P160C. In these examples, cross-linking was reduced, but not entirely prevented in the presence of DNA.

In the third class of cysteine-substituted mutants, homodimer formation was either not affected by or, in some cases, was stimulated in the presence of DNA (Table 4.5, bottom panel). Included in this class are: A139C, G148C, E151C, F153C, R154C, E155C, D156C and E157C. In Figure 4.6B, the cross-linking experiment is shown, using A139 as an example. In the absence of DNA, there is considerable homodimer formed (lane 2) and the homodimer increases in the presence of *ompF* and *ompC* DNA (lanes 4 and 6). This result suggests that the homodimer cross-linked across the  $\beta$  sheet is capable of binding to DNA. It is this third class of cysteine substitutions that is the focus of the remaining study.

The eight cysteine substitutions in this class were subjected to oxidation using hydrogen peroxide. Of this group, E151C and R154C did not cross-link and thus, were not considered further (data not shown). F153C was also not characterized, because the level of cross-linked dimer formed was considerably lower than the others (Table 4.5). All five of the mutant proteins selected for further study were comparable to wild-type OmpR in their ability to activate porin gene expression (Table 4.2). The results of our cross-linking experiments are summarized in Figure 4.7.

#### **4.3.8 The cross-linked proteins are phosphorylated by the kinase EnvZ**

It was of interest to determine whether the cross-linked dimers could be phosphorylated, a further indication of their functional state. A representative experiment with the mutant A139C is shown in Figure 4.8. When the cytoplasmic domain of EnvZ (EnvZc) is incubated with [ $\gamma^{32}\text{P}$ ]-ATP and the products separated on SDS PAGE, a radiolabeled band corresponding to EnvZ-P is evident (lane 1). Upon addition of A139C, phosphotransfer occurs and the mutant is phosphorylated (lanes 2-4). The level of EnvZ-P decreases, and as observed with wild-type OmpR, A139C-P does not increase over time, as EnvZ stimulates A139C-P turnover. When A139C is oxidized upon exposure to  $\text{H}_2\text{O}_2$ , both the monomer and the dimer are phosphorylated (Figure 4.8B). Similar results were obtained with cysteine substitutions G148C, E155C, D156C, and E157C (data not shown). Thus, both monomeric and dimeric mutant proteins are capable of phosphorylation by the kinase EnvZ.

#### **4.3.9 The cross-linked proteins bind to DNA**

In order to test whether the dimer interface across the  $\beta$  sheet was functional, we examined the ability of the cross-linked dimers to bind to DNA. We performed electrophoretic mobility assays in the absence and presence of the cross-linking reagent BMH (see Figure 4.9). The results using the F1 binding site are shown in panel A, the results with the C1 binding site are shown in panel B. Identical experiments performed with

each substitution in the presence of DTT (left) or in the presence of BMH (right) are shown. Three types of effects were observed, (i) mutants in which the cross-linked products were capable of binding to F1 and C1, (ii) mutants in which cross-linking inhibited binding to both F1 and C1 and (iii) mutants in which differential effects were observed at F1 DNA compared to C1. With mutants A139C and G148C, the binding to F1 or C1 in the presence of DTT is nearly identical to the binding in the presence of BMH (compare left panel with the right panel in both A and B), thus both mutants bind to F1 and C1 DNA. If the cross-linked homodimers were incapable of DNA binding, the concentration dependence in the presence of BMH would be shifted to significantly higher (monomer) concentrations.

The mutant E155C is impaired for binding at both *ompF* and *ompC* in the presence of the cross-linker. This is apparent by the fact that binding in the presence of BMH is shifted to higher protein concentrations, indicating that binding is most likely due to the monomer present in the reaction.

The D156C and E157C mutants are examples where binding at F1 is uninhibited by the presence of the cross-linker, but the cross-linked dimer is impaired in binding at C1. This result is consistent with the observed decrease in cross-linking of D156C in the presence of *ompC* DNA (Table 4.5). Thus, some of the cross-linked dimers are capable of



binding to DNA when homodimer formation is produced via cross-linking, indicating that a functional interface is formed.

We wished to demonstrate that the cases where we did not observe altered DNA binding in the presence of cross-linker correspond to cross-linked protein binding DNA. Figure 4.10 shows that the cross-linking reaction was working as expected at these lower protein levels. In this example, G148C was incubated in the presence or absence of cross-linker as for the DNA binding experiments and run on a reducing SDS-PAGE gel. Thus, Figure 4.10A shows G148C at 0, 1.3, 2.6, 5.3, 10.6, and 21  $\mu\text{M}$  (lanes 1-6) and Figure 4.10B shows G148C in the presence of cross-linker at the same range of concentrations. The amount of cross-linked protein was quantified as before and agrees with the results presented in Table 4.5, on average 29% of the protein was present as a dimer. We then diluted G148C to 71% of its original concentration, and performed the DNA binding assay again in the presence of DTT. This is shown in Figure 4.11. The left panel shows G148C binding at F1 and the right panel is G148C at C1. In each panel, the left half corresponds to diluted G148C bound in the presence of DTT. The concentration of G148C on the left of each panel ranges from 0.9 to 14.7  $\mu\text{M}$ . The right hand side of each panel is the undiluted G148C bound in the presence of the BMH cross-linker, in exactly the same manner as the results shown in Figure 4.9 (Concentrations range from 1.3 to 21  $\mu\text{M}$ ). Thus, for each set of binding experiments, the concentration of G148C monomer is

constant, but the right hand side of each panel contains more protein in the form of cross-linked G148C dimer. If the cross-linked protein did not participate in DNA binding we would expect both sides of each panel to give the same DNA binding pattern. We can clearly see that the right hand sides of both panels show an increase in DNA binding. At F1 (left panel), the diluted G148C begins to bind at 1.8  $\mu$ M (lane 3, left side) and a strong shifted complex is formed at 3.6  $\mu$ M (lane 4, left side). However, when the cross-linked protein is used (right side), binding is detectable as early as lane 2 (1.3  $\mu$ M), and is readily apparent by 2.6  $\mu$ M (lane 3). This indicates that the dimer produced by cross-linking does bind to DNA. With binding to C1 (right panel), the same trend is observed. While diluted protein forms only a faint complex in lane 2 (0.8  $\mu$ M), the cross-linked protein forms a dark band in lane 2. Since the additional protein in the reactions on the right hand side is cross-linked, the cross-linked protein contributes to the observed DNA binding. Since proteins cross-linked as homodimers through residues of the  $\beta$  sheet that begins the carboxyl terminus are capable of binding to DNA, the OmpR dimer cannot be formed as proposed (Harrison-McMonagle, P. *et al.*, 1999).

#### **4.3.10 The cross-linked proteins bind only to the high affinity site C1**

The specific binding of cross-linked proteins to the high affinity F1 and C1 sites demonstrates that cross-linking across the  $\beta$ -sheet can provide a functional OmpR dimer interface. However, we have previously

shown that in order to activate transcription at *ompC*, both the high affinity site and low affinity sites must be occupied (Mattison, K. *et al.*, 2002a; Mattison, K. *et al.*, 2002b). We used DNase I footprinting to determine whether the cross-linked protein could protect the entire upstream promoter region of *ompC* (shown in Figure 4.12). Figure 4.12A indicates that when G148C is incubated with DTT, to prevent disulfide bond formation across the cysteines, the protein is able to protect all of the *ompC* binding sites, C1, C2, and C3. This pattern of protection is similar to that observed with wild-type OmpR (Mattison, K. *et al.*, 2002a; Mattison, K. *et al.*, 2002b). In contrast, G148C fails to protect the low affinity C2 and C3 sites when the cross-linker BMH is present in the reaction (Figure 4.12B). The cross-linked protein protects the high affinity C1 site, in agreement with the electrophoretic mobility shift assay (Figure 4.9), but it is prevented from binding at the downstream sites. Either the presence of the cross-linker prevents G148C from binding to the low affinity sites, or constraining the protein as a result of cross-linking prevents low affinity site binding.

## **4.4 Discussion**

### **4.4.1 Oligomerization occurs after DNA binding**

A previous report demonstrated increased cross-linking of OmpR dimers upon phosphorylation (Nakashima, K. *et al.*, 1991b). Two mutants were isolated which were defective in this dimerization, and this was proposed to account for their OmpF<sup>-</sup> OmpC<sup>-</sup> phenotype. We have

shown here that DNA binding has a much more pronounced effect on OmpR dimer formation than does phosphorylation (Figure 4.1). Dimers of OmpR are increasingly detected when the protein is phosphorylated, but this effect is negligible when compared to that seen upon interaction of OmpR with DNA (Figure 4.1). Higher concentrations of OmpR than those shown in Figure 4.1 are required before the OmpR-P dimer is prominent (unpublished results). The E96A and R115S mutants isolated by Nakashima *et al.* were also found to be defective in DNA binding. The authors suggested that the dimerization defect may result in an inability of OmpR-P to bind DNA. In light of the evidence presented here, we propose that the lack of porin gene expression in the two mutant strains is a result of their failure to bind DNA and that the dimerization defect is secondary. The ability of OmpR and OmpR-P to form dimers is strongly dependent on their ability to bind to DNA and the dimerization is unlikely to occur in solution at physiological protein concentrations.

#### **4.4.2 F140C is OmpC<sup>-</sup> and dominant to wild-type**

The observation that F140C is OmpC<sup>-</sup> and this effect is dominant to wild-type (Tables 4.2 and 4.3) indicates that the mutant is capable of forming mixed oligomers with the wild-type OmpR protein and that these mixed oligomers are inactive. The phenylalanine residue at position 140 forms part of the hydrophobic core of OmpRc (Martinez-Hackert, E. and A. M. Stock, 1997a). Perhaps the cysteine substitution interferes with the proper folding of the protein, although its behavior during purification

and its ability to activate transcription of *ompF* suggest that this possibility is unlikely (Table 4.2).

#### **4.4.3 An asymmetric tandem model for OmpR dimer formation**

We present a new model for OmpR dimer formation at specific DNA binding sites (Figure 4.13). Members of the winged helix-turn-helix family of DNA binding proteins use many diverse mechanisms of DNA recognition, and therefore OmpR may use a previously uncharacterized manner of recognizing promoter sequences (Kenney, L. J., 2002). Therefore, since our cross-linking results are in conflict with the currently proposed tandem dimer orientation, we constructed a new model from the available data (Harrison-McMonagle, P. *et al.*, 1999). The model is shown in Figure 4.13. The sequence of the F1 OmpR binding site was used as the DNA molecule for the model; the structure is depicted in the most thermodynamically stable conformation for the base pairs involved. The OmpR monomers were then positioned on the DNA such that the recognition helices protected the appropriate base pairs based on the known hydroxyl radical footprint of OmpR binding to this region (Huang, K. J. and M. M. Igo, 1996). The orientation of the monomers with respect to each other was based both on the cleavage patterns obtained in the earlier study and on our cross-linking data (Harrison-McMonagle, P. *et al.*, 1999). In particular, we positioned A139, G148, D156, and E157 from one monomer in close proximity to the corresponding residues from the second monomer, since cysteine

helix of OmpR does not fit into the major groove. We have chosen to place the amino terminus of this helix in contact with major groove bases such that V203 interacts with the DNA (pink residue, Figure 4.13).

Residues outside of the recognition helix are also implicated in DNA binding by mutations which render OmpR incapable of binding DNA. These include T162 in  $\alpha$  helix 1 of OmpRc, R182 in  $\alpha$ 2, and T224 and G229 in  $\beta$  strands 6 and 7 of wing 2, respectively (Kato, M. *et al.*, 1995). T162 is shown in yellow in Figure 4.13. It is apparent that in our model, the hydroxyl group of the threonine residue is positioned such that it can hydrogen bond with the phosphate backbone of the DNA and stabilize the DNA-bound structure. The distances between the hydroxyl group and the phosphate moiety are 6Å and 3Å, for the left and right side monomers in Figure 4.13A, respectively. The arginine at position 182 is the cyan residue in Figure 4.13. This arginine extends down into close proximity with the DNA backbone, being separated from the phosphate by 10Å in the left side monomer and 3Å in the right side monomer in Figure 4.13A. This charge-charge interaction may also stabilize DNA-bound OmpR. T224 and G229 are not depicted in the model shown in Figure 4.13, but it is apparent that the  $\beta$  hairpin corresponding to wing 2 is in close proximity to DNA and that residues in this region may be involved in interactions with the DNA.

The final two residues highlighted in Figure 4.13 are P179 and S181 in dark green and light green, respectively. These residues are

thought to interact with RNA Polymerase; when they are mutated OmpR is able to bind DNA but not to activate transcription (Aiba, H. *et al.*, 1994; Kato, M. *et al.*, 1995; Pratt, L. A. and T. J. Silhavy, 1994). The residues are positioned such that when OmpR binds at F3 or C3 they are on the face of OmpR that would be located adjacent to the RNA Polymerase binding site at -35, as shown by the orientation in Figure 4.13A. It is interesting that this model provides a clear explanation for how two residues adjacent in the primary amino acid sequence can be important for different functions of the protein. The serine at position 181 is positioned optimally for interaction with RNA Polymerase, while the arginine residue at position 182 points down and contributes to DNA binding (light green and cyan residues, Figure 4.13).

While the cross-linked dimers were able to interact with the high affinity F1 and C1 sites (Figure 4.9), when G148C was cross-linked it protected only the C1 site and not the downstream C2 and C3 sites. It is not surprising that the cross-linked protein, while able to bind specific DNA, is overly constrained and as such cannot adjust to the conditions required for interactions between dimers, which normally allows for binding at the lower affinity C2 and C3 binding sites.

This new model provides a basis for further molecular studies of OmpR function. The interactions of this regulator with DNA and with RNA Polymerase are predicted by the model and the testing of these

predictions will further our understanding of the mechanism of OmpR-mediated transcriptional activation.

## **4.5 Materials and Methods**

### **4.5.1 Construction of mutants by PCR**

*ompR* was subcloned into the pBluescriptKS vector using the *HindIII* and *XbaI* restriction enzyme sites. The point mutations were introduced into *ompRC67A*, in which the endogenous cysteine of OmpR is replaced with an alanine. This cysteine-less protein behaves as wild-type OmpR in all assays tested (unpublished results) and ensures that any reactivity is due solely to the introduced cysteine. For each PCR reaction, two complementary oligonucleotides containing the desired mutation were used. The sequences of the oligonucleotides used are shown in Table 4.1. PCR reactions were performed as described (Mattison, K. *et al.*, 2002a; Tran, V. K. *et al.*, 2000).

### **4.5.2 Protein purification**

All of the mutant proteins were expressed and purified as described for wild-type OmpR (Head, C. G. *et al.*, 1998). In some cases, where only low levels of protein expression were achieved, the resulting fractions were concentrated before use with Amicon® Ultra centrifugal filter devices (Millipore).

### **4.5.3 $\beta$ -galactosidase assays**

All of the cysteine mutants were subcloned into the expression vector pFR29\* using *XbaI* and *HindIII* restriction endonuclease cleavage



sites. pFR29\* is pFR29 from which the *envZ* gene has been removed (Russo, F. D. and T. J. Silhavy, 1991). The plasmids were transformed into strains containing an *ompR101* null mutation and either an *ompF-lacZ* or an *ompC-lacZ* fusion (MH513.101 and MH225.101) (Hall, M. N. and T. J. Silhavy, 1979, 1981c). To test for dominance of the mutant phenotypes, MH513 and MH225 were used, these strains contain a wild-type chromosomal copy of the *ompR* gene and either an *ompF-lacZ* or an *ompC-lacZ* fusion, respectively (Hall, M. N. and T. J. Silhavy, 1979, 1981c). For the data shown in Table 4.2, assays were performed as described (Mattison, K. *et al.*, 2002a) and cells were grown in minimal A medium where the salts were at 0.2x for assays of *ompF-lacZ* expression or minimal A medium with 2x salts and 20% sucrose for assays of *ompC-lacZ* expression. For the results in Table 4.3 and Figure 4.5, cells were grown in LB and assays performed as described (Mattison, K. *et al.*, 2002a).

#### **4.5.4 Phosphorylation of mutant proteins**

OmpR proteins were phosphorylated with acetyl phosphate and separated on a C4 column using reversed phase HPLC as described (Ames, S. K. *et al.*, 1999; Mattison, K. *et al.*, 2002a). The area under each peak was determined and used to calculate the percentage of OmpR phosphorylation under each set of conditions, as reported in Table 4.4. In other experiments, EnvZ115 was used to phosphorylate cysteine mutants as described (Igo, M. M. *et al.*, 1989a; Mattison, K. *et al.*,

2002a). These reactions were performed in the presence of 1 mM DTT or 1 mM H<sub>2</sub>O<sub>2</sub>.

#### **4.5.5 Cross-linking of mutant proteins**

For the experiment shown in Figure 4.1, 4  $\mu$ M OmpR was incubated with either nothing, 10  $\mu$ M F1 DNA (sequence as in (Head, C. G. *et al.*, 1998)), 25 mM acetyl phosphate, or 10  $\mu$ M F1 + 25 mM acetyl phosphate for 3 hours in 50 mM Tris-HCl (pH 7.5), 50 mM KCl, 20 mM MgCl<sub>2</sub>. 100  $\mu$ M bis-[Sulfosuccinimidyl]suberate (BS<sup>3</sup>, Pierce, Sulfo-NHS ester) was added for an hour and the reactions were separated by SDS-PAGE. The resulting gel was stained with Coomassie Blue.

For the experiments shown in Figures 4.3, 4.4, and 4.6 (summarized in Table 4.5), approximately 10  $\mu$ M of the appropriate cysteine mutant was mixed with no additions, 30  $\mu$ M F1 DNA, or 30  $\mu$ M C1 DNA in the presence or absence of 50 mM DTT. When two proteins were mixed in the same assay, 5  $\mu$ M of each protein was used. 25  $\mu$ M bis-Maleimidoethane (BMH, Pierce) was added to each reaction and they were incubated for 30 minutes. Reactions that were previously without reducing agent were quenched with 50 mM DTT. The products were separated by SDS-PAGE and stained with Coomassie Blue. The dried gels were scanned and quantified using IPLabGel software to determine the percent cross-linking. Alternatively, bis-Maleimidobutane (BMB, Pierce) or bis-Maleimidoethane (BMOE, Pierce) were used as cross-linking agents. BMH has a six carbon linker resulting in a spacer arm

16.1 Å long, BMB has a four carbon linker which gives a spacer of 10.9 Å, and BMOE has a two carbon linker and a length of 8.0 Å. For all mutants, except M159C, the results from the three cross-linkers with different spacer arms are averaged in Table 4.5, since there were no differences observed with the shorter spacers. M159C failed to cross-link with BMOE, thus, only the results from BMH and BMB cross-linking are included in the averages presented.

#### **4.5.6 Electrophoretic mobility shift assays**

For electrophoretic mobility shift assays of DNA binding, 7.5 µM F1 or C1 DNA (Head, C. G. *et al.*, 1998) was phosphorylated with 5 µCi γ-<sup>32</sup>P[ATP] using T4 Polynucleotide kinase (New England Biolabs) for 30 min at 37°C. The reaction was stopped by heat inactivating the kinase for 10 min at 65°C. 0.3 µM labeled DNA was then added to reaction mixtures containing various concentrations of OmpR in 50 mM Tris-HCl (pH 7.5), 50 mM KCl, 20 mM MgCl<sub>2</sub>, 25 mM acetyl phosphate. Half of the reactions contained 1 mM DTT. 20 µM BMH was added and the reactions were incubated at room temperature for three hours. 1 mM DTT was added to samples that had not previously contained reducing agent and loading buffer was added to all samples (50 mM Tris-HCl (pH 7.5), 50 mM KCl, 20 mM MgCl<sub>2</sub>, 0.1 mg/mL heparin, 10 % (v/v) glycerol). The samples were run on an 8% acrylamide, 1X TBE gel, the gels were dried and exposed to Kodak X-Omat XB-1 film. For the experiment shown in Figure 4.10, the same reactions were performed, except

unlabeled DNA was used. The products were separated on 12% SDS-PAGE and stained with Coomassie Brilliant Blue.

#### **4.5.7 DNase I footprinting**

DNA probes were prepared as described (Mattison, K. *et al.*, 2002a). Binding reactions contained: 300,000 cpm *ompC* DNA, 54 mM Tris-HCl (pH 7.6), 1 mM EDTA, 70 mM KCl, 12 % (v/v) glycerol, 20 mM MgCl<sub>2</sub>, 50 mg/ml poly [d(I-C)], 25 mM acetyl phosphate and a range of G148C concentrations. In addition, one set of samples contained 1 mM DTT while the other contained 25  $\mu$ M BMH. The reactions were incubated for three hours at room temperature before cleavage with DNase I, precipitation, and electrophoresis as described (Mattison, K. *et al.*, 2002a).

#### **4.6 Acknowledgments**

LJK thanks Stephen Farrand and George Ordal, University of Illinois Urbana-Champaign for stimulating discussions. KM is a pre-doctoral fellow of the American Heart Association Northwest Affiliate. NB was the recipient of a Research Fellowship from the American Heart Association Northwest Affiliate (2001) and an RUE from the National Science Foundation (2002). Supported by NSF MCB-9904658 and NIH GM-58746 to LJK.

Figure 4.1. OmpR cross-linking with BS<sup>3</sup>. OmpR was cross-linked as described in Materials and Methods. The sizes of molecular weight markers in kiloDaltons are indicated on the left. Lane 1 is OmpR alone, lane 2 is OmpR in the presence of the F1 DNA binding site. Lane 3 is OmpR-P and lane 4 is OmpR-P in the presence of F1.

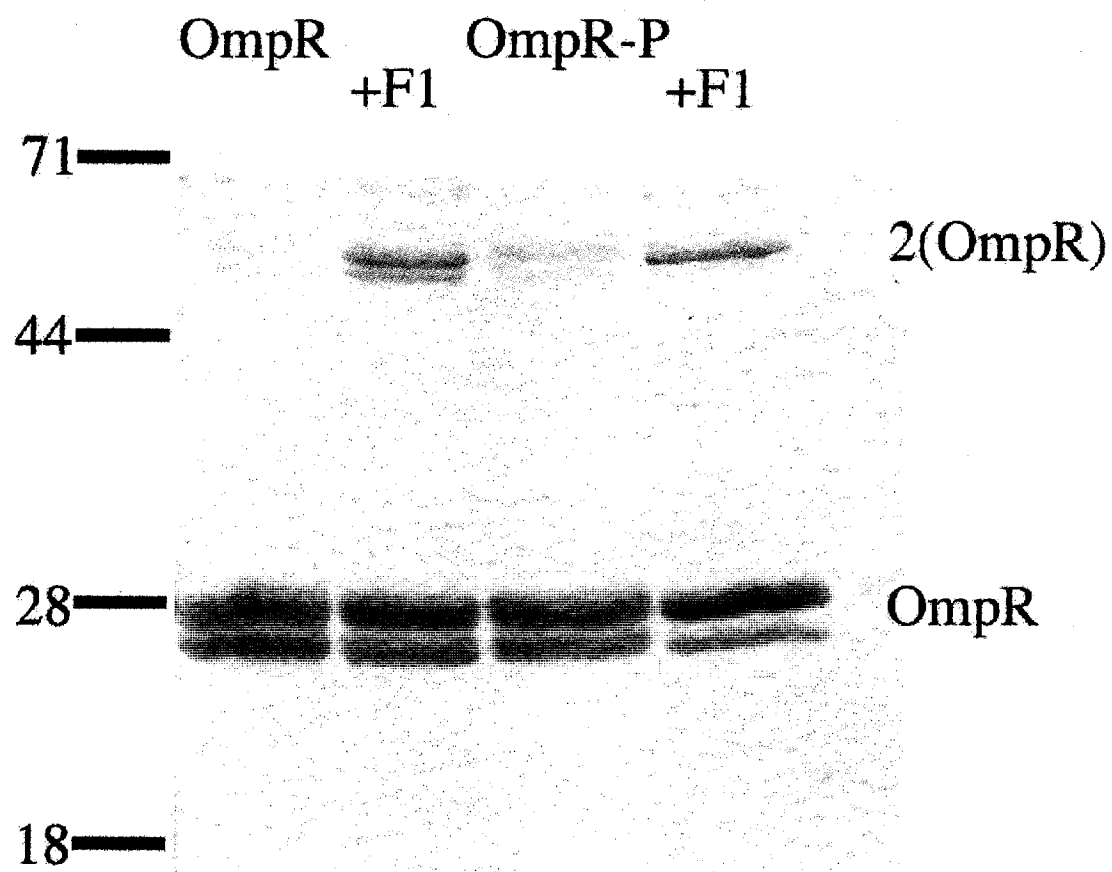
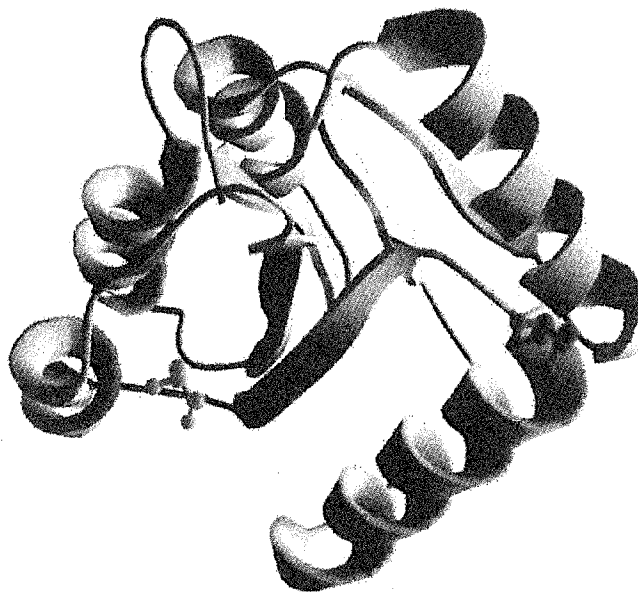


Figure 4.2. The (A) amino and (B) carboxyl terminal domains of OmpR. Coordinates were taken from the crystal structures of (A) CheY (PDB accession number 1CHN) (Bellssolell, L. *et al.*, 1994) and (B) OmpRc (PDB accession number 1OPC) (Martinez-Hackert, E. and A. M. Stock, 1997a) and the figures were generated using the Swiss PDB Viewer (DeepView) software. The yellow residue is an alanine at position 103 of CheY, which corresponds to A99 of OmpR. In red is a threonine at position 112 of CheY, which is located in the same position as N108 of OmpR. In blue is L161 of OmpR and in green is G227 of OmpR.

A



B





Figure 4.3. Cross-linking of four cysteine substitutions with BMH. 10  $\mu$ M each of (A) A99C, (B) N108C, (C) L161C, and (D) G227C were cross-linked as in Materials and Methods. In each case, lanes 1, 3, and 5 are reactions in the presence of DTT and lanes 2, 4, and 6 are in the presence of BMH. Lanes 1 and 2 are the proteins alone in solution, lanes 3 and 4 are in the presence of F1 and lanes 5 and 6 are in the presence of C1.

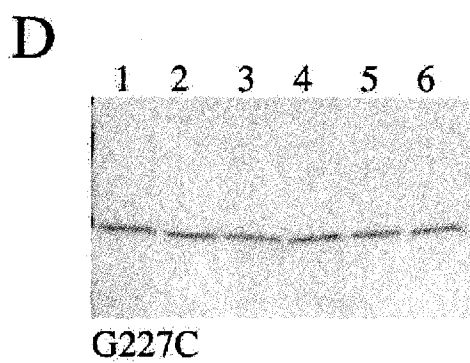
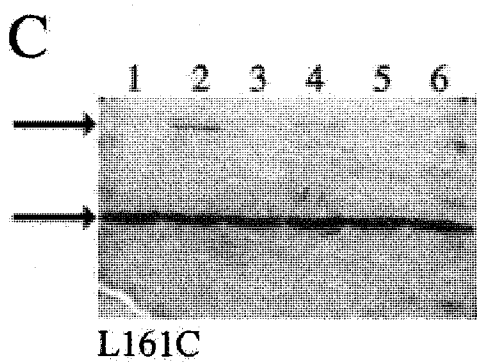
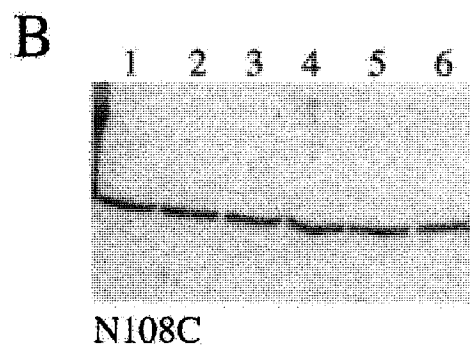
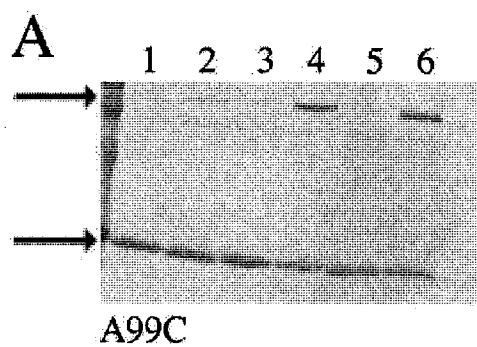


Figure 4.4. Cross-linking of combinations of cysteine substitutions with BMH. 5  $\mu$ M each (10  $\mu$ M total in each lane) of (A) A99C and N108C, (B) A99C and L161C, (C) A99C and G227C, and (D) L161C and G227C were cross-linked as in Materials and Methods. The cross-linking reactions are shown in lanes 2, 4, and 6, while lanes 1, 3, and 5 are in the presence of excess DTT so no cross-linking is observed. F1 DNA has been added in lanes 3 and 4, and C1 DNA is included in lanes 5 and 6.

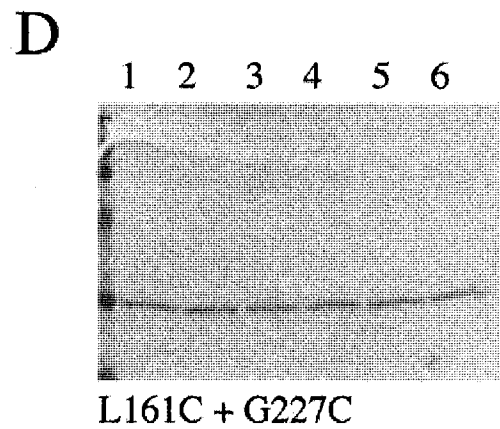
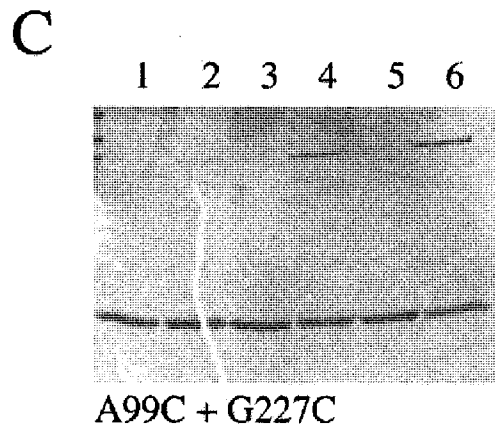
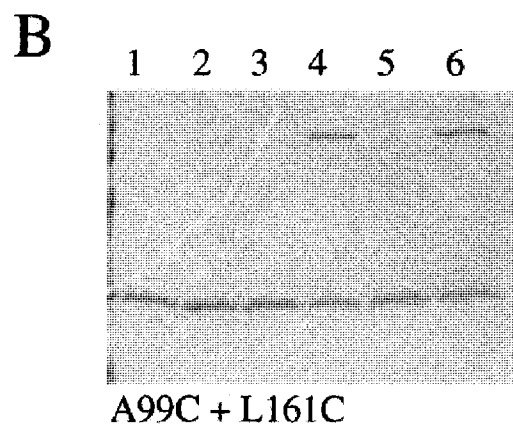
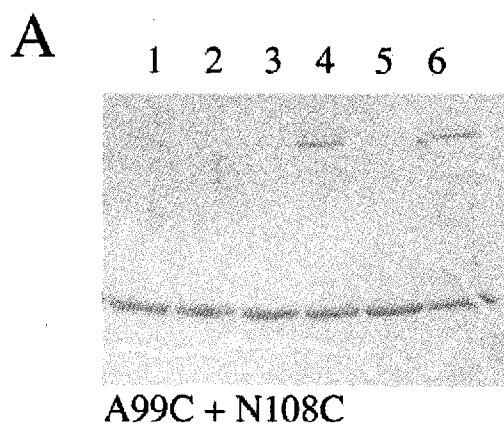


Figure 4.5. *In vivo* phenotype of the cysteine substitutions S163C and V225C.  $\beta$ -galactosidase assays were performed in LB as described (Mattison, K. *et al.*, 2002a). Data from *ompF-lacZ* fusion strains is shown on the left, and results with *ompC-lacZ* are on the right. Both strains lack a wild-type copy of *ompR*. Open bars show the strains alone (no expression in the absence of *ompR*), filled bars are the results when wild-type *ompR* is included. The light gray bars show  $\beta$ -galactosidase activity in the presence of *ompRS163C* and the dark gray bars are with *ompRV225C*. Data are the averages of at least three independent experiments, error bars represent the standard deviation of the mean.

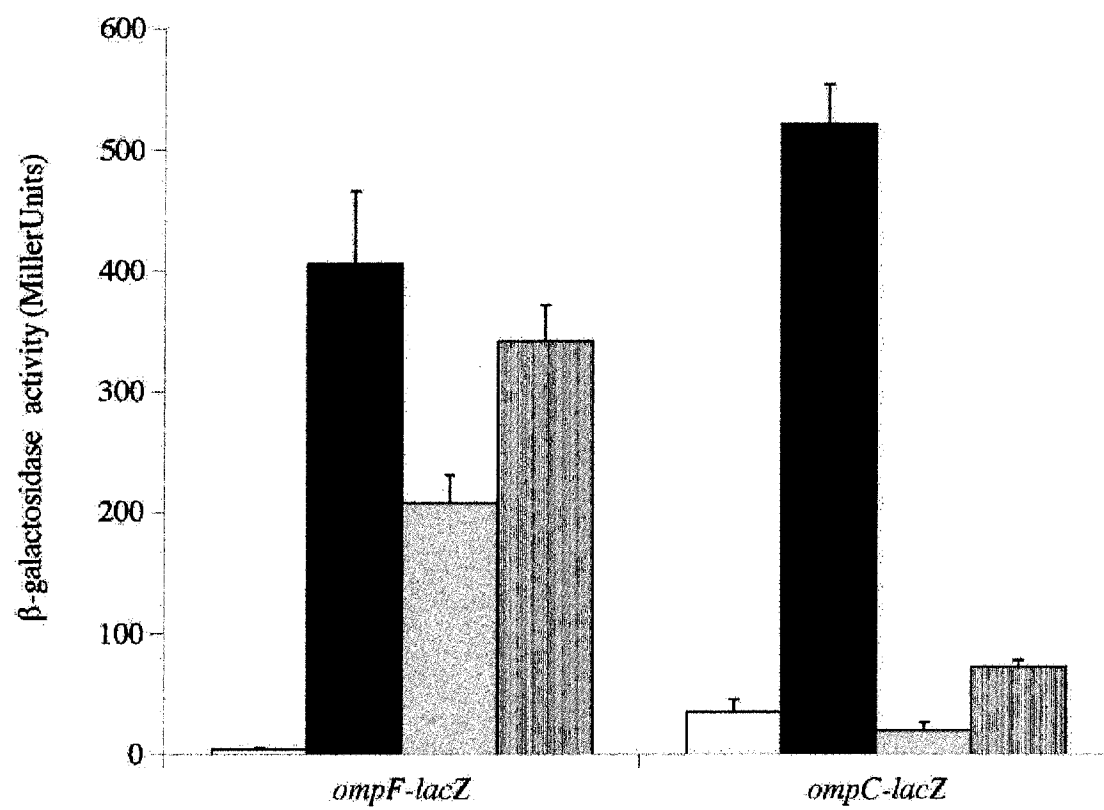
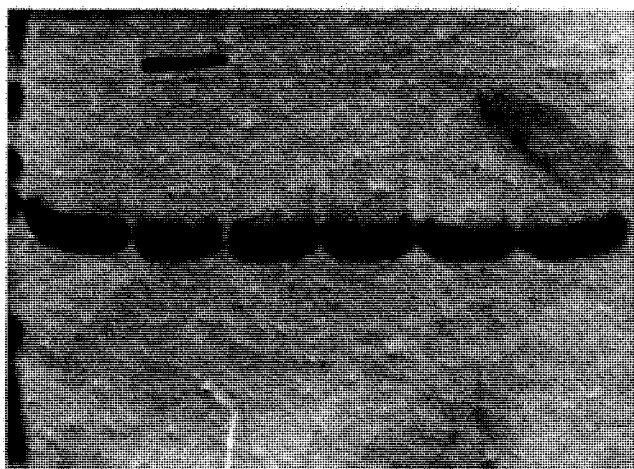


Figure 4.6. Cross-linking with BMH. 10  $\mu$ M (A) M152C and (B) A139C were cross-linked as described in Materials and Methods. For both gels, the cross-linking reactions are shown in lanes 2, 4, and 6. Lanes 1, 3, and 5 are controls where DTT is also present to quench the cross-linker. Cross-linking of the protein when free in solution can be seen in lanes 1 and 2. Lanes 3-6 show cross-linking when the protein is bound to DNA (F1, lanes 3, 4; C1, lanes 5, 6).

A

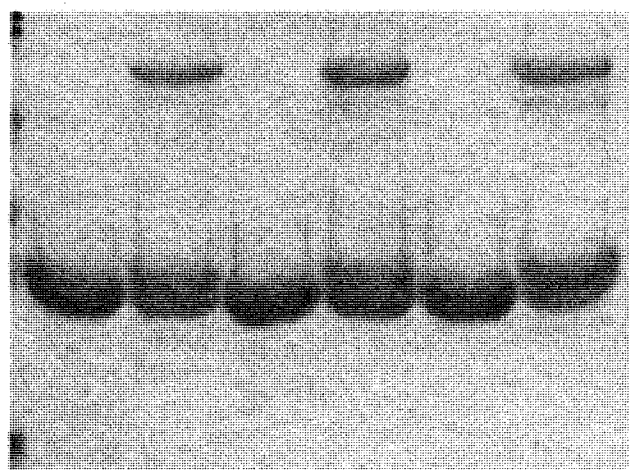
1 2 3 4 5 6



M152C

B

1 2 3 4 5 6

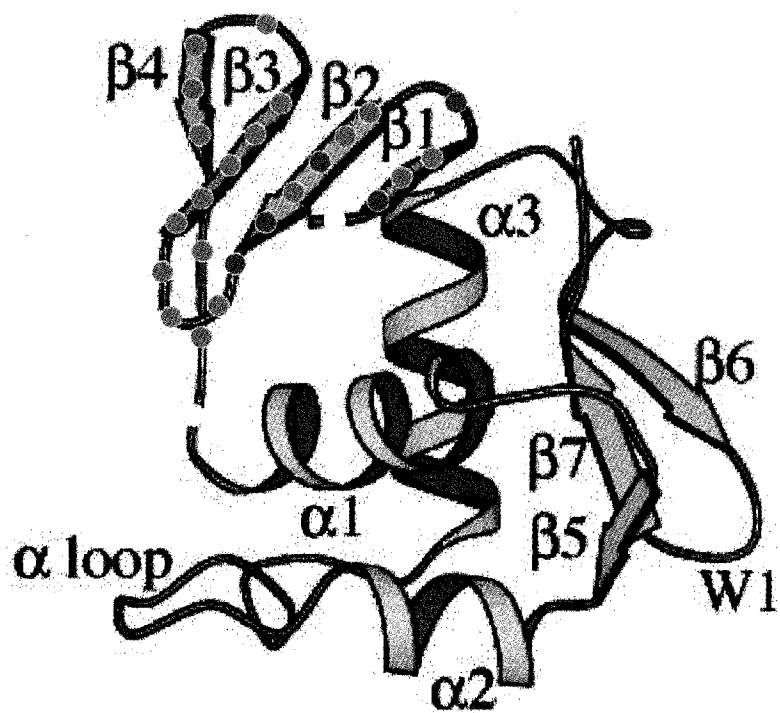


A139C



Figure 4.7. Summary of the cross-linking results with maleimide cross-linkers. Results reported in Table 5 are summarized graphically on a cartoon of the OmpR carboxyl terminal domain taken from (Martinez-Hackert, E. and A. M. Stock, 1997a). Dots are individual residues from I138 to L161. (A) represents cross-linking in the absence of DNA and (B) is cross-linking in the presence of DNA. Green dots indicate that a cross-linked dimer is formed, blue dots indicate that no cross-linking is observed. The orange dots in (B) indicate that cross-linking was still observed in the presence of DNA but that the levels of cross-linked dimer were less than when the protein was free in solution.

A



B

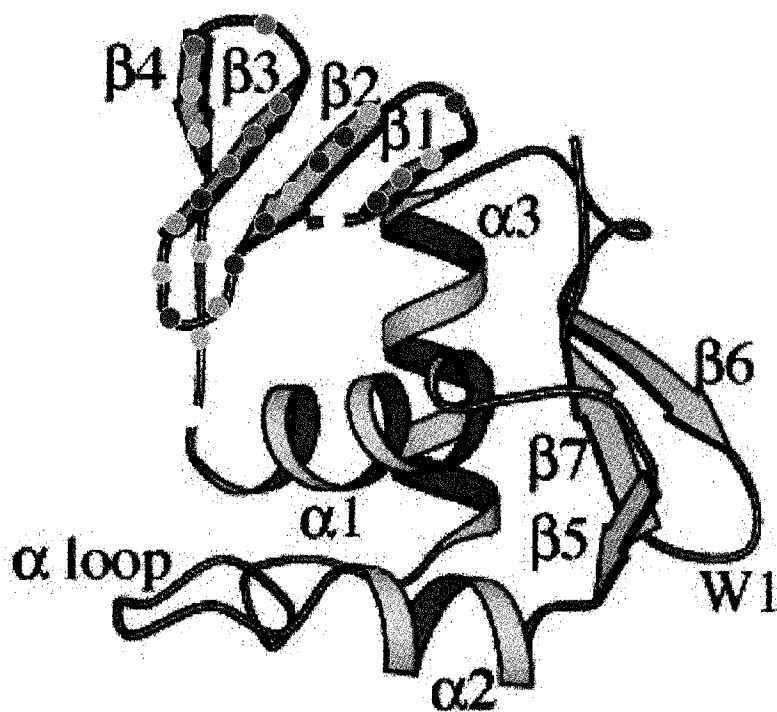
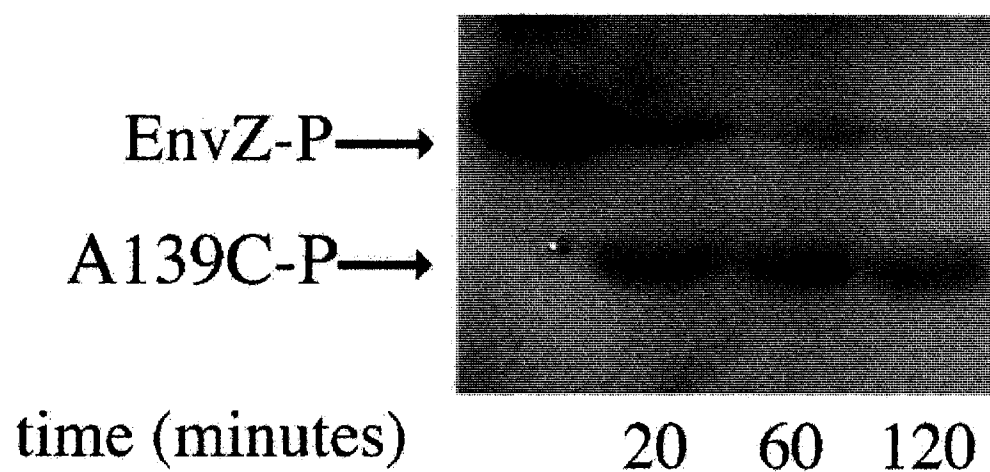


Figure 4.8. Example of phosphorylation of cross-linked cysteine mutants. A139C in the presence of (A) DTT or (B) H<sub>2</sub>O<sub>2</sub> was phosphorylated with EnvZ115 as described (Mattison, K. *et al.*, 2002a). The reaction was stopped at 20, 60 or 120 minutes, run by SDS-PAGE, and visualized by autoradiography.

## A. DTT



## B. H<sub>2</sub>O<sub>2</sub>

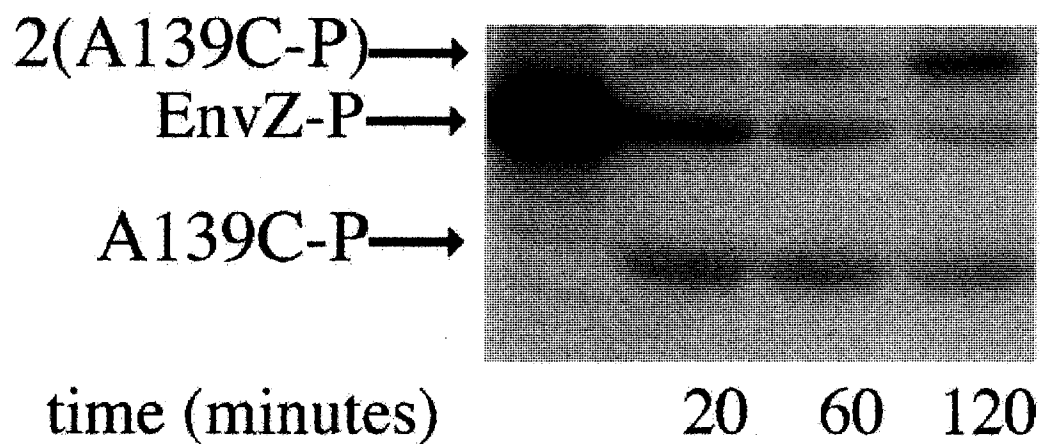
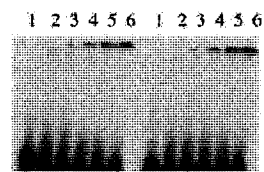


Figure 4.9. DNA binding by cross-linked cysteine mutants. DNA binding at (A) the F1 site and (B) the C1 site. In each panel, the left hand side shows binding in the presence of DTT and the right hand side is binding in the presence of the BMH cross-linking reagent. The concentrations of protein used from lanes 1-6 for A139C, G148C and E155C are 0, 1.3, 2.6, 5.3, 10.6, and 21  $\mu$ M. For D156C, 0.6, 1.2, 2.4, 4.8, and 9.6  $\mu$ M. For E157C, 0.4, 0.9, 1.8, 3.5, and 7.0  $\mu$ M.

A. F1

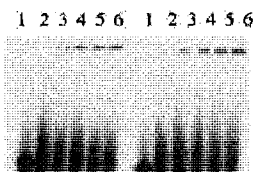
+DTT +BMH

A139C

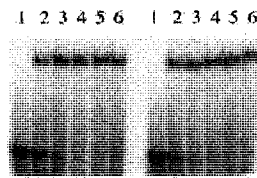
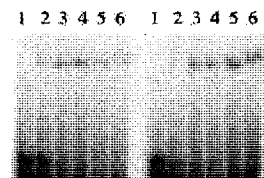


B. C1

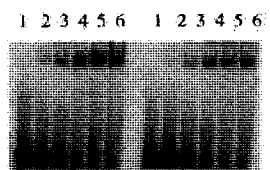
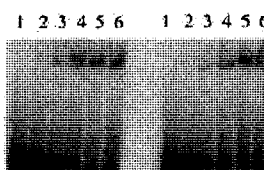
+DTT +BMH



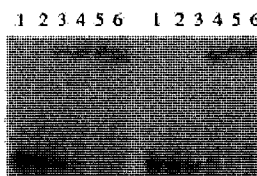
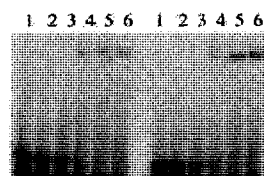
G148C



E155C



D156C



E157C

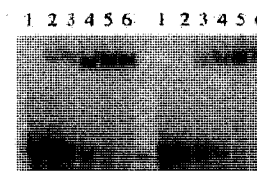
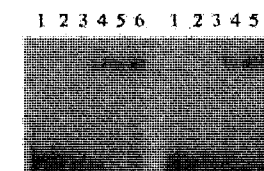
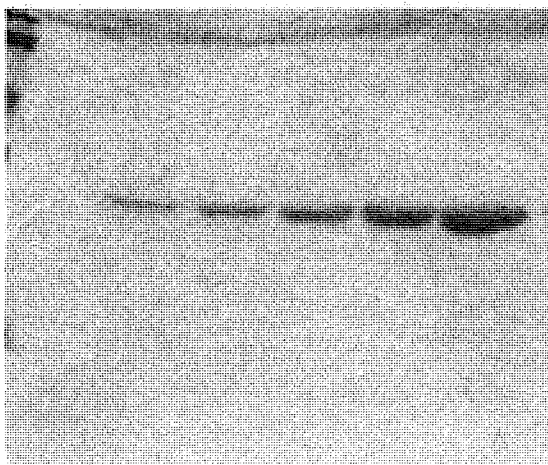


Figure 4.10. Example of cross-linking by diluted proteins. G148C was incubated exactly as for the DNA binding reactions except that the DNA used was not radiolabeled. Thus in each panel the protein concentrations are (lanes 1-6) 0, 1.3, 2.6, 5.3, 10.6, and 21  $\mu$ M. (A) is in the presence of DTT, and (B) is in the presence of the BMH cross-linker. Analysis of (B) with IP LabGel software indicates that (lanes 2-6) 24%, 27%, 25%, 33%, and 37% of the protein was cross-linked in each lane. The average amount of cross-linked dimer present is 29%.

**A**

1 2 3 4 5 6



**B**

1 2 3 4 5 6

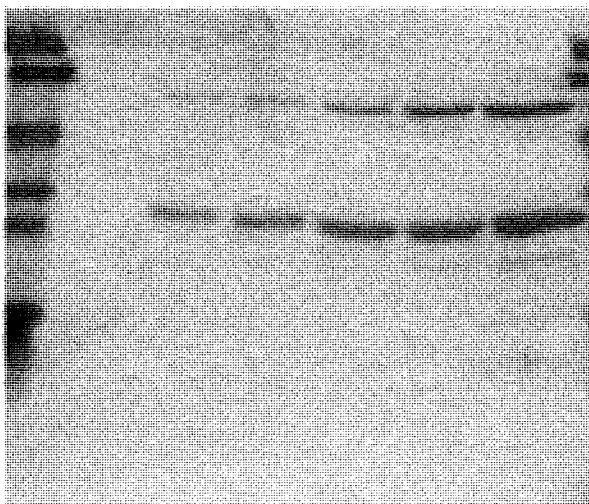




Figure 4.11. DNA binding by diluted protein. The left hand panel is DNA binding at the F1 site and the right hand panel is DNA binding at C1. In each panel, the left hand side indicates binding by diluted G148C in the presence of DTT and the right hand side is binding of G148C (not diluted) in the presence of the BMH cross-linking reagent. The concentrations of protein used for the diluted samples from lanes 1-6 are 0.9, 1.8, 3.6, 7.2, 14.4  $\mu$ M and for the undiluted samples from lanes 1-6 are 1.3, 2.6, 5.3, 10.6, 21  $\mu$ M. Based on the calculation of 29% G148C cross-linking (Figure 10), the concentration of monomeric protein is the same in each assay. Differences in binding affinity are due to DNA binding by G148C dimers.

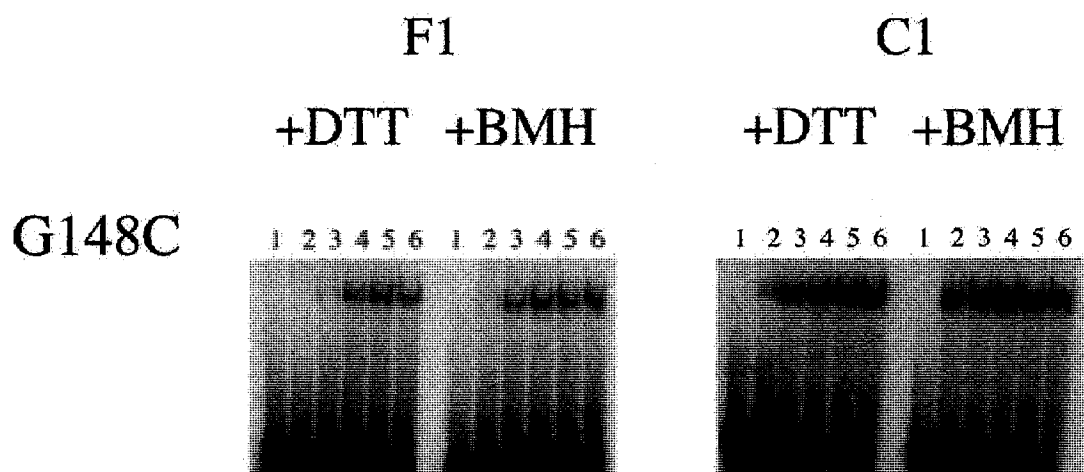
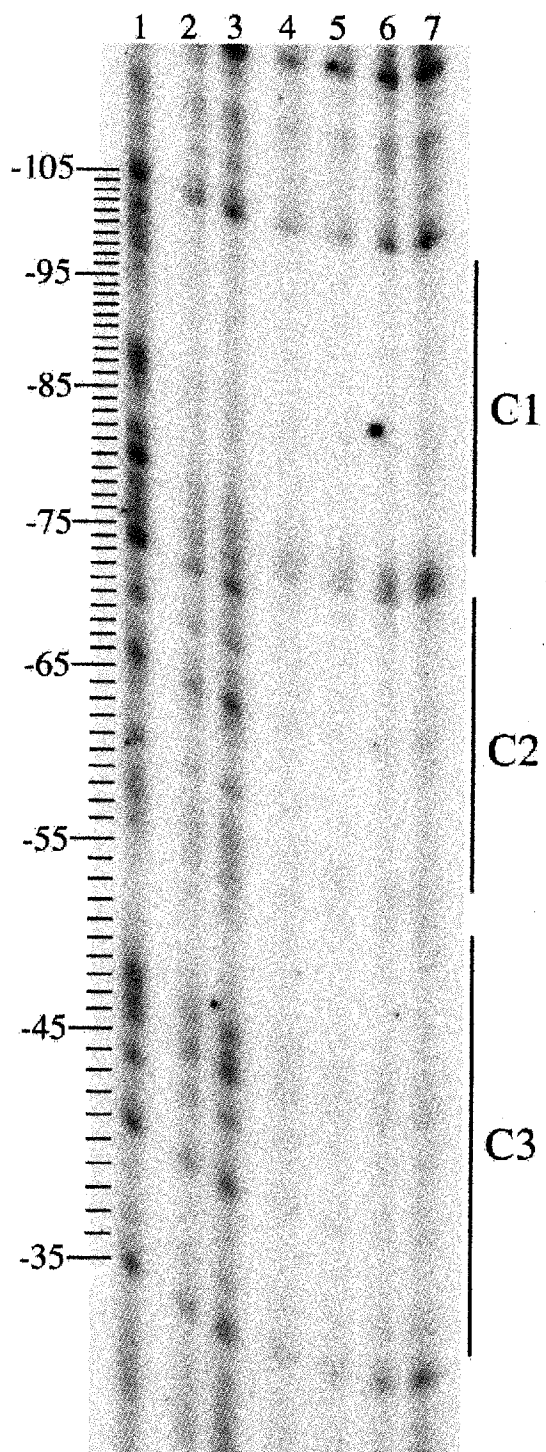


Figure 4.12. DNase I footprinting analysis of (A) uncross-linked and (B) cross-linked G148C binding at the *ompC* promoter. (A) G148C binding at *ompC* in the absence of cross-linker. Lane 1 is DNase I cleavage in the absence of G148C and lanes 2-7 show the cleavage pattern in the presence of 0.05, 0.1, 0.2, 0.5, 1.0, 2.0, and 4.0  $\mu$ M G148C incubated in DTT to prevent oxidation of the unique cysteine. (B) Cross-linked G148C bound at the *ompC* promoter region. Lane 1 is DNase I cleavage in the absence of G148C and lanes 2-7 show the cleavage pattern in the presence of 0.05, 0.1, 0.2, 0.5, 1.0, 2.0, and 4.0  $\mu$ M G148C that has been incubated with the BMH cross-linking reagent. For both panels, the previously identified OmpR binding sites are indicated to the right and the position of each band relative to the transcriptional start site of the promoter is indicated to the left.

# A. +DTT



# B. +BMH

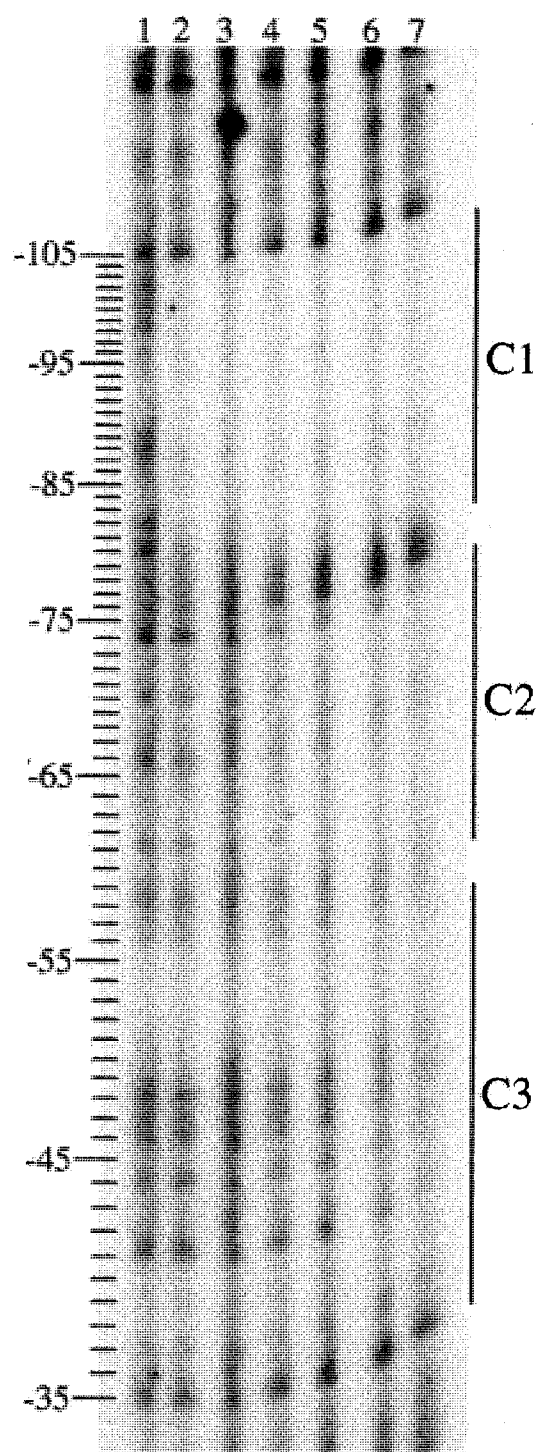


Figure 4.13. Model of OmpR dimerization. The dimer is depicted in the usual orientation, with the upstream DNA relative to the transcriptional start site on the left (A) and in the inverse orientation to show the  $\beta$  sheet that is involved in the interaction between the monomers (B). Several residues are shown: T162 in yellow, P179 in dark green, S181 in light green, R182 in cyan, and V203 in pink. The figure was generated using the Swiss PDB Viewer (DeepView). DNA corresponds to the sequence for the F1 site of the *ompF* promoter and was modeled by Ann E. Maris. Coordinates for OmpRc are taken from PDB coordinates numbered 1OPC (Martinez-Hackert, E. and A. M. Stock, 1997a).

A



B

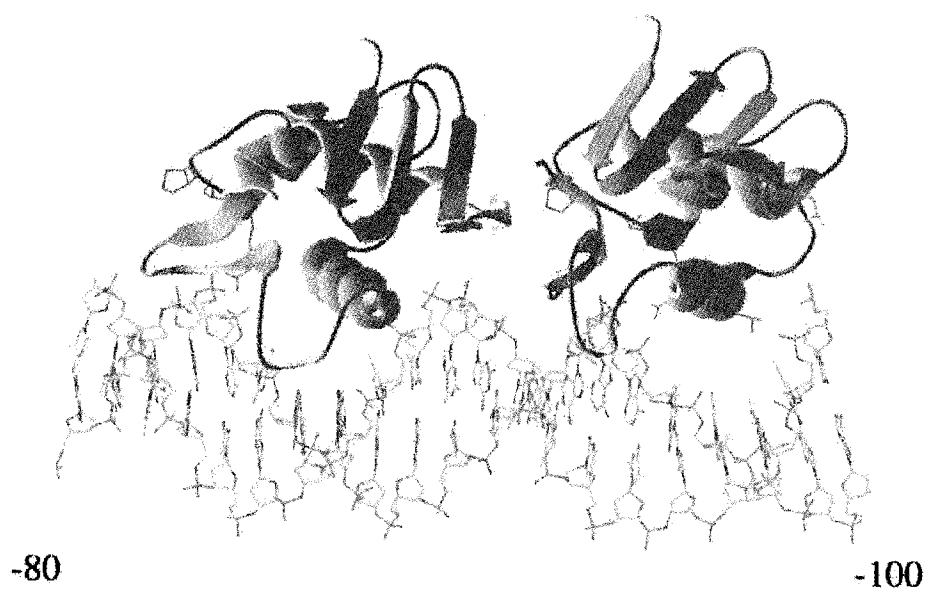


Table 4.1. Sequence of oligonucleotides used for site-directed mutagenesis. The oligonucleotides listed along with their complements were used as primers for PCR reactions as described in (Tran, V. K. *et al.*, 2000). In all cases the template was *ompRC67A*.

OmpR mutant	Oligonucleotide sequence (5'-3')
A99C	GGAGATTGGCTGCGACGACTACA
N108C	AAAACCGTTTTGCCCGCGTGAAC
I138C	AGAGGCGGTATGCGCTTTCGGTA
A139C	GGCGGTAATTTGCTTCGGTAAGT
F140C	GGTAATTGCTTGCGGTAAGTTCA
G141C	GCGGTAATTGCTTTCTGCAAGTTCAAACCTAAC
K142C	GTAATTGCTTTTCGGTTGCTTCAAACCTAACCTC
F143C	TTTCGGTAAGTGCAAACCTTAACC
K144C	CGGTAAGTTCTGCCTTAACCTCG
L145C	TAAGTTCAAATGCAACCTCGGTA
N146C	GTTCAAACCTTGCCCTCGGTACGC
L147C	CAAACCTTAAGTGCAGTACGCGCG
G148C	ACTTAACCTCTGCACGCGCGAAA
T149C	TAACCTCGGTTGCCGCGAAATGT
R150C	CCTCGGTACGTGCGAAATGTTCC
E151C	CGGTACGCGCTGCATGTTCCGCG
M152C	TACGCGCGAATGCTTCCGCGAAG
F153C	GCGCGAAATGTGCCGCGAAGACG
R154C	CGAAATGTTCTGCGAAGACGAGC
E155C	AATGTTCCGCTGCGACGAGCCGA
D156C	GTTCCGCGAATGCGAGCCGATGC
E157C	CCGCGAAGACTGCCCCGATGCCGC
P158C	CGAAGACGAGTGCATGCCGCTCA
M159C	AGACGAGCCGTGCCCCGCTCACCA
P160C	CGAGCCGATGTGCCTCACCAGCG
L161C	GCCGATGCCGTGCACCAGCGGTG
S163C	GCCGCTCACCTGCGGTGAGTTTG
G227C	GACCGTCTGGTGCCTAGGCTACGTC



Table 4.2. Phenotypes of cysteine mutants in the  $\beta$  sheet.  $\beta$ -galactosidase assays were performed in *ompF-lacZ* and *ompC-lacZ* fusion strains which lack a wild-type copy of OmpR. When wild-type OmpR is introduced into these strains, the level of  $\beta$ -galactosidase activity observed was taken to be 100%. A plus indicates that the mutant protein mediated at least 90% of the  $\beta$ -galactosidase levels as compared to wild-type OmpR. In all other cases, the percent expression relative to wild-type is indicated. Percentages shown are derived from averages of at least three independent experiments.

OmpR Protein	OmpF expression	OmpC expression
I138C	+	+
A139C	+	+
F140C	+	17%
G141C	+	48%
K142C	15%	24%
F143C	+	+
K144C	+	+
L145C	+	+
N146C	+	19%
L147C	+	+
G148C	+	+
T149C	+	+
R150C	+	19%
E151C	+	+
M152C	+	+
F153C	+	+
R154C	+	+
E155C	+	+
D156C	+	+
E157C	+	+
P158C	+	+
M159C	+	+
P160C	+	+

Table 4.3. Dominance of the cysteine mutants in the  $\beta$  sheet to wild-type OmpR.  $\beta$ -galactosidase assays were performed in *ompF-lacZ* and *ompC-lacZ* fusion strains which contain a wild-type copy of OmpR. The activity detected in the unmodified fusion strains is taken as 100%. The percentage  $\beta$ -galactosidase activity in the presence of the mutant proteins is expressed relative to this level. Values shown are averages of three independent experiments. The mutants in which expression was wild-type in the absence of *ompR* were not tested and are denoted nd to indicate this.

OmpR Protein Added	OmpF expression (%)	OmpC expression (%)
None	100	100
Wild-type	218	90
F140C	nd	41
G141C	nd	18
K142C	100	100
N146C	nd	37
R150C	nd	15

Table 4.4. Phosphorylation of the cysteine mutants with acetyl phosphate. Proteins were phosphorylated with acetyl phosphate and analyzed as described (Ames, S. K. *et al.*, 1999). The area under each peak on the HPLC chromatogram was used to determine the % phosphoprotein for each sample. The fold-increase represents the ratio of OmpR-P formed in the presence of F1 or C1 DNA to OmpR-P formed with acetyl phosphate alone.

OmpR Protein	AcPi (%)	AcPi + F1 (%)	Fold Increase	AcPi + C1 (%)	Fold Increase
I138C	13	67	5.2	82	6.3
A139C	10	89	9.3	88	9.2
F140C	16	64	4.0	14	-
G141C	29	90	3.1	90	3.1
K142C	20	87	4.4	86	4.3
F143C	22	92	4.2	90	4.1
K144C	8	32	4.0	72	9.0
L145C	41	83	2.0	90	2.2
N146C	31	43	1.4	57	1.8
L147C	48	74	1.5	90	1.9
G148C	20	80	4.0	78	3.9
T149C	25	89	3.6	91	3.6
R150C	25	59	2.4	88	3.5
E151C	30	73	2.4	84	2.8
M152C	15	78	5.2	90	6.0
F153C	14	52	3.7	83	5.9
R154C	25	84	3.4	90	3.6
E155C	20	66	3.3	75	3.8
D156C	11	62	5.6	67	6.1
E157C	42	69	1.6	82	2.0
P158C	19	58	3.1	78	4.1
M159C	29	81	2.8	85	2.9
P160C	17	58	3.4	83	4.9

Table 4.5. Cross-linking of the cysteine mutants with maleimide based cross-linkers. Proteins were cross-linked as described in Materials and Methods and the percent dimer formed was quantified using IPLabGel software. The numbers shown represent averages from at least three experiments using BMH, BMB, or BMOE. No difference was noted in cross-linking intensities using the three reagents. The exception is M152C, which cross-links very poorly in the presence of BMOE, this value was not used in calculating the average and is indicated by the asterisk (\*). The ‡ is a reminder that F140C fails to bind C1 DNA (see Table 4) and so this reaction is essentially in the absence of DNA.

Class	OmpR Substitution	Cross-linking (% of total protein)	+ompF	+ompC
I	I138C	0	0	0
	G141C	0	0	0
	K144C	0	0	0
	N146C	0	0	0
	L147C	0	0	0
II	F140C	46	0	25 <sup>†</sup>
	K142C	26	2	15
	F143C	11	0	0
	L145C	38	11	9
	T149C	46	0	0
	R150C	57	39	41
	M152C	16	0	0
	P158C	33	24	20
	M159C*	24	12	7
	P160C	37	21	17
III	A139C	19	20	22
	G148C	13	32	34
	E151C	26	30	21
	F153C	8	9	17
	R154C	7	3	16
	E155C	15	33	33
	D156C	30	33	21
	E157C	29	41	37



## **Chapter 5**

### **Phosphorylation Alters the Interaction of the Response Regulator**

#### **OmpR with its Sensor Kinase EnvZ**

**(Journal of Biological Chemistry 277: 11143-11148, 2002)**

### **5.0 Preface**

In the following paper, I conducted all of the experiments in Figures 5.2, 5.3, 5.4, 5.5 and 5.6. The model shown in Figure 5.1 was adapted from (Ames, S. K. *et al.*, 1999).

## 5.1 Abstract

OmpR and EnvZ comprise a two component system that regulates the porin genes *ompF* and *ompC* in response to changes in osmolarity. EnvZ is autophosphorylated by intracellular ATP on a histidine residue and it transfers the phosphoryl group to an aspartic acid residue of OmpR. EnvZ can also dephosphorylate phospho-OmpR (OmpR-P) to control the cellular level of OmpR-P. At low osmolarity, OmpR-P levels are low because of either low EnvZ kinase or high EnvZ phosphatase activities. At high osmolarity, OmpR-P is elevated. It has been proposed that EnvZ phosphatase is the activity that is regulated by osmolarity. OmpR is a two-domain response regulator; phosphorylation increases its affinity for DNA, and DNA binding stimulates phosphorylation. The step that is affected by DNA depends upon the phosphodonor employed. In the present work, we have used fluorescence anisotropy and phosphotransfer assays to examine OmpR interactions with EnvZ. Our results indicate that phosphorylation greatly reduces the affinity of OmpR for the kinase, while DNA does not affect their interaction. The results presented cast serious doubts on the role of the EnvZ phosphatase in response to signaling *in vivo*.

## 5.2 Introduction

The predominant paradigm for signal transduction in prokaryotes is the two component regulatory system (See (Hoch, J. A. and T. J. Silhavy, 1995) for reviews and references). The first component is a sensor kinase, often a membrane protein, which senses the appropriate environmental signal and is phosphorylated from intracellular ATP on a histidine residue. The sensor phosphokinase then transfers the phosphoryl group to an aspartic acid residue of the second component, the response regulator. Phosphorylation of the response regulator generally leads to its activation, often by increasing its affinity for DNA with a subsequent effect on transcription. In a postulated second level of regulation, it has been suggested that the sensor kinase can also stimulate dephosphorylation of the phosphorylated response regulator via a phosphatase activity, thus limiting the level of activated regulator and resetting the system.

The two component regulatory system that governs expression of the outer membrane porins OmpF and OmpC consists of the sensor kinase EnvZ and the response regulator OmpR. Activation of EnvZ by an unknown signal, related to the osmolarity of the growth medium, leads to phosphorylation of OmpR at aspartate 55 (Delgado, J. *et al.*, 1993; Igo, M. M. *et al.*, 1989a; Igo, M. M. *et al.*, 1989b). Phosphorylation of OmpR results in an increased affinity for the regulatory regions upstream from the *ompF* and *ompC* genes (Aiba, H. *et al.*, 1989c; Head, C. G. *et al.*,

1998; Huang, K. J. and M. M. Igo, 1996; Rampersaud, A. *et al.*, 1994). Recent *in vitro* studies demonstrated that the corollary is also true, i.e. the presence of DNA increases the level of OmpR phosphorylation (Ames, S. K. *et al.*, 1999; Qin, L. *et al.*, 2001). As a result of these studies, we proposed that OmpR exists as an equilibrium mixture of four distinct states (see Figure 5.1): (A) unphosphorylated OmpR, (B) phosphorylated OmpR, (C) unphosphorylated OmpR bound to DNA with low affinity, and (D) phosphorylated OmpR bound to DNA with high affinity. A similar model has been proposed for the single domain response regulator CheY, where the switch protein FliM substitutes for DNA (Schuster, M. *et al.*, 2001; Silversmith, R. E. and R. B. Bourret, 1999).

Interestingly, the reaction step that is most affected by the presence of DNA depends upon the phosphodonor employed. When phosphorylating with the small molecule phosphodonor, acetyl phosphate, DNA binding dramatically stimulates the rate of phosphorylation with little effect on the dephosphorylation rate of OmpR-P. Estimates of initial rates indicate that phosphorylation by acetyl phosphate is at least 25-fold faster in the presence of DNA than in its absence (i.e.  $C \rightarrow D$  is much faster than  $A \rightarrow B$ , Figure 5.1) (Ames, S. K. *et al.*, 1999). Furthermore, DNA binding slows dephosphorylation about 2-fold ( $D \rightarrow C$  is slightly slower than  $B \rightarrow A$ , Figure 5.1) (Ames, S. K. *et al.*, 1999). In contrast, when phosphorylating with the phospho-kinase (EnvZ-P), the step most affected by DNA binding is the rate of EnvZ-

stimulated OmpR-P dephosphorylation (i.e.  $D \rightarrow C$  is much slower than  $B \rightarrow A$ , Figure 5.1) (Qin, L. *et al.*, 2001). In either case, the overall effect of DNA is to increase the net rate of OmpR-P formation on the order of 50-fold.

The EnvZ kinase has the following enzymatic activities:

- |  |                     |
|--|---------------------|
| (a) $\text{EnvZ} + \text{ATP} \rightarrow \text{EnvZ-P} + \text{ADP}$                | autophosphorylation |
| (b) $\text{EnvZ-P} + \text{OmpR} \rightarrow \text{EnvZ} + \text{OmpR-P}$            | phosphotransfer     |
| (c) $\text{EnvZ} + \text{OmpR-P} \rightarrow \text{EnvZ} + \text{OmpR} + \text{P}_i$ | phosphatase         |

As a result, by controlling either the phosphotransfer activity (b) or the phosphatase activity (c), EnvZ can modulate the level of OmpR-P *in vivo*.

A current model for osmoregulation proposes that at high osmolarity, the level of OmpR-P increases due to a reduction in dephosphorylation rate catalyzed by the kinase EnvZ (Jin, T. and M. Inouye, 1993).

Unphosphorylated OmpR does not play a role in porin gene expression, since *envZ* deletion strains are effectively OmpF<sup>-</sup> OmpC<sup>-</sup> (Slauch, J. M. and T. J. Silhavy, 1989). Results from the EnvZ/OmpR system have been extended to other two component regulatory systems leading to the conclusion that phosphatase activity of the sensor kinase is the step regulated or altered by signal input (Castelli, M. E. *et al.*, 2000; Montagne, M. *et al.*, 2001; Nakano, M. M. and Y. Zhu, 2001; Wanner, B. L., 1996; Williams, S. B. and V. Stewart, 1997).

Along these lines, a central role for the regulation of phosphatase activity has been proposed by Jin *et al.* (Jin, T. and M. Inouye, 1993).

Furthermore, Qin *et al.* proposed that when OmpR-P binds to DNA, it is effectively made inaccessible to EnvZ, and thus DNA binding inhibits EnvZ stimulation of OmpR-P breakdown. If this explanation were correct, it would be difficult to reconcile with the proposed role of the EnvZ phosphatase activity in breaking down OmpR-P and re-setting its levels *in vivo* (Russo, F. D. and T. J. Silhavy, 1991). In other words, how does EnvZ dephosphorylate OmpR-P bound to DNA if the OmpR-P/DNA complex is inaccessible? In the present work, we have demonstrated that phosphorylation of OmpR dramatically reduces its interaction with EnvZ. Furthermore, the ability of EnvZ to interact with OmpR or OmpR-P is not affected by the presence of specific DNA. Our data suggest that the direct stimulation of OmpR-P breakdown by EnvZ probably does not play a role *in vivo*.

## **5.3 Results**

### **5.3.1 Phosphorylation decreases the affinity of OmpR for EnvZ**

We wanted to determine whether or not phosphorylation of OmpR altered its interaction with EnvZ. For these experiments, OmpR was labeled with fluorescein at the amino terminus and the labeled protein was separated from the free label. EnvZc was then added incrementally. Representative binding curves are shown in Figure 5.2. For the curves shown in Figure 5.2A, fluorescein-labeled OmpR was phosphorylated with phosphoramidate. In this particular experiment, the affinity for EnvZc binding to OmpR is 589 nM (triangles). The average  $K_d$  for EnvZc

binding to OmpR from 10 independent experiments is  $425 \pm 127$  nM. EnvZc binds to OmpR-P with such low affinity that its  $K_d$  is beyond the detection limit of the assay (circles). We were consistently unable to detect saturable binding of EnvZc to OmpR-P. Thus, phosphorylation has a dramatic effect on OmpR/EnvZ interactions, decreasing the affinity of OmpR for EnvZ by at least 10-fold.

It has recently been suggested that OmpR-P/DNA and OmpR-P/EnvZ interactions are mutually exclusive (Qin, L. *et al.*, 2001). We set out to examine this proposal directly, i.e. to determine whether DNA binding by OmpR or OmpR-P altered its affinity for the EnvZ kinase. In Figure 5.2B, the dissociation constant ( $K_d$ ) for EnvZc binding to OmpR is 519 nM (filled triangles); for EnvZc binding to OmpR in the presence of *ompC* DNA (C1-C2-C3) the  $K_d$  is 568 nM (open triangles). The average  $K_d$  for EnvZc binding to OmpR in the presence of *ompC* DNA from six separate curves is  $385 \pm 162$  nM. The dissociation constants are the same, within the error of the assay. The presence of *ompC* DNA did not alter the binding of EnvZc to OmpR (Figure 5.2B) or to OmpR-P (Figure 5.2A, compare closed circles with open circles). Thus, although phosphorylation has a dramatic effect on the affinity of OmpR for EnvZc (Figure 5.2A), the presence of specific DNA does not affect the ability of EnvZc to bind to OmpR (Figure 5.2B). This result is in conflict with the recently proposed role for DNA in the OmpR/OmpR-P equilibrium mediated by EnvZ (Qin, L. *et al.*, 2001).

### 5.3.2 The role of DNA in phosphorylation

We have been studying the native linker in OmpR and its role in OmpR/DNA and OmpR/EnvZ interactions. We have engineered and expressed a mutant in which the native Q linker (Wootton, J. C. and M. H. Drummond, 1989) is replaced with a linker of equal length, but substituted with glycine and lysine residues (hereafter referred to as GGK). The GGK mutant is able to activate expression of *ompF* but not *ompC* (OmpF<sup>+</sup> OmpC<sup>-</sup>). GGK is also able to protect the *ompF* and *ompC* regulatory regions in a DNase I footprinting assay; a complete characterization of the mutant is described elsewhere. In the present work, we first examined the steady-state phosphorylation of GGK by the small molecule phosphodonor, acetyl phosphate (Figure 5.3).

Unphosphorylated OmpR runs as a single peak on C4 reversed phase HPLC (Figure 5.3A). Acetyl phosphate phosphorylates OmpR at aspartate 55, and an additional peak that corresponds to OmpR-P appears (Figure 5.3B) (Ames, S. K. *et al.*, 1999; Head, C. G. *et al.*, 1998). As reported previously, when a two-fold molar excess of specific DNA is included in the reaction, OmpR-P levels increase nearly 2-fold (Figure 5.3C)(Ames, S. K. *et al.*, 1999). The GGK mutant also elutes as a single peak on C4 reversed phase HPLC (Figure 5.3D) and acetyl phosphate is similarly able to phosphorylate GGK (Figure 5.3E). The addition of DNA also increases the steady-state level of phosphorylated GGK (Figure 5.3F). Thus, when



acetyl phosphate is used as a phosphodonor, GGK phosphorylates and responds to DNA similarly to wild-type OmpR.

### 5.3.3 The effect of DNA on GGK phosphorylation by EnvZ

We next determined the effect of DNA on the phosphorylation of GGK by the EnvZ kinase. EnvZ is autophosphorylated upon incubation with [ $\gamma$ - $^{32}$ P]ATP (Figure 5.4 A and B, lane 1). When OmpR is added to the reaction, the phosphoryl group is transferred from EnvZ-P to OmpR and OmpR-P is formed (Figure 5.4A, lanes 2-4). Similarly, incubation of GGK with EnvZ-P results in the formation of GGK-P (Figure 5.4B, lanes 2-4). When OmpR is added to EnvZ-P in the presence of either *ompF* DNA (Figure 5.4A lanes 5-7) or *ompC* DNA (Figure 5.4A lanes 8-10), the level of residual OmpR-P is increased compared with no addition of DNA. However, when GGK is added to the reaction in the presence of *ompF* or *ompC* DNA, a decrease in the amount of GGK-P is observed (Figure 5.4B lanes 5-10). This behavior is in striking contrast to that observed with wild-type OmpR (Figure 5.4A lanes 5-10). Even though the interaction of GGK with DNA appears to be similar to wild-type OmpR in stimulating phosphorylation from acetyl phosphate (Figure 5.3), the interaction of GGK-P with the kinase EnvZ is dramatically altered in the presence of DNA. The decrease in the amount of GGK-P upon incubation with EnvZ-P and DNA (Figure 5.4) indicates either that the kinase is less able to phosphorylate DNA-bound GGK (C  $\rightarrow$  D is slow, Figure 5.1), or that EnvZ rapidly dephosphorylates DNA-bound GGK-P (D  $\rightarrow$  C is fast, Figure 5.1).

#### **5.3.4 The GGK mutant displays increased turnover in the presence of EnvZ and DNA**

To distinguish between these two possibilities, we measured  $P_i$  release from GGK-P in the presence and absence of DNA and compared it to wild-type OmpR (Figure 5.5). If the kinase is less able to phosphorylate GGK in the presence of DNA, then  $P_i$  production should be low. If the kinase rapidly dephosphorylates DNA-bound GGK, and rephosphorylation occurs, then a high level of  $P_i$  should be released. In the presence of EnvZ and ATP, wild-type OmpR is phosphorylated and dephosphorylated, the net result is  $P_i$  release at a rate of 7.1 nmol/ml/minute (closed triangles). The presence of specific DNA decreases the  $P_i$  produced by wild-type OmpR to a rate of 0.4 nmol/ml/minute (open triangles). In contrast, the mutant GGK phosphoprotein turns over very slowly, and  $P_i$  production is low (closed circles). Because GGK is being phosphorylated under these conditions (Figure 5.4), dephosphorylation of GGK-P must be inhibited. Surprisingly, the addition of DNA greatly enhances  $P_i$  production by the mutant protein (open circles). This stimulated rate in turnover of GGK-P in the presence of DNA approaches that observed with wild-type OmpR in the absence of DNA (compare closed triangles with open circles). The rate of  $P_i$  production by GGK increases from 0.3 nmol/ml/minute to 4.7 nmol/ml/minute upon addition of DNA. DNA binding has the opposite effect from wild-type OmpR on GGK-P dephosphorylation by EnvZ. For

GGK, the  $D \rightarrow C$  transition is faster than the  $B \rightarrow A$  transition, while for OmpR, the  $D \rightarrow C$  transition is much slower than the  $B \rightarrow A$  transition (Figure 5.1). Furthermore, GGK-P and EnvZ *must* interact when GGK-P is bound to DNA, because this mutant shows an increase in the rate of EnvZ-stimulated dephosphorylation upon DNA binding (Figure 5.5, open circles). Our interpretation is that the presence of the altered linker sequence prevents the  $B \rightarrow A$  transition (Figure 5.1) required for spontaneous dephosphorylation. When the mutant protein is bound to DNA, GGK-P can transition to an EnvZ-bound form if EnvZ is present, stimulating dephosphorylation of the protein. While this result is obtained with an OmpR mutant, it emphasizes the point that OmpR binding to DNA cannot remove it from solution and prevent interaction with EnvZ, as previously proposed (Qin, L. *et al.*, 2001).

#### 5.4 Discussion

In the present work, we have demonstrated that phosphorylation of OmpR reduces its affinity by at least 10-fold for the kinase EnvZ. The average apparent dissociation constant for EnvZc binding to OmpR is 425 nM. When OmpR was phosphorylated using phosphoramidate (generating nearly 100% OmpR-P), we were unable to measure a  $K_d$  for EnvZc binding because the interaction was of such low affinity. This has important consequences for the hypothesis that the phosphatase activity of EnvZ plays a regulatory role and controls OmpR-P levels *in vivo* (see below).

A previous study used native gel electrophoresis to examine the effect of DNA on the interaction OmpR/OmpR-P and EnvZ (Qin, L. *et al.*, 2001). The authors concluded that OmpR-P bound to DNA was prevented from interacting with EnvZ, and this inability to interact prevents EnvZ from dephosphorylating OmpR-P. We can now interpret these results in light of our present findings. In a solution containing OmpR and OmpR-P, OmpR has a higher affinity for EnvZ and OmpR-P has a higher affinity for DNA. The  $K_d$  for OmpR binding to an *ompC* binding site, C1, is 101 nM, the  $K_d$  for OmpR-P is 8 nM (Head, C. G. *et al.*, 1998). Thus, in the mixed population of OmpR and OmpR-P present in the previous study, OmpR interacts predominantly with EnvZ and OmpR-P interacts predominantly with DNA (Qin, L. *et al.*, 2001). Significant EnvZ/OmpR-P interactions would not be expected to occur. The dramatic decrease in affinity of OmpR-P for the EnvZ kinase demonstrated in the present work makes it unlikely that reverse phosphotransfer from OmpR-P to EnvZ is the mechanism of dephosphorylation of OmpR-P (Dutta, R. and M. Inouye, 1996), or that EnvZ plays a major role in dephosphorylating OmpR-P *in vivo* (Jin, T. and M. Inouye, 1993). However, when the ratio of EnvZ to OmpR is adjusted to high EnvZ concentrations relative to OmpR (i.e. *in vitro*), EnvZ can dephosphorylate OmpR-P. It is important to note that this reaction is slow compared with the duration of the EnvZ binding assay presented here (see Materials and Methods and Figure 5.5).

In the bacterial chemotaxis system, the phosphatase CheZ also does not appear to be important for signaling *in vivo* (Blat, Y. *et al.*, 1998). Deletion of *cheZ*, which accelerates dephosphorylation of the response regulator, CheY-P, did not alter the cellular response to the excitatory stimulus aspartate (Kim, C. *et al.*, 2001). Furthermore, CheY has a reduced affinity for its cognate kinase CheA upon phosphorylation. Measurements using isothermal titration calorimetry demonstrated that the affinity of CheA for CheY was 2  $\mu\text{M}$  and it was reduced 6-fold upon phosphorylation in the presence of magnesium (Li, J. *et al.*, 1995). Thus, it appears that dephosphorylation acts similarly in the chemotaxis and osmoregulatory systems. In both cases, phosphorylation of the response regulators dramatically decreases their affinity for the sensor kinases (Figure 5.2A, as shown in this work and (Li, J. *et al.*, 1995)), and dephosphorylation does not appear to be the regulated step in signaling (Kim, C. *et al.*, 2001). With an intracellular concentration of OmpR of 1  $\mu\text{M}$ , and EnvZ concentration on the order of 10 nM, an apparent  $K_d$  of > 5  $\mu\text{M}$  for EnvZ binding to OmpR-P indicates that these two partners would only rarely be associated. These estimates are based on 10 copies of EnvZ and 1000 copies of OmpR per cell (Liljestrom, P., 1986a).

From the results presented here, we propose that OmpR binds to DNA (A  $\rightarrow$  C pathway, Figure 5.1), is phosphorylated by EnvZ (C  $\rightarrow$  D) and then undergoes a conformational change that enhances its binding affinity and may promote an interaction with RNA Polymerase (D  $\rightarrow$  E).

As a consequence of this conformational change, OmpR-P is not a substrate for dephosphorylation by EnvZ (D and B forms do not interact with EnvZ). If the EnvZ phosphatase activity is important *in vivo*, OmpR-P must undergo a transition to a form that EnvZ can dephosphorylate. A possible candidate might be a conformational change associated with RNA Polymerase binding during transcriptional activation. The possibility that OmpR-P must be released in order for EnvZ to dephosphorylate it can be eliminated because DNA did not alter the affinity of OmpR-P and EnvZ (Figure 5.2A).

The behavior of the glycine-rich linker mutant GGK is significantly different from that of wild-type OmpR. This behavior emphasizes the importance of the linker region in OmpR action (Ames, S. K. *et al.*, 1999). In the case of the GGK mutant, GGK-P turnover and  $P_i$  production is slow in the absence of DNA and DNA binding increases the rate of dephosphorylation of GGK-P (D  $\rightarrow$  C is faster than B  $\rightarrow$  A). If the GGK mutant were removed from the reaction as a consequence of binding to DNA, i.e. it were no longer a substrate for  $P_i$  release by EnvZ (as predicted by Qin *et al.* (Qin, L. *et al.*, 2001)), then the presence of DNA would not stimulate  $P_i$  turnover. Our result of the stimulation of  $P_i$  production by GGK in the presence of DNA (Figure 5.5) is not consistent with the explanation provided by Inouye and co-workers for the loss of EnvZ-stimulated OmpR-P breakdown upon DNA binding (Qin, L. *et al.*,

2001). However, the altered turnover we observed with the GGK mutant most likely contributes to its OmpF<sup>+</sup> OmpC<sup>-</sup> phenotype.

#### **5.4.1 *In vivo* relevance**

The fundamental question arising from this work is whether or not there is an *in vivo* role for the stimulation of OmpR-P breakdown by EnvZ that is observed *in vitro*. The results presented here suggest that the affinity of EnvZ for OmpR-P is too low to play a role *in vivo* in dephosphorylating OmpR-P. They are most consistent with a model in which the autophosphorylation of EnvZ or the phosphotransfer to OmpR (or both) increases with increasing osmolarity. This view is further supported by a recent study that reported elevated EnvZ autokinase activity at high potassium concentrations, with no change in the phosphotransfer or phosphatase activities (Jung, K. *et al.*, 2001). Spontaneous dephosphorylation of OmpR-P would then lead to OmpR-P decay. Measurements of OmpR-P turnover have reported a half-life of OmpR-P of 1-2 h, i.e. too long for spontaneous dephosphorylation to account for signal shut off (Igo, M. M. *et al.*, 1989b). In other studies, about 60% of the OmpR-P was dephosphorylated within the first 10 min (Kenney, L. J., unpublished results). Given our present findings, the kinetics of OmpR-P dephosphorylation bears careful reexamination. It is also important to emphasize that our studies are performed with an EnvZ construct that lacks the periplasmic and transmembrane domains, which could alter EnvZ/OmpR and EnvZ/OmpR-P interactions.

It has been suggested that this phosphatase activity of EnvZ is regulated in response to osmolarity, i.e. at high osmolarity the kinase activity remains constant, and the phosphatase activity decreases, increasing the cellular level of OmpR-P (Jin, T. and M. Inouye, 1993). This hypothesis is based on the results of experiments with a chimeric kinase, Taz, in which the periplasmic domain of the aspartate receptor has been fused to the carboxyl terminus of EnvZ (Utsumi, R. *et al.*, 1989). This chimeric construct only responds to high concentrations of aspartate (1-5 mM), compared with the natural aspartate receptor which binds aspartate with a  $K_d$  of 1.2  $\mu$ M (Biemann, H.-P. and D. E. J. Koshland, 1994), and its effect on *ompF* expression has not been reported. The behavior of Taz therefore seems unlikely to accurately represent EnvZ signaling *in vivo*. *In vitro* demonstration of the phosphatase activity is beyond dispute (Aiba, H. *et al.*, 1989b; Igo, M. M. *et al.*, 1989b; Qin, L. *et al.*, 2001) and mutations in EnvZ have been isolated that influence it (Aiba, H. *et al.*, 1989b; Dutta, R. *et al.*, 2000; Hall, M. N. and T. J. Silhavy, 1981c; Hsing, W. *et al.*, 1998; Matsuyama, S. *et al.*, 1986). However, these substitutions also alter EnvZ autophosphorylation and phosphotransfer activities and so their *in vivo* actions should be interpreted with caution.

The results presented here demonstrate that OmpR-P has a significantly lower affinity for the EnvZ kinase than does OmpR, and suggest that alternate mechanisms must be proposed if the phosphatase



activity of EnvZ controls OmpR-P levels *in vivo*. For example, it is possible that in order for EnvZ to bind OmpR-P, the protein must undergo a conformational change. This might be a result of interaction with RNA Polymerase. However, such models that postulate extra roles for sensor kinases, beyond the environmental sensing step *in vivo*, involve additional assumptions and await further experimental investigation. Our present work emphasizes the need to separately characterize the partial biochemical reactions of the components in the signaling pathway in order to rationalize the mechanistic basis of the observed phenotypes.

## **5.5 Materials and Methods**

### **5.5.1 Protein purification**

OmpR was expressed and purified as previously described (Head, C. G. *et al.*, 1998; Tran, V. K. *et al.*, 2000). GGK was constructed by ligating synthetic oligonucleotides into engineered restriction sites in OmpR, resulting in the replacement of endogenous amino acids 124-137 of the linker region with Gly-Gly-Lys-Gly-Gly-Lys-Gly-Gly-Lys-Gly-Gly-Lys-Gly-Gly. The protein was expressed as described (Head, C. G. *et al.*, 1998) and purified on a HiTrap Heparin column (Amersham Biosciences, Inc.). The construct encoding the soluble carboxyl terminal fragment of EnvZ (EnvZc) was a kind gift from Dr. Masayori Inouye; it was expressed and purified according to (Park, H. and M. Inouye, 1997).

### 5.5.2 Fluorescence anisotropy

OmpR was labeled at the amino terminus using an amine fluorescein labeling kit (Panvera). The labeled protein was purified using a series of three 5 ml desalting columns (Amersham Biosciences, Inc.). The labeling kit is optimized for amino-terminal labeling but does not exclude the possibility of labeling at surface lysines. However, the labeled protein was phosphorylated by EnvZ and responded to DNA as wild-type (Figure 5.6). For some experiments, fluorescein-labeled OmpR was phosphorylated using 25 mM phosphoramidate in a buffer of 50 mM Tris (pH 7.5), 50 mM KCl, 20 mM MgCl<sub>2</sub>. The amount of phosphorylated protein was determined to be greater than 95% by C4 reversed phase HPLC analysis, as previously described in (Head, C. G. *et al.*, 1998). EnvZc was titrated into a binding reaction containing 5 mM Na<sub>2</sub>HPO<sub>4</sub>/NaH<sub>2</sub>PO<sub>4</sub> (pH 7.4), 50 mM NaCl, 5 mM MgCl<sub>2</sub>, 0.05% (v/v) Tween-20, 50 µg/ml bovine serum albumin and 40 nM fluorescein-labeled OmpR or OmpR-P. 100 nM C1-C2-C3 DNA was included for some experiments. Fluorescent OmpR was excited at 490 nm and emission was measured at 530 nm in a Beacon Fluorimeter (Panvera). The samples were incubated in the fluorimeter for 30 s and five measurements were taken at 10 s intervals after each protein addition. A typical binding experiment lasted approximately 30 min. Each point plotted in the figures is an average of five measurements. The data were analyzed according to (Head, C. G. *et al.*, 1998).

### **5.5.3 Phosphorylation by acetyl phosphate**

OmpR and GGK were phosphorylated using acetyl phosphate (Sigma) as in (Kenney, L. J. *et al.*, 1995). For some experiments, DNA was added in a 2:1 molar ratio of protein to DNA (Ames, S. K. *et al.*, 1999). 10  $\mu$ M protein in a total volume of 200  $\mu$ l was injected onto a C4 reversed phase HPLC column and eluted as described (Head, C. G. *et al.*, 1998; Tran, V. K. *et al.*, 2000).

### **5.5.4 Phosphorylation by EnvZ115**

OmpR and GGK were phosphorylated as reported in (Tran, V. K. *et al.*, 2000), for some samples a 2-fold molar excess of F123 or C123 DNA was included in the reaction.

### **5.5.5 ATPase assays**

The reactions were carried out in a 0.6 ml volume containing 125 mM NaCl, 4 mM MgCl<sub>2</sub>, 60 mM Tris-HCl (pH 7.5), 0.75 mM EDTA, 3  $\mu$ M EnvZc-his and 1.5  $\mu$ M OmpR or GGK. 3  $\mu$ M C1-C2-C3 DNA was included for some experiments. Reactions were initiated and conducted as described (Kenney, L. J., 1997). The P<sub>i</sub> produced in the presence of EnvZ was subtracted from the total P<sub>i</sub> produced in the presence of OmpR or GGK.

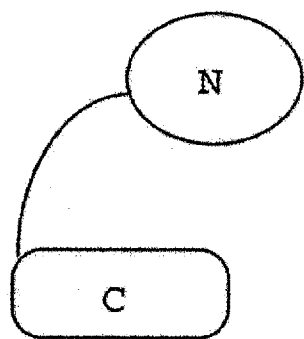
## **5.6 Acknowledgements**

LJK would like to thank the following for helpful discussions: Vic DiRita, University of Michigan; Barry Wanner, Purdue University; Jeffery F. Miller, University of California at Los Angeles; Jack H. Kaplan and our

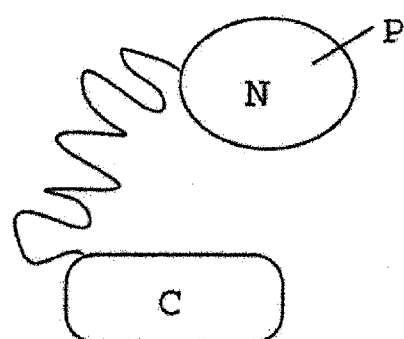
laboratory members Ricardo Oropeza, Don Walthers, Xiuhong Feng and Judith Dietvorst from Oregon Health Sciences University. Supported by NIH GM58746 and NSF MCB9904658. KM is a Predoctoral fellow of the American Heart Association-Northwest affiliate.

Figure 5.1. Model for OmpR phosphorylation and DNA binding. OmpR is depicted as a two-domain protein with the amino terminus (oval) joined to the carboxyl terminus (rectangular) by a flexible linker region. The protein is shown (A) alone, (B) phosphorylated, (C) bound to DNA, and (D) phosphorylated and bound to DNA. The arrows depict transitions between these states.

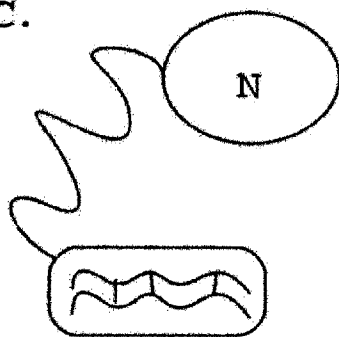
A.



B.



C.



D.

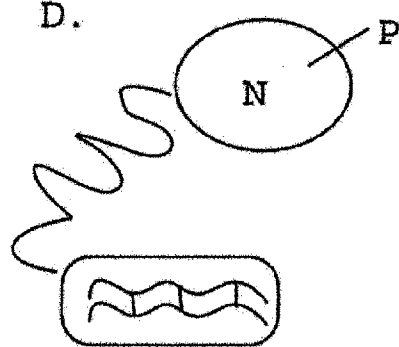


Figure 5.2. EnvZc binding to OmpR by fluorescence anisotropy. (A) Triangles show OmpR binding to EnvZc with a  $K_d$  of 589 nM. The average  $K_d$  for EnvZc binding to OmpR from ten independent experiments is  $425 \pm 127$  nM. Closed circles indicate that OmpR-P binds EnvZc with only very low affinity. This binding is unchanged in the presence of C1-C2-C3 DNA (open circles). A saturable binding curve for EnvZc binding to OmpR-P was never obtained using this approach ( $n=4$ ). (B) OmpR binds to EnvZc with a  $K_d$  of 519 nM (closed triangles). In the presence of specific DNA, EnvZc still binds OmpR, with a  $K_d$  of 568 nM (open triangles). The average  $K_d$  for EnvZc binding to OmpR from ten independent experiments is  $425 \pm 127$  nM and for EnvZc binding to OmpR + C1-C2-C3 from six separate curves is  $385 \pm 162$  nM.

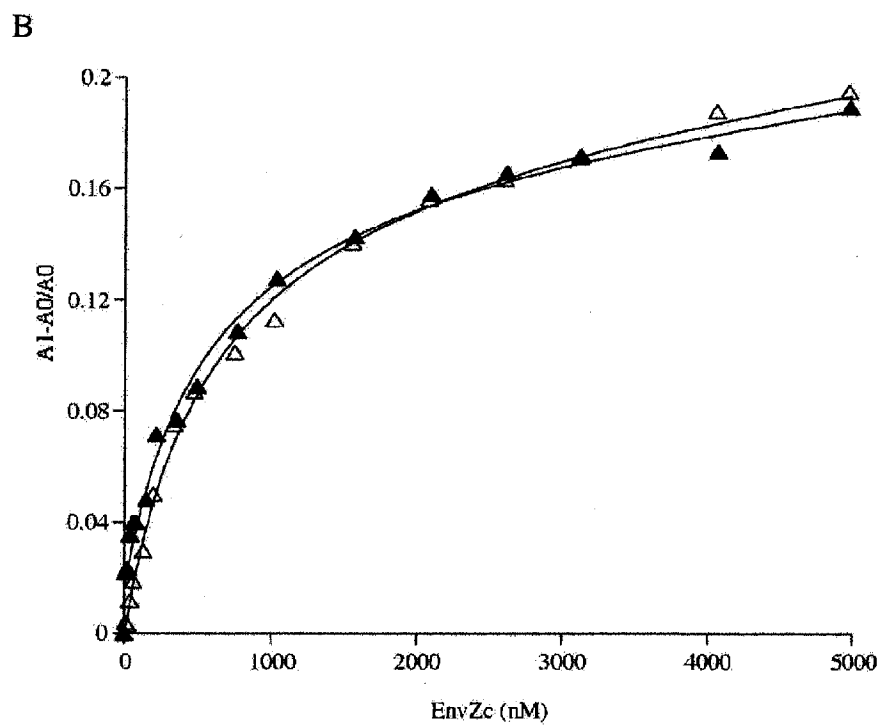
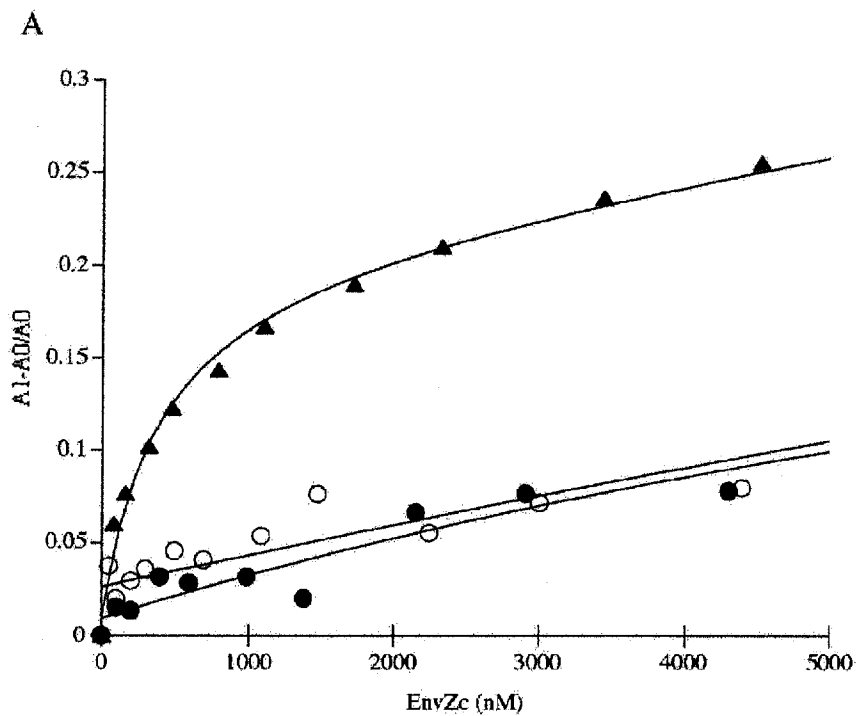




Figure 5.3. Phosphorylation of OmpR and GGK by acetyl phosphate. C4 reversed phase HPLC elution profiles for (A) OmpR (B) OmpR + acetyl phosphate (C) OmpR + acetyl phosphate + C1-C2-C3 (D) GGK (E) GGK + acetyl phosphate (F) GGK + acetyl phosphate + C1-C2-C3.

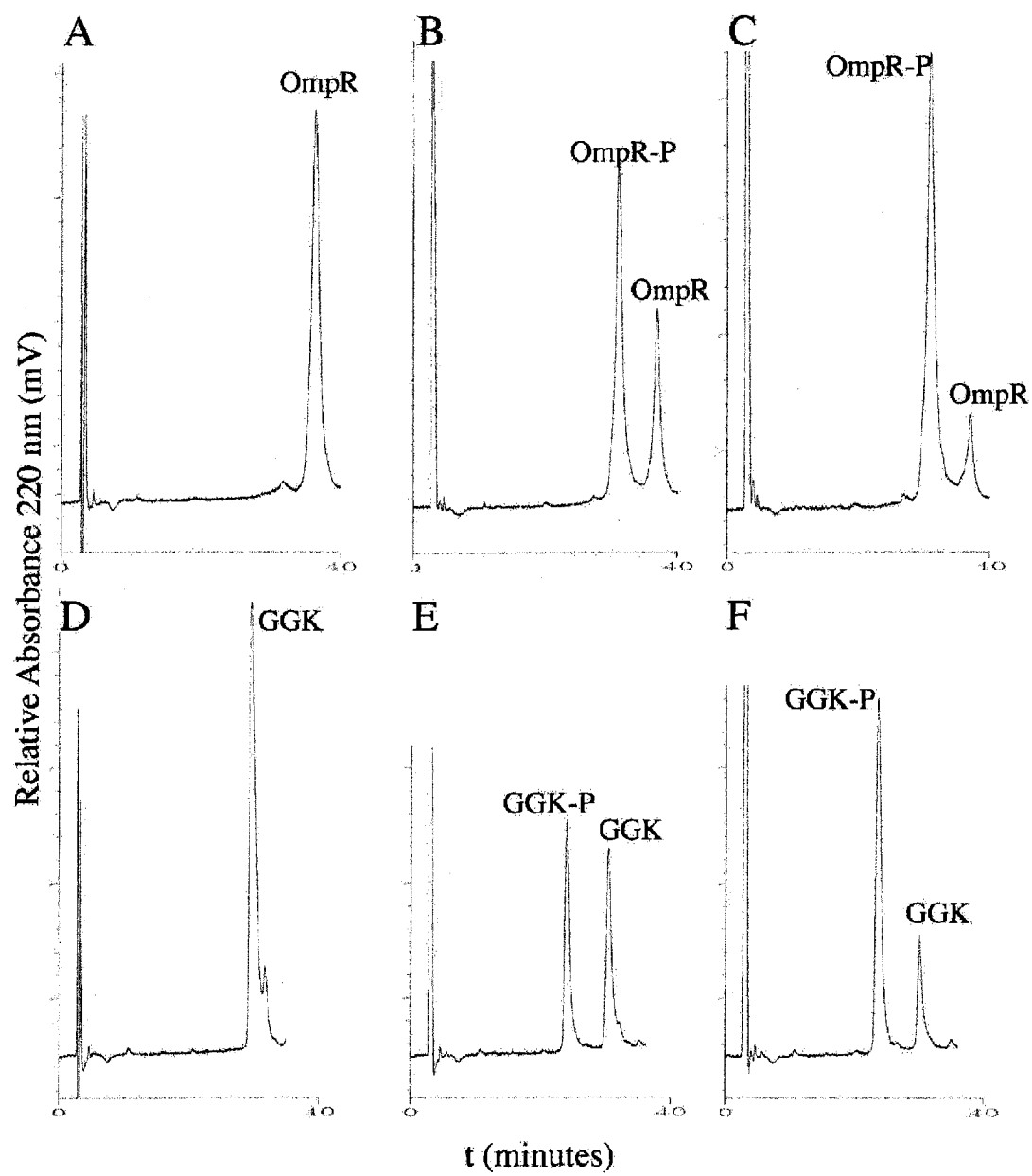


Figure 5.4. EnvZ115 phosphorylation of OmpR and GGK. (A) Lane 1 shows EnvZ after autophosphorylation with [ $\gamma$ - $^{32}$ P]ATP. Lanes 2-4 show OmpR-P produced 5, 20, and 60 minutes after the addition of OmpR to the reaction. Lanes 5-7 are identical to lanes 2-4 but the reaction contains F1-F2-F3 DNA. Lanes 8-10 are identical to lanes 2-4 but the reaction contains C1-C2-C3 DNA. (B) As for A, except the assay was performed with GGK.

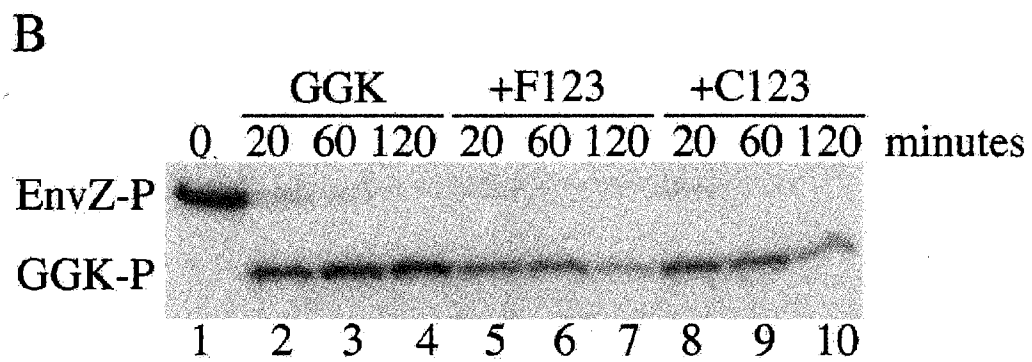
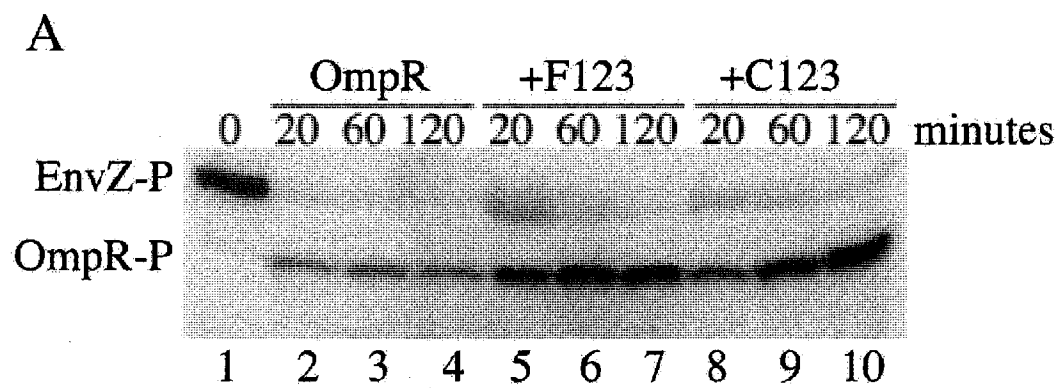


Figure 5.5. ATPase assay with OmpR and GGK. Closed triangles show the  $P_i$  released after incubation of OmpR with EnvZ and ATP, open triangles indicate that  $P_i$  release is slowed when DNA is included in the reaction. Closed circles indicate that GGK does not stimulate the ATPase activity of EnvZ, and open circles show that upon addition of DNA, GGK greatly stimulates  $P_i$  production. Reactions were performed in quadruplet; error bars indicate the standard deviation.

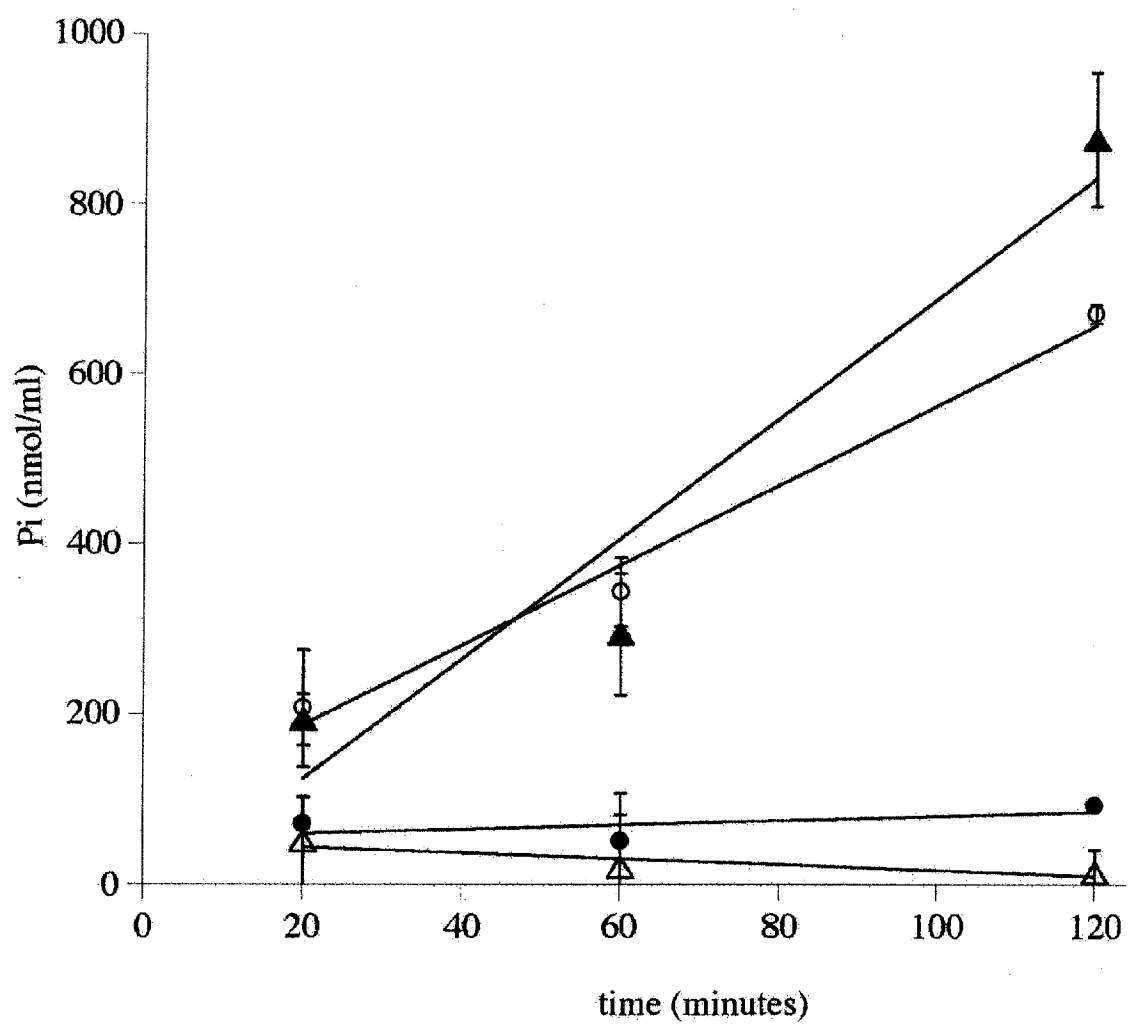
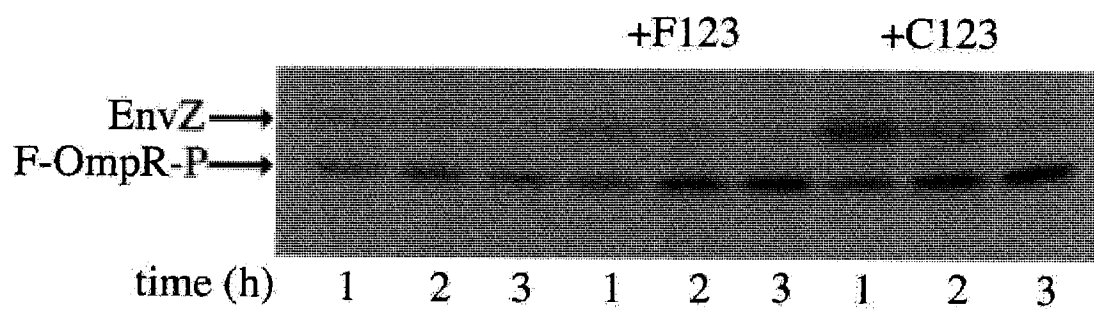


Figure 5.6. Phosphorylation of fluorescein labeled OmpR. Fluorescein labeled OmpR was phosphorylated with EnvZ115 as described in Materials and Methods. A 2-fold molar excess of *ompF* or *ompC* promoter DNA was included in some reactions as indicated. The stimulation of FS-OmpR phosphorylation by DNA is similar to that observed with unlabeled OmpR (see Figure 5.4).





## **Chapter 6**

### **A phosphatase mutant of EnvZ demonstrates altered binding to the response regulator OmpR**

#### **6.0 Preface**

I performed all of the experiments shown in this Chapter.

## 6.1 Abstract

The two component signaling system composed of the EnvZ sensor kinase and the OmpR response regulator controls the expression of the OmpF and OmpC porins in response to changing environmental osmolarity. *In vitro*, EnvZ has been shown to possess both OmpR kinase and OmpR-P phosphatase activities, and it has been proposed that the dephosphorylation of OmpR-P is an important signaling mechanism *in vivo*. The isolation of point mutants in EnvZ defective in OmpR-P dephosphorylation has provided support for this hypothesis. We have examined the phosphatase mutant EnvZ T247R in order to clarify whether its *in vivo* phenotype is due to its inability to dephosphorylate OmpR-P. We find that while EnvZ T247R does not significantly dephosphorylate OmpR-P, neither does wild-type EnvZ when the reaction is performed at a molar ratio of EnvZ:OmpR comparable to that found *in vivo*. The EnvZ T247R mutant has a higher affinity for both OmpR and OmpR-P than does the wild-type enzyme, and we propose that characteristics of this mutant other than its inability to dephosphorylate OmpR-P may account for its *in vivo* phenotype.

## 6.2 Introduction

Two component signal transduction systems are the primary means by which prokaryotic organisms sense and respond to changing environmental conditions (Hoch, J. A. and T. J. Silhavy, 1995). In their simplest form, these systems consist of a membrane bound sensor kinase, which senses environmental conditions, and a cytoplasmic response regulator, which mediates the appropriate intracellular response. In the EnvZ/OmpR system, EnvZ is a histidine kinase that spans the inner membrane (Forst, S. *et al.*, 1987; Liljestrom, P., 1986b). In response to an unknown signal related to extracellular osmolarity, EnvZ is phosphorylated by cytosolic ATP at histidine 243 (Roberts, D. L. *et al.*, 1994). The phosphoryl group is then transferred to aspartic acid 55 of the OmpR regulator (Delgado, J. *et al.*, 1993). This signaling pathway controls the expression of the genes for the outer membrane porins OmpF and OmpC. *ompF* is expressed under conditions of low osmolarity, while at high osmolarity *ompF* transcription is repressed and transcription from the *ompC* locus is activated (van Alphen, W. and B. Lugtenberg, 1977).

In the affinity model of porin gene regulation, it is the increasing amount of OmpR-P present in the cell as osmolarity increases that determines the gene expression profiles of *ompF* and *ompC* (Russo, F. D. and T. J. Silhavy, 1991). However, DNA binding studies revealed only slight differences in the affinity of OmpR-P for the *ompF* and *ompC*

upstream promoter regions (Head, C. G. *et al.*, 1998). We have recently suggested that a conformational change in OmpR-P is responsible for differentiating between the *ompF* and *ompC* promoters (Mattison, K. *et al.*, 2002a; Mattison, K. *et al.*, 2002b).

*In vitro*, in addition to the aforementioned autophosphorylation and phosphotransfer activities, the EnvZ kinase stimulates dephosphorylation of OmpR-P. We have proposed that this phosphatase activity is not relevant *in vivo*, in light of the finding that OmpR-P and EnvZ interact only with low affinity (Mattison, K. and L. J. Kenney, 2002). However, there are mutations in EnvZ that decrease the phosphatase activity, and they have the expected OmpF<sup>-</sup> OmpC<sup>c</sup> phenotype *in vivo*. The purpose of this study was to characterize the phosphatase mutant known as EnvZ11, which has an arginine residue in the place of the endogenous threonine at position 247 (T247R) (Aiba, H. *et al.*, 1989b; Hall, M. N. and T. J. Silhavy, 1981c). In this work, we have examined the autophosphorylation, phosphotransfer, and phosphatase activities of the EnvZ T247R mutant and found that *in vitro*, it is indeed defective in dephosphorylation of OmpR-P. However, at ratios of EnvZ to OmpR that mimic those detected in the cell, neither EnvZ nor EnvZ T247R is capable of dephosphorylating OmpR-P. Furthermore, OmpR-binding studies show that EnvZ T247R binds to OmpR differently than does wild-type EnvZ. This leads us to postulate a mechanism whereby the stabilization of OmpR-P achieved by EnvZ T247R is simply a

by-product of its high affinity for OmpR in the presence of magnesium ions. By binding OmpR and OmpR-P with abnormally high affinity in the presence of  $Mg^{2+}$ , EnvZ T247R may simply exclude  $Mg^{2+}$  from the OmpR active site, a process which is known to stabilize phosphorylated response regulators *in vitro* and is often achieved by the addition of EDTA (Weinstein, M. *et al.*, 1993; Zhu, Y. *et al.*, 2000). Thus, the defect in the phosphatase activity of EnvZ T247R detected *in vitro* may not be the reason for its aberrant regulation of *ompF* and *ompC* expression *in vivo*.

### 6.3 Results

A point mutant of the EnvZ kinase which results in the replacement of a threonine at position 247 by an arginine residue has been previously isolated and characterized (Aiba, H. *et al.*, 1989b; Hall, M. N. and T. J. Silhavy, 1981c). When the mutation is present, *E. coli* fail to express the OmpF porin (OmpF<sup>-</sup>) and constitutively express the OmpC porin (OmpC<sup>c</sup>) (Hall, M. N. and T. J. Silhavy, 1981c). *In vitro*, the mutant protein appears to mediate efficient phosphorylation of the OmpR regulator while failing to stimulate its dephosphorylation (Aiba, H. *et al.*, 1989b). Previously, the deficiency in phosphatase activity of the mutant protein was thought to account for its porin expression phenotype. In accordance with the affinity model, a high level of OmpR-P in the cell would lead to an absence of OmpF expression and constitutive expression of OmpC (Russo, F. D. and T. J. Silhavy, 1991). Our recent work has led us to postulate that firstly, the difference in affinity of

OmpR-P for the *ompF* and *ompC* promoter regions fails to account for the regulation of these loci by increasing amounts of OmpR-P and secondly, that the phosphatase activity of EnvZ is unlikely to control OmpR-P levels *in vivo* (Head, C. G. *et al.*, 1998; Mattison, K. and L. J. Kenney, 2002; Mattison, K. *et al.*, 2002a; Mattison, K. *et al.*, 2002b). In light of these studies, we have re-examined the biochemical characteristics of the EnvZ T247R mutation in order to reconcile its resultant phenotype with our currently proposed model of EnvZ/OmpR regulation.

### **6.3.1 EnvZ T247R is phosphorylated slightly faster than EnvZ**

We began our study of the phosphatase mutant, EnvZ T247R, by determining its rate of autophosphorylation in comparison to that of EnvZ. Figure 6.1 shows that the mutant kinase has a rate of phosphorylation slightly faster than that of wild-type EnvZ. In Figure 6.1A, EnvZ is phosphorylated by  $\gamma$ -[ $^{32}\text{P}$ ]ATP and the reaction is stopped at time points ranging from 10 seconds - 8 minutes. In Figure 6.1B, the T247R mutant is phosphorylated following the same time course. Figure 6.1C shows the intensity of the phosphorylated bands; triangles represent EnvZ and circles represent the T247R mutant. The fold difference in phosphorylation can be determined in two ways. By simple point-by-point comparison, EnvZ T247R is phosphorylated between 1.8 and 1.5-fold more than wild-type EnvZ. By linear regression of the first 5 time points (10 seconds - 4 minutes, as shown in Figure 6.1C), the initial rate of EnvZ T247R phosphorylation is 1.5-fold faster than that of wild-

type OmpR. This is in agreement with previous studies that found a 1.5 to 2-fold increase in the maximum amount of label incorporation into the T247R mutant (Aiba, H. *et al.*, 1989b; Dutta, R. *et al.*, 2000). Thus, the T247R mutation in EnvZ slightly improves autophosphorylation of the kinase, but this effect is small and does not intuitively account for the dramatic OmpF<sup>-</sup> OmpC<sup>c</sup> phenotype of the mutation *in vivo*.

### **6.3.2 OmpR-P produced by EnvZ T247R or by low amounts of EnvZ is relatively stable**

In order to compare the phosphotransfer and phosphatase activities of EnvZ and EnvZ T247R, we performed kinase assays with varying amounts of EnvZ and a constant amount of OmpR. The results are shown in Figure 6.2. In Figure 6.2A, wild-type EnvZ is used to phosphorylate OmpR at either a 1:5 EnvZ:OmpR (left panel) or a 1:100 EnvZ:OmpR (right panel) ratio. When EnvZ is present at levels 5 times less than OmpR, significant phospho-transfer occurs after 10 seconds (0.2 minutes, lane 1). After five minutes, both phospho-transfer and dephosphorylation have occurred, resulting in a decrease in the intensity of the OmpR-P band (lane 2). It is readily apparent after 20 minutes of incubation that OmpR-P is being efficiently dephosphorylated (lane 3), and after 2 hours there is very little phospho-protein remaining (lane 5). By contrast, when 100-fold less EnvZ than OmpR is present in the reaction mixture, no turnover is detected. OmpR-P increases over the entire two hours of incubation (Figure 6.2A, right panel).

Figure 6.2B shows the same experiment using EnvZ T247R. Similarly to wild-type EnvZ, at a ratio of 1:5, T247R readily transfers the phosphoryl group to OmpR in 10 seconds. However, dephosphorylation of OmpR-P is not apparent, in fact, OmpR-P increases over time (Figure 6.2B, left panel). At the 1:100 ratio, OmpR-P is also seen to increase over the two hour assay in the presence of EnvZ T247R (Figure 6.2B, right panel). Thus, EnvZ T247R is defective in phosphatase activity *in vitro*, but when low amounts of EnvZ are present, this behavior is not different from that of wild-type EnvZ (compare right panels of Figure 6.2A and B).

In order to quantify the amount of phosphatase activity when varying amounts of EnvZ are present in the reaction mixture, we used an ATPase assay, which detects free inorganic phosphate ( $P_i$ ) production. Figure 6.3A shows that with wild-type EnvZ, the amount of OmpR-P turnover, as indicated by the increase in free  $P_i$ , decreases as less EnvZ is used in the assay. The filled triangles show that when a 5-fold molar excess of EnvZ is present, the rate of  $P_i$  production is 11.2 nmol/mL/minute. At equimolar amounts of EnvZ and OmpR,  $P_i$  production decreases to 3.1 nmol/mL/minute (filled circles). As EnvZ decreases further, to 5-fold less than OmpR (filled diamonds), the rate of  $P_i$  production also decreases to a barely detectable 0.4 nmol/mL/minute. At a ratio of 1:100 EnvZ:OmpR, the rate of  $P_i$  production is below the detection limit of the assay, linear regression gives a rate of 0.1 nmol/mL/minute (filled squares). While comparison with the gels in



Figure 6.2 indicates that this chromogenic ATPase assay is less sensitive than the radioactive kinase assay, it is clearly apparent that the amount of OmpR-P turnover depends on the amount of EnvZ included in the assay.

We performed the same ATPase assay with EnvZ T247R and found that none of the ratios tested gave appreciable  $P_i$  production levels (Figure 6.3B, open triangles, circles, diamonds, and squares). Not until a 20:1 molar excess of EnvZ T247R was included in the assay did we detect appreciable OmpR-P turnover, at a rate of 3.6 nmol  $P_i$  produced per mL per minute (Figure 6.3B, crosses). Concomitant with the lower sensitivity of this assay, we were able to detect OmpR-P turnover using a radioactive kinase assay run on gels at a 5:1 molar excess of EnvZ T247R (Figure 6.3C). We conclude that the T247R mutant of EnvZ does retain the ability to stimulate turnover of OmpR-P but at severely reduced levels compared to the wild-type protein.

In order to quantitate the amount of phosphatase activity remaining in the T247R mutant using a more sensitive detection system than the ATPase assay shown in Figure 6.3A and B, we detected OmpR-P by C4 reversed phase HPLC. OmpR was phosphorylated with the small molecule phospho-donor phosphoramidate, and the samples were spun through gel filtration columns to remove any excess phospho-donor. The percent phospho-protein present immediately after this step was determined and taken to be 100% in the graphical representations

shown in Figure 6.4. The open triangles in Figure 6.4A show OmpR-P that has been purified and incubated at room temperature for up to one hour. OmpR-P is maintained at 100% for the duration of the 60-minute assay. The open squares in Figure 6.4A show OmpR-P levels after the addition of EDTA and EnvZ. EnvZ contributes to the turnover of OmpR-P even in the absence of  $Mg^{2+}$ , as the levels of OmpR-P decrease to approximately 60% over the course of the experiment. The stimulatory effect of EnvZ does not cause a linear decrease in the amount of OmpR-P, rather dephosphorylation occurs quickly at early time points, after which OmpR-P levels appear to stabilize. This is true in all cases where EnvZ stimulates OmpR-P dephosphorylation (see below). The open circles in Figure 6.4A show the rapid dephosphorylation of OmpR-P stimulated by EnvZ in the presence of  $Mg^{2+}$ . Only 40% of the initial OmpR-P remains after 5 minutes, after this OmpR-P slowly decreases to approximately 20% of starting values over the hour of incubation. Figure 6.4B shows the same reactions using T247R instead of wild-type EnvZ. The closed triangles in Figure 6.4B show that OmpR-P is stable over the course of one hour. When EDTA and T247R are included in the reaction, again no turnover is detected, indicating that in the absence of  $Mg^{2+}$ , T247R is unable to contribute to OmpR-P dephosphorylation (closed squares). However, when T247R is incubated with OmpR-P in the presence of  $Mg^{2+}$ , some dephosphorylation of OmpR-P is apparent (closed circles). This is in agreement with the assay shown in Figure 6.3C, where T247R

is able to mediate slow turnover of OmpR-P at levels much reduced compared to wild-type EnvZ. We postulate that the decreased phosphatase activity of T247R is not apparent using the radioactive kinase assays because of the large amount (40%) of OmpR-P still present after the incubation. In summary, the T247R mutant of EnvZ is able to mediate some OmpR-P dephosphorylation *in vitro*, at levels much reduced compared to wild-type EnvZ. The amount of phosphatase activity present in the reactions can be summarized as EnvZ + Mg<sup>2+</sup> > T247R + Mg<sup>2+</sup> > EnvZ + EDTA > T247R + EDTA.

Both EnvZ and T247R can be shown to possess some phosphatase activity *in vitro*, and the phosphatase activity of T247R is greatly reduced compared to that of EnvZ (Figures 6.2, 6.3 and 6.4). However, since neither EnvZ nor T247R stimulate turnover of OmpR-P when much less EnvZ than OmpR is present, as is the case *in vivo* (Figures 6.2 and 6.3)(Cai, S. J. and M. Inouye, 2002; Liljestrom, P., 1986a), we question whether this *in vitro* phenomenon is relevant to the *in vivo* phenotype of the *envZT247R* mutation.

### **6.3.3 EnvZ T247R binds OmpR and OmpR-P with higher affinity than EnvZ**

We began our study using isothermal titration calorimetry to assess the binding affinities of OmpR and EnvZ in the presence or absence of Mg<sup>2+</sup>. Figure 6.5 shows a representative experiment in which the dissociation constant for EnvZ binding to OmpR in the absence of

Mg<sup>2+</sup> is 1.5  $\mu$ M. There was an exothermic event detected as EnvZ was titrated into the reaction cell, as indicated by the control injections in the top curve. This combines with the binding of EnvZ to OmpR, an endothermic reaction, to result in the experimental result shown the lower curve of the top panel. In the bottom panel, the control injections have been subtracted from the experimental such that the kilocalories of heat absorbed are zero when binding is saturated. By averaging six such data sets, EnvZ binds OmpR in the absence of Mg<sup>2+</sup> with a  $K_d$  of  $1.7 \pm 0.7$   $\mu$ M (Table 6.1). When Mg<sup>2+</sup> was included in the binding assay, EnvZ bound to OmpR with a  $K_d$  of  $4.2 \pm 0.6$   $\mu$ M, a 2.5-fold decrease in binding affinity (Table 6.1). While these dissociation constants are higher than those previously reported using fluorescence anisotropy measurements (Mattison, K. and L. J. Kenney, 2002), the ITC assays are performed in a buffer of 960-1100 milliosmoles, while the FA experiments were in 1/3 PBS, which is only 110 milliosmoles. It is not surprising that increasing the salt concentration decreases the affinity of this interaction.

We next used ITC to measure the affinity of the interaction between EnvZ T247R and OmpR. In the buffer lacking Mg<sup>2+</sup>, T247R had a similar affinity for OmpR as wild-type EnvZ,  $1.4 \pm 0.4$   $\mu$ M (Table 6.1). However, when we performed binding experiments with T247R and OmpR in the presence of Mg<sup>2+</sup>, we obtained aberrant binding curves that did not fit the single-set-of-sites equations (data not shown).

In order to compare the affinities of EnvZ and T247R for OmpR in the presence of  $Mg^{2+}$ , we returned to the fluorescence anisotropy assay. Representative curves are shown in Figure 6.6. Figure 6.6A shows that T247R binds to OmpR with higher affinity than EnvZ in the presence of  $Mg^{2+}$ . The filled triangles show EnvZ binding to OmpR with a  $K_d$  of 1.0  $\mu M$ . The filled circles show T247R binding to OmpR with a  $K_d$  of 183 nM. The average of 10 independent experiments indicates that EnvZ binds OmpR with a  $K_d$  of  $425 \pm 127$  nM, and the average of five curves indicates that T247R binds OmpR with a  $K_d$  of  $136 \pm 42$  nM. Figure 6.6B shows that T247R similarly has a higher affinity for OmpR-P than EnvZ. Open triangles show EnvZ binding to OmpR, this interaction is not saturable by this assay and is estimated to have a  $K_d$  of  $> 3 \mu M$  (Mattison, K. and L. J. Kenney, 2002). Open circles indicate that T247R binds OmpR-P with a higher affinity of 510 nM. The average  $K_d$  of T247R binding to OmpR-P from 3 separate curves is  $327 \pm 131$  nM. While the binding affinities for OmpR-P are in the appropriate range for ITC measurements, unfortunately OmpR-P is not soluble at the high concentrations needed to detect changes in the heat of an isothermal chamber upon protein-protein interaction.

We conclude that the failure of T247R to mediate wild-type levels of OmpR-P turnover stems not from an inability of the mutant kinase to interact with OmpR or OmpR-P, but rather from an altered effect of  $Mg^{2+}$

on the interaction between the mutant kinase and the response regulator.

Our use of OmpR-P in fluorescence anisotropy assays has been questioned based on the assumption that OmpR-P will not be maintained in solution in the presence of EnvZ and  $Mg^{2+}$  (Mattison, K. and L. J. Kenney, 2002; Yoshida, T. *et al.*, 2002a). What the authors fail to note is that there is a 10, 000-fold molar excess of phosphoramidate present in the reactions, which allows for re-phosphorylation of any OmpR-P that has been dephosphorylated. In order to show this, we phosphorylated OmpR using phosphoramidate, added EnvZ, and incubated the reactions for 5, 15, or 60 minutes. It takes approximately 30 minutes to complete a typical fluorescence anisotropy binding curve. The results of the dephosphorylation experiment are shown in Figure 6.7. Figure 6.7A shows that after phosphorylation followed by a 5 minute incubation with EnvZ, 45% of the protein is phosphorylated. Comparing Figure 6.7A to Figures 6.7B and 6.7C, it is apparent that the faster migrating peak corresponding to phospho-OmpR is increasing over time, even though EnvZ is present in the reaction. In Figure 6.7B, after 15 minutes of incubation with EnvZ, OmpR-P has increased to 61% of the total protein. After a 60 minute incubation, 70% of the OmpR in the reaction mix is phosphorylated (Figure 6.7C). It is clear that under our conditions, OmpR-P is indeed present in the OmpR-EnvZ binding reactions.

## 6.4 Discussion

The findings in this study reinforce our previous conclusion that the phosphatase activity of EnvZ may not be relevant *in vivo* (Mattison, K. and L. J. Kenney, 2002). When the level of EnvZ used in a kinase reaction is reduced, OmpR-P is just as stable as in the presence of wild-type EnvZ as it is in the presence of the phosphatase mutant T247R (see Figure 6.2A and 6.2B, right panels). The ratio of EnvZ:OmpR used corresponds to an early estimate of the amounts of EnvZ and OmpR present in a cell (10 and 1000 molecules, respectively) (Liljestrom, P., 1986a). More current work estimates there are 100 molecules of EnvZ and 3500 molecules of OmpR per cell (Cai, S. J. and M. Inouye, 2002). This does not alter the significance of our result, since Figure 6.3 clearly shows a decrease in the phosphatase activity as EnvZ concentration decreases. Furthermore, the T247R mutant clearly retains some phosphatase activity, it simply requires higher levels of T247R for this to become apparent (Figure 6.3C).

Our EnvZ/OmpR binding studies lead to two conclusions, firstly that the presence of  $Mg^{2+}$  reduces the affinity of the EnvZ/OmpR interaction and secondly that the OmpF<sup>-</sup> OmpC<sup>+</sup> phenotype of the EnvZ T247R mutant may be due to altered binding between the kinase and the response regulator in the presence of  $Mg^{2+}$ . Our finding that  $Mg^{2+}$  decreases the affinity of the OmpR/EnvZ interaction appears to contradict the findings of Cai and Inouye (Cai, S. J. and M. Inouye,

2002), however there are notable differences between the two systems. These authors determined binding affinities by Coomassie staining gels of histidine-tagged proteins bound to a  $\text{Ni}^{2+}$  column. We feel that our binding assay more accurately portrays the behavior of the molecules in solution as the binding event is measured with no post-binding sample manipulation. Furthermore, the previous study added 5 mM  $\text{Mg}^{2+}$  in the presence of various nucleotides, while here we modify the buffer only with 20 mM  $\text{Mg}^{2+}$ . Either the amount of  $\text{Mg}^{2+}$  added or the absence of nucleotide may alter the binding affinity.

Binding to  $\text{Mg}^{2+}$  is known to cause conformational changes centered at the active site in the homologous response regulator CheY (Bellolell, L. *et al.*, 1994; Stock, A. M. *et al.*, 1993) and binding to  $\text{Mg}^{2+}$  reduces the affinity of CheY for its cognate kinase CheA (Li, J. *et al.*, 1995). Such conformational changes in and around the active site of OmpR may account for the decreased affinity observed in the presence of  $\text{Mg}^{2+}$  (Table 6.1). One known effect of excluding  $\text{Mg}^{2+}$  from the active site of related response regulators is stabilization of the phospho-protein (Weinstein, M. *et al.*, 1993). One can envision that a response regulator binds  $\text{Mg}^{2+}$ , which allows phosphorylation to occur, but the resulting  $\text{Mg}^{2+}$ -bound phospho-protein is inherently unstable, in part due to the conformational changes induced by  $\text{Mg}^{2+}$  binding. In the CheY system,  $\text{Mg}^{2+}$  has been proposed to stabilize the transition state required for dephosphorylation, thus allowing more efficient dephosphorylation



(Stock, A. M. *et al.*, 1993; Zhao, R. *et al.*, 2002). When EDTA is introduced into the system,  $Mg^{2+}$  is removed from the active site, and the resulting conformational change stabilizes the phospho-protein.

The T247R mutation of EnvZ not only stabilizes OmpR-P (Figures 6.2 and 6.3), it also increases the affinity of the kinase for OmpR in the presence of  $Mg^{2+}$  (Figure 6.6). While EnvZ has an endogenous arginine located near the phospho-histidine, at position 246, this residue is oriented away from the phosphorylated histidine residue ((Tomomori, C. *et al.*, 1999), center red residue in Figure 6.8). The arginine introduced by the T247R mutation is directed outwards from the coiled coil, as is the phosphorylated histidine (bottom and top residues, green and blue respectively, in Figure 6.8). It is possible that the presence of this arginine residue increases the density of positive charges directed towards the active site of OmpR, and as such decreases the ability of  $Mg^{2+}$  to stay bound at the active site. We propose that OmpR-P is stabilized in the presence of T247R EnvZ because the mutant kinase stimulates the release of  $Mg^{2+}$  from the active site. A possible consequence of this proposal is that the introduced arginine residue may functionally substitute for  $Mg^{2+}$  in the phospho-transfer reaction. This was previously suggested based on the observation that T247R had significant autophosphorylation activity in the absence of  $Mg^{2+}$  (Dutta, R. *et al.*, 2000).

The orientation of the mutated residue, shown in green in Figure 6.8, indicates that it may destabilize  $Mg^{2+}$  binding at the active site of OmpR and this explains the *in vitro* characterization of the mutant as lacking phosphatase activity (Figures 6.2 and 6.3). However, both the wild-type kinase and the T247R mutant behave similarly when physiologically relevant ratios of protein are used in phosphorylation assays (Figures 6.2 and 6.3) (Cai, S. J. and M. Inouye, 2002; Liljestrom, P., 1986a). This *in vitro* defect in phosphatase activity therefore fails to account for the *in vivo* OmpF<sup>-</sup> OmpC<sup>c</sup> phenotype of the mutant (Aiba, H. *et al.*, 1989b; Hall, M. N. and T. J. Silhavy, 1981c). It is interesting to note that early studies of the T247R mutant also showed that the phosphatase defect did not fully account for the gene expression phenotype in mutant strains. OmpR-P purified from strains containing the *envZT247R* mutation was found at levels 4-fold higher than those seen in wild-type cells grown at low osmolarity (Forst, S. *et al.*, 1990). However, the difference in DNA binding between these two protein preparations was found to be 250-fold, indicating that some other conformational effect resulted in a 60-fold increase in the DNA binding affinity of OmpR-P (Forst, S. *et al.*, 1989a). This discrepancy between the amount of OmpR-P purified and the DNA binding by the mutant protein also holds true for cells containing wild-type *envZ* grown in high osmolarity, and for another phosphatase mutant *envZV241G* (Forst, S. *et al.*, 1989a; Forst, S. *et al.*, 1990; Waukau, J. and S. Forst, 1992).

and the protocol described previously (Mattison, K. *et al.*, 2002a). The protein was expressed and purified as for the wild-type EnvZ (Park, H. and M. Inouye, 1997).

### **6.5.2 ATPase assays**

The reactions were carried out in a 0.6-ml volume containing 125 mM NaCl, 4 mM MgCl<sub>2</sub>, 60 mM Tris-HCl (pH 7.5), 0.75 mM EDTA, 1.5  $\mu$ M OmpR and varying amounts of EnvZc-his or EnvZcT247R-his (0.015, 0.3, 1.5, or 7.5  $\mu$ M). Reactions were performed as described (Kenney, L. J., 1997). The P<sub>i</sub> produced in the presence of EnvZc-his (or EnvZcT247R-his) alone was subtracted from the reported values in the presence of OmpR.

### **6.5.3 Phosphorylation reactions**

For autophosphorylation experiments, 15  $\mu$ M EnvZc-his or EnvZcT247R-his were phosphorylated in reaction containing phosphorylation buffer (50 mM Tris-HCl (pH7.5), 50 mM KCl, 20 mM MgCl<sub>2</sub>) and 5  $\mu$ Ci [ $\gamma$ -<sup>32</sup>P]ATP for 10sec, 30 sec, 1 min, 2 min, 4 min, or 8 min. At indicated times, the reaction was stopped by adding denaturing sample buffer (124 mM Tris-HCl (pH 6.8), 20% (v/v) glycerol, 4% (w/v) SDS, 8% (v/v)  $\beta$ -mercaptoethanol, 0.025% (w/v) bromophenol blue) and the products were separated by SDS-PAGE. The resulting gels were exposed to a phosphorimager cassette and the signal intensity in each band was analyzed using IPLabGel software.

For phospho-transfer experiments, EnvZc-his or EnvZcT247R-his (30, 6, 1.2, or 0.06  $\mu$ M) was phosphorylated in phosphorylation buffer with 5  $\mu$ Ci [ $\gamma$ - $^{32}$ P]ATP for 15 minutes at room temperature. 6  $\mu$ M OmpR was added and the phosphotransfer reaction was allowed to continue for 0.17, 5, 20, 60 or 120 minutes. The reactions were stopped with the addition of denaturing sample buffer and the products were separated by SDS-PAGE. The dried gel was exposed to Kodak X-Omat Blue XB-1 film in the presence of an intensifying screen.

For the phosphatase experiments, 10  $\mu$ M OmpR was phosphorylated with 25 mM phosphoramidate in 2.5 mM Tris-HCl (pH 7.5), 2.5 mM KCl, 1 mM  $\text{MgCl}_2$  for one hour at room temperature. OmpR-P was purified from the phosphoramidate by applying the sample to a Bio-Spin 6 gel filtration column (Bio-Rad) pre-equilibrated with the buffer used for phosphorylation. 10 mM EDTA was added to some samples to chelate the  $\text{Mg}^{2+}$ . 10  $\mu$ M EnvZc-his or 10  $\mu$ M EnvZcT247R-his was added to some samples. Samples were frozen using an EtOH/ $\text{CO}_2$  bath at the time points indicated and run on a C4 reversed phase HPLC column as described (Mattison, K. *et al.*, 2002a; Tran, V. K. *et al.*, 2000). The amount of OmpR-P present directly after the gel purification step was taken as 100% and all values presented are relative to this number (64% OmpR-P). For the assays to show that OmpR-P persists in the presence of phosphoramidate and EnvZ, the above protocol was followed except that the samples were not gel purified or treated with EDTA.

#### **6.5.4 Fluorescence anisotropy**

EnvZcT247R-his was used in binding reactions exactly as described for EnvZc-his in ref. (Mattison, K. and L. J. Kenney, 2002).

#### **6.5.5 Isothermal Titration Calorimetry**

All titrations were carried out in a VP-ITC MicroCalorimeter from MicroCal, LLC, Northampton, MA. Data acquisition and analysis were performed with Origin® software, also from MicroCal. EnvZc-his (or EnvZcT247R-his) and OmpR were dialyzed before each experiment in TGED (20 mM Tris-HCl (pH 7.6), 1 mM EDTA, 5% (v/v) glycerol and 0.1 mM DTT) with the addition of the indicated salts (see Table 6.1). Titrations were performed at 25 °C, with a syringe stirring speed of 300 rpm. A typical experiment consisted of 25-30 injections of 350  $\mu$ M EnvZc into 35  $\mu$ M OmpR where the individual injections were 4-10  $\mu$ L each and were made every 2 minutes. The calibrated cell feedback signal ( $\mu$ cal/sec) was collected every 2 sec. In every case, the area of the first sample injection was not used for the analysis since anomalous values were obtained. This has been observed by others using ITS analysis (Li, J. *et al.*, 1995). The data were analyzed by fitting a single-set-of-sites model, which calculates values for the binding stoichiometry,  $n$ , the association constant,  $K_a$ , and the enthalpy of binding,  $\Delta H$ .

#### **6.6 Acknowledgments**

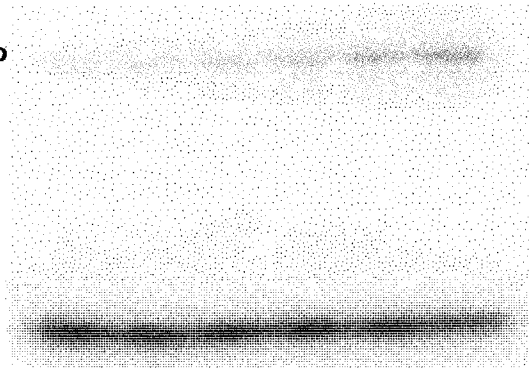
We would like to thank Thomas O'Hare, Gary Thomas, Margie T. Borra, David Murray, Marshall Miller, Richard Brennan and Hans Peter

Bächinger from OHSU for help and advice regarding ITC. Supported by NIH GM58746 and NSF MCB9904658. KM is a predoctoral fellow of the American Heart Association-Northwest affiliate.

Figure 6.1. Autophosphorylation of EnvZ and EnvZ T247R. EnvZ (A) and EnvZ T247R (B) were phosphorylated as described in Materials and Methods for 10 s, 30 s, 1 min, 2 min, 4 min, and 8 min. The resulting gels were exposed on a phosphorimager cassette and the bands were quantitated using IPLabGel software. The first 5 time points are plotted and fit to a line in (C).

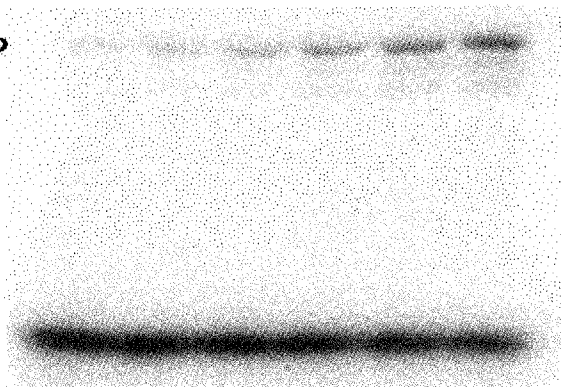
A

EnvZ-P



B

T247R-P



C

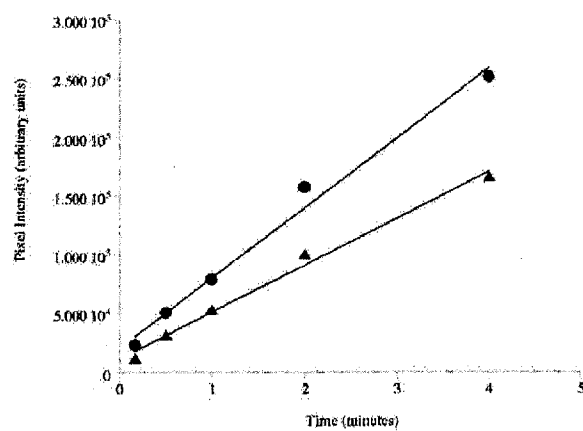




Figure 6.2. Phosphorylation of OmpR by EnvZ and EnvZ T247R. EnvZ (A) and EnvZ T247R (B) were used to phosphorylate OmpR as described in Materials and Methods. Each panel shows the phospho-proteins that result after 10s, 5 min, 20 min, 60 min and 120 min of incubation. The left panels show phosphorylation when 5 times more OmpR than EnvZ is present and the right panels show the reaction in the presence 100 times more OmpR than EnvZ.

A

EnvZ:OmpR

1:5

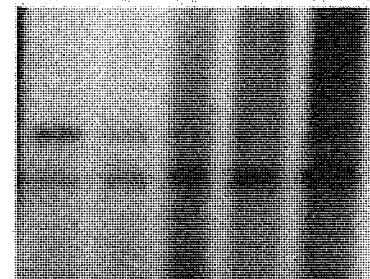
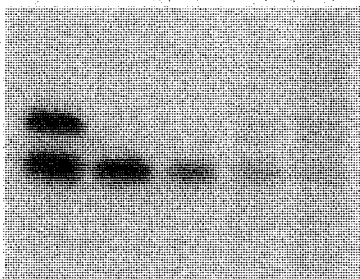
1:100

Time  
(minutes)

0.2 5 20 60 120

0.2 5 20 60 120

EnvZ-P  
OmpR-P



B

T247R:OmpR

1:5

1:100

Time  
(minutes)

0.2 5 20 60 120

0.2 5 20 60 120

T247R-P  
OmpR-P

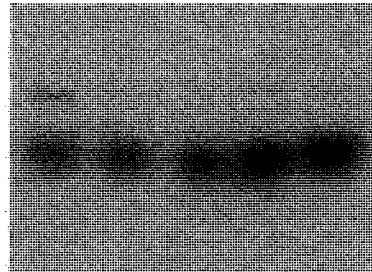
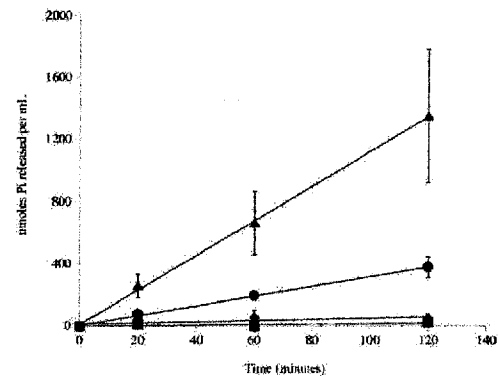
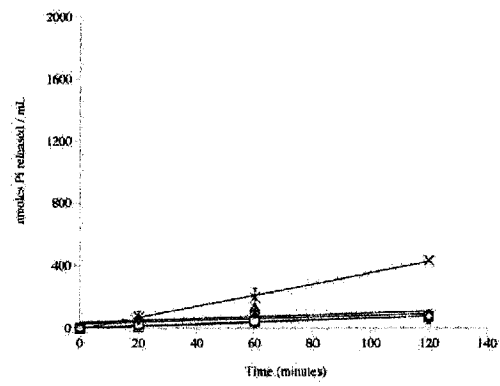


Figure 6.3. ATPase assay with EnvZ and EnvZ T247R. EnvZ (A) and EnvZ T247R (B) were used in an ATPase assay as described in Experimental Procedures and (Kenney, L. J., 1997). (A),  $P_i$  release after incubation of OmpR with ATP and EnvZ; closed triangles, 5:1 EnvZ:OmpR; closed circles, 1:1 EnvZ:OmpR; closed diamonds, 1:5 EnvZ:OmpR; closed squares, 1:100 EnvZ:OmpR. (B),  $P_i$  release after incubation of OmpR with ATP and EnvZ T247R; crosses, 20:1 EnvZ:OmpR; open triangles, 5:1 EnvZ:OmpR; open circles, 1:1 EnvZ:OmpR; open diamonds, 1:5 EnvZ:OmpR; open squares, 1:100 EnvZ:OmpR. The amount of  $P_i$  produced represents the OmpR-stimulated component. At least three independent experiments were performed over 120 min, the error bars represent the standard deviation of the mean for each time point. The average rates reported in the text are derived from the slope of the lines shown, the lines were positioned by least-squares linear regression. (C) Phosphorylation and dephosphorylation of OmpR by a 5-fold molar excess of T247R. T247R was used to phosphorylate OmpR as described in the Materials and Methods. The reactions were stopped after 10 seconds, 5 minutes, 20 minutes, 60 minutes, and 120 minutes.

A



B



C

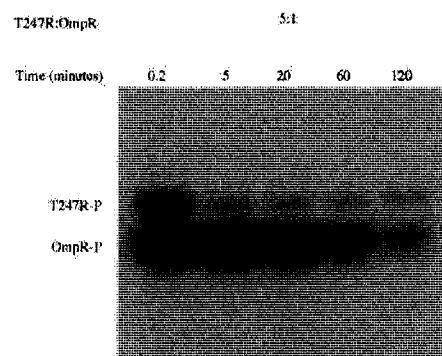
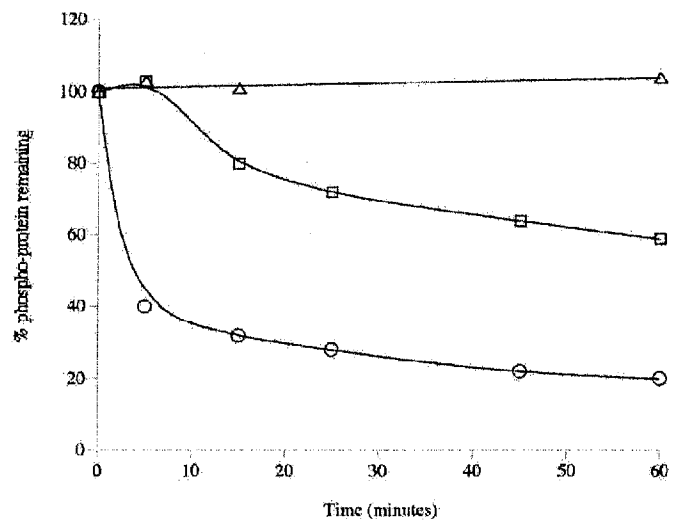


Figure 6.4. Dephosphorylation of OmpR-P by EnvZ and EnvZ T247R. OmpR was phosphorylated using the small molecule phospho-donor phosphoramidate and OmpR-P was purified. The phospho-protein was quantified by C4 reversed phase HPLC and the amount of OmpR-P detected after purification is taken as 100%. Samples were then incubated alone (triangle), in the presence of EnvZ and  $Mg^{2+}$  (circles), or in the presence of EnvZ and EDTA (squares). (A) Shows incubations with wild-type EnvZ (open symbols) and (B) shows the incubations with the EnvZ T247R mutant (filled symbols). The amount of OmpR-P remaining after various time points was quantified by C4 reversed phase HPLC and expressed as a percentage of the starting value.

A



B

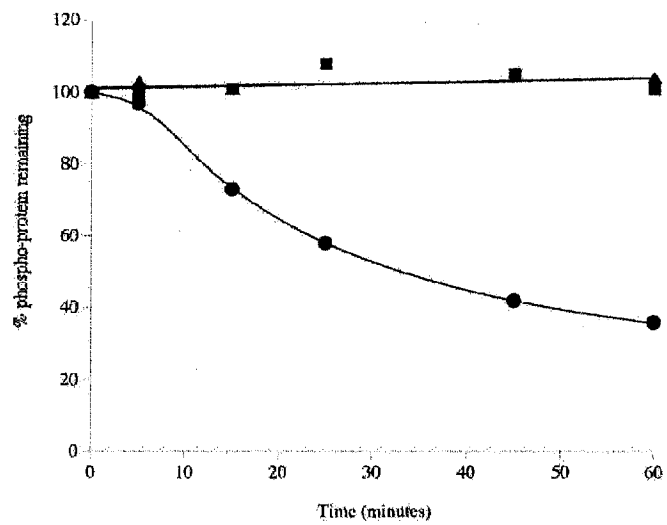


Figure 6.5. Isothermal titration calorimetry of OmpR with EnvZ. The top curve is a control experiment with EnvZ injected into TGED + 200 mM NaCl. The second curve is EnvZ injected into OmpR in the same buffer. The bottom panel shows the integrated areas for the experimental curve after the values from the control curve have been subtracted. When the data are fit using the single set of sites model, best fit curves give a  $K_d$  of 1.5  $\mu$ M for the EnvZ/OmpR interaction.

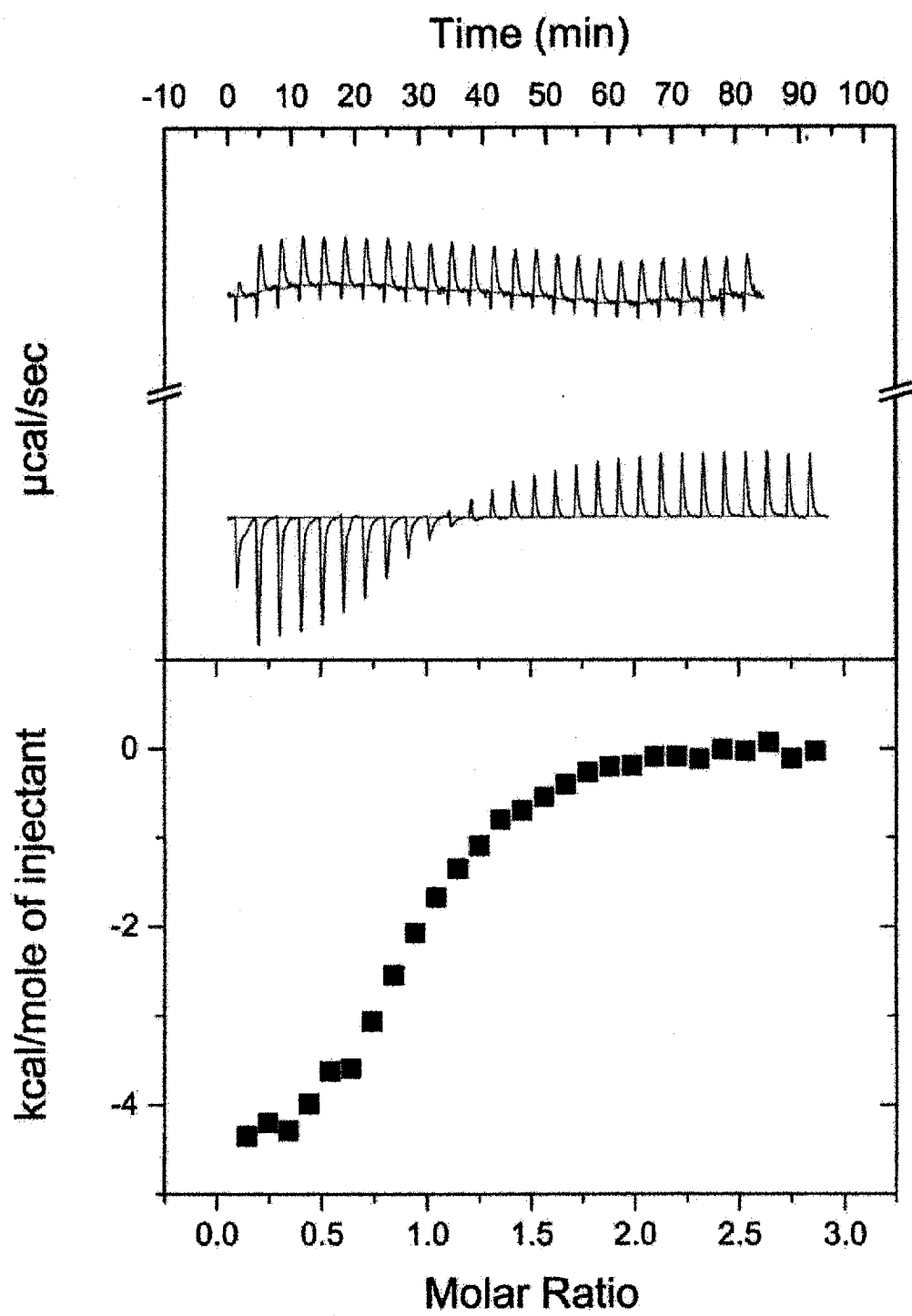
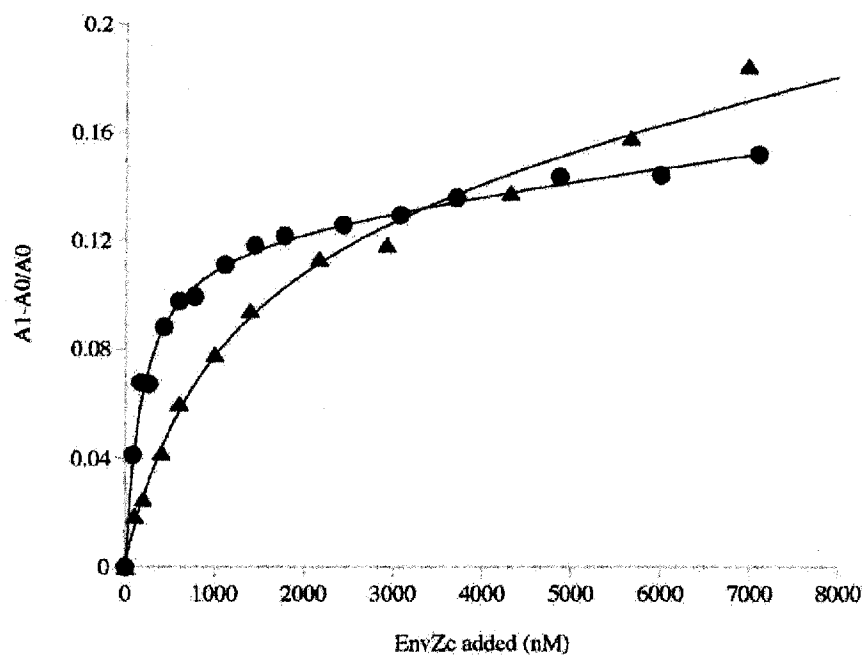




Figure 6.6. Fluorescence anisotropy of OmpR with EnvZ and EnvZ T247R. EnvZ (triangles) or EnvZ T247R (circles) was titrated in to a reaction containing fluorescein-labeled OmpR (A, filled symbols) or OmpR-P (B, open symbols). The curves are representative of multiple experiments, the average values for all curves are reported in the text. (A) The  $K_d$  for OmpR binding to EnvZ in the curve shown is 1.0  $\mu\text{M}$  (filled triangles). For OmpR binding to EnvZ T247R in the curve shown the  $K_d$  is 183 nM (filled circles). (B) In the curve shown, OmpR-P binds EnvZ with non-specific affinity (open triangles) and OmpR-P binds EnvZ T247R with an affinity of 510 nM (open circles).

A



B

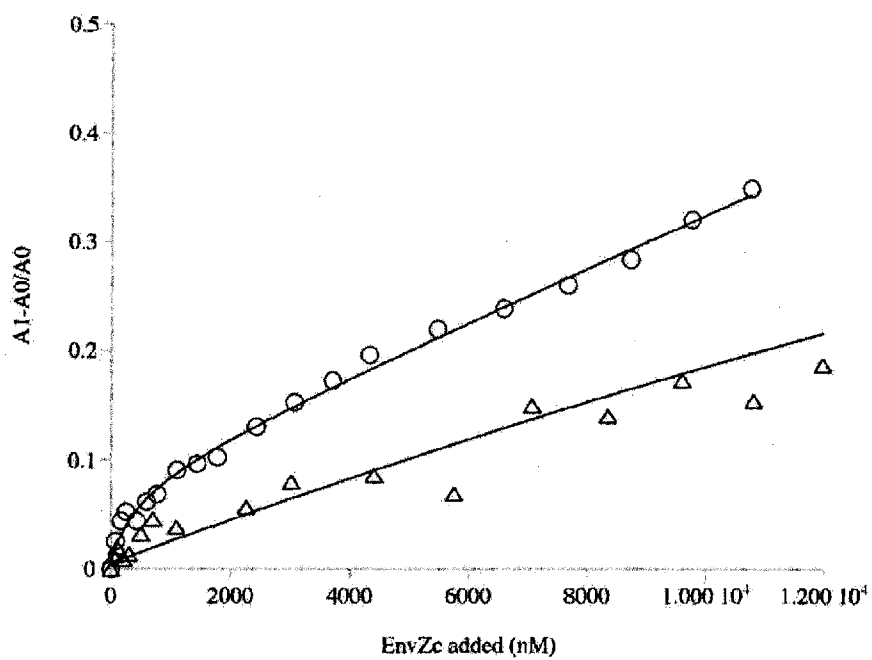


Figure 6.7. OmpR-P is maintained in the presence of EnvZ and phosphoramidate. OmpR was phosphorylated using the phospho-donor phosphoramidate for 30 minutes at room temperature. EnvZ was then added and the samples were incubated for various amounts of time. (A) is the sample after a 5 minute incubation with EnvZ, (B) shows the sample incubated with EnvZc for 15 minutes, and (C) is the sample incubated with EnvZc for 60 minutes. It is clear that even in the presence of EnvZc and  $Mg^{2+}$ , OmpR-P is maintained when there is an excess of phosphoramidate present in the reaction.

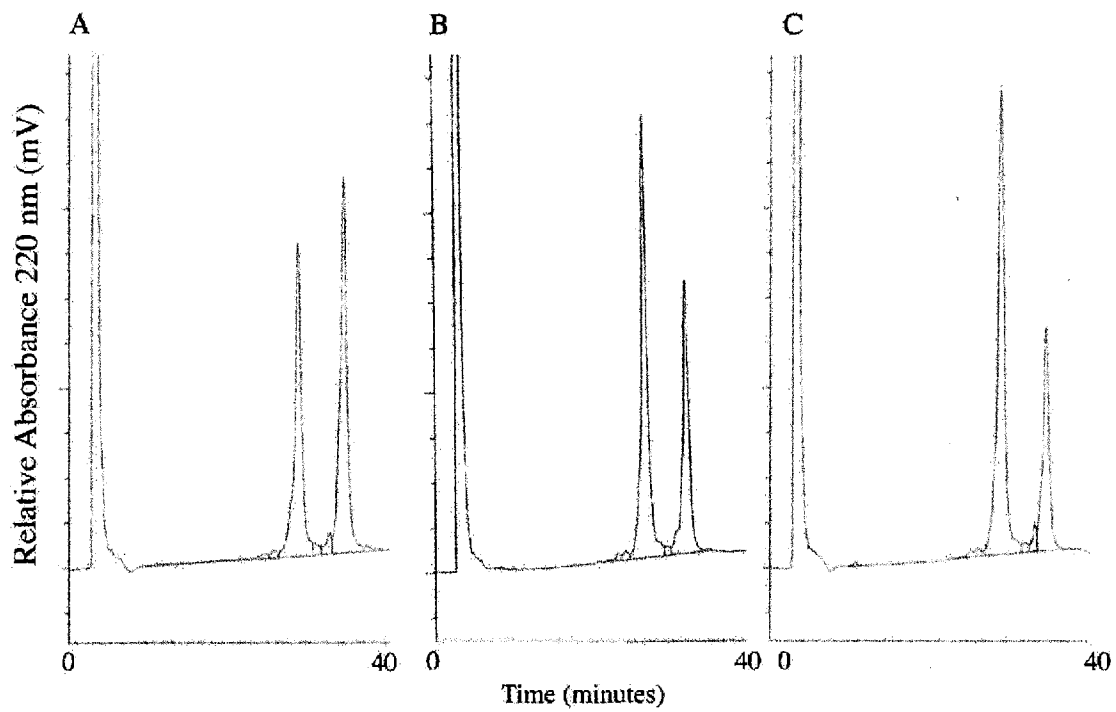


Figure 6.8. Residue positioning in the dimerization domain of EnvZ.

Ribbon diagram of the region surrounding the phosphorylated histidine at position 243 of EnvZ. The coordinates were taken from one set of NMR data derived by (Tomomori, C. *et al.*, 1999) (PDB # 1JOY) and the ribbon diagram generated using the Swiss PDB Viewer (DeepView). The threonine residue at position 247 was mutated to arginine to demonstrate the predicted position of the residue in the mutant protein. The top blue residue is the histidine at position 243, the central red residue is the endogenous arginine at position 246, and the bottom green residue is the introduced arginine at position 247.

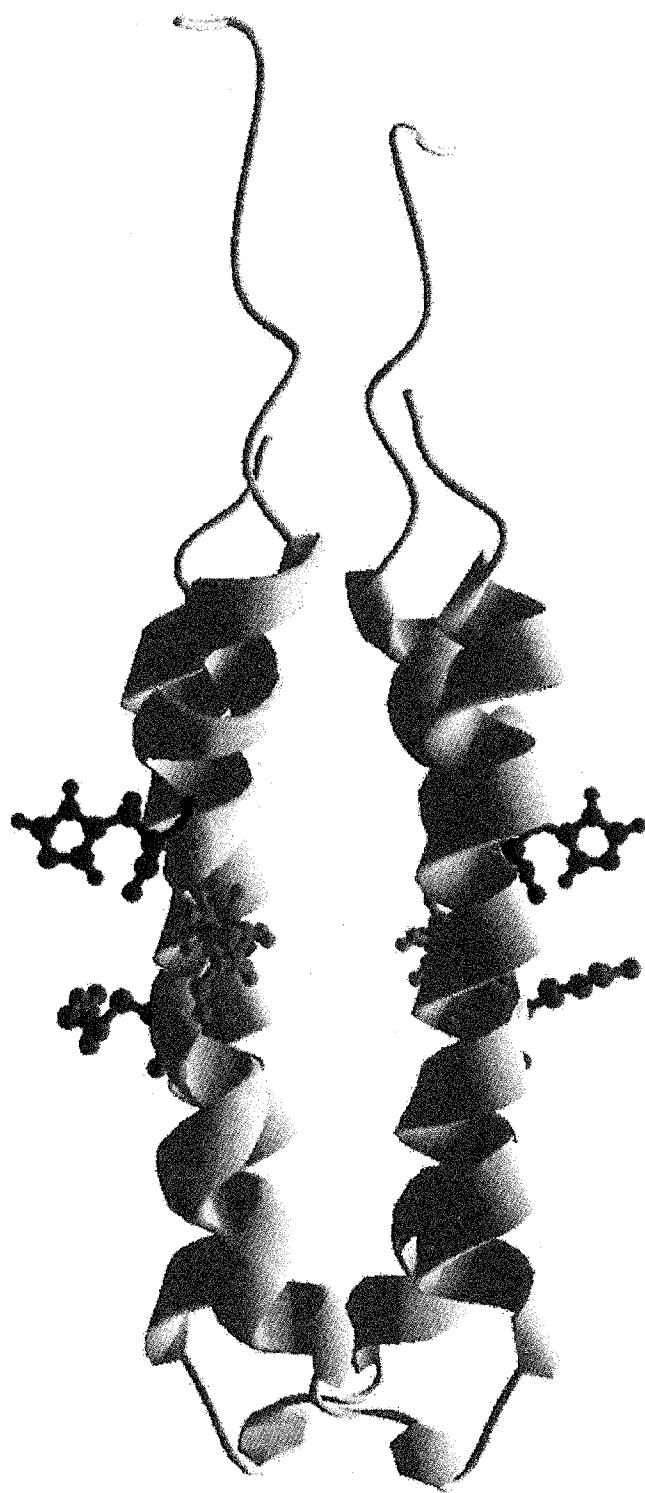


Table 6.1. Isothermal titration calorimetry data. All experiments are titrations of EnvZc into OmpR. The first column shows the EnvZ protein used, either wild-type (WT) or the EnvZ T247R mutant (T247R). The second column shows the buffer used for both OmpR and EnvZ proteins. TGED is 20 mM Tris-HCl (pH 7.6), 5% (v/v) glycerol, 1 mM EDTA, 0.1 mM DTT. Additions to this basic buffer are indicated. The third column (n) shows the calculated ratio of EnvZ:OmpR in the interaction, these are all close to 1, as expected. In the fourth column the calculated enthalpy of the reaction is shown. The fifth column shows the calculated affinity constant for the interaction, the dissociation constants are presented in column 6 for ease of comparison with our fluorescence anisotropy results. The average  $K_d$  values were calculated from the data shown (column 7).

EnvZc	Buffer	n	$\Delta H$ (cal/mole)	$K_a$ ( $M^{-1} \times 10^{-5}$ )	$K_d$ ( $\mu M$ )	Average $K_d$ ( $\mu M$ )
WT	TGED + 200 mM NaCl	0.916	-4770	6.468	1.5	$1.7 \pm 0.7$
		1.006	-6420	3.358	2.9	
		0.897	-5105	7.196	1.3	
	TGED + 100 mM NaCl 20 mM KCl	1.093	-5923	4.360	2.2	
		0.758	-4651	9.754	1.0	
		0.747	-4903	6.972	1.4	
WT	TGED + 100 mM NaCl 20 mM MgCl <sub>2</sub>	0.745	-6723	2.654	3.7	$4.2 \pm 0.6$
		0.816	-7093	2.050	4.8	
		0.841	-6430	2.490	4.0	
T247R	TGED + 100 mM NaCl 20 mM KCl	1.142	-6449	7.069	1.4	$1.4 \pm 0.4$
		0.845	-6253	9.675	1.0	
		0.863	-6624	5.242	1.9	
		0.916	-7713	7.710	1.2	



## **Chapter 7**

### **Discussion**

#### **7.0 Preface**

In this section I have tried not to repeat the discussions from the preceding Chapters, rather I have used this space to address those topics that I feel are important general conclusions of the thesis. I point out data or opinions in the field that conflict with our conclusions and models, and I suggest how further studies will help clarify these issues.

## 7.1 A new model for porin gene osmoregulation

In Chapters 2 and 3 of this dissertation, I present alternatives to the affinity model for porin gene regulation (Figures 2.12 and 3.6). These models predict that the osmoregulation of *ompF* and *ompC* is mediated by alternate conformations of OmpR-P, and not by changing phosphoprotein levels. This is contrary to the affinity model, which predicts that the increase in OmpR-P concentration at high osmolarity leads to the repression of *ompF* and the activation of *ompC* (Russo, F. D. and T. J. Silhavy, 1991). Our laboratory has previously shown that OmpR-P does not have sufficiently different binding affinities at the *ompF* and *ompC* promoter regions to support the requirements of an affinity model (Head, C. G. *et al.*, 1998). The new models presented here are not contradicted by any of the available biochemical data.

However, our models do not account for the genetic data which indicate that EnvZ is required for osmoregulation of porin gene expression (Garrett, S. *et al.*, 1983). The question remains, what role does EnvZ phosphotransfer play in this regulation? All models propose that OmpR-P is the active form of the protein, and this activation of OmpR upon phosphorylation accounts for one requirement of EnvZ in the system. However, the EnvZ kinase is also required for osmoregulation, and our models fail to describe how this might occur. It is possible that a combination of the affinity model and the conformational changes we describe is required to accurately predict the

way the EnvZ/OmpR system controls the expression of OmpF and OmpC at low and high osmolarity.

Reconstitution of the system *in vitro* would provide an excellent opportunity to examine these issues. In my attempts to perform *in vitro* transcription reactions, I found that low concentrations of OmpR-P activate transcription from *ompF*, while higher concentrations of the activator repress transcription from this locus, indicating that for regulation of *ompF*, the affinity model may have some relevance (unpublished results). This is in agreement with published studies of *ompF* transcription *in vitro* (Aiba, H. and T. Mizuno, 1990; Igo, M. M. *et al.*, 1989a). However, *in vitro* transcription reactions using the *ompC* promoter region are more complicated. I consistently detected multiple *ompC* transcripts in attempting to study activation of this promoter (unpublished results). Two other studies have found that transcription of *ompC in vitro* yields the three transcripts that I observed (Ikenaka, K. *et al.*, 1986; Norioka, S. *et al.*, 1986). The one study that achieved transcription of *ompC* from only the expected promoter does not appear to use a different technique, and this issue will have to be resolved before *in vitro* studies will provide more information (Aiba, H. and T. Mizuno, 1990). The utility of an *in vitro* system is that specific mutagenesis of both OmpR and the promoter regions may be used to define the factors contributing to osmoregulation.

## 7.2 Some OmpR mutants bind at C1 but not C2 and C3

The second major finding common to chapters 2 and 3 is that some mutants have a DNA binding defect that has not previously been reported. T83I, G129D and GGK were all found to protect the C1 region from DNase I digestion without binding at the downstream C2 and C3 regions of the *ompC* promoter (Figures 2.8 and 3.5). This defect is specific to binding at *ompC*, as DNase I footprints at *ompF* showed normal patterns of protection. Furthermore, constraint of the OmpR dimer interface leads to this defective pattern of binding, as a cross-linked dimer binds at C1 but not at the downstream sites (Figure 4.12). This DNA binding defect has important implications, especially for the isolation and characterization of activation mutants, which have the ability to bind to DNA but not to activate transcription. Previously, this phenotype has been supposed to indicate that the mutants fail to interact productively with RNA Polymerase (Pratt, L. A. and T. J. Silhavy, 1994). Our studies, presented here as Chapters 2 and 3, show that such mutants may simply fail to bind the promoter-proximal region required to activate transcription (Maeda, S. and T. Mizuno, 1990). Indeed, recent studies in our laboratory indicate that mutants previously thought to have defects in their interaction with RNA Polymerase actually fail to bind at C2 and C3 (D. Walthers and L. J. Kenney, unpublished results).

Since the *ompF* and *ompC* promoters are bound differently by the various mutant and cross-linked proteins, it is interesting to consider

that the promoter sequences may direct different modes of OmpR-P binding, depicted as different conformations in the models proposed in Chapters 2 and 3 (Figure 2.12 and 3.6). Sequences both in and between the OmpR binding sites might contribute to different modes of OmpR binding. In particular, the bases between the F1 and F2 sites are significantly different from those between the C1 and C2 sites (Figure 2.11). This difference could explain the ability of the mutants to bind beyond F1 and not beyond C1. In and around the F1/F2 junction there is a stretch of 6 T·A base pairs (Figure 2.11). Sequences like this, containing four or more consecutive T·A (or A·T) base pairs are known as T-tracts (or A-tracts) (Han, G. W. *et al.*, 1997; Leroy, J. L. *et al.*, 1988; Suter, B. *et al.*, 2000). These sequences adopt a slightly different structure than typical B-form DNA in that they are essentially straight and rigid (DiGabriele, A. D. *et al.*, 1989; Han, G. W. *et al.*, 1997; Leroy, J. L. *et al.*, 1988; Nelson, H. C. *et al.*, 1987). In addition, these sequences deviate from B-form DNA by having a compressed minor groove and a shorter helical repeat of only 10 bp (Alexeev, D. G. *et al.*, 1987; Han, G. W. *et al.*, 1997; Peck, L. J. and J. C. Wang, 1981; Rhodes, D. and A. Klug, 1980, 1981). In fact, in and around the F1 binding site there are four T-tract sequences, which may confer a unique conformation to this promoter sequence (Figure 2.11). By contrast, the sequence separating C1 from C2 is AGC, within a stretch of ATAGCG (Figure 2.11). This sequence does not share the special T-tract properties seen at *ompF*,

there are only two minimal T-tract sequences in the entire *ompC* promoter region, and none of them are found in regions external to the OmpR binding sites (Figure 2.11). The unique structure of the T-tracts may provide an environment where OmpR dimers readily interact at *ompF*. At *ompC*, the normal B-form DNA may situate the OmpR dimers such that they must be capable of conformational changes like those depicted in Figures 2.12 and 3.6 for oligomerization and binding at the downstream C2 and C3 sites. This would explain the inability of the mutant proteins to oligomerize along the *ompC* sequence without undergoing some conformational transition necessary for normal binding at *ompC*. DNase I cleavage is observed in between the C1 and C2 sites when wild-type OmpR is bound, indicating that the DNA separating C1 and C2 is more accessible than that in the corresponding region of *ompF* (Figures 2.8, 2.11 and 3.5). This hypothesis can be directly tested by interrupting the T-tract between F1 and F2 by substituting one of the thymidine bases with A or G. Pyrimidine-purine transitions are particularly effective at disrupting A tract structure (Leroy, J. L. *et al.*, 1988; MacDonald, D. *et al.*, 2001). According to this hypothesis, a disrupted T-tract in between F1 and F2 is not expected to interfere with binding by wild-type OmpR. The mutation is expected to confer a binding phenotype at *ompF* to the mutants T83I, G129D, and GGK analogous to that observed at *ompC*, i.e. the F1 site is predicted to be bound in the absence of F2 and F3 binding.

### 7.3 A new model for OmpR dimerization

In Chapter 4, I describe cross-linking studies which do not support the previous model for OmpR dimer formation (Harrison-McMonagle, P. *et al.*, 1999). We have proposed a new model for the dimer interface based on these results (Figure 4.13). This study suggests a role for the  $\beta$ -sheet at the amino terminal end of OmpRc in forming the dimer interface. This  $\beta$ -sheet is conserved among OmpR family members, but has not been previously assigned a functional role in osmoregulation (Martinez-Hackert, E. and A. M. Stock, 1997b). The asymmetric tandem dimer model that is proposed in Chapter 4 fits most of the available data (see section 4.4). One discrepancy is that the *ompC* promoter region may be inverted without disrupting transcriptional activation by OmpR (Maeda, S. and T. Mizuno, 1988). This indifference to binding site orientation is easiest to explain by a symmetric head-to-head type of dimer model. We did at first attempt to construct such a model, but the distances between the cysteine-substituted sites were too great to explain the cross-linking data. If the  $\beta$ -sheet is capable of movement away from the hydrophobic core of OmpRc, then a head-to-head interface is possible. We were unwilling to propose such movement, since removal of the  $\beta$ -sheet from OmpRc had no effect on function (unpublished results). However, OmpR interacts with the carboxyl terminal domain of the  $\alpha$  subunit of RNA Polymerase ( $\alpha$ -CTD) (Kato, N. *et al.*, 1996; Matsuyama, S. and S. Mizushima, 1987; Sharif, T. R. and M. M. Igo, 1993; Slauch, J. M.

*et al.*, 1991). The amino terminal domain of the  $\alpha$  subunit interacts with the rest of the RNA Polymerase complex, while the carboxyl terminus is tethered to the complex by a flexible linker, which allows it to bind to transcriptional activators in different ways (Gaal, T. *et al.*, 1996; Hayward, R. S. *et al.*, 1991; Igarashi, K. and A. Ishihama, 1991). The flexibility of  $\alpha$ -CTD may be sufficient to interact with the inverted OmpR activator in an asymmetric model such as the one we have proposed.

#### **7.4 The role of the EnvZ phosphatase in osmoregulation**

Both Chapters 5 and 6 of this thesis present evidence that indicates the phosphatase activity of EnvZ is unlikely to play a role *in vivo*. We feel that the *in vitro* phosphatase activity displayed by this kinase is only achieved due to the high levels of purified protein used in the assays. This conclusion has been controversial in the field and publications have followed which attempt to discredit it. (Cai, S. J. and M. Inouye, 2002; Yoshida, T. *et al.*, 2002a; Yoshida, T. *et al.*, 2002b). In one study, the authors use  $\text{Ni}^{++}$  beads to precipitate histidine-tagged EnvZc and the OmpR bound to it. They use a competition assay to argue that OmpR and OmpR-P bind EnvZc with similar affinities, in contrast to our finding (Figure 5.2) (Yoshida, T. *et al.*, 2002b). This is a very different assay from ours, and does not directly detect the interaction of OmpR or OmpR-P with EnvZ. Their analysis is compromised since the lowest concentration of protein used is 4  $\mu\text{M}$ , while the EnvZ/OmpR interaction has a  $K_d$  of approximately 0.5-1  $\mu\text{M}$  (Mattison, K. and L. J. Kenney, 2002;



Yoshida, T. *et al.*, 2002a)(Table 6.1). In addition, an earlier description of this technique from their laboratory stated that OmpR-P bound EnvZ with lower affinity than OmpR, although the data were not shown (Hidaka, Y. *et al.*, 1997). In a second study, fluoresceinated OmpR was used in fluorescence anisotropy assays as we described. The affinity reported for the interaction between OmpR and EnvZ is only slightly different from ours, although the equations used do not include a term which corrects for the linear increase in polarization as protein concentration becomes high (Yoshida, T. *et al.*, 2002a). The calculated dissociation constant for the interaction between EnvZ and OmpR-P is not reported, although in the graphical representation shown it appears to be lower than the affinity between EnvZ and OmpR (Yoshida, T. *et al.*, 2002a). The last study uses quantitative Western blotting to show that there are approximately 3500 molecules of OmpR and 100 molecules of EnvZ per cell (Cai, S. J. and M. Inouye, 2002). This slightly changes the ratio of OmpR to EnvZ in the cell from previous estimates, but does not change the pattern that we show in Chapter 6, where the phosphatase activity is less evident at lower protein concentrations (Figures 6.2 and 6.3). None of these publications have cast serious doubts on our findings. Future studies of the phosphatase mutant of EnvZ will be very interesting in detailing the role that  $Mg^{2+}$  plays in the stability of OmpR-P. It will be useful to directly test our proposed alternate explanation for the *in vivo* phenotypes of such phosphatase mutants. These studies of

the EnvZ phosphatase activity reinforce that the physiological relevance of *in vitro* reaction conditions must always be considered.

## **7.5 Conclusion**

The studies presented in this thesis present new models for the regulation of porin gene expression by the response regulator OmpR (Chapters 2 and 3). These models postulate conformational changes in OmpR that are responsible for the reciprocal regulation of OmpF and OmpC at low and high osmolarity. Together with the new model for the OmpR dimer interface in Chapter 4, these models provide a basis for detailed molecular studies which will clarify OmpR function. This thesis has also shown that the interaction of EnvZ with OmpR-P is of very low affinity (Chapter 5). Given the low concentration of EnvZ present in the cell, this makes it unlikely that EnvZ dephosphorylates OmpR-P *in vivo*. We show that a phosphatase mutant has altered interactions with the OmpR regulator, and present an intriguing hypothesis where  $Mg^{2+}$  bound in the OmpR-P active site might change the inherent stability of OmpR-P (Chapter 6). Testing of this model may provide more evidence that the EnvZ phosphatase does not control the concentration of phosphorylated OmpR in the cell.

## References

- Aiba, H., N. Kato, M. Tsuzuki and T. Mizuno (1994). Mechanism of gene activation by the *Escherichia coli* positive regulator, OmpR: a mutant defective in transcriptional activation. *FEBS Lett* **351**: 303-307.
- Aiba, H., S. Matsuyama, T. Mizuno and S. Mizushima (1987). Function of *micF* as an antisense RNA in osmoregulatory expression of the *ompF* gene in *Escherichia coli*. *J Bacteriol* **169**: 3007-3012.
- Aiba, H. and T. Mizuno (1990). Phosphorylation of a bacterial activator protein, OmpR, by a protein kinase, EnvZ, stimulates the transcription of the *ompF* and *ompC* genes in *Escherichia coli*. *FEBS Lett* **261**: 19-22.
- Aiba, H., T. Mizuno and S. Mizushima (1989a). Transfer of phosphoryl group between two regulatory proteins involved in osmoregulatory expression of the *ompF* and *ompC* genes in *Escherichia coli*. *J Biol Chem* **264**: 8563-8567.
- Aiba, H., F. Nakasai, S. Mizushima and T. Mizuno (1989b). Evidence for the physiological importance of the phosphotransfer between the two regulatory components, EnvZ and OmpR, in osmoregulation in *Escherichia coli*. *J Biol Chem* **264**: 14090-14094.
- Aiba, H., F. Nakasai, S. Mizushima and T. Mizuno (1989c).  
Phosphorylation of a bacterial activator protein, OmpR, by a

- protein kinase, EnvZ, results in stimulation of its DNA-binding ability. *J Biochem (Tokyo)* **106**: 5-7.
- Alexeev, D. G., A. A. Lipanov and I. Skuratovskii (1987). Poly(dA)·poly(dT) is a B-type double helix with a distinctively narrow minor groove. *Nature* **325**: 821-823.
- Allen, M. P., K. B. Zumbrennen and W. R. McCleary (2001). Genetic evidence that the alpha5 helix of the receiver domain of PhoB is involved in interdomain interactions. *J Bacteriol* **183**: 2204-2211.
- Ames, S. K., N. Frankema and L. J. Kenney (1999). C-terminal DNA binding stimulates N-terminal phosphorylation of the outer membrane protein regulator OmpR from *Escherichia coli*. *Proc Natl Acad Sci U S A* **96**: 11792-11797.
- Andersen, J., N. Delihias, K. Ikenaka, P. J. Green, O. Pines, O. Ilercil and M. Inouye (1987). The isolation and characterization of RNA coded by the *micF* gene in *Escherichia coli*. *Nucleic Acids Res* **15**: 2089-2101.
- Andersen, P. A., I. Kaasen, O. B. Styrvold, G. Boulnois and A. R. Strom (1988). Molecular cloning, physical mapping and expression of *bet* genes governing the osmo-regulatory choline-glycinebetaine pathway of *Escherichia coli*. *J Gen Microbiol* **134**: 1737-1746.
- Appleby, J. L. and R. B. Bourret (1998). Proposed signal transduction role for conserved CheY residue Thr87, a member of the response regulator active-site quintet. *J Bacteriol* **180**: 3563-3569.

- Appleby, J. L. and R. B. Bourret (1999). Activation of CheY mutant D57N by phosphorylation at an alternative site, Ser-56. *Mol Microbiol* **34**: 915-925.
- Appleyard, M. V. C. L., W. L. McPheat and M. J. R. Stark (2000). A novel 'two-component' protein containing histidine kinase and response regulator domains required for sporulation in *Aspergillus nidulans*. *Curr Genet* **37**: 364-372.
- Arakawa, T. and S. N. Timasheff (1985). The stabilization of proteins by osmolytes. *Biophys J* **47**: 411-414.
- Argast, M. and W. Boos (1980). Co-regulation in *Escherichia coli* of a novel transport system for sn-glycerol-3-phosphate and outer membrane protein Ic (e, E) with alkaline phosphatase and phosphate-binding protein. *J Bacteriol* **143**: 142-150.
- Argos, P. (1990). An investigation of oligopeptides linking domains in protein tertiary structures and possible candidates for general gene fusion. *J Mol Biol* **211**: 943-958.
- Aubry, L. and R. Firtel (1999). Integration of signaling networks that regulate *Dictyostelium* differentiation. *Annu Rev Cell Dev Biol* **15**: 469-517.
- Baikalov, I., I. Schroder, M. Kaczor-Grzeskowiak, K. Grzeskowiak, R. P. Gunsalus and R. E. Dickerson (1996). Structure of the *Escherichia coli* response regulator NarL. *Biochemistry* **35**: 11053-11061.

- Bellsolell, L., J. Prieto, L. Serrano and M. Coll (1994). Magnesium binding to the bacterial chemotaxis protein CheY results in large conformational changes involving its functional surface. *J Mol Biol* **238**: 489-495.
- Bergstrom, L., L. Qin, S. Harlocker, L. A. Egger and M. Inouye (1998). Hierarchical and co-operative binding of OmpR to a fusion construct containing the *ompC* and *ompF* upstream regulatory sequences of *Escherichia coli*. *Genes Cells* **3**: 777-788.
- Biemann, H.-P. and D. E. J. Koshland (1994). Aspartate receptors of *Escherichia coli* and *Salmonella typhimurium* bind ligand with negative and half-of-the-sites cooperativity. *Biochemistry* **33**: 629-634.
- Birck, C., L. Mourey, P. Gouet, B. Fabry, J. Schumacher, P. Rousseau, D. Kahn and J. P. Samama (1999). Conformational changes induced by phosphorylation of the FixJ receiver domain. *Structure Fold Des* **7**: 1505-1515.
- Blanco, A. G., M. Sola, F. X. Gomis-Ruth and M. Coll (2002). Tandem DNA Recognition by PhoB, a Two-Component Signal Transduction Transcriptional Activator. *Structure (Camb)* **10**: 701-713.
- Blat, Y., B. Gillespie, A. Bren, F. W. Dahlquist and M. Eisenbach (1998). Regulation of phosphatase activity in bacterial chemotaxis. *J Mol Biol* **284**: 1191-1199.

- Bourret, R. B., N. W. Charon, A. M. Stock and A. H. West (2002). Bright Lights, Abundant Operons-Fluorescence and Genomic Technologies Advance Studies of Bacterial Locomotion and Signal Transduction: Review of the BLAST Meeting, Cuernavaca, Mexico, 14 to 19 January 2001. *J Bacteriol* **184**: 1-17.
- Bourret, R. B., J. F. Hess and M. I. Simon (1990). Conserved aspartate residues and phosphorylation in signal transduction by the chemotaxis protein CheY. *Proc Natl Acad Sci U S A* **87**: 41-45.
- Brennan, R. G. (1993). The winged helix-turn-helix DNA-binding motif: another helix-turn-helix takeoff. *Cell* **74**: 773-776.
- Brissette, R. E., K. Tsung and M. Inouye (1991a). Suppression of a mutation in OmpR at the putative phosphorylation center by a mutant EnvZ protein in *Escherichia coli*. *J Bacteriol* **173**: 601-608.
- Brissette, R. E., K. L. Tsung and M. Inouye (1991b). Intramolecular second-site revertants to the phosphorylation site mutation in OmpR, a kinase-dependent transcriptional activator in *Escherichia coli*. *J Bacteriol* **173**: 3749-3755.
- Buckler, D. R., G. S. Anand and A. M. Stock (2000). Response-regulator phosphorylation and activation: a two-way street? *Trends Microbiol* **8**: 153-156.
- Buckler, D. R., Y. Zhou and A. M. Stock (2002). Evidence of Intradomain and Interdomain Flexibility in an OmpR/PhoB Homolog from *Thermotoga maritima*. *Structure (Camb)* **10**: 153-164.

- Cai, S. J. and M. Inouye (2002). EnvZ-OmpR interaction and osmoregulation in *Escherichia coli*. *J Biol Chem* **277**: 24155-24161.
- Cairney, J., I. R. Booth and C. F. Higgins (1985). Osmoregulation of gene expression in *Salmonella typhimurium*: *proU* encodes an osmotically induced betaine transport system. *J Bacteriol* **164**: 1224-1232.
- Calera, J. A. and R. A. Calderone (1999). Identification of a putative response regulator two-component phosphorelay gene (CaSSK1) from *Candida albicans*. *Yeast* **15**: 1243-1254.
- Casadaban, M. J. (1976). Transposition and fusion of the *lac* genes to selected promoters in *Escherichia coli* using bacteriophages lambda and Mu. *J Mol Biol* **104**: 541-555.
- Castelli, M. E., E. Garcia Vescovi and F. C. Soncini (2000). The phosphatase activity is the target for Mg<sup>2+</sup> regulation of the sensor protein PhoQ in Salmonella. *J Biol Chem* **275**: 22948-22954.
- Cayley, S., B. A. Lewis and M. T. Record (1992). Origins of the osmoprotective properties of betaine and proline in *Escherichia coli* K-12. *J Bacteriol* **174**: 1586-1595.
- Chen, Q. and R. J. Kadner (2000). Effect of altered spacing between *uhpT* promoter elements on transcription activation. *J Bacteriol* **182**: 4430-4436.



- Cho, H. S., S. Y. Lee, D. Yan, X. Pan, J. S. Parkinson, S. Kustu, D. E. Wemmer and J. G. Pelton (2000). NMR structure of activated CheY. *J Mol Biol* **297**: 543-551.
- Comeau, D. E., K. Ikenaka, K. Tsung and M. Inouye (1985). Primary characterization of the protein products of the *Escherichia coli* *ompB* locus: structure and regulation of synthesis of the OmpR and EnvZ proteins. *J Bacteriol* **164**: 578-584.
- Coyer, J., J. Andersen, S. Forst, M. Inouye and N. Delihias (1990). *micF* RNA in *ompB* mutants of *Escherichia coli*: different pathways regulate *micF* RNA levels in response to osmolarity and temperature change. *J Bacteriol* **172**: 4143-4150.
- Csonka, L. N. (1989). Physiological and genetic responses of bacteria to osmotic stress. *Microbiol Rev* **53**: 121-147.
- Cui, C., D. O. Smith and J. Adler (1995). Characterization of mechanosensitive channels in *Escherichia coli* cytoplasmic membrane by whole-cell patch clamp recording. *J Membr Biol* **144**: 31-42.
- D'Agostino, I. B. and J. J. Kieber (1999). Phosphorelay signal transduction: the emerging family of plant response regulators. *TIBS* **24**: 452-456.
- Da Re, S., J. Schumacher, P. Rousseau, J. Fourment, C. Ebel and D. Kahn (1999). Phosphorylation-induced dimerization of the FixJ receiver domain. *Mol Microbiol* **34**: 504-511.

- Dairi, T., K. Inokuchi, T. Mizuno and S. Mizushima (1985). Positive control of transcription initiation in *Escherichia coli*. A base substitution at the Pribnow box renders *ompF* expression independent of a positive regulator. *J Mol Biol* **184**: 1-6.
- Decad, G. M. and H. Nikaido (1976). Outer membrane of gram-negative bacteria. XII. Molecular-sieving function of cell wall. *J Bacteriol* **128**: 325-336.
- Delgado, J., S. Forst, S. Harlocker and M. Inouye (1993). Identification of a phosphorylation site and functional analysis of conserved aspartic acid residues of OmpR, a transcriptional activator for *ompF* and *ompC* in *Escherichia coli*. *Mol Microbiol* **10**: 1037-1047.
- DiGabriele, A. D., M. R. Sanderson and T. A. Steitz (1989). Crystal lattice packing is important in determining the bend of a DNA dodecamer containing an adenine tract. *Proc Natl Acad Sci U S A* **86**: 1816-1820.
- Dutta, R. and M. Inouye (1996). Reverse phosphotransfer from OmpR to EnvZ in a kinase-/phosphatase+ mutant of EnvZ (EnvZ.N347D), a bifunctional signal transducer of *Escherichia coli*. *J Biol Chem* **271**: 1424-1429.
- Dutta, R., L. Qin and M. Inouye (1999). Histidine kinases: diversity of domain organization. *Mol Microbiol* **34**: 633-640.
- Dutta, R., T. Yoshida and M. Inouye (2000). The critical role of the conserved Thr247 residue in the functioning of the osmosensor

- EnvZ, a histidine Kinase/Phosphatase, in *Escherichia coli*. *J Biol Chem* **275**: 38645-38653.
- Egger, L. A. and M. Inouye (1997). Purification and characterization of the periplasmic domain of EnvZ osmosensor in *Escherichia coli*. *Biochem Biophys Res Commun* **231**: 68-72.
- Ellison, D. W. and W. R. McCleary (2000). The unphosphorylated receiver domain of PhoB silences the activity of its output domain. *J Bacteriol* **182**: 6592-6597.
- Epstein, W. and S. G. Schultz (1965). Cation transport in *Escherichia coli* V. regulation of cation content. *J. Gen. Physiol.* **49**: 221-234.
- Forst, S., D. Comeau, S. Norioka and M. Inouye (1987). Localization and membrane topology of EnvZ, a protein involved in osmoregulation of OmpF and OmpC in *Escherichia coli*. *J Biol Chem* **262**: 16433-16438.
- Forst, S., J. Delgado and M. Inouye (1989a). DNA-binding properties of the transcription activator (OmpR) for the upstream sequences of *ompF* in *Escherichia coli* are altered by *envZ* mutations and medium osmolarity. *J Bacteriol* **171**: 2949-2955.
- Forst, S., J. Delgado and M. Inouye (1989b). Phosphorylation of OmpR by the osmosensor EnvZ modulates expression of the *ompF* and *ompC* genes in *Escherichia coli*. *Proc Natl Acad Sci U S A* **86**: 6052-6056.

- Forst, S., J. Delgado, G. Ramakrishnan and M. Inouye (1988). Regulation of *ompC* and *ompF* expression in *Escherichia coli* in the absence of *envZ*. *J Bacteriol* **170**: 5080-5085.
- Forst, S., J. Delgado, A. Rampersaud and M. Inouye (1990). In vivo phosphorylation of OmpR, the transcription activator of the *ompF* and *ompC* genes in *Escherichia coli*. *J Bacteriol* **172**: 3473-3477.
- Forst, S., I. Kalve and W. Durski (1995). Molecular analysis of OmpR binding sequences involved in the regulation of *ompF* in *Escherichia coli*. *FEMS Microbiol Lett* **131**: 147-151.
- Foussard, M., S. Cabantous, J.-D. Pedelacq, V. Guillet, S. Tranier, L. Mourey, C. Birck and J. P. Samama (2001). The molecular puzzle of two-component signaling cascades. *Microbes and Infection* **3**: 417-424.
- Friedman, D. I. (1988). Integration host factor: a protein for all reasons. *Cell* **55**: 545-554.
- Gaal, T., W. Ross, E. E. Blatter, H. Tang, X. Jia, V. V. Krishnan, N. Assa-Munt, R. H. Ebright and R. L. Gourse (1996). DNA-binding determinants of the alpha subunit of RNA polymerase: novel DNA-binding domain architecture. *Genes Dev* **10**: 16-26.
- Galanos, C. and O. Luderitz (1975). Electrodialysis of lipopolysaccharides and their conversion to uniform salt forms. *Eur J Biochem* **54**: 603-610.

- Ganguli, S., H. Wang, P. Matsumura and K. Volz (1995). Uncoupled phosphorylation and activation in bacterial chemotaxis. The 2.1-A structure of a threonine to isoleucine mutant at position 87 of CheY. *J Biol Chem* **270**: 17386-17393.
- Garrett, S., R. K. Taylor and T. J. Silhavy (1983). Isolation and characterization of chain-terminating nonsense mutations in a porin regulator gene, *envZ*. *J Bacteriol* **156**: 62-69.
- Garrett, S., R. K. Taylor, T. J. Silhavy and M. L. Berman (1985). Isolation and characterization of delta *ompB* strains of *Escherichia coli* by a general method based on gene fusions. *J Bacteriol* **162**: 840-844.
- Giaever, H. M., O. B. Styrvold, I. Kaasen and A. R. Strom (1988). Biochemical and genetic characterization of osmoregulatory trehalose synthesis in *Escherichia coli*. *J Bacteriol* **170**: 2841-2849.
- Goudreau, P. N., P.-J. Lee and A. M. Stock (1998). Stabilization of the phospho-aspartyl residue in a two-component signal transduction system in *Thermotoga maritima*. *Biochemistry* **37**: 14575-14584.
- Gowrishankar, J. (1986). Identification of osmoresponsive genes in *Escherichia coli*: evidence for participation of potassium and proline transport systems in osmoregulation. *J Bacteriol* **164**: 434-445.
- Hackenbeck, R. and J. B. Stock (1996). Analysis of two-component signal transduction systems involved in transcriptional regulation. *Methods Enzymol* **273**: 281-300.

- Halkides, C. J., M. M. McEvoy, E. Casper, P. Matsumura, K. Volz and F. W. Dahlquist (2000). The 1.9 Å resolution crystal structure of phosphono-CheY, an analogue of the active form of the response regulator, CheY. *Biochemistry* **39**: 5280-5286.
- Hall, M. N. and T. J. Silhavy (1979). Transcriptional regulation of *Escherichia coli* K-12 major outer membrane protein 1b. *J Bacteriol* **140**: 342-350.
- Hall, M. N. and T. J. Silhavy (1981a). Genetic analysis of the major outer membrane proteins of *Escherichia coli*. *Annu Rev Genet* **15**: 91-142.
- Hall, M. N. and T. J. Silhavy (1981b). Genetic Analysis of the *ompB* locus in *Escherichia coli*. *J Mol Biol* **151**: 1-15.
- Hall, M. N. and T. J. Silhavy (1981c). The *ompB* locus and the regulation of the major outer membrane porin proteins of *Escherichia coli* K12. *J Mol Biol* **146**: 23-43.
- Han, G. W., M. L. Kopka, D. Cascio, K. Grzeskowiak and R. E. Dickerson (1997). Structure of a DNA analog of the primer for HIV-1 RT second strand synthesis. *J Mol Biol* **269**: 811-826.
- Harlocker, S. L., L. Bergstrom and M. Inouye (1995). Tandem binding of six OmpR proteins to the *ompF* upstream regulatory sequence of *Escherichia coli*. *J Biol Chem* **270**: 26849-26856.
- Harrison-McMonagle, P., N. Denissova, E. Martinez-Hackert, R. H. Ebright and A. M. Stock (1999). Orientation of OmpR monomers

- within an OmpR:DNA complex determined by DNA affinity cleaving. *J Mol Biol* **285**: 555-566.
- Hawley, D. K. and W. R. McClure (1983). Compilation and analysis of *Escherichia coli* promoter DNA sequences. *Nucleic Acids Res* **11**: 2237-2255.
- Hayward, R. S., K. Igarashi and A. Ishihama (1991). Functional specialization within the alpha-subunit of *Escherichia coli* RNA polymerase. *J Mol Biol* **221**: 23-29.
- Head, C. G., A. Tardy and L. J. Kenney (1998). Relative binding affinities of OmpR and OmpR-phosphate at the *ompF* and *ompC* regulatory sites. *J Mol Biol* **281**: 857-870.
- Hidaka, Y., H. Park and M. Inouye (1997). Demonstration of dimer formation of the cytoplasmic domain of a transmembrane osmosensor protein, EnvZ, of *Escherichia coli* using Ni-histidine tag affinity chromatography. *FEBS Lett* **400**: 238-242.
- Hoch, J. A. and T. J. Silhavy (1995). Two component signal transduction. American Society for Microbiology Press, Washington, D.C.
- Hsing, W., F. D. Russo, K. K. Bernd and T. J. Silhavy (1998). Mutations that alter the kinase and phosphatase activities of the two-component sensor EnvZ. *J Bacteriol* **180**: 4538-4546.
- Hsing, W. and T. J. Silhavy (1997). Function of conserved histidine-243 in phosphatase activity of EnvZ, the sensor for porin osmoregulation in *Escherichia coli*. *J Bacteriol* **179**.

- Huang, K. J. and M. M. Igo (1996). Identification of the bases in the *ompF* regulatory region, which interact with the transcription factor OmpR. *J Mol Biol* **262**: 615-628.
- Huang, K. J., C. Y. Lan and M. M. Igo (1997). Phosphorylation stimulates the cooperative DNA-binding properties of the transcription factor OmpR. *Proc Natl Acad Sci U S A* **94**: 2828-2832.
- Huang, K. J., J. L. Schiebel and M. M. Igo (1994). A distant upstream site involved in the negative regulation of the *Escherichia coli ompF* gene. *J Bacteriol* **176**: 1309-1315.
- Igarashi, K., A. Hanamura, K. Makino, H. Aiba, T. Mizuno, A. Nakata and A. Ishihama (1991). Functional map of the alpha subunit of *Escherichia coli* RNA polymerase: two modes of transcription activation by positive factors. *Proc Natl Acad Sci U S A* **88**: 8958-8962.
- Igarashi, K. and A. Ishihama (1991). Bipartite functional map of the *E. coli* RNA polymerase alpha subunit: involvement of the C-terminal region in transcription activation by cAMP-CRP. *Cell* **65**: 1015-1022.
- Igo, M. M., A. J. Ninfa and T. J. Silhavy (1989a). A bacterial environmental sensor that functions as a protein kinase and stimulates transcriptional activation. *Genes Dev* **3**: 598-605.
- Igo, M. M., A. J. Ninfa, J. B. Stock and T. J. Silhavy (1989b). Phosphorylation and dephosphorylation of a bacterial



- transcriptional activator by a transmembrane receptor. *Genes Dev* **3**: 1725-1734.
- Igo, M. M. and T. J. Silhavy (1988). EnvZ, a transmembrane environmental sensor of *Escherichia coli* K-12, is phosphorylated *in vitro*. *J Bacteriol* **170**: 5971-5973.
- Ikenaka, K., G. Ramakrishnan, M. Inouye and K. Tsung (1986). Regulation of the *ompC* gene of *Escherichia coli*. Involvement of three tandem promoters. *J Biol Chem* **261**: 9316-9320.
- Inokuchi, K., H. Furukawa, K. Nakamura and S. Mizushima (1984). Characterization by deletion mutagenesis *in vitro* of the promoter region of *ompF*, a positively regulated gene of *Escherichia coli*. *J Mol Biol* **178**: 653-668.
- Inokuchi, K., M. Itoh and S. Mizushima (1985). Domains involved in osmoregulation of the *ompF* gene in *Escherichia coli*. *J Bacteriol* **164**: 585-590.
- Ishige, K., S. Nagasawa, S. Tokishita and T. Mizuno (1994). A novel device of bacterial signal transducers. *EMBO J* **13**: 5195-5202.
- Janiak-Spens, F., J. M. Sparling, M. Gurfinkel and A. H. West (1999). Differential stabilities of phosphorylated response regulator domains reflect functional roles of the yeast osmoregulatory SLN1 and SSK1 proteins. *J Bacteriol* **181**: 411-417.
- Jin, T. and M. Inouye (1993). Ligand binding to the receptor domain regulates the ratio of kinase to phosphatase activities of the

- signaling domain of the hybrid *Escherichia coli* transmembrane receptor, Taz1. *J Mol Biol* **232**: 484-492.
- Jo, Y., F. Nara, S. Ichihara, T. Mizuno and S. Mizushima (1986). Purification and characterization of the OmpR protein, a positive regulator involved in osmoregulatory expression of the *ompF* and *ompC* genes in *Escherichia coli*. *J Biol Chem* **261**: 15252-15256.
- Jovanovich, S. B., M. Martinell, M. T. Record and R. R. Burgess (1988). Rapid response to osmotic upshift by osmoregulated genes in *Escherichia coli* and *Salmonella typhimurium*. *J Bacteriol* **170**: 534-539.
- Jung, K., K. Hamann and A. Reverman (2001). K<sup>+</sup> stimulates specifically the autokinase activity of purified and reconstituted EnvZ of *Escherichia coli*. *J Biol Chem* **276**: 40896-40902.
- Kaback, H. R. and T. F. Deuel (1969). Proline uptake by disrupted membrane preparations from *Escherichia coli*. *Arch Biochem Biophys* **132**: 118-129.
- Kanamaru, K., H. Aiba and T. Mizuno (1990). Transmembrane signal transduction and osmoregulation in *Escherichia coli*: I. Analysis by site-directed mutagenesis of the amino acid residues involved in phosphotransfer between the two regulatory components, EnvZ and OmpR. *J Biochem (Tokyo)* **108**: 483-487.
- Kanamaru, K. and T. Mizuno (1992). Signal transduction and osmoregulation in *Escherichia coli*: a novel mutant of the positive

- regulator, OmpR, that functions in a phosphorylation-independent manner. *J Biochem (Tokyo)* **111**: 425-430.
- Kato, M., H. Aiba, S. Tate, Y. Nishimura and T. Mizuno (1989). Location of the phosphorylation site and DNA binding site of a positive regulator, OmpR, involved in the activation of the osmoregulatory genes of *Escherichia coli*. *FEBS Lett* **249**: 168-172.
- Kato, M., M. Tsuzuki, H. Aiba and T. Mizuno (1995). Gene activation by the *Escherichia coli* positive regulator OmpR: a mutational study of the DNA-binding domain of OmpR. *Mol Gen Genet* **248**: 399-406.
- Kato, N., H. Aiba and T. Mizuno (1996). Suppressor mutations in  $\alpha$ -subunit of RNA polymerase for a mutant of the positive regulator, OmpR, in *Escherichia coli*. *FEMS Microbiol Lett* **139**: 175-180.
- Kenney, L. J. (1997). Kinase activity of EnvZ, an osmoregulatory signal transducing protein of *Escherichia coli*. *Arch Biochem Biophys* **346**: 303-311.
- Kenney, L. J. (2000). Response-regulator phosphorylation and activation: a two-way street? response. *Trends Microbiol* **8**: 155-156.
- Kenney, L. J. (2002). Structure/function relationships in OmpR and other winged-helix transcription factors. *Curr Opin Microbiol* **5**: 135-141.
- Kenney, L. J., M. D. Bauer and T. J. Silhavy (1995). Phosphorylation-dependent conformational changes in OmpR, an osmoregulatory

- DNA-binding protein of *Escherichia coli*. *Proc Natl Acad Sci U S A* **92**: 8866-8870.
- Kim, C., M. Jackson, R. Lux and S. Khan (2001). Determinants of chemotactic signal amplification in *Escherichia coli*. *J Mol Biol* **307**: 119-135.
- Koch, A. L. (1971). The adaptive response of *Escherichia coli* to a feast and famine existence. *Adv Microb Physiol* **6**: 147-217.
- Kondo, H., A. Nakagawa, J. Nishihira, Y. Nishimura, T. Mizuno and I. Tanaka (1997). *Escherichia coli* positive regulator OmpR has a large loop structure at the putative RNA polymerase interaction site. *Nat Struct Biol* **4**: 28-31.
- Laimins, L. A., D. B. Rhoads and W. Epstein (1981). Osmotic control of *kdp* operon expression in *Escherichia coli*. *Proc Natl Acad Sci U S A* **78**: 464-468.
- Landfald, B. and A. R. Strom (1986). Choline-glycinebetaine pathway confers a high level of osmotic tolerance in *Escherichia coli*. *J Bacteriol* **165**: 849-855.
- Leonardo, M. R. and S. Forst (1996). Re-examination of the role of the periplasmic domain of EnvZ in sensing of osmolarity signals in *Escherichia coli*. *Mol Microbiol* **22**: 405-413.
- Leroy, J. L., E. Charretier, M. Kochoyan and M. Gueron (1988). Evidence from base-pair kinetics for two types of adenine tract structures in

- solution: their relation to DNA curvature. *Biochemistry* **27**: 8894-8898.
- Lewis, R. J., J. A. Brannigan, K. Muchova, I. Barak and A. J. Wilkinson (1999). Phosphorylated aspartate in the structure of a response regulator protein. *J Mol Biol* **294**: 9-15.
- Lewis, R. J., S. Krzywda, J. A. Brannigan, J. P. Turkenburg, K. Muchova, E. J. Dodson, I. Barak and A. J. Wilkinson (2000). The *trans*-activation domain of the sporulation response regulator SpoOA revealed by X-ray crystallography. *Mol Microbiol* **38**: 198-212.
- Li, J., R. V. Swanson, M. I. Simon and R. M. Weis (1995). The response regulators CheB and CheY exhibit cooperative binding to the kinase CheA. *Biochemistry* **34**: 14626-14636.
- Liljestrom, P. (1986a). Structure and expression of the *ompB* operon of *Salmonella typhimurium* and *Escherichia coli*, Thesis Dissertation. University of Helsinki, Helsinki, Finland.
- Liljestrom, P. (1986b). The EnvZ protein of *Salmonella typhimurium* LT-2 and *Escherichia coli* K-12 is located in the cytoplasmic membrane. *FEMS Microbiol Lett* **36**: 145-150.
- Liljestrom, P., I. Laamanen and E. T. Palva (1988). Structure and expression of the *ompB* operon, the regulatory locus for the outer membrane porin regulon in *Salmonella typhimurium* LT-2. *J Mol Biol* **201**: 663-673.

- Liljestrom, P., P. L. Maattanen and E. T. Palva (1982). Cloning of the regulatory locus *ompB* of *Salmonella typhimurium* LT-2. I. Isolation of the *ompR* gene and identification of its gene product. *Mol Gen Genet* **188**: 184-189.
- Luderitz, O., M. A. Freudenberg, C. Galanos, V. Lehmann, E. T. Rietschel and D. M. Shaw (1982). Lipopolysaccharides of gram-negative bacteria. *Curr Top Membr Transp* **17**: 79-151.
- Lukat, G. S., B. H. Lee, J. M. Mottonen, A. M. Stock and J. B. Stock (1991). Roles of the highly conserved aspartate and lysine residues in the response regulator of bacterial chemotaxis. *J Biol Chem* **266**: 8348-8354.
- Lukat, G. S., A. M. Stock and J. B. Stock (1990). Divalent metal ion binding to the CheY protein and its significance to phosphotransfer in bacterial chemotaxis. *Biochemistry* **29**: 5436-5442.
- MacDonald, D., K. Herbert, X. Zhang, T. Polgruto and P. Lu (2001). Solution structure of an A-tract DNA bend. *J Mol Biol* **306**: 1081-1098.
- Mach, H., C. R. Middaugh and R. V. Lewis (1992). Statistical determination of the average values of the extinction coefficients of tryptophan and tyrosine in native proteins. *Anal Biochem* **200**: 74-80.
- Madhusudan, J. Zapf, J. M. Whiteley, J. A. Hoch, N. H. Xuong and K. I. Varughese (1996). Crystal structure of a phosphatase-resistant

- mutant of sporulation response regulator Spo0F from *Bacillus subtilis*. *Structure* **4**: 679-690.
- Maeda, S. and T. Mizuno (1988). Activation of the *ompC* gene by the OmpR protein in *Escherichia coli*. The *cis*-acting upstream sequence can function in both orientations with respect to the canonical promoter. *J Biol Chem* **263**: 14629-14633.
- Maeda, S. and T. Mizuno (1990). Evidence for multiple OmpR-binding sites in the upstream activation sequence of the *ompC* promoter in *Escherichia coli*: a single OmpR- binding site is capable of activating the promoter. *J Bacteriol* **172**: 501-503.
- Maeda, S., Y. Ozawa, T. Mizuno and S. Mizushima (1988). Stereospecific positioning of the *cis*-acting sequence with respect to the canonical promoter is required for activation of the *ompC* gene by a positive regulator, OmpR, in. *J Mol Biol* **202**: 433-441.
- Maeda, S., K. Takayanagi, Y. Nishimura, T. Maruyama, K. Sato and T. Mizuno (1991). Activation of the osmoregulated *ompC* gene by the OmpR protein in *Escherichia coli*: a study involving synthetic OmpR-binding sequences. *J Biochem (Tokyo)* **110**: 324-327.
- Makino, K., M. Amemura, T. Kawamoto, S. Kimura, H. Shinagawa, A. Nakata and M. Suzuki (1996). DNA binding of PhoB and its interaction with RNA polymerase. *J Mol Biol* **259**: 15-26.
- Maris, A. E., M. R. Sawaya, M. Kaczor-Grzeskowiak, M. R. Jarvis, S. M. Bearson, M. L. Kopka, I. Schroder, R. P. Gunsalus and R. E.

- Dickerson (2002). Dimerization allows DNA target site recognition by the NarL response regulator. *Nat Struct Biol* **9**: 771-778.
- Martinez-Flores, I., R. Cano, V. H. Bustamante, E. Calva and J. L. Puente (1999). The *ompB* operon partially determines differential expression of OmpC in *Salmonella typhi* and *Escherichia coli*. *J Bacteriol* **181**: 556-562.
- Martinez-Hackert, E. and A. M. Stock (1997a). The DNA-binding domain of OmpR: crystal structures of a winged helix transcription factor. *Structure* **5**: 109-124.
- Martinez-Hackert, E. and A. M. Stock (1997b). Structural relationships in the OmpR family of winged-helix transcription factors. *J Mol Biol* **269**: 301-312.
- Matsubara, M., S. Kitaoka, S. Takeda and T. Mizuno (2000). Tuning of the porin expression under anaerobic growth conditions by His-to-Asp cross-phosphorelay through both the EnvZ-osmosensor and ArcB-anaerosensor in *Escherichia coli*. *Genes Cells* **5**: 555-569.
- Matsubara, M. and T. Mizuno (1999). EnvZ-independent phosphotransfer signaling pathway of the OmpR-mediated osmoregulatory expression of OmpC and OmpF in *Escherichia coli*. *Biosci Biotechnol Biochem* **63**: 408-414.
- Matsuyama, S., K. Inokuchi and S. Mizushima (1984). Promoter exchange between *ompF* and *ompC*, genes for osmoregulated major



- outer membrane proteins of *Escherichia coli* K-12. *J Bacteriol* **158**: 1041-1047.
- Matsuyama, S., T. Mizuno and S. Mizushima (1986). Interaction between two regulatory proteins in osmoregulatory expression of *ompF* and *ompC* genes in *Escherichia coli*: a novel *ompR* mutation suppresses pleiotropic defects caused by an *envZ* mutation. *J Bacteriol* **168**: 1309-1314.
- Matsuyama, S. and S. Mizushima (1985). Construction and characterization of a deletion mutant lacking *micF*, a proposed regulatory gene for OmpF synthesis in *Escherichia coli*. *J Bacteriol* **162**: 1196-1202.
- Matsuyama, S. and S. Mizushima (1987). Novel *rpoA* mutation that interferes with the function of OmpR and EnvZ, positive regulators of the *ompF* and *ompC* genes that code for outer- membrane proteins in *Escherichia coli* K12. *J Mol Biol* **195**: 847-853.
- Mattison, K. and L. J. Kenney (2002). Phosphorylation alters the interaction of the response regulator OmpR with its sensor kinase EnvZ. *J Biol Chem* **277**: 11143-11148. (This corresponds to Chapter 5)
- Mattison, K., R. Oropeza, N. Byers and L. J. Kenney (2002a). A phosphorylation site mutant of OmpR reveals different binding conformations at *ompF* and *ompC*. *J Mol Biol* **315**: 497-511. (This corresponds to Chapter 2)

- Mattison, K., R. Oropeza and L. J. Kenney (2002b). The linker region plays an important role in the interdomain communication of the response regulator OmpR. *J Biol Chem* **277**: 32714-32721. (This corresponds to Chapter 3)
- Mayover, T. L., C. J. Halkides and R. C. Stewart (1999). Kinetic characterization of CheY phosphorylation reactions: comparison of P-CheA and small molecule phosphate donors. *Biochemistry* **38**: 2259-2271.
- McCleary, W. R. (1996). The activation of PhoB by acetyl phosphate. *Mol Microbiol* **20**: 1155-1163.
- McCleary, W. R. and J. B. Stock (1994). Acetyl phosphate and the activation of two-component response regulators. *J Biol Chem* **269**: 31567-31572.
- McCleary, W. R., J. B. Stock and A. J. Ninfa (1993). Is acetyl phosphate a global signal in *Escherichia coli*? *J Bacteriol* **175**: 2793-2798.
- Meury, J. (1994). Immediate and transient inhibition of the respiration of *Escherichia coli* under hyperosmotic shock. *FEMS Microbiol Lett* **121**: 281-286.
- Meury, J., A. Robin and P. Monnier-Champeix (1985). Turgor-controlled K<sup>+</sup> fluxes and their pathways in *Escherichia coli*. *Eur J Biochem* **151**: 613-619.
- Milner, J. L., S. Grothe and J. M. Wood (1988). Proline porter II is activated by a hyperosmotic shift in both whole cells and

- membrane vesicles of *Escherichia coli* K-12. *J Biol Chem* **262**: 14900-14905.
- Mizuno, T. (1987). Static bend of DNA helix at the activator recognition site of the *ompF* promoter in *Escherichia coli*. *Gene* **54**: 57-64.
- Mizuno, T., H. Kasai and S. Mizushima (1987). Construction of a series of *ompC-ompF* chimeric genes by in vivo homologous recombination in *Escherichia coli* and characterization of their translational products. *Mol Gen Genet* **207**: 217-223.
- Mizuno, T., M. Kato, Y. L. Jo and S. Mizushima (1988). Interaction of OmpR, a positive regulator, with the osmoregulated *ompC* and *ompF* genes of *Escherichia coli*. Studies with wild-type and mutant OmpR proteins. *J Biol Chem* **263**: 1008-1012.
- Mizuno, T. and S. Mizushima (1986). Characterization by deletion and localized mutagenesis *in vitro* of the promoter region of the *Escherichia coli ompC* gene and importance of the upstream DNA domain in positive regulation by the OmpR protein. *J Bacteriol* **168**: 86-95.
- Mizuno, T. and S. Mizushima (1987). Isolation and characterization of deletion mutants of *ompR* and *envZ*, regulatory genes for expression of the outer membrane proteins OmpC and OmpF in *Escherichia coli*. *J Biochem (Tokyo)* **101**: 387-396.
- Mizuno, T., E. T. Wurtzel and M. Inouye (1982). Osmoregulation of gene expression. II. DNA sequence of the *envZ* gene of the *ompB* operon

- of *Escherichia coli* and characterization of its gene product. *J Biol Chem* **257**: 13692-13698.
- Montagne, M., A. Martel and H. Le Moual (2001). Characterization of the catalytic activities of the PhoQ histidine protein kinase of *Salmonella enterica* serovar *Typhimurium*. *J Bacteriol* **183**: 1787-1791.
- Moore, J. B., S. P. Shiau and L. J. Reitzer (1993). Alterations of highly conserved residues in the regulatory domain of nitrogen regulator I (NtrC) of *Escherichia coli*. *J Bacteriol* **175**: 2692-2701.
- Munro, G. F., K. Hercules, J. Morgan and W. Sauerbier (1972). Dependence of putrescine content of *Escherichia coli* on the osmotic strength of the medium. *J Biol Chem* **247**: 1272-1280.
- Nakae, T. (1976). Outer membrane of *Salmonella*. Isolation of protein complex that produces transmembrane channels. *J Biol Chem* **251**: 2176-2178.
- Nakae, T. and H. Nikaido (1973). Permeability of model membranes containing phospholipids and lipopolysaccharides: some preliminary results. *J Infect Dis* **128**: S30-S34.
- Nakae, T. and H. Nikaido (1975). Outer membrane as a diffusion barrier in *Salmonella typhimurium*. Penetration of oligo- and polysaccharides into isolated outer membrane vesicles and cells with degraded peptidoglycan layer. *J Biol Chem* **250**: 7359-7365.

- Nakano, M. M. and Y. Zhu (2001). Involvement of ResE phosphatase activity in down-regulation of ResD- controlled genes in *Bacillus subtilis* during aerobic growth. *J Bacteriol* **183**: 1938-1944.
- Nakashima, K., K. Kanamaru, H. Aiba and T. Mizuno (1991a). Osmoregulatory expression of the porin genes in *Escherichia coli*: evidence for signal titration in the signal transduction through EnvZ- OmpR phosphotransfer. *FEMS Microbiol Lett* **66**: 43-47.
- Nakashima, K., K. Kanamaru, H. Aiba and T. Mizuno (1991b). Signal transduction and osmoregulation in *Escherichia coli* : a novel type of mutation in the phosphorylation domain of the activator protein, OmpR, results in a defect in its phosphorylation-dependent DNA binding. *J Biol Chem* **266**: 10775-10780.
- Nara, F., S. Matsuyama, T. Mizuno and S. Mizushima (1986). Molecular analysis of mutant *ompR* genes exhibiting different phenotypes as to osmoregulation of the *ompF* and *ompC* genes of *Escherichia coli*. *Mol Gen Genet* **202**: 194-199.
- Nelson, H. C., J. T. Finch, B. F. Luisi and A. Klug (1987). The structure of an oligo(dA)·oligo(dT) tract and its biological implications. *Nature* **330**: 221-226.
- Nikaido, H. and T. Nakae (1979). The outer membrane of gram-negative bacteria. *Adv Microb Physiol* **20**: 163-250.

- Nikaido, H. and E. Y. Rosenberg (1983). Porin channels in *Escherichia coli*: studies with liposomes reconstituted from purified proteins. *J Bacteriol* **153**: 241-252.
- Nikaido, H. and M. Vaara (1985). Molecular basis of bacterial outer membrane permeability. *Microbiol Rev* **49**: 1-32.
- Nogami, T., T. Mizuno and S. Mizushima (1985). Construction of a series of *ompF-ompC* chimeric genes by *in vivo* homologous recombination in *Escherichia coli* and characterization of the translational products. *J Bacteriol* **164**: 797-801.
- Norioka, S., G. Ramakrishnan, K. Ikenaka and M. Inouye (1986). Interaction of a transcriptional activator, OmpR, with reciprocally osmoregulated genes, *ompF* and *ompC*, of *Escherichia coli*. *J Biol Chem* **261**: 17113-17119.
- Ostrow, K. S., T. J. Silhavy and S. Garrett (1986). *cis*-acting sites required for osmoregulation of *ompF* expression in *Escherichia coli* K-12. *J Bacteriol* **168**: 1165-1171.
- Ozawa, Y., T. Mizuno and S. Mizushima (1987). Roles of the Pribnow box in positive regulation of the *ompC* and *ompF* genes in *Escherichia coli*. *J Bacteriol* **169**: 1331-1334.
- Park, H. and M. Inouye (1997). Mutational analysis of the linker region of EnvZ, an osmosensor in *Escherichia coli*. *J Bacteriol* **179**: 4382-4390.

- Park, H., S. K. Saha and M. Inouye (1998). Two-domain reconstitution of a functional protein histidine kinase. *Proc Natl Acad Sci U S A* **95**: 6728-6732.
- Peck, L. J. and J. C. Wang (1981). Sequence dependence of the helical repeat of DNA in solution. *Nature* **292**: 375-378.
- Perroud, B. and D. LeRudulier (1985). Glycine betaine transport in *Escherichia coli*: osmotic modulation. *J Bacteriol* **161**: 393-401.
- Pratt, L. A., W. Hsing, K. E. Gibson and T. J. Silhavy (1996). From acids to *osmZ*: multiple factors influence synthesis of the OmpF and OmpC porins in *Escherichia coli*. *Mol Microbiol* **20**: 911-917.
- Pratt, L. A. and T. J. Silhavy (1994). OmpR mutants specifically defective for transcriptional activation. *Journal of Molecular Biology* **243**: 579-594.
- Pratt, L. A. and T. J. Silhavy (1995). Identification of base pairs important for OmpR-DNA interaction. *Mol Microbiol* **17**: 565-573.
- Pruss, B. M. (1998). Acetyl phosphate and the phosphorylation of OmpR are involved in the regulation of the cell division rate in *Escherichia coli*. *Arch Microbiol* **170**: 141-146.
- Qin, L., R. Dutta, H. Kurokawa, M. Ikura and M. Inouye (2000). A monomeric histidine kinase derived from EnvZ, an *Escherichia coli* osmosensor. *Mol Microbiol* **36**: 24-32.

- Qin, L., T. Yoshida and M. Inouye (2001). The critical role of DNA in the equilibrium between OmpR and phosphorylated OmpR mediated by EnvZ in *Escherichia coli*. *Proc Natl Acad Sci U S A* **98**: 908-913.
- Ramakrishnan, G., K. Ikenaka and M. Inouye (1985). Uncoupling of osmoregulation of the *Escherichia coli* K-12 *ompF* gene from *ompB*-dependent transcription. *J Bacteriol* **163**: 82-87.
- Ramani, N., L. Huang and M. Freundlich (1992). *In vitro* interactions of integration host factor with the *ompF* promoter-regulatory region of *Escherichia coli*. *Mol Gen Genet* **231**: 248-255.
- Rampersaud, A., S. L. Harlocker and M. Inouye (1994). The OmpR protein of *Escherichia coli* binds to sites in the *ompF* promoter region in a hierarchical manner determined by its degree of phosphorylation. *J Biol Chem* **269**: 12559-12566.
- Rampersaud, A. and M. Inouye (1991). Procaine, a local anesthetic, signals through the EnvZ receptor to change the DNA binding affinity of the transcriptional activator protein OmpR. *J Bacteriol* **173**: 6882-6888.
- Rampersaud, A., S. Norioka and M. Inouye (1989). Characterization of OmpR binding sequences in the upstream region of the *ompF* promoter essential for transcriptional activation. *J Biol Chem* **264**: 18693-18700.
- Reyrat, J. M., M. David, J. Batut and P. Boistard (1994). FixL of *Rhizobium meliloti* enhances the transcriptional activity of a



- mutant FixJD54N protein by phosphorylation of an alternate residue. *J Bacteriol* **176**: 1969-1976.
- Rhodes, D. and A. Klug (1980). Helical periodicity of DNA determined by enzyme digestion. *Nature* **286**: 573-578.
- Rhodes, D. and A. Klug (1981). Sequence-dependent helical periodicity of DNA. *Nature* **292**: 378-380.
- Richey, B., D. S. Cayley, M. C. Mossing, C. Kolka, C. F. Anderson, T. C. Farrar and M. T. Record (1987). Variability in the intracellular ionic environment of *Escherichia coli*: differences between *in vitro* and *in vivo* effects of ion concentrations on protein-DNA interactions and gene expression. *J Biol Chem* **262**: 7157-7164.
- Roberts, D. L., D. W. Bennett and S. A. Forst (1994). Identification of the site of phosphorylation on the osmosensor, EnvZ, of *Escherichia coli*. *J Biol Chem* **269**: 8728-8733.
- Robinson, V. L., D. R. Buckler and A. M. Stock (2000). A tale of two components: a novel kinase and a regulatory switch. *Nature Structural Biology* **7**: 626-633.
- Russo, F. D. and T. J. Silhavy (1991). EnvZ controls the concentration of phosphorylated OmpR to mediate osmoregulation of the porin genes. *J Mol Biol* **222**: 567-580.
- Russo, F. D., J. M. Slauch and T. J. Silhavy (1993). Mutations that affect separate functions of OmpR the phosphorylated regulator of porin transcription in *Escherichia coli*. *J Mol Biol* **231**: 261-273.

- Schindler, M. and M. J. Osborn (1979). Interaction of divalent cations and polymixin B with lipopolysaccharide. *Biochemistry* **18**: 4425-4430.
- Schleyer, M., R. Schmid and E. P. Bakker (1993). Transient, specific and extremely rapid release of osmolytes from growing cells of *Escherichia coli* K-12 exposed to hypoosmotic shock. *Arch Microbiol* **160**: 424-431.
- Schuster, M., R. E. Silversmith and R. B. Bourret (2001). Conformational coupling in the chemotaxis response regulator CheY. *Proc Natl Acad Sci U S A* **98**: 6003-6008.
- Sharif, T. R. and M. M. Igo (1993). Mutations in the alpha subunit of RNA polymerase that affect the regulation of porin gene transcription in *Escherichia coli* K-12. *J Bacteriol* **175**: 5460-5468.
- Sheridan, R. C., J. F. McCullough and Z. T. Wakefield (1971). Phosphoramidic acid and its salts. *Inorganic Synthesis* **13**: 23-26.
- Shine, J. and L. Dalgarno (1975). Determinant of cistron specificity in bacterial ribosomes. *Nature* **254**: 34-38.
- Silversmith, R. E. and R. B. Bourret (1999). Throwing the switch in bacterial chemotaxis. *Trends Microbiol* **7**: 16-22.
- Skarphol, K., J. Waukau and S. Forst (1997). Role of His243 in the phosphatase activity of EnvZ in *Escherichia coli*. *J Bacteriol* **179**: 1413-1416.

- Slauch, J. M., S. Garrett, D. E. Jackson and T. J. Silhavy (1988). EnvZ functions through OmpR to control porin gene expression in *Escherichia coli* K-12. *J Bacteriol* **170**: 439-441.
- Slauch, J. M., F. D. Russo and T. J. Silhavy (1991). Suppressor mutations in *rpoA* suggest that OmpR controls transcription by direct interaction with the alpha subunit of RNA polymerase. *J Bacteriol* **173**: 7501-7510.
- Slauch, J. M. and T. J. Silhavy (1989). Genetic analysis of the switch that controls porin gene expression in *Escherichia coli* K-12. *J Mol Biol* **210**: 281-292.
- Slauch, J. M. and T. J. Silhavy (1991). *cis*-acting *ompF* mutations that result in OmpR-dependent constitutive expression. *J Bacteriol* **173**: 4039-4048.
- Sola, M., F. X. Gomis-Ruth, L. Serrano, A. Gonzalez and M. Coll (1999). Three-dimensional crystal structure of the transcription factor PhoB receiver domain. *J Mol Biol* **285**: 675-687.
- Stock, A. M., E. Martinez-Hackert, B. F. Rasmussen, A. H. West, J. B. Stock, D. Ringe and G. A. Petsko (1993). Structure of the Mg<sup>2+</sup>-bound form of CheY and mechanism of phosphoryl transfer in bacterial chemotaxis. *Biochemistry* **32**: 13375-13380.
- Stock, A. M., J. M. Mottonen, J. B. Stock and C. E. Schutt (1989). Three-dimensional structure of CheY, the response regulator of bacterial chemotaxis. *Nature* **337**: 745-749.

- Stock, A. M., V. L. Robinson and P. N. Goudreau (2000). Two-component signal transduction. *Annu Rev Biochem* **69**: 183-215.
- Stock, J. B., B. Rauch and S. Roseman (1977). Periplasmic space in *Salmonella typhimurium* and *Escherichia coli*. *J Biol Chem* **252**: 7850-7861.
- Suter, B., G. Schnappauf and F. Thoma (2000). Poly(dA·dT) sequences exist as rigid DNA structures in nucleosome-free yeast promoters *in vivo*. *Nucleic Acids Res* **28**: 4083-4089.
- Tanaka, T., S. K. Saha, C. Tomomori, R. Ishima, D. Liu, K. I. Tong, H. Park, R. Dutta, L. Qin, M. Swindells, T. Yamazaki, A. M. Ono, M. Kainosho, M. Inouye and M. Ikura (1998). NMR structure of the histidine kinase domain of the *E. coli* osmosensor EnvZ. *Nature* **396**: 88-92.
- Tate, S., M. Kato, Y. Nishimura, Y. Arata and T. Mizuno (1988). Location of DNA-binding segment of a positive regulator, OmpR, involved in activation of the *ompF* and *ompC* genes of *Escherichia coli*. *FEBS Lett* **242**: 27-30.
- Taylor, R. K., S. Garrett, E. Sodergren and T. J. Silhavy (1985). Mutations that define the promoter of *ompF*, a gene specifying a major outer membrane porin protein. *J Bacteriol* **162**: 1054-1060.
- Taylor, R. K., M. N. Hall and T. J. Silhavy (1983). Isolation and characterization of mutations altering expression of the major

- outer membrane porin proteins using the local anaesthetic procaine. *J Mol Biol* **166**: 273-282.
- Tempest, D. W., J. L. Meers and C. M. Brown (1970). Influence of environment on the content and composition of microbial free amino acid pools. *J Gen Microbiol* **64**: 171-185.
- Tokishita, S., A. Kojima, H. Aiba and T. Mizuno (1991). Transmembrane signal transduction and osmoregulation in *Escherichia coli*: functional importance of the periplasmic domain of the membrane-located protein kinase, EnvZ. *J Biol Chem* **266**: 6780-6785.
- Tokishita, S., A. Kojima and T. Mizuno (1992). Transmembrane signal transduction and osmoregulation in *Escherichia coli*: functional importance of the transmembrane regions of membrane-located protein kinase, EnvZ. *J Biochem (Tokyo)* **111**: 707-713.
- Tokishita, S. and T. Mizuno (1994). Transmembrane signal transduction by the *Escherichia coli* osmotic sensor, EnvZ: intermolecular complementation of transmembrane signaling. *Mol Microbiol* **13**: 435-444.
- Tokishita, S., H. Yamada, H. Aiba and T. Mizuno (1990). Transmembrane signal transduction and osmoregulation in *Escherichia coli*: II. The osmotic sensor, EnvZ, located in the isolated cytoplasmic membrane displays its phosphorylation and dephosphorylation abilities as to the activator protein, OmpR. *J Biochem (Tokyo)* **108**: 488-493.

- Tommassen, J. and B. Lugtenberg (1980). Outer membrane protein e of *Escherichia coli* K-12 is coregulated with alkaline phosphatase. *J Bacteriol* **143**: 151-157.
- Tomomori, C., T. Tanaka, R. Dutta, H. Park, S. K. Saha, Y. Zhu, R. Ishima, D. Liu, K. I. Tong, H. Kurokawa, H. Qian, M. Inouye and M. Ikura (1999). Solution Structure of the homodimeric core domain of *Escherichia coli* histidine kinase EnvZ. *Nature Structural Biology* **6**: 729-734.
- Tran, V. K., R. Oropeza and L. J. Kenney (2000). A single amino acid substitution in the C terminus of OmpR alters DNA recognition and phosphorylation. *J Mol Biol* **299**: 1257-1270.
- Tsui, P., V. Helu and M. Freundlich (1988). Altered osmoregulation of *ompF* in integration host factor mutants of *Escherichia coli*. *J Bacteriol* **170**: 4950-4953.
- Tsung, K., R. Brissette and M. Inouye (1990). Enhancement of RNA polymerase binding to promoters by a transcriptional activator, OmpR, in *Escherichia coli*: Its positive and negative effects on transcription. *Proc Natl Acad Sci U S A* **87**: 5940-5944.
- Tsung, K., R. E. Brissette and M. Inouye (1989). Identification of the DNA-binding domain of the OmpR protein required for transcriptional activation of the *ompF* and *ompC* genes of *Escherichia coli* by *in vivo* DNA footprinting. *J Biol Chem* **264**: 10104-10109.

- Tsuzuki, M., H. Aiba and T. Mizuno (1994). Gene activation by the *Escherichia coli* positive regulator, OmpR. Phosphorylation-independent mechanism of activation by an OmpR mutant. *J Mol Biol* **242**: 607-613.
- Tzeng, Y. L. and J. A. Hoch (1997). Molecular recognition in signal transduction: the interaction surfaces of the Spo0F response regulator with its cognate phosphorelay proteins revealed by alanine scanning mutagenesis. *J Mol Biol* **272**: 200-212.
- Utsumi, R., R. E. Brissette, A. Rampersaud, S. A. Forst, K. Oosawa and M. Inouye (1989). Activation of bacterial porin gene expression by a chimeric signal transducer in response to aspartate. *Science* **245**: 1246-1249.
- van Alphen, W. and B. Lugtenberg (1977). Influence of osmolarity of the growth medium on the outer membrane protein pattern of *Escherichia coli*. *J Bacteriol* **131**.
- Villarejo, M. and C. C. Case (1984). *envZ* mediates transcriptional control by local anesthetics but is not required for osmoregulation in *Escherichia coli*. *J Bacteriol* **159**: 883-887.
- Volz, K. and P. Matsumura (1991). Crystal structure of *Escherichia coli* CheY refined at 1.7 Å resolution. *J Biol Chem* **266**: 15511-15519.
- Walthers, D., V. K. Tran and L. J. Kenney (2003). Interdomain linkers of homologous response regulators determine their mechanism of action. *J Bacteriol* **185**: 317-324.

- Wandersman, C., F. Moreno and M. Schwartz (1980). Pleiotropic mutations rendering *Escherichia coli* K-12 resistant to bacteriophage TP1. *J Bacteriol* **143**: 1374-1383.
- Wanner, B. L. (1996). in *Escherichia coli and Salmonella typhimurium*. (F. C. Neidhart, et al., eds.). American Society for Microbiology Press, Washington, D.C. **1**: 1359-1381.
- Waukau, J. and S. Forst (1992). Molecular analysis of the signaling pathway between EnvZ and OmpR in *Escherichia coli*. *J Bacteriol* **174**: 1522-1527.
- Waukau, J. and S. Forst (1999). Identification of a conserved N-terminal sequence involved in transmembrane signal transduction in EnvZ. *J Bacteriol* **181**: 5534-5538.
- Webber, C. A. and R. J. Kadner (1997). Involvement of the amino-terminal phosphorylation module of UhpA in activation of *uhpT* transcription in *Escherichia coli*. *Mol Microbiol* **24**: 1039-1048.
- Weinstein, M., A. F. Lois, G. S. Ditta and D. R. Helinski (1993). Mutants of the two-component regulatory protein FixJ of *Rhizobium meliloti* that have increased activity at the *nifA* promoter. *Gene* **134**: 145-152.
- Weinstein, M., A. F. Lois, E. K. Monson, G. S. Ditta and D. R. Helinski (1992). Isolation of phosphorylation-deficient mutants of the *Rhizobium meliloti* two-component regulatory protein, FixJ. *Mol Microbiol* **6**: 2041-2049.



- Williams, S. B. and V. Stewart (1997). Nitrate- and nitrite-sensing protein NarX of *Escherichia coli* K-12: mutational analysis of the amino-terminal tail and first transmembrane segment. *J Bacteriol* **179**: 721-729.
- Wood, J. (1999). Osmosensing by bacteria: signals and membrane-based sensors. *Microbiol Mol Biol Rev* **63**: 230-262.
- Wootton, J. C. and M. H. Drummond (1989). The Q-linker: a class of interdomain sequences found in bacterial multidomain regulatory proteins. *Protein Eng* **2**: 535-543.
- Wurtzel, E. T., M. Y. Chou and M. Inouye (1982). Osmoregulation of gene expression. I. DNA sequence of the *ompR* gene of the *ompB* operon of *Escherichia coli* and characterization of its gene product. *J Biol Chem* **257**: 13685-13691.
- Wurtzel, E. T., N. R. Movva, F. L. Ross and M. Inouye (1981). Two-step cloning of the *Escherichia coli* regulatory gene *ompB*, employing phage Mu. *J Mol Appl Genet* **1**: 61-69.
- Yamamoto, I., K. Takamatsu, Y. Ohshima, T. Ujiye and T. Satoh (1999). Site-directed mutagenesis of the response regulator DmsR for the *dmsCBA* operon expression in *Rhodobacter sphaeroides* f. sp. *Denitrificans*: An essential residue of proline-130 in the linker. *Biochim Biophys Acta* **1447**: 57-63.

- Yang, Y. and M. Inouye (1991). Intermolecular complementation between two defective mutant signal-transducing receptors of *Escherichia coli*. *Proc Natl Acad Sci U S A* **88**: 11057-11061.
- Yang, Y. and M. Inouye (1993). Requirement of both kinase and phosphatase activities of an *Escherichia coli* receptor (Taz1) for ligand-dependent signal transduction. *J Mol Biol* **231**: 335-342.
- Yoshida, T., S. J. Cai and M. Inouye (2002a). Interaction of EnvZ, a sensory histidine kinase, with phosphorylated OmpR, the cognate response regulator. *Mol Microbiol* **46**: 1283-1294.
- Yoshida, T., L. Qin and M. Inouye (2002b). Formation of the stoichiometric complex of EnvZ, a histidine kinase, with its response regulator, OmpR. *Mol Microbiol* **46**: 1273-1282.
- Zhao, H., T. Msadek, J. Zapf, Madhusan, J. A. Hoch and K. I. Varughese (2002). DNA complexed structure of the key transcription factor initiating development in sporulating bacteria. *Structure* **10**: 1041-1050.
- Zhao, R., E. J. Collins, R. B. Bourret and R. E. Silversmith (2002). Structure and catalytic mechanism of the *E. coli* chemotaxis phosphatase CheZ. *Nature Structural Biology*.
- Zhu, X., C. D. Amsler, K. Volz and P. Matsumura (1996). Tyrosine 106 of CheY plays an important role in chemotaxis signal transduction in *Escherichia coli*. *J Bacteriol* **178**: 4208-4215.

- Zhu, X., J. Rebello, P. Matsumura and K. Volz (1997a). Crystal structures of CheY mutants Y106W and T87I/Y106W. *J Biol Chem* **272**: 5000-5006.
- Zhu, X., K. Volz and P. Matsumura (1997b). The CheZ binding surface of CheY overlaps the CheA and FliM binding surfaces. *J Biol Chem* **272**: 23758-23764.
- Zhu, Y., L. Qin, T. Yoshida and M. Inouye (2000). Phosphatase activity of histidine kinase EnvZ without kinase catalytic domain. *Proc Natl Acad Sci U S A* **97**: 7808-7813.